ROLE OF MACROPHAGES IN GROWTH AND PROGRESSION OF BREAST CANCER

By

RAJSHRI SINGH

Enrol. No. LIFE01200804013

Bhabha Atomic Research Centre, Mumbai

A thesis submitted to the

Board of Studies in Life Sciences

In partial fulfillment of requirements

for the Degree of

DOCTOR OF PHILOSOPHY

of

HOMI BHABHA NATIONAL INSTITUTE

February, 2015

Homi Bhabha National Institute

Recommendations of the Viva Voce Committee

As members of the Viva Voce Committee, we certify that we have read the dissertation prepared by Mrs. Rajshri Singh entitled " Role of macrophages in growth and progression of breast cancer" and recommend that it may be accepted as fulfilling the thesis requirement for the award of Degree of Doctor of Philosophy.

Chairman – Dr. S.V.Chiplunkar	Date: 29/5/15
Guide / Convener – Dr. Bhavani S. Shankar	Date: 29/5/15
Examiner – Dr. R.S.Jayshree	Date: 29/5/15
Member 1 – Dr. M.G.R.Rajan	Date: 29-5-15
Member 2- Dr. J.R.Bandekar	Date: 29-5-2015

Final approval and acceptance of this thesis is contingent upon the candidate's submission of the final copies of the thesis to HBNI.

I hereby certify that I have read this thesis prepared under my direction and recommend that it may be accepted as fulfilling the thesis requirement.

Date: 29/5/15

Place: MUMBAI

Guide

STATEMENT BY AUTHOR

This dissertation has been submitted in partial fulfillment of requirements for an advanced degree at Homi Bhabha National Institute (HBNI) and is deposited in the Library to be made available to borrowers under rules of the HBNI.

Brief quotations from this dissertation are allowable without special permission, provided that accurate acknowledgement of source is made. Requests for permission for extended quotation from or reproduction of this manuscript in whole or in part may be granted by the Competent Authority of HBNI when in his or her judgment the proposed use of the material is in the interests of scholarship. In all other instances, however, permission must be obtained from the author.

Rajshri Singh

DECLARATION

I, hereby declare that the investigation presented in the thesis has been carried out by me. The work is original and has not been submitted earlier as a whole or in part for a degree / diploma at this or any other Institution / University.

Rajshri Singh

List of Publications arising from the thesis

Journal

1. "TGF-β1-ROS-ATM-CREB signaling axis in macrophage mediated migration of human breast cancer MCF7 cells." Singh R, Shankar BS, Sainis KB, 2014, Jul; 26(7):1604-15. Cellular Signaling.

Conferences

1. Singh R., Shankar B., Cherian S., Kulkarni R.K., Sainis K.B. Expression of inducible nitric oxide synthase (iNOS) in human breast cancer and its relation to p53, γH2AX and Ki67. 37th Annual Conference of Indian Immunology Society, Jammu, Feb., 2011, p87. Book of Abstracts.
2. Singh R., Shankar B., Sainis K.B. Macrophages increase invasion of human breast cancer MCF7 cells through DNA damage mediated activation of CREB. 32nd Annual Convention of Indian Association for Cancer Research (IACR) & International Symposium on "Infection & Cancer", New Delhi, Feb., 2013, p114. Book of Abstracts.

Rajshri Singh

Dedicated to my parents

and family

ACKNOWLEDGEMENTS

The PhD program that I had been through was truly a once in a lifetime experience. I am using this opportunity to express my gratitude to everyone who supported me throughout this study.

Foremost, I would like to express my sincere gratitude to Dr. K.B. Sainis for his support for my Ph.D study and research, for his motivation, enthusiasm and immense knowledge. It has been a pleasure working under your mentorship and your simplicity and passion towards research has been an inspiration to me.

My deepest gratitude is to my guide, Dr. Bhavani Shankar. The constant moral support, constructive advice and criticism, untiring interest throughout the pursuit of the research were really helpful. Mam taught me how to question thoughts and express ideas. Her guidance helped me in all the time of research and writing of this thesis. I am deeply grateful to her for the patience and support she gave to overcome many crisis situations, academically and emotionally through the rough road to finish this thesis. Without her help and encouragement this dissertation would not have been written (or ever finished!).

I would like to express my sincere thanks to the members of the doctoral committee: Dr. Zingde, Dr. MGR Rajan, Dr. Chiplunlar, Dr. Sheshadri and Dr. Bandekar for critically analyzing my work and giving their constructive advices which lead to huge improvement in the work I produced.

I would like to thank Dr. Susan Cherian, always willing to help and giving her best suggestions. Many thanks to Sulbha mam, Kishore sir and Sanjhana mam for helping me to collect patient's samples. My research would not have been possible without their help.

Although there are no words to describe my heartfelt thanks to Dr. Nitin and Dr. Richa for their support in IHC work. I will always be indebted with gratitude for all your help and support.

I gratefully thank Dr. Bhakti Basu for the academic support and the facilities provided to carry out the 2D gel work.

I am very grateful to Dr. S.K.Apte and Dr. Hema Rajaram, Dean Life Sciences, HBNI. I do hereby acknowledge senior colleagues who have been very kind enough to extend their help for instruments and experiments, whenever I approached them- Dr. B.L. Das, Dr. Anu Ghosh, Dr. S. Santosh, Dr. B.N. Pandey, Dr. H.S. Mishra, Dr. Savitha Kulkarni and Dr. A.V.S.N. Rao.

I wish to acknowledge Dr. Sarin, Dr. Amin and Dr. Poonam from ACTREC for the help they provided in IHC sample acquisition.

My colleagues Prayag, Shyama, Vipul, Poonam and Kavitha have all extended their support in a very special way and I gained a lot from them. I find myself fortunate enough to express my sincere and profound sense of gratitude to all these lab members as I don't believe without their love and backing I would have wrote this acknowledgement. I loved your company in the lab. I thank Birliptha for helping me as a lab trainee. I really had a memorable time there and all the best for your future endeavors. I am also thankful to Narendra ji, Munankar ji and Punitha who maintained our lab so efficiently. Thanks all for providing great friendly atmosphere in our research lab.

I would like to cease this opportunity to thank all my friends in other labs for providing very friendly environment and constant help in my work- C Vijay, Chitra mam, Alka mam Mritunjaya, Saikat, Sejal, Vasumati, Shree, Sneh, Divya, Vinay Sir, Nishad, Ravi, Pampi Di,

Pramod, Sudhir, Sayali, Bakkiam, Raghavendra, Himanshu, Nilantana, Narsimbhan sir and Pratiksha mam. It is a pleasure to express my gratitude wholeheartedly to RB&HSD office staff.

Many friends have helped me stay sane through these difficult years. Their support and care helped me overcome setbacks and stay focused on my research work. I greatly value their friendship and I deeply appreciate their belief in me.

I appreciate the financial support from DAE that funded for the research.

Last but not the least, sincere thanks to all my family members for their support and encouragement throughout. Words cannot express how grateful I am to my parents for all of the sacrifices that they have made on my behalf. Your prayer for me was what sustained me this far. I also thank my brother Gajendra for his constant motivation and care. I am very much indebted to my in-laws who supported me in every possible way to see the completion of this work.

I must express my very profound gratitude to my husband, Sandeep for providing me with unfailing support and continuous encouragement throughout my years of study and through the process of researching and writing this thesis. This accomplishment would not have been possible without him. Your love, support and constant patience have taught me so much about sacrifice, discipline and compromise. Thank you. My heart goes out in gratitude to my newborn baby who without even knowing the purpose of all this struggle, endured with me, inspired me and became one of my biggest source of strength in thesis writing. A very special thanks to my newborn beloved daughter Prisha.

Finally, I would like to thank everybody who was important to the successful realization of thesis, as well as expressing my apology that I could not mention personally one by one.

Above all, I owe it all to Almighty God for granting me the wisdom, health and strength to undertake this research task and enabling me to its completion.

SYNOPSIS

Homi Bhabha National Institute

Ph. D. PROGRAMME

1. **Name of the Student: Rajshri Singh**

2. **Name of the Constituent Institution: BARC**

3. **Enrolment No. : LIFE 01200804013**

4. **Title of the Thesis: Role of macrophages in growth and progression of breast cancer.**

5. **Board of Studies: Life Sciences**

SYNOPSIS

Introduction

The tumor microenvironment is composed of malignant and immune cells, cytokines, chemokines and stromal components including extracellular matrix (ECM) and plays an important role in facilitating cancer progression and metastasis. Interactions between tumor and immune cells through the soluble factors they secrete influence the tumor cell survival and proliferation, integrity of the ECM, invasion, angiogenesis and metastasis [1]. The importance of macrophages, one of the prominent infiltrating immune cells, in growth and metastasis of breast

cancer is well documented. Macrophages participate in a number of pathophysiological settings, due to high plasticity of their functional responses. Macrophages populate the microenvironment of most if not all tumors. They secrete a variety of growth factors, cytokines, chemokines and enzymes that regulate tumor growth, angiogenesis, invasion and metastasis [2]. The tumor associated macrophages (TAM)-derived conditioned medium can induce angiogenesis in various *in vivo* model systems [3].

Focal macrophage infiltration is an important prognostic factor in breast invasive carcinoma and reduced survival is associated with high infiltration rates [4]. A large number of studies indicate that many of the inflammatory components present in the tumor microenvironment actively support cancer development and progression [1, 2, 5, 6]. But how the inflammation link operates in breast cancer is still an open question. Breast cancer is no longer seen as a single disease but rather a multifaceted disease comprised of distinct biological subtypes with diverse natural history, presenting a varied spectrum of clinical, pathologic and molecular features with different prognostic and therapeutic implications. Consensus regarding the definitive prognostic/predictive analysis is yet to be reached, but significant progress continues to be made in the ongoing search for a specific, rigorous and reproducible method of identifying successful treatment algorithms utilizing biological markers. The hypothesis of this study is that macrophages influence the growth and progression of breast cancer. To test this hypothesis the effect of monocyte and macrophage conditioned media was tested on growth and migration of breast cancer cells *in vitro*. The importance of some of the prominent proteins identified during this *in vitro* study was also evaluated in archived fibroadenoma and invasive ductal carcinoma (IDC) samples. The specific aims of the studies included in this thesis are:

1. To study the role of macrophages and inflammatory mediators in growth and migration of breast cancer cell lines *in vitro*.
2. To identify the soluble factors secreted by macrophages responsible for tumor growth promotion.
3. To understand the relationship between inflammatory response, DNA damage and survival factor signaling pathways in breast cancer by immunohistochemical labeling of representative markers: iNOS (inflammation), CD68 (macrophage), pCREB (pro-survival transcription factor), γ-H2AX (DNA damage) and p53 (tumor suppressor protein) in benign fibroadenomas as well malignant invasive ductal carcinoma.
4. To identify if any of these proteins could serve as a biomarker of malignancy or metastasis.

The work embodied in this thesis is divided into four chapters: Chapter 1: General introduction and review of literature. Chapter 2: Materials and Methods. Chapter 3: Results. Chapter 4: General Discussion and conclusion. The 'Results' chapter is further sub divided into three sections (3.1): Role of macrophages in non invasive and invasive breast cancer cell lines. (3.2): Characterization of monocyte and macrophage conditioned media. (3.3): Evaluation of the expression of biomarkers pCREB, iNOS, CD68, γH2AX and p53 proteins in fibroadenoma and invasive ductal carcinoma by immunohistochemistry.

Chapter 1. This chapter describes the general information on breast cancer and review of literature on role of macrophages in cancer progression. TAMs promote cancer metastasis through several mechanisms, including promotion of angiogenesis, induction of tumor growth, and enhancement of tumor cell migration and invasion. A variety of cytokines and growth

factors, such as tumor necrosis factor (TNF-α), transforming growth factor-β (TGF-β), hepatocyte growth factor (HGF), epidermal growth factor (EGF) etc., have been implicated in tumor-stroma cross-talk. The TGF-β-pathway is one of the major pathways altered in tumors, including breast cancer [7, 8].

Metastasis is a biological cascade of multiple steps: loss of cellular adhesion, increased motility and invasiveness, entry and survival in the circulation, exit into new tissue and eventual colonization at a distant site. Mechanisms that induce epithelial mesenchymal transition (EMT) involve multiple extracellular triggers and intracellular signaling pathways [9-11]. These include oncogenic signaling [12], Wnt3/β catenin signaling, increased reactive oxygen species (ROS) [11] as well as DNA damage [10]. This chapter describes the various signaling and survival pathways involved in macrophage mediated cancer progression. In response to DNA damage or extracellular signals, expression of several transcription factors like Cyclic AMP (cAMP) response element binding protein (CREB), nuclear factor kappa-light-chain-enhancer of activated B cells (NF-κB), c-fos and c-jun allows the cells to overcome stressful or deleterious environment. Previous studies have reported the tumor promoting function of CREB in breast cancer, melanoma, and hepatocellular carcinoma [13-15]. CREB also acts as a proto-oncogene to regulate hematopoiesis and to contribute to the leukemia phenotype [16, 17]. In melanoma, CREB activation regulates the expression of many genes important for invasion, inflammation, and survival including MCAM/MUC18, MMP2, IL-8, and BCL2 [18-20].

Macrophages are a key component of a chronic inflammatory response and constitute part of the heterogeneous population of cells in tumors. Macrophages and nitric oxide (NO) have been implicated in the activation of p53 [21] in inflammatory bowel disease (IBD) and the activation of the Akt pathway in breast cancer [22]. The literature related to different clinical

markers used for breast cancer and their regulatory effect on various cellular processes would be described in this chapter.

Chapter 2. This chapter describes the details of materials used along with their sources and common experimental methods used in this study. Detailed protocols of different techniques and approaches used in this study will be described under three different categories: (i) cell culture techniques including maintenance of cell lines, preparation of conditioned medium, colony forming assay, cell cycle analysis, estimation of ROS and RNS, flow cytometric analysis, immunofluorescence, wound healing, migration assay, si-RNA mediated transfection, and western blots, (ii) techniques used for characterization of CM like ELISA, 1D and 2D gel electrophoresis, MALDI analysis and preparation of exosomes and (iii) clinical techniques including archived breast cancer biopsy sample collection, tissue microarray (TMA) preparation, IHC labeling, scoring and statistical analysis.

Chapter 3. The results obtained from this study have been presented in three sections.

3.1. Role of macrophages in non invasive and invasive breast cancer cell lines.

In this study, the macrophage – tumor interaction was studied by employing monocyte conditioned medium (MCM) and macrophage conditioned medium (MϕCM) treatment to epithelial breast cancer cell line, MCF7 and invasive breast cancer cell line, MDA-MB-231. Differential effects of MϕCM were observed in these two cell lines differing in their invasive nature. MϕCM treatment resulted in increased merging of colonies accompanied by EMT responses in MCF7 cells and larger sized, multinucleated cells resembling senescence type phenotype in MDA-MB-231 cells. The macrophage conditioned media contained various pro-inflammatory cytokines like TNF-α, IL-1β and IL-6. These cytokines in turn induced secretion of

TGF-β1 in MCF7 cells. As a multifunctional factor, TGF-β1 is involved in the regulation of many biological processes and induced concomitant apoptosis and EMT responses in hepatocytes [23, 24]. It has been referred to as a "double edged sword" because of its dual function as tumor suppressor and tumor promoter (reviewed in [25]). TGF-β1 caused apoptosis in some of the cells and significant increase in reactive oxygen species (ROS) and reactive nitrogen species (RNS) generation in the surviving cells. This oxidative and nitrosative stress resulted in DNA damage response signaling as observed by expression of phosphorylated ATM and H2AX proteins. In contrast, there was no increase in apoptosis, ROS, RNS or DNA damage in MDA-MB-231 cells. CREB, a 43 kDa-basic/leucine zipper (bZip) transcription factor plays important roles in cell differentiation [26], survival [27, 28], proliferation [17], development [29], cell cycle progression [30] and glucose metabolism [31]. A significant increase in pCREB and total CREB was observed in MϕCM treated MCF7 cells in contrast to MDA-MB-231 cells where basal level expression of CREB was higher and was unaffected by the treatments. There was a marked increase in vimentin expression (a EMT marker) as well as increase in migration of MCF7 cells treated with MϕCM. MϕCM induced expression of pCREB and invasion in MCF7 cells was significantly decreased following neutralization of pro-inflammatory cytokines (TNF-α, IL-1β and IL-6 in the conditioned media) or treatment with N-acetyl cysteine (NAC) or inhibitors of iNOS and ATM/ATR. Decreased phosphorylation of pCREB as well as decreased migration was observed in MCF7 cells with siRNA mediated downregulation of ATM.

3.2. Characterization of monocyte and macrophage conditioned media.

The tumor promoting activities of TAM are the result of the ability to express numerous mediators, such as growth factors, angiogenic molecules, ECM degrading enzymes, inflammatory cytokines and chemokines. In order to identify the constituents of the conditioned

media, two approaches were followed. The proteins were precipitated using ammonium sulfate or concentrated through centricon filtration with a 10 kDa cutoff. The conditioned media concentrated using centricon filters could not be absorbed onto isoelectric focusing (IEF) strips or move in the electric field indicating the presence of lipid components. Exosomes are small membrane vesicles that can be secreted *in vitro* by most cell types and the general idea is that they could play roles as "intercellular messengers", transferring various kinds of informations or signals between cells. To determine if exosomes secreted by macrophages were involved in the induction of EMT signals in breast cancer cells, they were purified and the supernatant obtained following ultra centrifugation was collected and termed as exosomes free conditioned medium (EFCM). The protein profile of exosomes secreted by monocytes and macrophages were similar and the exosomes from both cell types was taken up by MCF7 cells indicating that it did not play a major role in the growth promoting effects exerted by MϕCM. On the other hand the effect of EFCM and EFMϕCM on the growth of MCF7 cells was identical to MCM and MϕCM. The EFMϕCM treatment resulted in decrease in the colony forming ability in MCF7 and MDA-MB-231 cells along with an increase in merging of colonies in MCF7 cells. These results thus confirmed that the soluble mediators present in the CM and not exosomes were responsible for the observed changes.

Presence of some of the cytokines was detected using ELISA. The cytokines IFN-γ and TGF-β1 were absent in MCM and MϕCM whereas the pro inflammatory cytokines like TNF-α, IL-1β and IL-6 were present only in MϕCM. In order to further characterize the proteins present in MϕCM, the conditioned media were subjected to 2D electrophoresis. The proteins were precipitated with ammonium sulfate for this purpose. Though the number of proteins observed in MϕCM was higher in 1D, this difference was not seen in 2D gel electrophoresis. This could

happen due to proteins with lower or higher pI or multicomplex proteins. Hence the proteins were separated in 1D gel electrophoresis followed by MALDI analysis of the differentially expressed proteins The protein samples were subjected to peptide mass fingerprint (PMF) analysis by MALDI-TOF and protein IDs were generated. The proteins upregulated in MϕCM were found to be isoforms of matrix metalloproteinase 1 (MMP1) pre proprotein variant, MMP 9 pre proprotein variant, chitinase-2, plasminogen activator inhibitor-2, myoferlin, L-plastin, dual specificity protein kinase CLK3, etc. These proteins are known to have their role in breast cancer growth and progression. TNF-α is an important mediator during the inflammatory phase of wound healing and TNFα stimulates secretion of active MMP-2. Confirmation of the identity of MMPs was also carried out by gelatin zymography.

3.3. Expression of pCREB, iNOS, CD68, γ-H2AX and p53 protein in fibroadenomas and invasive ductal carcinoma samples by IHC.

The relationship between inflammatory mediators, DNA damage, survival signaling and migration was studied in breast cancer cells *in vitro*. To confirm if these biomarkers have a practical relevance and can be used to predict malignancy or metastasis, CD68, a macrophage marker, iNOS, a marker for inflammation, pCREB, a pro-survival transcription factor, γ-H2AX, effector of the DNA damage response pathway and p53 as a representative tumor suppressor protein were assessed in fibroadenoma and invasive ductal carcinoma samples by IHC labeling. Three cores (2 mm each) from each of these donor samples representing different areas of tumor were placed on a recipient paraffin block in the form of tissue microarray (TMA). Tissue sections (5-7 μm thick) were cut from the TMA paraffin embedded blocks on a microtome and mounted on the slides. After appropriate deparaffinzation, rehydration and unmasking of the antigens, they were labeled with various antibodies. The images of stained

tissues were taken with Metasystems Imager. Z2 Zeiss microscope enabled with Metaviewer V2 software. The scoring for protein expression for each sample was given as the product of intensity of labeling and percentage positive cells. The labeling of 91 IDC samples and 23 fibroadenoma samples was carried out. There was a statistically significant increase in iNOS and CD68 expression ($p<0.01$) in IDC as compared to fibroadenoma. No such difference was observed with respect to pCREB as a marker.

Chapter 4. This chapter covers the general discussion and conclusions on the results obtained in the study. Macrophages play an ambiguous role in cancers. Macrophages and tumor cells mutually influence each other's behaviour in majority of cancers, with the tumor cell attracting macrophages and sustaining their survival and they, in turn, producing a myriad of factors to promote or regulate tumor growth and angiogenesis. The main finding of this study is that the pro-inflammatory cytokines secreted by macrophages induce secretion of TGF-β1 in MCF7 cells. This results in apoptosis in a fraction of cells. In the remaining cells, there is increase in oxidative stress and DNA damage which trigger CREB mediated survival signaling inducing EMT responses. The data presented herein not only provide evidence that macrophage mediated release of soluble factors result in EMT responses in tumor cells but also point out that a differential effect on tumors depending on their invasive nature. There was a statistically significant increase in expression of markers CD68 and iNOS in IDC as compared to the fibroadenoma samples. The expression and correlation of iNOS, CD68, pCREB, γ-H2AX and p53 in breast cancer samples will be discussed in this chapter in light of their value as prognostic or predictive factors and in turn their potential for integration into clinical practice.

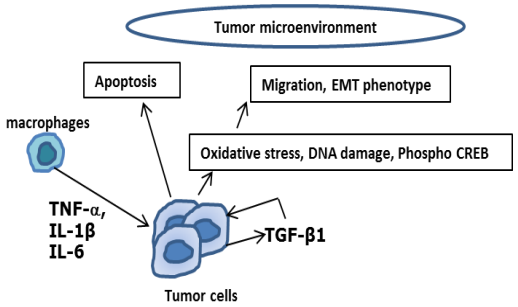

Figure1: The schematic representation of the effect of MϕCM on MCF7 cells

References:

1. Lin WW, Karin M: **A cytokine-mediated link between innate immunity, inflammation, and cancer**. *J Clin Invest* 2007, **117**(5):1175-1183.
2. Lewis CE, Pollard JW: **Distinct role of macrophages in different tumor microenvironments**. *Cancer Res* 2006, **66**(2):605-612.
3. Polverini PJ, Leibovich SJ: **Induction of neovascularization in vivo and endothelial proliferation in vitro by tumor-associated macrophages**. *Lab Invest* 1984, **51**(6):635-642.
4. Leek RD, Lewis CE, Whitehouse R, Greenall M, Clarke J, Harris AL: **Association of macrophage infiltration with angiogenesis and prognosis in invasive breast carcinoma**. *Cancer Res* 1996, **56**(20):4625-4629.
5. Soria G, Ben-Baruch A: **The inflammatory chemokines CCL2 and CCL5 in breast cancer**. *Cancer Lett* 2008, **267**(2):271-285.
6. Goldberg JE, Schwertfeger KL: **Proinflammatory cytokines in breast cancer: mechanisms of action and potential targets for therapeutics**. *Curr Drug Targets* 2010, **11**(9):1133-1146.
7. Wakefield LM, Roberts AB: **TGF-beta signaling: positive and negative effects on tumorigenesis**. *Curr Opin Genet Dev* 2002, **12**(1):22-29.
8. Roberts AB, Wakefield LM: **The two faces of transforming growth factor beta in carcinogenesis**. *Proc Natl Acad Sci U S A* 2003, **100**(15):8621-8623.
9. Polyak K, Weinberg RA: **Transitions between epithelial and mesenchymal states: acquisition of malignant and stem cell traits**. *Nat Rev Cancer* 2009, **9**(4):265-273.
10. Chiba N, Comaills V, Shiotani B, Takahashi F, Shimada T, Tajima K, Winokur D, Hayashida T, Willers H, Brachtel E *et al*: **Homeobox B9 induces epithelial-to-mesenchymal transition-associated radioresistance by accelerating DNA damage responses**. *Proc Natl Acad Sci U S A* 2012, **109**(8):2760-2765.
11. Rhyu DY, Yang Y, Ha H, Lee GT, Song JS, Uh ST, Lee HB: **Role of reactive oxygen species in TGF-beta1-induced mitogen-activated protein kinase activation and epithelial-mesenchymal transition in renal tubular epithelial cells**. *J Am Soc Nephrol* 2005, **16**(3):667-675.
12. Vuoriluoto K, Haugen H, Kiviluoto S, Mpindi JP, Nevo J, Gjerdrum C, Tiron C, Lorens JB, Ivaska J: **Vimentin regulates EMT induction by Slug and oncogenic H-Ras and migration by governing Axl expression in breast cancer**. *Oncogene* 2011, **30**(12):1436-1448.
13. Kim SW, Hong JS, Ryu SH, Chung WC, Yoon JH, Koo JS: **Regulation of mucin gene expression by CREB via a nonclassical retinoic acid signaling pathway**. *Mol Cell Biol* 2007, **27**(19):6933-6947.

14. Jean D, Harbison M, McConkey DJ, Ronai Z, Bar-Eli M: **CREB and its associated proteins act as survival factors for human melanoma cells**. *J Biol Chem* 1998, **273**(38):24884-24890.
15. Sofi M, Young MJ, Papamakarios T, Simpson ER, Clyne CD: **Role of CRE-binding protein (CREB) in aromatase expression in breast adipose**. *Breast Cancer Res Treat* 2003, **79**(3):399-407.
16. Crans-Vargas HN, Landaw EM, Bhatia S, Sandusky G, Moore TB, Sakamoto KM: **Expression of cyclic adenosine monophosphate response-element binding protein in acute leukemia**. *Blood* 2002, **99**(7):2617-2619.
17. Shankar DB, Sakamoto KM: **The role of cyclic-AMP binding protein (CREB) in leukemia cell proliferation and acute leukemias**. *Leuk Lymphoma* 2004, **45**(2):265-270.
18. Melnikova VO, Dobroff AS, Zigler M, Villares GJ, Braeuer RR, Wang H, Huang L, Bar-Eli M: **CREB inhibits AP-2alpha expression to regulate the malignant phenotype of melanoma**. *PLoS One* 2010, **5**(8):e12452.
19. White PC, Shore AM, Clement M, McLaren J, Soeiro I, Lam EW, Brennan P: **Regulation of cyclin D2 and the cyclin D2 promoter by protein kinase A and CREB in lymphocytes**. *Oncogene* 2006, **25**(15):2170-2180.
20. Zhang X, Odom DT, Koo SH, Conkright MD, Canettieri G, Best J, Chen H, Jenner R, Herbolsheimer E, Jacobsen E *et al*: **Genome-wide analysis of cAMP-response element binding protein occupancy, phosphorylation, and target gene activation in human tissues**. *Proc Natl Acad Sci U S A* 2005, **102**(12):4459-4464.
21. Ying L, Hofseth LJ: **An emerging role for endothelial nitric oxide synthase in chronic inflammation and cancer**. *Cancer Res* 2007, **67**(4):1407-1410.
22. Prueitt RL, Boersma BJ, Howe TM, Goodman JE, Thomas DD, Ying L, Pfiester CM, Yfantis HG, Cottrell JR, Lee DH *et al*: **Inflammation and IGF-I activate the Akt pathway in breast cancer**. *Int J Cancer* 2007, **120**(4):796-805.
23. Yang Y, Pan X, Lei W, Wang J, Shi J, Li F, Song J: **Regulation of transforming growth factor-beta 1-induced apoptosis and epithelial-to-mesenchymal transition by protein kinase A and signal transducers and activators of transcription 3**. *Cancer Res* 2006, **66**(17):8617-8624.
24. Yang Y, Pan X, Lei W, Wang J, Song J: **Transforming growth factor-beta1 induces epithelial-to-mesenchymal transition and apoptosis via a cell cycle-dependent mechanism**. *Oncogene* 2006, **25**(55):7235-7244.
25. Derynck R, Akhurst RJ, Balmain A: **TGF-beta signaling in tumor suppression and cancer progression**. *Nat Genet* 2001, **29**(2):117-129.
26. Ionescu AM, Schwarz EM, Vinson C, Puzas JE, Rosier R, Reynolds PR, O'Keefe RJ: **PTHrP modulates chondrocyte differentiation through AP-1 and CREB signaling**. *J Biol Chem* 2001, **276**(15):11639-11647.
27. Riccio A, Ahn S, Davenport CM, Blendy JA, Ginty DD: **Mediation by a CREB family transcription factor of NGF-dependent survival of sympathetic neurons**. *Science* 1999, **286**(5448):2358-2361.
28. Conkright MD, Montminy M: **CREB: the unindicted cancer co-conspirator**. *Trends Cell Biol* 2005, **15**(9):457-459.
29. Rudolph D, Tafuri A, Gass P, Hämmerling GJ, Arnold B, Schütz G: **Impaired fetal T cell development and perinatal lethality in mice lacking the cAMP response element binding protein**. *Proc Natl Acad Sci U S A* 1998, **95**(8):4481-4486.
30. Shankar DB, Cheng JC, Kinjo K, Federman N, Moore TB, Gill A, Rao NP, Landaw EM, Sakamoto KM: **The role of CREB as a proto-oncogene in hematopoiesis and in acute myeloid leukemia**. *Cancer Cell* 2005, **7**(4):351-362.
31. Mayr BM, Canettieri G, Montminy MR: **Distinct effects of cAMP and mitogenic signals on CREB-binding protein recruitment impart specificity to target gene activation via CREB**. *Proc Natl Acad Sci U S A* 2001, **98**(19):10936-10941.

Publications in Refereed Journal

1. "TGF-β1-ROS-ATM-CREB signaling axis in macrophage mediated migration of human breast cancer MCF7 cells." Singh R, Shankar BS, Sainis KB, 2014, Jul; 26 (7):1604-15. Cellular Signaling.

Other Publications: Symposium presentations:

1. Singh R., Shankar B., Cherian S., Kulkarni R.K., Sainis K.B. Expression of inducible nitric oxide synthase (iNOS) in human breast cancer and its relation to p53, γH2AX and Ki67. 37th Annual Conference of Indian Immunology Society, Jammu, Feb., 2011, p87. Book of Abstracts.

2. Singh R., Shankar B., Sainis K.B. Macrophages increase invasion of human breast cancer MCF7 cells through DNA damage mediated activation of CREB. 32nd Annual Convention of Indian Association for Cancer Research (IACR) & International Symposium on "Infection & Cancer", New Delhi, Feb., 2013, p114. Book of Abstracts.

INDEX

Index

LIST OF FIGURES

LIST OF TABLES

ABBREVIATIONS

1D PAGE	One Dimensional Polyacrylamide Gel Electrophoresis
2D PAGE	Two Dimensional Polyacrylamide Gel Electrophoresis
9-1-1	Complex Rad9–Hus1–Rad1 Complex
ACN	Acetonitrile
ANOVA	Analysis Of Variance
AP-1	Activating Protein-1
ATF	Activating Transcription Factor
ATM	Ataxia-Telangiectasia Mutated
ATR	Ataxia Telangiectasia and Rad3 related
ATRIP	ATR Interacting Protein
αSMA	α-Smooth Muscle Actin
BAFF	B-Cell Activating Factor
bFGF	Basic Fibroblast Growth Factor
BRCA1	Breast Cancer Susceptibility Gene 1
bZip	Basic Leucine Zipper 1
CAFs	Cancer Associated Fibroblasts

CBP	Cyclic AMP Response Element-Binding Protein
CCL	Chronic Lymphocytic Leukemia
Cdks	Cyclin-Dependent Kinase
CHAPS	3-[(3-Cholamidopropyl) Dimethyl ammonio] -1- Propane sulfonate
CHCA	A-Cyano-4-Hydroxycinnamic Acid
Chk1	Checkpoint Kinase 1
cIAP1	Cellular Inhibitor Of Apoptosis Protein-1
CIN	Cervical Intraepithelial Neoplasia
CKI	Cyclin-Dependent Kinase Inhibitor
CLK3	CDC-Like Kinase 3
CM	Conditioned Medium
COX-2	Cyclooxygenase-2
CREB	cAMP Response Element-Binding Protein
CSF-1	Colony Stimulating Factor 1
CXCL12	(C-X-C Motif) Ligand 12
DAF-FMDA	Diaminofluorescein-Diacetate
DAPI	4', 6-Diamidino-2-Phenylindole Dazolylcarbocyanine Iodide

DC	Dendritic Cells
DCFDA	Dichlorofluorescein diacetate
DCIS	Ductal Carcinoma *In Situ*
DDR	DNA Damage Response
Df	Degree Of Freedom
DMEM	Dulbecco's Modified Eagle's Medium
DMSO	Dimethyl Sulfoxide
DNA	Deoxyribonucleic Acid
DNA-PK	DNA-Dependent Protein Kinase
DSBs	Double Strand Breaks
DTT	Dithiothreitol
ECM	Extracellular Matrix
EDTA	Ethylene Diamine Tetraacetic Acid
EFCM	Exosome Free Conditioned Medium
EGF	Epidermal Growth Factor
EGFR	Epidermal Growth Factor Receptor
Egr-1	Early Growth Response-1

ELISA	Enzyme-Linked Immunosorbent Assay
EMT	Epithelial-Mesenchymal Transition
ER	Estrogen-Receptor
ERK	Extracellular Signal-Regulated Kinase
EVs	Extracellular Vesicles
FADD	Fas-Associated Protein with Death Domain
FAP	Familial Adenomatous Polyposis
FBS	Fetal Bovine Serum
GAPDH	Glyceraldehyde 3-Phosphate Dehydrogenase
Gp130	Glycoprotein 130
H & E	Hematoxylin And Eosin
HER2	Human Epidermal Growth Factor Receptor 2
HGF	Hepatocyte Growth Factor
HIF	Hypoxia-Inducible Factor 1
HRP	Horseradish Peroxidase
IAA	Iodoacetamide
IACR	International Association Of Cancer Registries

IBD	Inflammatory Bowel Disease
ICAM-1	Intercellular Adhesion Molecule-1
IDC	Invasive Ductal Carcinoma
IEF	Isoelectric Focusing
IFN-γ	Interferon Gamma
IHC	Immunohistochemistry
IL-10	Interleukin-10
IL-17A	Interleukin -17A
IL-1β	Interleukin-1β
IL-4	Interleukin-4
IL-6	Interleukin-6
iNOS	Inducible Nitric Oxide Synthase
IPG	Immobilized Ph Gradient
IR	Ionizing Radiation
IRAK-M	Interleukin-1 (IL-1) Receptor-Associated Kinase
IRS	Immunoreactive Score
JAK/STAT	Janus Kinase/Signal Transducers And Activators Of Transcription

JC-1	5,5′,6,6′-tetrachloro-1,1′,3,3′-tetraethylbenzimidazolylcarbocyanine iodide
JNK	C-Jun N-Terminal Kinases
KID	Kinase-Inducible Domain
L NMMA	L-NG-Monomethylarginine, Acetate
LIF	Leukemia Inhibitory Factor
LINE-1	Long Interspersed Nucleotide Element-1
LN Mets	Lymph Node Metastasis
L-NNA	Nitro-L-Arginine
MALDI-TOF	Matrix Assisted Laser Desorption/Ionization-Time Of Flight
MAPK	Mitogen-Activated Protein Kinases
MCM	Monocyte Conditioned Medium
MCP-1	Monocyte-Chemoattractant Protein
M-CSF	Macrophage Colony-Stimulating Factor 1
MECs	Myoepithelial Cells
MFI	Mean Fluorescence Intensity
MHC	Major Histocompatibility Complex
MIN	Multiple Intestinal Neoplasia

MMP	Matrix Metalloproteinases
MMTV	Mouse Mammary Tumor Virus
MRN	MRE11/RAD50/NBN
MSK-1	Mitogen- And Stress-Activated Kinase 1
Mϕ	Macrophage
MϕCM	Macrophage Conditioned Medium
NAC	N-Acetyl-Cysteine
NCBI	National Center For Biotechnology Information
NF-κB	Nuclear Factor Kappa-Light-Chain-Enhancer Of Activated B Cells
NGF	Nerve Growth Factor
NHEJ	Non-Homologous End Joining
NK Cells	Natural Killer Cells
NKG2D	Natural Killer Group 2, Member D
NO	Nitric Oxide
NOX	NADPH Oxidase
NPI	Nottingham Prognostic Index
NST	Non Specific Type

PARP	Poly (ADP-Ribose) Polymerase
PBS	Phosphate Buffered Saline
PCR	Polymerase Chain Reaction
PD-L1	Programmed Death-Ligand 1
PGE2	Prostaglandin E2
PI3K	Phosphatidylinositol 3-Kinase
PKC	Protein Kinase C
PMA	Phorbol 12-Myristate 13-Acetate
PMF	Peptide Mass Fingerprinting
PMN	Polymorphonuclear Neutrophils
PR	Progesterone Receptor
PVDF	Polyvinylidene Difluoride
RIP	Receptor Interacting Protein
RISC	RNA-Induced Silencing Complex
RNS	Reactive Nitrogen Species
ROS	Reactive Oxygen Species
RPA	Replication Protein-A

RPMI 1640	Roswell Park Memorial Institute (RPMI) 1640
SBR	Scarff-Bloom-Richardson
SDF	Stroma-Derived Factor
SDS	Sodium Dodecyl Sulfate
siRNA	Small Interfering RNA
TAM	Tumor Associated Macrophage
TFA	Trifluoroacetic Acid
TGFβR2	Transforming Growth Factor Beta Receptor 2
TGF-β	Transforming Growth Factor Beta
TILs	Tumor-Infiltrating Lymphocytes
TIMP	Tissue Inhibitor of Matrix Metalloproteinases
Tipα	TNF-α -Inducing Protein
TMA	Tissue Microarray
TME	Tumor Microenvironment
TNFR1	TNF Receptor 1
TNF-α	Tumor Necrosis Factor Alpha
TNM	Tumor, Node, Metastasis

TORC	Transducer of Regulated CREB Activity
TPA	12-O-Tetradecanoylphorbol 13-Acetate
TRAF2	TNF Receptor-Associated Factor 2
Tregs	T-Regulatory Cells
ULBP1-5	UL16-Binding Proteins 1–5
VEGF	Vascular Endothelial Growth Factor
VSI	Vessel Space Invasion

CHAPTER 1

INTRODUCTION

1.1 Incidence of breast cancer

Breast cancer is the most common cancer in women worldwide. In 2012, 1.7 million women were diagnosed with breast cancer and 6.3 million five year breast cancer survivors. Since the 2008 estimates, breast cancer incidence has increased by more than 20%, while mortality has increased by 14%. Breast cancer is also the most common cause of cancer death among women (5, 22,000 deaths in 2012) and the most frequently diagnosed cancer among women in 140 of 184 countries worldwide [1]. It now represents one in four of all cancers in women (Figure 1).

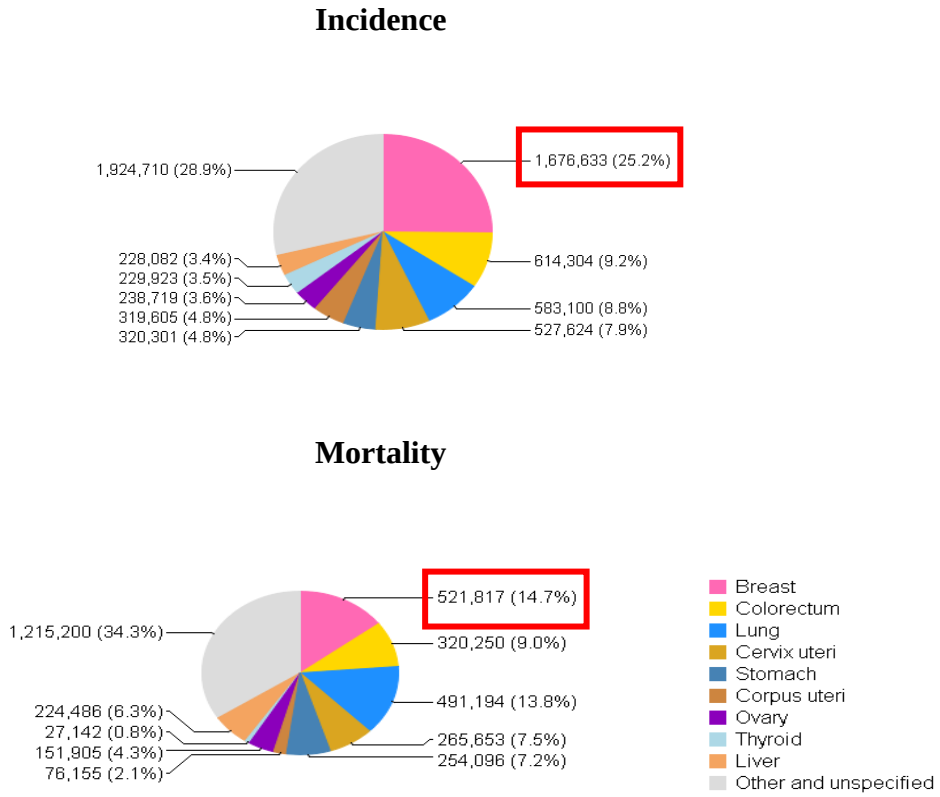

Figure 1: Distribution of cancers in the world. The pie charts depict estimated incidence of all the women's cancers in the year 2012 and the corresponding cancer related deaths worldwide [1].

In India, breast cancer is the most common cancer (followed by cervical cancer) with an estimated 144,937 new diagnoses. It is the most common cause of cancer-related deaths with 70,218 breast cancer deaths in 2012 [1] (Figure 2). The age-standardized incidence rate for breast cancer in India is 22.9 per 100,000, one-third that of Western countries although mortality rates are disproportionately higher [2, 3]. Breast cancer accounts for 27% of all new cancer diagnoses and 21.5% of all cancer deaths among women in India. Breast cancer in urban areas of India is three times higher than in rural parts of the country [1].

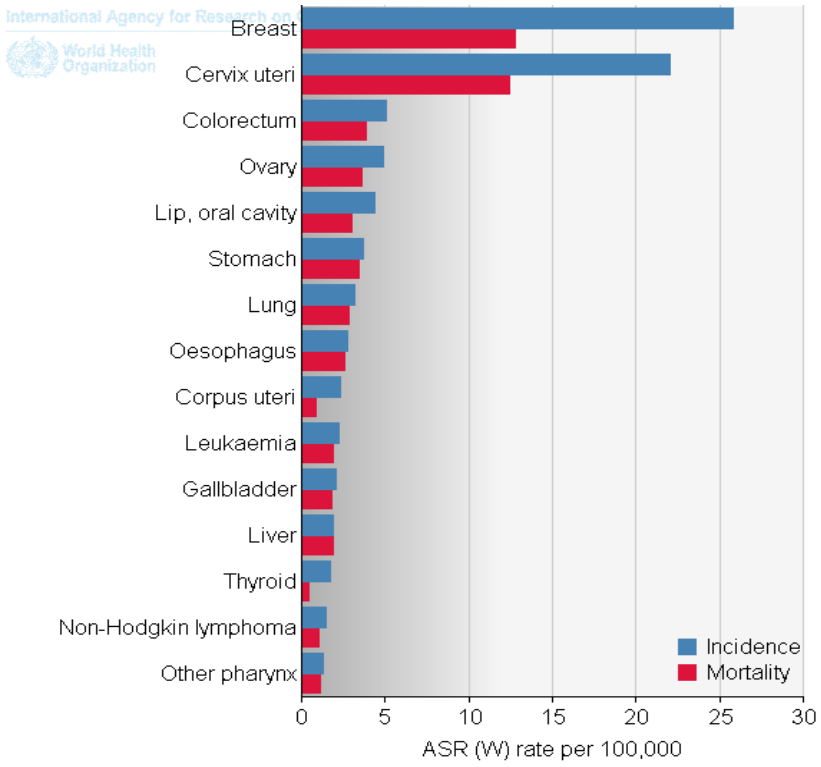

Figure 2: Distribution of cancers in India. Age-standardised incidence and mortality rates of most common cancers in India [1].

1.1.1 Epidemiology of breast cancer in India

In India, the disease peaks at a younger age (e.g. 40-50 years) as suggested by age incidence rates, as compared to Western countries [4] and as a result, the majority of new diagnoses occur in pre-menopausal women. Studies have shown a rising trend with steadily increasing rates since the mid-1980's [5] [6, 7] with the largest increase observed in Mumbai. According to National Cancer Registry Programme projections, the number of breast cancer deaths in India will climb to 106,124 in 2015 and to 123,634 in 2020 (Programme NCR, 2009). The majority of new cases are advanced stage and locally advanced at the time of diagnosis [8]. The increasing burden of disease may be associated with lifestyle factors such as later age at marriage, first child birth, reduced breastfeeding and westernization of diet and sedentary physical activity patterns [9] [10]. Breast cancer rates tend to be higher in women with higher education and in specific communities that have adopted a more westernized lifestyle, such as the Christians and the Parsis, and are lowest in the Muslim communities [11]. Differences in the prevalence of transforming growth factor beta signaling pathway associated gene polymorphisms (TGF-β1 & TGF-βR1) have also been linked to the lower rates observed in certain sub-populations such as those from western India compared to the Parsis [12].

1.2 Breast cancer and its microenvironment

The normal structure of the breast consists of lobes which arise from multiple lobules and connect to a common terminal interlobular duct. These ducts then continue to their outlet at the nipple. Histologically, a single layer of luminal epithelial cells line the lobules and ducts which is surrounded by transversely oriented myoepithelial cells. The surrounding tissue or stroma is

separated from these structures with a basement membrane. The breach of the basement membrane distinguishes invasive carcinoma from carcinoma *in situ*. The surrounding stroma comprises of extra cellular matrix (ECM) and discrete cells (e.g., fibroblasts, immune cells and adipocytes) and organized structures (e.g., blood vessels), each of which contribute to the overall configuration of the local microenvironment [13].

The components of the microenvironment like macrophages, myoepithelial and endothelial cells and several ECM molecules play critical roles in mammary duct morphogenesis [14]. Studies on epithelial-mesenchymal interactions in tissue differentiation have demonstrated that the terminal differentiation of both embryonic and adult epithelia is strongly influenced by embryonic mesenchyme [15]. In cell culture also, the influence of ECM was observed where normal mammary epithelial cells formed acini in laminin-rich three-dimensional matrix and became responsive to lactogenic hormones and capable of milk proteins production [16].

The tumor microenvironment is progressively accepted as a major regulator of carcinogenesis [17]. Dvorak's famous assessment 'tumors are wounds that do not heal', is being revisited now at the molecular level with the understanding of the role of tumor micro environment in cancer progression [18].

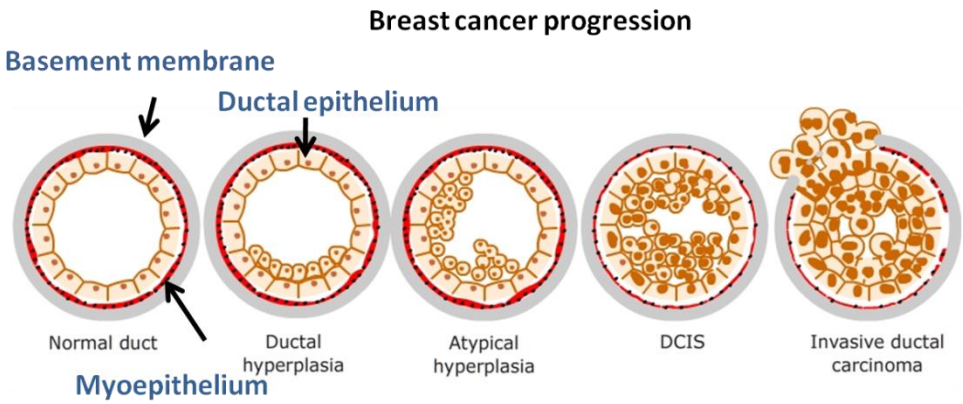

Figure 3: Model of breast cancer progression. Ductal carcinoma *in situ* (DCIS) is an intraductal neoplastic proliferation of epithelial cells that is separated from the breast stroma by an intact layer of basement membrane and myoepithelial cells. Invasive ductal carcinoma is defined by breakdown of the basement membrane, loss of myoepithelial cells, and invasion of the tumor cells into the surrounding stroma and the vasculature [19].

Breast tumors evolve through defined stages via sequential progression, starting with epithelial hyperproliferation to *in situ*, and later invasive ductal carcinoma, and finally progressing to metastatic disease [20]. Clinical and experimental studies suggest that invasive ductal carcinoma (IDC) arise from ductal carcinoma *in situ* (DCIS) (Figure 3) [19, 21]. In DCIS lesions, the proliferating neoplastic cells are confined to the duct (Figure 3). The loss of myoepithelial cell layer and basement membrane is seen in the transition of breast cancer from *in situ* to invasive ductal carcinoma which is a critical, but poorly understood step (Figure 3). The metastatic disease result from the subsequent spread of tumor cells to distant sites and the components of the tumor microenvironment has been implicated in each of these steps of cancer progression [22].

1.3 Clinical classification of breast cancer

1.3.1 Histological basis of breast cancer.

Carcinoma of the breast is considered as a heterogeneous group of diseases. The World Health Organization has established the formal histological typing for classification of breast cancer (1982) based upon the histological properties of the cancer and is not an indication of the origin of the tumor within the breast. The invasive carcinomas, majorly originate from the terminal duct lobules irrespective of its histological type [23]. It is divided into non invasive or *in situ* carcinomas and invasive breast cancer. *In situ* lesions are defined as the abnormal proliferation of cells that is not invading into the surrounding basement membrane, whereas invasive lesions are those in which the cells transgress this membrane.

The prevalence of the different histological types of breast cancer is well documented. The most common type of invasive breast cancer is of ductal carcinoma of no special type (NST) followed by lobular carcinoma and the rarer special types of breast cancer (Table 1).

Table 1: WHO classification of Breast carcinoma*

	Tumor type	% of presenting lesions
1.	***In situ* carcinoma**	10 %
	In situ ductal carcinoma	
	In situ lobular carcinoma	
	In situ carcinoma with microinvasion	
2.	**Infiltrating carcinoma**	
	Infiltrating ductal carcinoma	65 %
	Infiltrating lobular carcinoma	10 %

3.	**Carcinoma with particular clinical manifestations**	
	Pagets disease of the nipple	1 % - 4 %
	Inflammatory carcinoma	1 % - 5 %
4.	**Others**	3 % - 10 %
	Medullary carcinoma	
	Mucoid / colloid carcinoma	
	Tubular carcinoma	
	Adenoid cystic carcinoma	

* [24]

Ductal carcinoma of no special type (NST) is diagnosed in the lesions which does not exhibit any histological features. Macroscopically it is seen as a grey or white surface with a gritty texture on sectioning. The lesion itself may be spiculated or stellate in nature, infiltrating the surrounding tissue though some lesion may be more circumscribed. Histologically, the cells can be seen as glandular structures, sheets, cords or trabeculae associated with or without necrotic areas. The tumor cells themselves can exhibit a range of cytological features in the nucleus, cytoplasm and differences in mitotic rate.

1.3.2 Tumor grading

Grading system classifies the heterogeneous group of tumors. The grading of a cancer is a microscopic account of how similar the tumor is to normal breast tissue. The most commonly recommended and used histological grading system is the Elston and Ellis modification of the Bloom and Richardson system [25]. This grading system scores a tumor on three components; tubule formation, nuclear pleomorphism and mitotic rate. These three components are designated a score (1-3) and the total score determines the overall histological grade. The scoring is determined as shown in table 2.

Table 2: Modified Bloom and Richardson Grading System of breast cancer*

S.No.	Characteristics	Scores
1.	**Tubule Formation**	
	(% of tumor exhibiting gland formation)	
	>75% of tumor	1
	10- 75% of tumor	2
	<10% of tumor	3
2.	**Pleomorphism**	
	(Variation in size and shape of nuclei)	
	Mild	1
	Moderate	2
	Marked	3
3.	**Mitotic activity**	
	<6 mitosis/ 10hpf#	1
	7- 15 mitosis/ 10hpf	2
	>15 mitosis/ 10hpf	3
Total Score is derived from adding scores for the 3 parameters which varies from 3- 9.		
	Grade 1 (well differentiated)	3-5
	Grade 2 (moderately differentiated)	6-7
	Grade 3 (poorly differentiated)	8-9

*[25] # high power field

1.3.3 Staging of breast cancer

Staging of all types of cancers refers to the grouping of the patients according to their disease burden. This grouping of patients guides in the treatment of their disease and also allows the prediction of clinical outcomes as well as comparison of patients for the purpose of research. The staging of breast cancer is based on the TNM (tumor, nodes and metastases) system. Once the TNM status has been assessed, the patients are placed in a particular stage group. The TNM staging is based on both clinical (examination and imaging) and pathological findings.

Table 3: Tumor size groups for breast cancer*

Tumor staging groups	Subset	Description
T1		Tumor 2cm or less.
	T1is	*In situ* disease only.
	T1mic	Microinvasion< 0.1cm
	T1a	Tumor >0.1cm <0.5cm
	T1b	Tumor >0.5cm <1cm
	T1c	Tumor >1cm <2cm
T2		Tumor >2cm <5cm
T3		Tumor >5cm
T4		Tumor with extension.
	T4a	Chest wall extension not including pectoralis.
	T4b	Oedema or ulceration of the skin.
	T4c	Both T4a and T4b
	T4	Inflammatory carcinoma.

*[26]

The lymph node stage is determined clinically with examination and imaging but most commonly assessed after surgical excision of a sample during the surgery on the breast cancer. Table 4 shows the major pathological lymph node (N) groups and its sub groups.

Distant metastasis (M) is clinically apparent either on physical examination at the point of diagnosis or on staging imaging such as CT scans of the chest and abdomen or isotope bone scans. Routine staging imaging tends to be restricted to patients who are lymph node positive or are going on to chemotherapy. There are only 3 major M groups; MX- metastasis not assessed, M0- no distant metastasis and M1- distant metastasis present.

The TNM groups are then combined to place the patient into one of the overall staging groups. These stages of disease range from Stage 0 to Stage 4 (Table 5).

Table 4: Lymph node staging groups for breast cancer*

Node Staging group	Subset	Description
pNX		Regional nodes not available for assessment
pN0		No regional lymph node metastasis.
pN1		Metastasis in 1-3 axillary nodes or internal mammary nodes (not clinically apparent).
	pN1mi	Micro metastasis >0.2mm <2mm.
	pN1a	Metastasis in 1-3 axillary nodes.
	pN1b	Metastasis in internal mammary nodes.
	pN1c	pN1a and pN1b
pN2		Metastasis in 4-9 axillary nodes or clinically apparent internal mammary nodes.
	pN2a	Metastasis in 4-9 axillary nodes (at least 1 deposit >2.0mm.
	pN2b	Clinically apparent internal mammary metastasis in

	absence of axillary.
pN3	10 or more involved axillary nodes or internal mammary nodes; or 1 or more lateral supraclavicular nodes.

***[26]**

Table 5: Staging groups for breast cancer*

Stage Group	Tumor	Nodes	Metastasis
Stage 0	Tis	N0	M0
Stage I	T1	N0	M0
Stage II A	T0	N1	M0
	T1	N1	M0
	T2	N0	M0
Stage II B	T2	N1	M0
	T3	N0	M0
Stage III A	T0	N2	M0
	T1	N2	M0
	T2	N2	M0
	T3	N1	M0
	T3	N2	M0
Stage III B	T4	N0	M0
	T4	N1	M0
	T4	N2	M0
Stage III C	Any T group	N3	M0
Stage IV	Any T group	Any N group	M1

*[26]

1.3.4 Nottingham Prognostic Index (NPI)

Breast cancer is similar to all types of cancer, in respect of an unpredictable condition and in uncertainity of the outcome of treatment. The important prognostic factors are lymph node involvement, tumor size and tumor grade. The Nottingham prognostic index (NPI) [27] is a predictive index of the clinical outcome of breast cancer which has been devised combining the following factors: tumor size, node involvement and modified Scarff Bloom Richardson (SBR) grading system. The NPI can be calculated as:

NPI = 0.2 x tumor size (cm) + lymph node stage + histological tumor grade

The lymph node stage is 1 (if there are no nodes affected), 2 (if up to 3 nodes are affected) or 3 (if more than 3 nodes are affected). Similarly the tumor grade is scored as 1 (for grade I), 2 (for a grade II) or 3 (for a grade III).

Applying the formula results in scores which fall into three bands:

- a score of less than 3.4 - suggests a good outcome with a 15 year survival in 80% cases.
- a score of between 3.4 to 5.4 - suggests an intermediate level with a 15 year survival in 42% cases.
- a score of more than 5.4 - suggests a poor outcome with a 15 year survival in 13% cases.

Beside this, there are other important independent prognostic variables like lympho vascular invasion and estrogen and progesterone receptor status which are useful in determining the clinical outcome of the breast cancer. The presence or absence of lympho vascular invasion is considered to be useful in predicting local recurrences.

1.3.5 Hormone receptor status

1.3.5.a Estrogen and progesterone receptors status: Presence of hormone receptors is a powerful predictive factor for the likelihood of benefit from adjuvant hormonal therapy including aromatase inhibitors (e.g., anastrozole, letrozole) and tamoxifen, an oral selective estrogen receptor modulator [28, 29]. As a prognostic factor, ER and/or PR positivity is associated with reduced mortality compared to women with ER and/or PR negative disease [30]. Studies support better survival rates in carcinomas with >1% ER positive cells as compared to carcinomas that are completely devoid of ER [31].

1.3.5.b HER2/neu: Approximately 10% to 34% of invasive breast cancers overexpress the HER2 receptor. As a prognostic factor, overexpression is associated with increased tumor aggressiveness, rate of recurrence and mortality in node-positive patients, while a more variable influence in node-negative patients [32]. It is a strong prognostic factor for relapse and poor overall survival, particularly in node-positive patients [33]. In all cases of invasive breast carcinoma, amplification and/or overexpression of the Her2/neu gene is routinely evaluated using immunohistochemistry and/or fluorescence *in-situ* hybridization (FISH). As a predictive factor, Her2/neu status strongly predicts response to treatment with the anti-Her2 monoclonal antibody trastuzumab, and is predictive of resistance to alkylator-based chemotherapy, need for higher dose chemotherapy as well as benefit from adjuvant anthracyclines and tamoxifen resistance [32, 34].

1.3.6 Proliferation rate: Proliferation can be measured by mitotic count which are included as part of the grading system. Ki-67, a proliferation marker has repeatedly been confirmed as an independent predictive and prognostic factor in early breast cancer [35]. Breast

cancer with high Ki-67 expression responds better to chemotherapy [36, 37], but is associated with poor prognosis.

1.3.7Aneuploidy: Carcinomas with an abnormal DNA content (aneuploidy) have a slightly worse prognosis as compared to carcinomas with DNA content similar to normal cells.

1.4 Influence of microenvironment on tumor progression.

1.4.1. Myoepithelial cells

The loss of myoepithelial cell layer and basement membrane is a key characteristic of progression (Figure 1). The inhibition of tumor growth by normal myoepithelial cells is demonstrated in xenograft studies. The spontaneous progression of DCIS-like lesions to IDC was efficiently suppressed in MCFDCIS mice xenograft model (resembles human basal-like DCIS) with the co-injection of normal myoepithelial cells whereas it was augmented with fibroblasts [38]. The gene expression profiling of myoepithelial cells and immunohistochemical analysis of luminal epithelial and myoepithelial cells from MCFDCIS xenografts and human breast tissues identified the specific expression of transforming growth factor β1 (TGF-β1) and hedgehog pathways. The enhanced invasion was associated with the downregulation of TGFBR2, SMAD4, or GLI1 in MCFDCIS cells resulting in decreased myoepithelial cells [38]. The precise mechanism by which loss of the myoepithelial cell layer occurs in tumors is still unanswered. One assumption is that the signals transduced by tumor epithelial and stromal cells interfere with differentiation of myoepithelial cells from their progenitors.

1.4.2. Cancer-associated fibroblasts

The extracellular environment is maintained by the normal fibroblasts through the production and remodeling of the ECM. Carcinoma-associated fibroblasts (CAFs) are heterogeneous group of cells, with a subset identified as myofibroblasts expressing alpha smooth muscle actin (αSMA), fibroblast activation protein (FAP), desmin, S100A4 protein, and Thy-1 [39]. CAFs participate in tumor growth progression and increase tumor angiogenesis via CXCR4 signaling by the secretion of stromal derived factor (SDF)-1/CXCL12 which act in a paracrine fashion [40]. Co-culture of normal mammary fibroblasts with breast cancer cells 'stimulate' the fibroblasts to secrete HGF and thereby increase tumor promotion [41] as well as invasion via the paracrine activation of c-Met [42].

Multiple hypotheses have been proposed for the origin of CAFs. One of them is that the persistent aberrant signaling from tumor epithelial cells modifies the phenotype of native interstitial fibroblasts to CAF. Alternatively, they can be differentiated from bone marrow-derived mesenchymal stem cells which are recruited to the tumor site via endocrine stimulation by tumor-derived factors [43]. However, a recent study demonstrated that MDA-MB-231 xenografts 'instigate' the growth and metastasis of weakly tumorigenic cell lines via the activation and recruitment of bone marrow-derived hematopoietic cells [44].

1.4.3. Matrix remodeling components

Matrix metalloproteineases (MMPs) are a large family of endopeptidases, which are synthesized primarily by fibroblasts and contribute to tissue remodeling and wound healing. MMPs can activate chemokines, cytokines, adhesion molecules, growth factors (such as the release of insulin-like growth factor from ECM by MMP-3 and -7), or promote angiogenesis (for

example, activation of angiogenic factors by MMP-1, -2, -9, and -14) besides degrading ECM components thereby contributing to tumor progression [45].

The abnormal collagen cross-linking in breast tumors results in stiffening of ECM and contributes to progression as the forces generated by this stiffening lead to enhanced expression of integrin and growth factors. The collagen cross-linking is promoted by lysyl oxidase, an amine oxidase commonly expressed in breast tumors and its inhibition in the MMTV-Neu model (in which the expression of the oncogene neu is driven by the Mouse Mammary Tumor Virus promoter) of breast cancer, decreases the tumor burden [45]. In addition, elevated expression of lysyl oxidase-like 2 is associated with worse prognosis in early stage estrogen receptor (ER)-negative breast cancers [46].

1.4.4. Leukocytes

The innate immune system consist of different cell subsets which includes natural killer (NK) cells, dendritic cells (DC), neutrophils, and macrophages (Mϕ).The link between inflammation and cancer with the role of infiltrating leukocytes in tumor development are widely accepted. The mechanisms mediating immune and tumor cell cross-talk are poorly understood. The immune cells are one of the most vibrant cell populations in the breast tumor microenvironment, and are involved in healing wounds and remodeling of breast tissue in pregnancy and involution [47]. Increased infiltration of leukocytes is observed in DCIS with focal myoepithelial cell layer disruptions [48], suggesting their role in invasive progression.

The inhibition of tumor formation and organ metastasis in NOD/SCID mice (which lacks T and B cells as compared to NOD/SCID/γ^{null} (NSG) mice (which lacks T, B, and NK cells) suggest that NK cells are responsible for inhibiting the formation of progressively growing rapid

large tumors of breast cancer cells in SCID mice [49]. In breast cancer, although association between NK-cell infiltration and clinical outcome in patients is not certain, the expression of NK-cell ligands do play a crucial role in tumor immunoediting and concomitant immune escape [50]. The clinical prognostic value analysis of activating NK-cell receptor NKG2D ligands MIC-A/B and ULBP1-5 in early stage breast cancer has revealed that expression of MIC-A/B and ULBP-2 results in a favorable outcome concerning relapse-free survival [51].

Dendritic cells are key regulators of B and T lymphocyte function because of their superior ability to capture, process and present tumor-associated antigens [52]. The DC maturation process determines the presentation of processed tumor antigens and the subsequent activation of $CD4^+$ and $CD8^+$ T cells [53]. Tumor microenvironment induced DC to differentiate into regulatory DCs with a $CD11c^{low}$ $CD11b^{high}$ Ia^{low} phenotype and elevated expression of IL-10, nitric oxide, VEGF, and arginase I which inhibit T-cell proliferation both *in vitro* and *in vivo*. Several studies have shown that tumor-associated DCs can induce regulatory T lymphocytes (Tregs) ($CD4^+CD25^+FOXP3^+$) expansion and become not only incapable of inducing specific immune responses but also immunosuppressive [54, 55]. Furthermore, breast cancer cells have been reported to promote the differentiation of DCs into a phenotype that expresses IL-10 and transforming growth factor (TGF-β), which, in turn, induce the expansion of Treg [56].

Tregs and cytokines have also been implicated in the immune cell infiltration of tumors. Invasive breast cancer associated with an unfavorable prognosis has been reported to exhibit elevated levels of intratumoral Tregs, with ER/PR negativity and Her2 overexpression [57]. Furthermore, enrichment of Tregs in invasive ductal carcinoma of the breast correlates with upregulation of interleukin (IL)-17A expression and increased invasive ability [58].

Recent data have revealed the importance of tumor-infiltrating lymphocytes (TILs) in regulating the clinical progression of various epithelial cancers [59]. The prognostic power of intratumoral $CD8^+$ T cells immune-scoring determined by IHC in colorectal cancers has been shown to be superior to standard tumor staging (AJCC/UICC-TNM classification) methods [60]). A higher frequency of $CD8^+$ lymphocytes in stroma surrounding the tumor augment an active cell-mediated anti-tumor immune response against breast tumors and was associated with better patient survival [61]. The gene expression profiling of breast cancer-associated stroma that was enriched for cytotoxic $CD8^+$ T cell genes and natural killer cell activity has also revealed a gene signature predictive of good prognosis (>98% 5-year survival) [62].

Several studies have shown that tumor-associated macrophages (TAMs) facilitate angiogenesis, ECM degradation, and tumor invasion through activation of epidermal growth factor receptor signaling, secretion of proteases and paracrine signaling between tumor cells [63, 64]. Loss of macrophages in colony stimulating factor (CSF)-1 deficient mice model (Csf1op/op) had no effect on tumor initiation but dramatically reduced malignant progression [65]. Similar responses were seen in xenografts derived from human MCF-7 cells in immuno deficient mice when treated with either mouse CSF-1 antisense oligonucleotide or small interfering RNAs. These treatments suppressed mammary tumor growth by decreasing macrophage infiltration, production of MMPs, vascular endothelial growth factor (VEGF)-A and endothelial cell proliferation [66]. Besides macrophages, other immune cells have also been implicated in breast cancer development.

While intratumoral B cells and $CD8^+$ T-cell infiltrates are generally associated with better prognosis, $CD4^+$ T cells, particularly T-regulatory cells and tumor-associated macrophages (TAMs) have been associated with worse outcomes. Studies have shown reduced overall

survival with high levels of macrophages and $CD4^+$ T cells, while high levels of $CD8^+$ T cells combined with low levels of macrophages and $CD4^+$ T cells correlated with increased overall survival [64] .

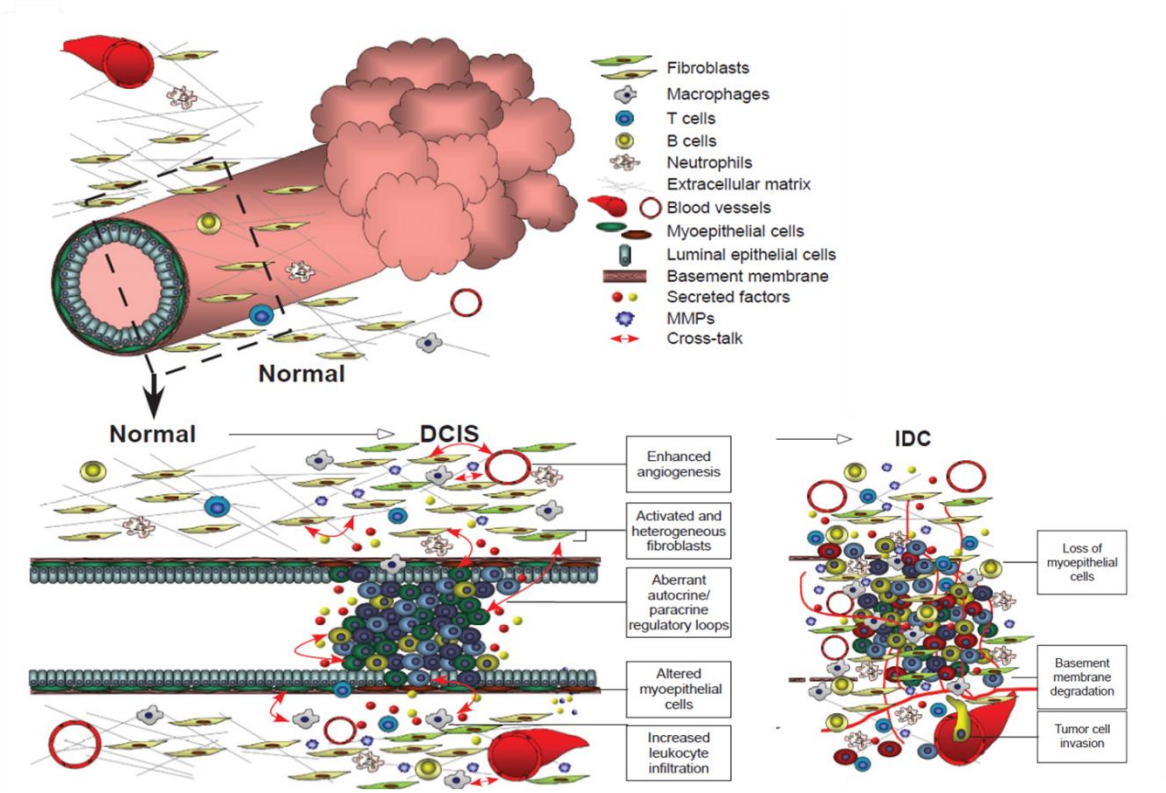

Figure 4: Progression of normal breast tissue to invasive breast cancer. Alterations of the microenvironment from normal duct to DCIS to IDC. In phenotypically normal tissue, epithelial structures consist of central luminal epithelial cells enclosed by a continuous basement membrane, while the primarily collagenous stroma contains fibroblasts, immune cells and vasculature. The progression to DCIS is characterized by proliferative epithelial cells enclosed in a still-continuous basement membrane, increased numbers of fibroblasts and immune cell infiltrate and enhanced angiogenesis. IDC is defined by breakdown of the basement membrane, loss of myoepithelial cells and invasion of the tumor cells into the surrounding stroma and the vasculature (Adapted from [22]).

1.5 Macrophages and its role in cancer

A considerable component of the leukocytic infiltrate in human cancer is tumor-associated macrophages (TAMs). The clinical outcome of the tumor has been associated with the amount of tumor infiltrating macrophages [67, 68]. Macrophage infiltration is correlated with poor prognosis in breast cancer [62, 69], Hodgkin's lymphoma [70], T-cell lymphoma [71], cervical cancer [72, 73] and uveal melanoma [74]. It is linked with a favorable prognosis in colorectal and gastric cancer [75-77]. Several studies have demonstrated that the prognostic role of TAMs in the tumor microenvironment is influenced by their location with respect to tumor cells [78].

The six classical hallmarks of cancer include abnormal cell growth, avoidance of growth-inhibition, resistance to cell death, replication without limitation, maintained angiogenesis and invasion into circulation through breaching of basement membranes [79]. The growing knowledge on the biology of cancer has elucidated the role of immune system, specifically macrophages, on several aspects of tumor biology. Recent studies have accentuated that the cells of the tumor microenvironment can be assigned as novel hallmarks of cancer, beside the classical six hallmarks. TAMs as part of the tumor microenvironment have been included as novel hallmarks of cancer such as tumor-promoting inflammation and avoidance of immune destruction (reviewed in [80]). Moreover, they are actively involved in all classical six hallmarks by exerting tumor-sustaining properties [17, 79].

1.5.1 Origin and activation status of macrophages

In general, macrophages are believed to arise from circulating monocytes that emigrate from blood vessels and differentiate into macrophages in the peripheral tissue. A variety of tissue

associated macrophages play an important role in tissue homeostasis. The tissue macrophages generally are considered to exhibit an intrinsic anti-inflammatory phenotype under homeostatic environment [81]. The tissue macrophages are comprised of langerhans cells in the epidermis, metallophilic macrophages in the spleen, osteoclast's in the bone, alveolar macrophages in the lung, kupffer cells in the liver and microglial cells in the central nervous system [82].

Macrophages are subjected to a variety of concurrent stimuli *in vivo* whereas, single agent stimulation can polarize the macrophages into pro- or anti-inflammatory macrophages *in vitro*. Macrophages are classified into a simplified M1-like and M2-like phenotype according to the *in vitro* stimulus cognate to the Th1-Th2 dichotomy in T cell biology [83]. The inflammatory signals such as interferon, LPS and other bacterial stimuli polarize the macrophages to pro-inflammatory "classically activated" M1-like phenotype which mediates defense against bacteria, protozoa and viruses [81]. The "alternatively activated" M2-like phenotype is associated with wound healing and tissue repair which is induced by IL-4 or IL-13 ("M2a"), LPS or immune complexes ("M2b"), IL-10 ("M2c") [84, 85].

1.5.2 Tumor Associated Macrophages (TAMs)

Macrophages display an extreme functional plasticity which enables them to integrate and respond to different stimuli [86]. Distinct macrophage subsets have been described in cancer as they play a prominent role in tumor malignancy [68, 88, 87]. In human cancer, the residing macrophages are termed as tumor-associated macrophages (TAMs) as they can neither be classified into classical activated M1-like or alternatively activated M2-like macrophages.

1.5.2.a Mechanisms of macrophage recruitment and macrophage polarization

In preinvasive tumorous lesions, macrophages are among the first immune cells to infiltrate and exert their role during the progression into invasive cancer. The inflammation associated with cancer aids in recruitment of bone marrow derived cells [17, 89]. The chemotaxis of monocytes into the tumor environment is shown to be induced by growth factors like CSF-1 (colony stimulating factor 1), vascular endothelial growth factor (VEGF), monocyte chemotactic protein-1 (MCP-1) as well as several CCL chemokines and other molecules [90]. An inflammatory $Ly6C^{hi}$ monocyte subset has been shown as the major monocyte subset to localize into the tumor site giving rise to TAM subsets [91].

Macrophage colony-stimulating factor (M-CSF) differentiates monocytes into macrophages at the tumor site. The tumor cell-derived factors evoke the polarization of macrophages into one of the TAM subpopulations. The tumor cell derived mediators which drive the induction of a TAM related phenotype are M-CSF [92], IL-4, IL-10, IL-6 [92], transforming growth factor β1 (TGF-β1), prostaglandin E2 (PGE_2) [90, 93], hyaluron fragments [94] and leukemia inhibitory factor (LIF) [92]. In cervical cancer, monocytes are skewed towards a macrophage phenotype by the production of PGE_2 and IL-6 from tumor cells [93, 95].

Though the conditions in the tumor microenvironment are different from infection, researchers classify TAMs using M1-like/M2-like terminology based on the similarities in surface marker profiles. Despite the illustration by vast majority of reports that TAM phenotypes share properties with M2 macrophages, TAM with expression of both M2-like and M1-like markers have been described [96]. These TAMs show enhanced expression of genes encoding immunosuppressive cytokines (IL-10, TGF-β1), phagocytosis-related receptors/molecules (Msr2,

C1q) and inflammatory chemokines (CCL2, CCL5) as well as IFN-inducible chemokines (Cxcl9, Cxcl10, Cxcl16) [96]. The mixed M1-like ($CD14^+HLA\text{-}DR^+$) and M2-like ($CD14^+CD163^+$) TAM infiltration [97] have also been studied. These TAMs are associated with sarcomas as well as carcinoma [91]. In cutaneous squamous cell carcinoma, a mixed population of TAM is present with some TAMs expressing M2-like markers CD209 and CCL18 and others expressing M1-like markers STAT1, IL-23, IL-12 and CD127 and few expressing markers of both M1-like and M2-like macrophages. IL-1, IL-6 and tumor necrosis factor α (TNF-α) are the typical genes expressed by TAMs [90]. The underlining intracellular pathways activated in TAMs are still unclear. Several pathways such as Ets-driven transcriptional program as well as a Wnt-signaling pathway have been shown to be important for specific functions of TAMs and have been associated with invasion and metastasis in murine breast cancer [98, 99].

1.5.2.b Pro-inflammatory and growth promoting properties of TAMs

Tumor-promoting inflammation and avoidance of immune destruction represent novel additions to hallmarks of cancer [17]. The activation of different pathways in macrophages which support tumor cell growth has been studied. Various soluble growth factors, eg. IL-1, IL-6, TNF-α, TGF-β1, epidermal growth factor (EGF), platelet-derived growth factor (PDGF) produced by macrophages participate in tumor cell growth [90]. In chronic inflammation, tumor cells and inflammatory cells produce TNF-α which promotes cell survival by induction of anti-apoptotic molecules via TNFR1 and TNFR2 [100]. EGF plays an important role in murine breast cancer [101]. TAMs are major producers of EGF and there is interplay between EGF producing TAMs and EGFR expressing tumor cells, which reciprocally produce M-CSF to support macrophage survival. IL-6 expression by TAMs is induced by signal transducer and activator of transcription 3 (STAT3) pathways. This pro-inflammatory cytokine is known to induce

proliferation of malignant cells [100, 102, 103]. IL-6 has a pivotal role in Kaposi sarcoma, multiple myeloma, Hodgkin lymphoma, breast cancer, ovarian cancer and others [104-108]. TGF-β has been attributed with opposing roles. TGF-β signaling inhibited tumor growth by decreasing IL-6 signaling during the late stages of colitis-associated colon cancer [100, 109] whereas enhanced TGF-β1 secretion is associated with epithelial-mesenchymal transition (EMT) in carcinoma. Increased levels of adhesion molecules and MMPs during EMT result in higher invasiveness of epithelial tumor cells resulting in metastasis [109]. TGF-β production by tumor cells also induces IRAK-1 (Interleukin-1 receptor-associated kinase) a negative regulator of Toll-like receptor signaling, which is part of the immunosuppressive phenotype of TAM [110].

1.5.2.c Immunosuppressive properties of TAMs

In contradiction to the strong inflammatory properties of macrophages, TAMs also exert immunosuppressive functions. TAMs produce several chemokines which exhibit a growth promoting influence on tumor cells in cancer rather than provide immunity against pathogens. TGF-β1, IL-10 and PGE_2 derived from the tumor cells downregulate the expression of MHC class II molecules on TAMs [90]. The direct inhibition of immune responses by TAMs has also been described [111]. In the tumor microenvironment, IL-10 and TNF-α induce expression of PD-L1 on the membrane of TAMs which inhibits activated effector T cells through the PD-1 receptor [112].

Another indirect mechanism responsible for creating an anti-inflammatory tumor milieu is through the recruitment of other non-inflammatory immune cells into the tumor microenvironment. TAMs produce CCL17 and CCL22 which predominantly attract the Th2 and

Treg cells [78]. F4/80^{+} TAMs secrete large amounts of CCL20 which attracts CCR6^{+}Treg cells to the tumor site in a murine model of colorectal cancer [113].

1.5.2.d Invasion and metastasis promoting properties of TAMs

The invasion and metastasis of tumor cells is supported by various macrophage-associated mechanisms in the tumor microenvironment. TAMs allow tumor cells to invade and spread locally with the production of MMPs, cathepsins and other proteolytic enzymes which degrade the extracellular matrix [114, 115]. Invasion, the major hallmark of malignancy is an essential requirement for metastasis. The PyMT mouse tumor model (in which the expression of the oncogene is driven by the Mouse Mammary Tumor Virus promoter) study shows that the tissue invasion capacity of tumor cells is dependent on macrophages. Tumor cells produce CSF-1 and TNF-α which aid in recruitment of MMP- 2, -3, -7 and -9 producing cells. The coordinated migration of macrophages is prominently accompanied by invasion of tumor cells [116, 117]. Intravital imaging has shown that perivascular macrophages are involved in the extravasation of mammary tumors [118]. Reduction in the number of tumor cells entering the blood stream can occur due to inhibition of EGF signaling or destruction of macrophages [90]. Molecular investigations have revealed that increased Wnt signaling is exhibited in invasive TAMs, a unique subpopulation of TAMs promoting carcinoma cell motility [99].

EMT plays an important role in invasiveness apart from CSF-1/EGF signaling axis [119]. In a F9-teratocarcinoma model (model for analysis of the molecular mechanisms of differentiation), the expression of mesenchymal markers was correlated with TAM infiltration and depletion of macrophages resulted in a decrease of mesenchyme associated genes [120]. Growth of tumor cells in macrophage-conditioned media resulted in EMT and enhanced

invasiveness. Alternatively, EMT could be induced in cancer cells *in vitro* by treatment with TGF-β. Experimental data also suggest that TGF-β1 is the driving force of macrophage-induced EMT *in* vivo [109, 120].

1.5.2. e Lymphangiogenesis promoting properties of TAMs

Tumors show either a lymphatic (transport of tumor cells to lymph nodes and ultimately, to other parts of the body) or a haematogenic (cancer cells detach from the primary site, invade the vasculature by degradation of the surrounding tissue, migrate to the secondary organ) metastasis pattern depending on the tumor characteristics. A poor clinical prognosis in most malignant disease is predicted by the level of lymphangiogenesis. Tumor cells and macrophages produce excess of lymphangiopoietic vascular endothelial growth factors (VEGF)-C and –D. Macrophage infiltration is associated with peritumoral lymphangiogenesis in lung adenocarcinoma and cervical cancer [121, 122].

1.5.2.f Angiogenesis promoting properties of TAMs

Several pathways have been described for cancer angiogenesis. Cancer requires angiogenesis beyond a tumor size of a few millimeters. Angiogenesis is positively correlated with macrophage infiltration in various studies [123]. Macrophages are adapted to hypoxic conditions under the control of the transcription factor, hypoxia-inducible factor (HIF) [124]. The neoangiogenesis in cancer development is known as "angiogenic switch" induced by angiogenic factors, like VEGF. In macrophages, HIF-1 induced under hypoxic conditions produces pro-angiogenic molecules in the tumor microenvironment. Several macrophage derived molecules that are directly angiogenic (VEGF, TNF-α, IL-8, CXCL8 and bFGF) and others that modulate angiogenesis (e.g. MMP2, MMP-7, MMP-9, MMP-12, COX-2) have been

characterized [90]. VEGF is produced by a specialized subset of TAMs in hypoxic areas of breast cancer [90].

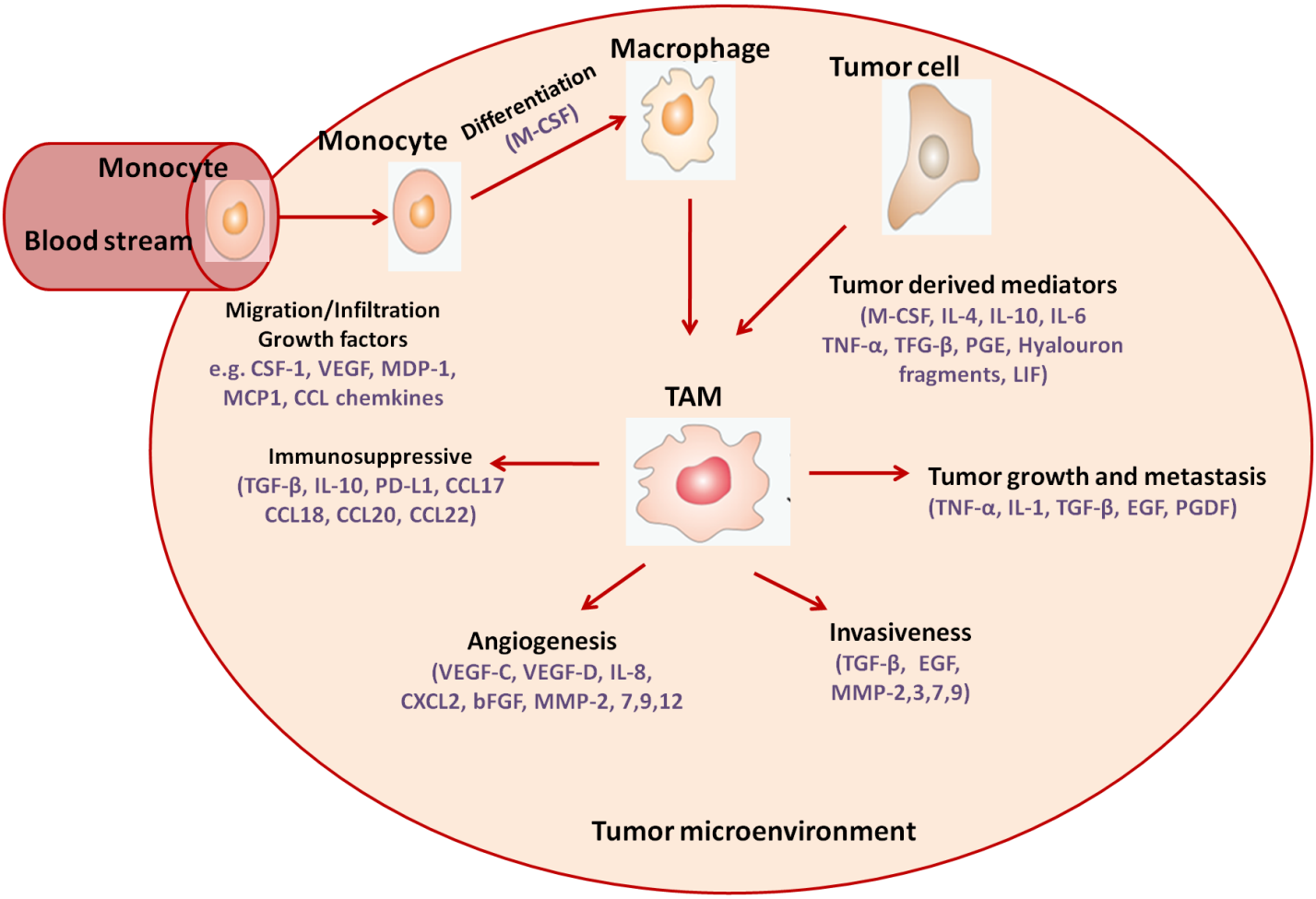

Figure 5: TAMs in the tumor microenvironment. Growth factors and chemokines attract the circulating monocytes into the tumor. Monocytes are differentiated to macrophages with the local presence of M-CSF. Soluble tumor derived factors initiate the polarization of macrophages into TAMs leading to the expression of molecules that support angiogenesis, tumor growth and metastasis. Conversely TAMs secrete factors that induce local immune suppression by recruitment of Treg cells or suppress T cell responses directly (Adapted from [80]).

1.6 Cytokines involved in cancer development

Cytokines are low-molecular-weight proteins that mediate cell-to-cell communication. They are synthesized by immune and stromal cells, such as fibroblasts and endothelial cells. Cytokines regulate proliferation, cell survival, differentiation, immune cell activation, cell migration and death. Depending on the tumor microenvironment and the balance of pro- and anti-inflammatory cytokines, can either modulate an anti tumoral response, or can induce cell transformation and malignancy during chronic inflammation, depending on their relative concentrations, cytokine receptor expression and the activation state of surrounding cells (reviewed by [125]).

1.6.1 Tumor Necrosis Factor (TNF-α)

Chronic inflammation can promote malignancy. Tumor necrosis factor (TNF-α) participates in chronic diseases as an inflammatory mediator and has been implicated in carcinogenesis [126]. Studies have shown that TNF-α-deficient mice are resistant to tetradecanoylphorbol-13-acetate- (TPA-) induced skin carcinogenesis. The effect of TNF-α seems to be more significant in the early stages of carcinogenesis including angiogenesis and invasion as compared to progression of carcinogenesis [127, 128]. This cytokine is recognized by two receptors: TNF-α receptor-1 (TNF-αR-1) which is ubiquitously expressed and TNF-αR-2, expressed mainly in immune cells [129]. Trimerization occurs upon TNF-α binding to TNF-α-Rs, leading to activation of at least four signaling pathways:

- a pro apoptotic pathway induced by caspase-8 interaction with Fas-associated death domain (FADD);

- an anti apoptotic platform activated by cellular inhibitor of apoptosis protein-1 (cIAP-1) and interacting with TNF-αR associated factor 2 (TRAF2);
- a TRAF2- and JNK-mediated AP-1 signaling pathway; and
- a receptor interacting protein (RIP) induced NF-κB [129].

However, there is controversy regarding the role of TNF-α in cancer. Evidences suggest a double-edged role of this prototypical proinflammatory cytokine in carcinogenesis. An anti-tumoral response in a murine model of sarcoma was elicited by high concentrations of TNF-α [130] and in contrast, low but sustained TNF-α production levels can induce a tumor phenotype [131].

A pro-tumor mechanism of TNF-α is based on the generation of reactive oxygen species (ROS) and reactive nitrogen species (RNS), which can induce DNA damage, thereby facilitating tumorigenesis [132, 133]. TNF-α-mediated inflammation has been linked to cancer in *H. pylori*-positive gastric lesions. *H.pylori*-secreted TNF-α -inducing protein (Tipα) increases TNF-α level in preneoplastic lesions [134]. The exposure of a prolonged TNF-α dose to the organoid model of normal human ovarian epithelial cells generated a precancerous phenotype. Role of TNF-α in tumorigenesis in ovarian epithelial cells has been suggested due to the observed structural and functional changes, like loss of epithelial polarity, cell invasion and overexpression of cancer markers [135].

The pro- or anti-tumoral TNF-α response within the tumor microenvironment also depends on its expression site in the tumor. Elevated levels of TNF-α in tumor islets resulted in high survival rates while increased stromal TNF-α content led to lower survival rates [136]. Studies in oral squamous cell carcinoma suggest that prolonged TNF-α exposure can enhance the

proportion of cancer stem cell phenotypes, increasing their tumor sphere forming ability, stem cell-transcription factor expression and tumorigenicity [137].

1.6.2 Interleukin 6 (IL-6)

IL-6 is another proinflammatory cytokine with a typical pro-tumorigenic effect. Elevated serum IL-6 levels have been detected in patients with systemic cancers as compared to healthy controls or patients with benign diseases and IL-6 has been proposed as a malignancy predictor [138].

IL-6 plays a key role in promoting proliferation and inhibiting apoptosis. It acts by binding to its receptor (IL-6Rα) and co-receptor gp130 (glycoprotein 130) which in turn activate the JAK/STAT signaling pathway of the Janus kinases (JAK) and signal transducers and activators of transcription (STATs) STAT1 and STAT3 [139]. STATs belong to a family of transcription factors closely associated with the tumorigenic processes. Several studies have highlighted the effect of the IL-6/JAK/STAT signaling pathway on cancer initiation and progression. IL-6 induced tumorigenesis via epigenetic alterations: hypermethylation of tumor suppressor genes as well as by hypomethylation of retrotransposon long interspersed nuclear element-1 (LINE-1) in oral squamous cell cancer lines *in vitro*, which is a frequent event in various cancers [140]. The stromal fibroblasts in a mouse gastric cancer model have also been shown to produce IL-6 [141]. The concomitant inhibition of signaling through the IL-6R/STAT3 pathway is required to efficiently induce apoptosis of multiple myeloma cells. [142]. Like TNF-α, IL-6 facilitates tumor development by promoting conversion of noncancer cells into tumor stem cells [143].

As pro-inflammatory cytokines are partially responsible for tumor induction, an increase in anti-inflammatory cytokines should limit the risk of cancer and reduce activation of signaling pathways. Nonetheless, evidence suggests more complex effects of anti-inflammatory cytokines such as TGF-β and IL-10 on tumor development.

1.6.3. Transforming Growth Factor β (TGF-β)

TGF-β is a powerful pleiotropic cytokine, with immune-suppressing and anti-inflammatory properties. TGF-β has a well-documented role in embryogenesis, cell proliferation, differentiation, apoptosis, adhesion and invasion [144]. Three isoforms have been identified as TGF-β1, TGF-β2 and TGF-β3. TGF-β binds to the cognate type II receptor (TGF- βRII) which induces the phosphorylation of type I TGF-β receptor (TGF-βRI) leading to the formation of a heterotetrameric complex that activates SMAD-dependent transcription [145]. SMAD transcription factors are structurally formed by a serine and threonine-rich linker region that connects two MAD (mothers against dpp) homology regions. The differential phosphorylation of these amino acid residues contributes to various cellular functions, including cytostatic effects, cell growth, invasion, extracellular matrix synthesis, cell cycle arrest and migration [146]. The differential phosphorylation of SMAD2 and SMAD3 by TGF-β receptor activation promotes their translocation into the nucleus, where they form a complex with SMAD4. SMAD4 further binds to DNA along with other transcription factors and induces gene expression [145]. The role of TGF-β in cancer is complex and paradoxical, varying by cell type and stage of tumorigenesis. The endogenous TGF-β–signaling network switch from tumor suppression to promotion of metastasis during the course of carcinogenic progression has been proposed to be initiated by a single, defined oncogenic event [147]. TGF-β1 acts as a tumor suppressor in early stages, inhibiting cell cycle progression and promoting apoptosis. Later, TGF-β1 enhances invasion and

metastasis by inducing epithelial-mesenchymal transition (EMT) [148]. In cancer induction, TGF-β exerts a tumor suppressor effect through cyclin-dependent kinase inhibitor (CKI), p21 upregulation and c-Myc downregulation [149]. In a conditional TGF-β RII knock-out mice model, the highly proliferative epithelia (such as rectal and genital) developed spontaneous squamous cell carcinomas and showed accelerated Ras mutations, reduced apoptosis and carcinoma progression [150], suggesting that a deficient TGF-β pathway contributes to tumorigenesis. There is consistent evidence demonstrating that TGF-β signaling changes are involved in human cancer. TGF-β receptor deletion or mutations have been associated with colorectal, prostate, breast and bladder cancer, co-relating with a more invasive and advanced carcinoma, higher degree of invasion and worse prognosis [151]. On the other hand, increased TGF-β1 mRNA and protein have also been observed in gastric carcinoma, non-small cell lung cancer and colorectal and prostate cancer [152].

In the tumor microenvironment, common sources of TGF-β are cancer and stromal cells, including immune cells and fibroblasts [153]. Bone matrix is also an abundant source of TGF-β and a common site for metastasis in many cancers, correlating with the tumor-promoting and invasive effects of this cytokine [154]. Specific therapy targeting this cytokine in advanced cancer patients has shown promising results in preclinical and clinical studies, using TGF-β inhibitors, specifically ligand traps, antisense oligonucleotides, receptor kinase inhibitors and peptide aptamers.

1.6.4. Interleukin 10 (IL-10)

Interleukin 10 (IL-10) is known to be a potent anti-inflammatory cytokine. Almost all immune cells, including T cells, B cells, monocytes, macrophages, mast cells, granulocytes,

dendritic cells and keratinocytes produce IL-10 [155]. IL-10 is secreted by tumor-infiltrating macrophages as well as tumor cells [156, 157]. When IL-10 binds to its receptor, Jak1 and Tyk2 tyrosine kinases phosphorylates an IL-10R intracellular domain. The phosphorylated IL-10R interaction with STAT1, STAT3 and STAT5, favors STAT translocation into the nucleus and induction of target gene expression [158]. Both pro- and anti tumoral effects of IL-10 are indicated in several studies. IL-10 downregulates proinflammatory cytokine expression by inhibiting NF-κB signaling and therefore can [159] act as an anti tumoral cytokine. IL-10 exerts anti tumoral activity in gliomas, melanomas and breast and ovarian carcinomas [100], through a mechanism involving MHC-I downregulation, thus inducing NK-mediated tumor cell lysis [160]. Due to its immunosuppressive effect on dendritic cells and macrophages, IL-10 can dampen antigen presentation, cell maturation and differentiation, allowing tumor cells to evade immune surveillance mechanisms [161]. IL-10 induces a sustained STAT3 phosphorylation and activation [162]. Through STAT3 activation, IL-10 can also have a pro-tumorigenic effect, mediated by an autocrine-paracrine loop involving Bcl-2 upregulation and resistance to apoptosis [163]. Elevated IL-10 levels are associated with poor prognosis in diffuse B cell lymphoma [164]. Increased production of BAFF, a TNF-α family member having role in tumor growth and survival through IL-10 expression by tumor cells and tumor-associated macrophages promotes Burkitt's lymphoma [165].

1.7 Oxidative stress and cancer

Oxidative stress is implicated in most of the known chronic pathologies [166]. The frequent occurrence of oxidative changes in biological environments is mainly due to the constant metabolic activity of mitochondria, which during the process of respiration gives rise to significant amounts of reactive oxygen species (ROS) (reviewed by [167]). Cells are equipped

with a wide range of redox sensors, which rapidly trigger the antioxidant defenses to compensate for the production of pro-oxidants. When the production of ROS is excessive or the antioxidant defenses are not sufficient, the condition called oxidative stress is established. The excessive ROS can promptly react with the surrounding cellular structures, resulting in oxidative modifications of DNA, lipid and protein [166, 168]. In cancer cells, oxidative changes have been described when compared to normal non-cancerous cells, suggesting a role of oxidative stress in malignant conditions [169]. Several studies have focused on investigating the redox changes that take place in solid tumors, especially in breast cancer. Most of the risk factors for breast cancer development and progression are to some extent implicated with ROS generation [168, 170]. Breast tumors are naturally embedded into an incredibly pro-oxidative environment, as the mammary gland is surrounded by adipose tissue. Therefore, the exceeding ROS quickly acts on the lipidic neighborhood yielding several active metabolites that can regulate a wide range of cellular processes. ROS generation also impacts other cell components, such as the DNA and the nuclear system of oxidative damage repair. Chemical processes induced by ROS on DNA provoke significant DNA damage by oxidation, methylation, de-amination and de-purination. ROS can also affect the DNA repair enzymes by oxidizing its catalytic moieties, which impedes the correct excision of the affected DNA sequences [166]. The protein machinery is affected by the high reactivity of ROS with the thiol residues, giving rise to an electrophilic stress status [166]. Completing this cycle of redox events, nitric oxide (NO) abundantly produced in the breast tumor environment yields a wide range of nitrogen-derived ROS, mostly peroxynitrite, driving nitrosative stress [171, 172].

ROS arise as a by-product of mitochondrial oxidative phosphorylation, oxygen metabolism and NADPH/NADPH oxidase (NOX) functions [173]. The induction of

carcinogenesis in non-tumorigenic breast cells lead to up-regulation of H-Ras gene expression, leading to extracellular signal-regulated kinase (ERK) pathway activation, Nox-1 expression and increased amounts of ROS. Also, increased TNF-α, MMP-2, MMP-9 and reduced E-cadherin were observed following increase in migratory and invasive activity. Ras-ERK-NOX-ROS pathway played an important role in both initiation and maintenance of chronically induced carcinogenesis [174].

The tumor microenvironment releases anti-inflammatory cytokines such as TGF-β. Boudreau and colleagues have demonstrated that TGF-β treatment of both normal and metastatic breast epithelial cells results in NOX-dependent superoxide production in the plasma membrane [175]. ROS-mediated signaling pathways contribute to initiation, promotion and progression of estrogen-dependent breast tumors [176]. Estrogens also play an important role in oxidative stress-mediated signaling. Estrogen-induced ROS promote *in vitro* and *in vivo* tumor formation in breast cancer cells [177].

The cellular redox environment is influenced by production of ROS [178]. p53 is a redox-active transcription factor and its cellular levels determine its biological function. At physiological levels, p53 positively regulates the expression of antioxidant genes to protect cells from damaging levels of ROS. At hypo-physiological levels of p53, it decreases basal transcription of antioxidant genes leading to increased ROS. The unbalanced induction of antioxidant enzymes by p53, at its hyper-physiological levels can result in oxidative stress [179].

Mitochondrial ROS may direct to inflammasome priming through several pathways such as inactivation of MAPK phosphatases which lead to sustained MAPK activity. Enhanced glycolysis in response to low oxygen tension in metastatic breast cancer cells increase HIF1-α as

compared to non tumorigenic breast cells [180]. The prominent transcription factors that drive glycolysis are HIF-1 and the oncoprotein Myc [181].

1.8 Nitrosative stress and cancer

Nitric oxide (NO) is a short-lived, endogenously produced gas that acts as a signaling molecule in the body. In 1987, Ignarro et al. and Palmer et al. simultaneously identified NO as the endothelium-derived relaxing factor [182, 183]. It is synthesized by nitric oxide synthase (NOS) enzymes and serves as a key signaling molecule in various physiological processes. The excessive and unregulated NO synthesis has been implicated as causal or contributing to pathophysiological conditions including cancer (reviewed in [184]). In various cancers such as cervical, breast, central nervous system, laryngeal and head and neck cancers, the expression of NOS has been detected [185-187]. The role of NO has been suggested to modulate different cancer-related events [188]. Many researchers have indicated that similar to TNF-α and TGF-β, NO may have dual effects in cancer. NO seems to promote tumor growth and proliferation at certain concentrations measurable in many different types of clinical samples and in contrast to this, NO also has tumoricidal effects at higher concentrations [189, 190].

In mammalian cells, there are three genes encoding distinct isoforms of NOS– NOS1, NOS2 and NOS3. They have 51-57% homology between isoforms and different localizations, regulation, catalytic properties and inhibitor sensitivity. NOS1, also known as nNOS (isoform first purified and cloned from neuronal tissue) and NOS3 or eNOS (isoform first found in endothelial cells) are also termed as constitutive since they are expressed continuously in neurons and endothelial cells, respectively. eNOS and nNOS produce low and transient concentrations of NO as they are also dependent on a rise in tissue calcium concentration for

activity. In contrast, NOS2 is an inducible, calcium-independent isoform, also called iNOS. Induction of NOS2 (iNOS) unlike NOS1 and NOS3, results in continuous production of NO [191]. It is inducible by immunological stimuli in virtually all nucleated mammalian cells. The enzyme once induced, continues to produce much higher NO concentrations for many hours or days.

The tumor suppressor gene p53 is an important regulator of NOS2, which senses raised cellular NO and inhibits NOS2 by a negative feedback loop [192]. This relationship has important implications in cancer. NO manifests its biological actions via a wide range of chemical reactions, contrary to conventional bio-signaling molecules that act by binding to specific receptor molecules. The precise reactions depend on the concentration of NO and on the variations in the composition of intra- and extracellular milieu [191]. Cells under normal physiological conditions produce small but significant amounts of NO contributing to its anti-inflammatory effects and antioxidant properties [193, 194]. However, with a high NO concentration in tissues, iNOS is upregulated and nitration (addition of NO_2), nitrosation (addition of NO^+) and oxidation effects are seen [194]. Interaction of NO with O_2 or O^{2-} results in formation of reactive nitrogen species (RNS). Dinitrogen trioxide (N_2O_3) and peroxynitrite (ONOO) which constitue RNS can induce two types of chemical stresses, nitrosative and oxidative. O^{2-} and NO may rapidly interact to produce the potent cytotoxic oxidants peroxynitrite (ONOO-) and its conjugate acid ONOOH. Peroxynitrite is a powerful oxidant having important implications in cancer as it oxidizes thiols or thioethers, nitrates tyrosine residues, nitrates and oxidizes guanosine, degrades carbohydrates, initiates lipid peroxidation and cleaves DNA [195, 196].

NO has been reported to exert dichotomous effects within the multistage model of cancer (Tables 6 and 7). It modulates different cancer related events including angiogenesis, apoptosis, cell cycle, invasion and metastasis [188] (Table 6). NO participates in genotoxic events and mediates DNA lesions by formation of toxic and mutagenic species, by direct modification of DNA, or by inhibition of DNA repair mechanisms [197]. DNA strand breaks and different types of mutations in DNA are also mediated by RNS [197, 198].

Positive correlation has been observed between NO biosynthesis and grade of malignancy as it increases tumor blood flow and promotes angiogenesis [199]. Nitrotyrosine, a biomarker of NO, was found to be correlated with VEGF-C expression and lymph node metastasis in breast cancer suggesting the role of NO in progression of breast carcinoma [200]. Switzer et al. showed that NOS2 expression in human breast tumors is functionally linked to poor patient survival [201].

Unlike other types of cancer, tumors of the breast are greatly influenced by steroid hormones. Recent findings implicate NO pathway in some of their effects. Estrogen and progesterone can regulate NOS and, in turn, the NO produced has profound consequences on tumor cell homeostasis [202, 203]. It has been found that estrogen stimulates eNOS release in breast tissue [204] where it acts as a free radical. eNOS expression has been found to be strongly correlated with estrogen receptor expression in a human breast cancer cell line, suggesting free radicals as possible causes of breast cancer [204]. Progesterone has been found to activate iNOS expression. The proliferative effect of estrogen has been shown to be mediated by low levels of NO produced by eNOS [205]. On the contrary, an increase in apoptosis in response to progesterone could implicate high levels of NO produced by induction of iNOS expression [205].

Table 6: Tumor promoting role of NO in cancer*

Role of nitric oxide (NO)	Mechanism by which NO acts
Genotoxic mechanisms	• Toxic and mutagenic species formation. • Direct modification of DNA– strand breaks, oxidation and deamination of nucleic acids. • Inhibition of systems required to repair DNA lesions [198].
Anti apoptotic effects	• GC to AT mutations in p53– loss of its repressor activity. • s-nitrosylation of the cysteine thiol leading to direct inhibition of caspase activity. • Inhibition of cytochrome c release. • Increase in Bcl-2 expression. • Suppression of ceramide generation. • Activation of cyclooxygenase [206].
Induction and promotion of angiogenesis (iNOS and eNOS)	• Dilatation of arteriolar vessels by eNOS. • VEGF release and NO stimulation of hyperpermeability of vascular endothelium. • Increased production of PGE2 resulting in increased tumor vasculature permeability. • Activation of COX-2 which stimulates production of proangiogenic factors and prostaglandins [207].
Limits host immune	• Suppression of proliferation and infiltration of leukocytes.

response against tumor	• Low leukocyte-endothelial interaction [195].
Promotes metastasis	• Promotion of lymphangiogenesis and spread to lymph nodes possibly through involvement of VEGF-C. • Upregulation of MMP-2 and −9. • Downregulation of TIMP-2 and-3 [207, 208].

*[181]

Table 7: Tumoricidal role of NO in cancer

Tumoricidal role of NO	Mechanism by which NO acts
Cytostatic and/or cytotoxic effect on tumor cells	• Suppression of cellular respiration • Shift in iron metabolism • Suppression of DNA synthesis • Modulation of proapoptotic proteins like caspases p53. [206, 209-211].

1.9 DNA Damage Response (DDR), genomic instability and cancer

Over 30 years ago, it was established that the cells within a tumor are derived from a single genetically unstable cell and that population as a whole continues to acquire further chromosomal abnormalities over time [212]. The precise mechanisms of acquisition of these abnormalities are still unclear. The presence of a specific type of genomic instability, termed as chromosomal instability (CIN) is often characterized in hereditary cancers. In these cancers, CIN

can often be attributed to mutation in DNA repair genes [213]. Microsatellite instability (MIN), a second form of genomic instability, is also associated with defects in DNA repair [214]. However, in non-hereditary sporadic tumors, the picture is less clear.

Pro-inflammatory leukocytes release genotoxic reactive oxygen and nitrogen species, which lead to genomic instability and growth-promoting alterations in the genome of the surrounding incipient cancer cells. In addition, activated leukocytes also secrete a number of growth-promoting cytokines, including IL-4, IL-6, IL-10, TGF-β and TNF-α, further fueling the oncogenic process through various mechanisms. Furthermore, established tumors have also been shown to maintain an inflammatory microenvironment further promoting malignant transformation and tumor maintenance.

A complex system of damage detection and repair is required in order to preserve the integrity of the genome. This system is termed the DNA damage response (DDR) and comprises of : DNA damage recognition, signals transduction through appropriate pathways and the activation of cellular responses ranging from DNA repair and chromatin remodeling to cell death activation if the irreparable damage is encountered [215, 216].

1.9.1 Damage signaling

Damage sensing is linked to an intricate signal transduction cascade that induces cell cycle arrest which provides an extended time to allow completion of lesion removal prior to replication or cell division [217, 218] (reviewed in [219]). The cell cycle can be arrested at the G1/S transition, within the S-phase, or at the G2/M transition depending on the nature of the DNA injury and the phase of the cell cycle in which the lesion is encountered [220].

Alternatively, apoptosis is triggered in order to protect the organism from potentially harmful cells, when too many injuries are encountered [221].

The recruitment of phosphatidyl inositol 3-kinase (PI3K)- ATM (Ataxia Telangiectasia mutated) following double strand breaks (DSBs) is mediated by the Mre11/Rad50/NBS1 (MRN) complex [222] in response to chromatin decondensation and relaxation of the double helix torsional stress [223]. This initiator kinase phosphorylates a large number of adaptor/transducer proteins, carrying the ATM-consensus sequence [224]. Multiple proteins that are phosphorylated by ATM include the tumor suppressor protein p53, structural maintenance of chromosomes (SMC) 1, (engages the S phase checkpoint), the breast and ovarian cancer susceptibility protein (BRCA1) and the checkpoint kinase Chk2 [225, 226].

Single-strand DNA (ssDNA) is formed by replication collapse caused by bulky lesions which induces the retraction of the replication fork. Replication Protein-A (RPA) binds to ssDNA and recruits ATM related protein (ATR) via its association with ATR interacting protein (ATRIP) and activates the checkpoint kinase Chk1 [227]. RPA covered ssDNA also triggers the Rad17-dependent loading of the RAD9-HUS1-RAD1 (9-1-1 complex), which is an important transducer of checkpoint activation upon DNA damage [228].

IR-induced DSBs also activates, a third PI3 kinase, DNA-dependent DNA repair protein kinase (DNA-PK, composed of its catalytic subunit DNA-PKcs and a regulatory Ku70/80 heterodimer). DNA-PKcs is essential for NHEJ in higher eukaryotes [229] and additionally functions in telomere maintenance and induction of apoptosis [230].

When genomic insults are encountered, a complicated set of different emergency strategies are called into action. Although many of the individual players are identified and the

downstream signaling cascades have been studied, their respective interactions and communication is still to be resolved.

1.9.2 DDR and γ-H2AX

The phosphorylation of the histone H2A-variant H2AX is the most prominent DDR-associated covalent histone modification in response to DNA damage by the checkpoint kinases ATM, ATR and DNA-PKcs.

H2AX is a histone H2A variant that constitutes 2–25% of mammalian histone H2A depending on the organism and cell type [231, 232]. H2AX is composed of a central globular domain, flanked by N-terminal and C-terminal tails which have sites for a variety of post-translational modifications such as acetylation, biotinylation, phosphorylation, methylation and ubiquitination [231, 233, 234]. H2AX is structurally similar to other H2A species except for the presence of a unique COOH terminal tail, containing a serine, four residues from the C terminus (omega-4) and its position as well as the surrounding motif is highly conserved [232]. The proteins responsible for the phosphorylation of the H2AX omega-4 serine are members of the PI3 kinase family, including ATM, ATR and DNA-PK [235, 236]. Upon DSB induction, one of these kinases phosphorylates many molecules of H2AX in chromatin regions varying from a few megabases (Mbp) to many tens of Mbp flanking the lesion [237, 238]. This phosphorylation event is dynamic, complex process and depends on interactions between MDC1, H2AX, ATM and other kinases [239]. These γ-H2AX foci co-localize with most of the DSB associated DDR factors and are thought to serve as docking sites for recruiting and retaining DNA repair and signaling factors to DSBs.

The amplified response of DDR is easily detected using antibodies to γ-H2AX, manifesting discrete nuclear foci that may be utilized to enumerate the number of DSBs in a cell and/or to examine the co-localization of other DNA repair proteins to the sites of double-strand damage [240]. This is a sensitive technique for detecting DNA double-strand damage in cells which reveals the presence of γ-H2AX foci in the nuclei of intact primary and cultured cancer cells, as well as in tissues [237, 241, 242]. These foci are believed to represent lesions arising from various kinds of endogenous and exogenous stress [243, 244]. γ-H2AX has recently been identified as a potentially useful biomarker with clinical implications because of the sensitivity and utility of γ-H2AX detection of DNA DSBs.

Mice lacking H2AX are radiation-sensitive and exhibit several features associated with defective DDR but they are only partially defective in DSB repair and are not fully compromised in checkpoint activation [245]. This notion argues that this impressive structural organization of γ-H2AX into large molecular assemblies only makes the DDR process more efficient but is not essential for DDR.

1.9.3 DDR and p53

p53 is a key player in the tumor suppressive DNA damage response. The TP53 tumor suppressor gene is located on the small arm of chromosome 17, consists of 11 exons and encodes a 53 KD protein with 393 amino acids, which is a cell cycle regulatory nuclear phosphoprotein. p53 is normally expressed at a low level in cells (reviewed by [246]).

p53 was the first tumor suppressor gene described in 1979 and functions to eliminate and inhibit the proliferation of abnormal cells, thereby preventing neoplastic development [247]. It is a negative regulator of cell cycle [248]. Abrogation of the negative growth regulatory functions

of p53 occurs in many, perhaps all, human tumors [247]. p53, a tumor suppressor protein is essential for preventing inappropriate cell proliferation and maintains genome integrity following genotoxic stress [247, 249].

Mice lacking the critical DDR gene TP53, are highly tumor-prone and regularly succumb to neoplastic disease [250]. Patients suffering from Li-Fraumeni syndrome, caused by germline mutations in the TP53 gene, are characterized by the development of multiple tumors early in life [251]. p53 gene is often found to be genetically altered in tumors and is one of the most frequently inactivated genes in human cancers [252]. Various mechanisms, including mutations within the gene itself, lesions that prevent its activation, or mutations of downstream mediators inhihit the function of p53 tumor suppressor in cancers [249]. Acquired mutations in the p53 gene are found in all major types of human cancers [253]. Mutation of the p53 gene is the most common genetic alteration in human cancer, affecting more than 50% of all tumors [254-256]. p53 mutations in breast cancers occur in only 20% of cases [257, 258]. Tumors carrying p53 mutations are more aggressive and correlate with poor prognosis for treatment. Thus, the loss of functional p53 during tumorigenesis likely represents an essential step in the switch to an angiogenic phenotype that is displayed by aggressive tumors [256].

A variety of target genes that are transcriptionally controlled by p53 have been identified as this mechanism of p53-mediated checkpoint responses is highly conserved and is involved in a complex signaling network [259]. The physiologically best understood p53-mediated checkpoint responses are probably induction of p21 and BH3-only proteins [259, 260]. The cell cycle inhibitor p21 binds and inhibits cyclin dependent kinases (CDKs), thus preventing progression through the cell cycle. In contrast, BH3-only proteins such as p53 upregulated modulator of apoptosis (PUMA) as well as the BH domain proteins Bcl-2-associated protein X

(Bax) and Bcl-2 antagonist/killer (Bak), are potent activators of apoptosis [261]. Both, senescence and apoptosis are potent tumor suppressive mechanisms that ultimately prevent the (neoplastic) proliferation of damaged cells.

1.9.3.a p53 interaction with the immune system

While the different p53-dependent cellular outcomes are largely the result of cell autonomous signaling cascades, p53 signaling also involves non-cell autonomous and systemic mechanisms. A widespread apoptosis or senescence is observed with reactivation of functional p53 in pre-existing p53-deficient tumors. This reactivation triggered lymphomas to apoptosis, while senescence was the primary response in sarcomas and liver carcinomas [262, 263]. Mice carrying liver carcinomas revealed an intimate relationship between p53 signaling and recruitment and activation of the innate immune system [263]. In liver carcinomas, p53 reactivation-induced senescence was associated with upregulation of a number of pro-inflammatory cytokines including CSF-1 and MCP-1, Chemokine CXC motif ligand (CXCL)1, and IL-15 which attract macrophages, neutrophils and natural killer cells, respectively [263]. These mRNAs were also induced by p53 reactivation in cultured hepatoma cells, indicating their specific expression in tumor cells.

Tumor cells utilize survival mechanisms integrating extracellular signals in response to changes in environment with specific changes in gene expression. In response to DNA damage or extracellular signals, expression of several transcription factors like CREB, NF-κB, c-fos and c-jun allows the cells to overcome stressful or deleterious environment and play a critical regulatory role as integrators of diverse signaling pathways with selective induction of gene expression [264-267].

NF-κB transcription factors act as crucial players in an elaborate system that allows cells to adapt and respond to environmental changes, a process pivotal for survival. Activation of NF-κB is through a large number of diverse external stimuli and NF-κB regulated expression of various genes play important and conserved roles in immune and stress responses and impact processes such as apoptosis, proliferation, differentiation and development [268]. AP1 (jun/fos) transcription factors (c-jun, junB, junD, c-fos, FosB, Fra-1 and Fra-2) are important drivers of cancer development [269]. The signaling cascade consists of upstream regulator proteins (novel protein kinase c and Ras), a MAPK module (MEKK1, MEK3 and p38δ) and AP1 transcription factors. Differentiation stimulus causes activation of this cascade and lead to sequential phosphorylation and activation of kinases in the MAPK module which in turn increases AP1 transcription factor level and binding to the DNA response element in the target gene. This leads to increased target gene transcription [270-273].

1.10 cAMP Response Element Binding Protein (CREB)

CREB is a 43-kDa leucine zipper transcription factor that belongs to the CREB/ATF family and regulates proliferation, differentiation and survival in a variety of cell types [274, 275] (reviewed in [276]). CREB contains a kinase-inducible domain (KID), two glutamine rich domains and a basic leucine zipper (bZIP) domain. The transactivation and phosphorylation of CREB occurs at KID and glutamine-rich domains [274, 275]. Various kinases phosphorylate a serine 133 (Ser-133) residue within the KID domain and this phosphorylation promotes the interaction of CREB with a number of transcription co-activators, particularly the histone acetyltransferases- CREB-binding protein (CBP) or p300 [277, 278]. Various stimuli such as growth factors, neurotransmitters, stress signals that increase intracellular cAMP or calcium levels phosphorylate and activate CREB. Nuclear translocation of transducer of regulated CREB

activity (TORC) coactivators also activate CREB by phosphorylation at Ser-133 [279, 280]. Activated CREB family member proteins bind to the cAMP response elements (CRE), promote the recruitment of co-activators such as CBP/p300 and thus initiate the transcriptional machinery and induce CREB target genes [281].

1.10.1 Phosphorylation and activation of CREB

Phosphorylation is one of the most important post-translational modifications that modulates the charge, activity, stability, cellular localization and downstream signal transduction, or have impact on crosstalk of proteins through other modifications [282]. CREB was one of the first transcription factors shown to be regulated by phosphorylation and act as an intracellular signaling second messenger in cells [274, 283, 284]. CREB is phosphorylated by forskolin mediated by the cAMP-dependent protein kinase (PKA) *in vitro* [283]. CREB is phosphorylated at Ser-133 by various kinases including ribosomal protein S6 kinase (pp90RSK), protein kinase C (PKC), protein kinase B/AKT and mitogen- and stress activated protein kinase (MSK-1) [274, 285]. Numerous stimuli such as neurotransmitters, growth factors or stress signals that increase intracellular cAMP or calcium levels were found to activate CREB in cells. Phosphorylation of CREB is induced by different growth factors such as mast/stem cell growth factor, basic fibroblast growth factor and granulocyte-macrophage colony-stimulating factor (GM-CSF) [286, 287]. CREB, when activated, dimerizes and binds to the promoter regions of its target gene containing CRE site, TGACGTCA, or CRE half sites CGTCA/TGACG and for CREB-mediated transcription, pCREB promotes the recruitment of its transcriptional coactivators CBP/p300. Thus, CREB can regulate various cellular mechanisms through modulation of its target genes.

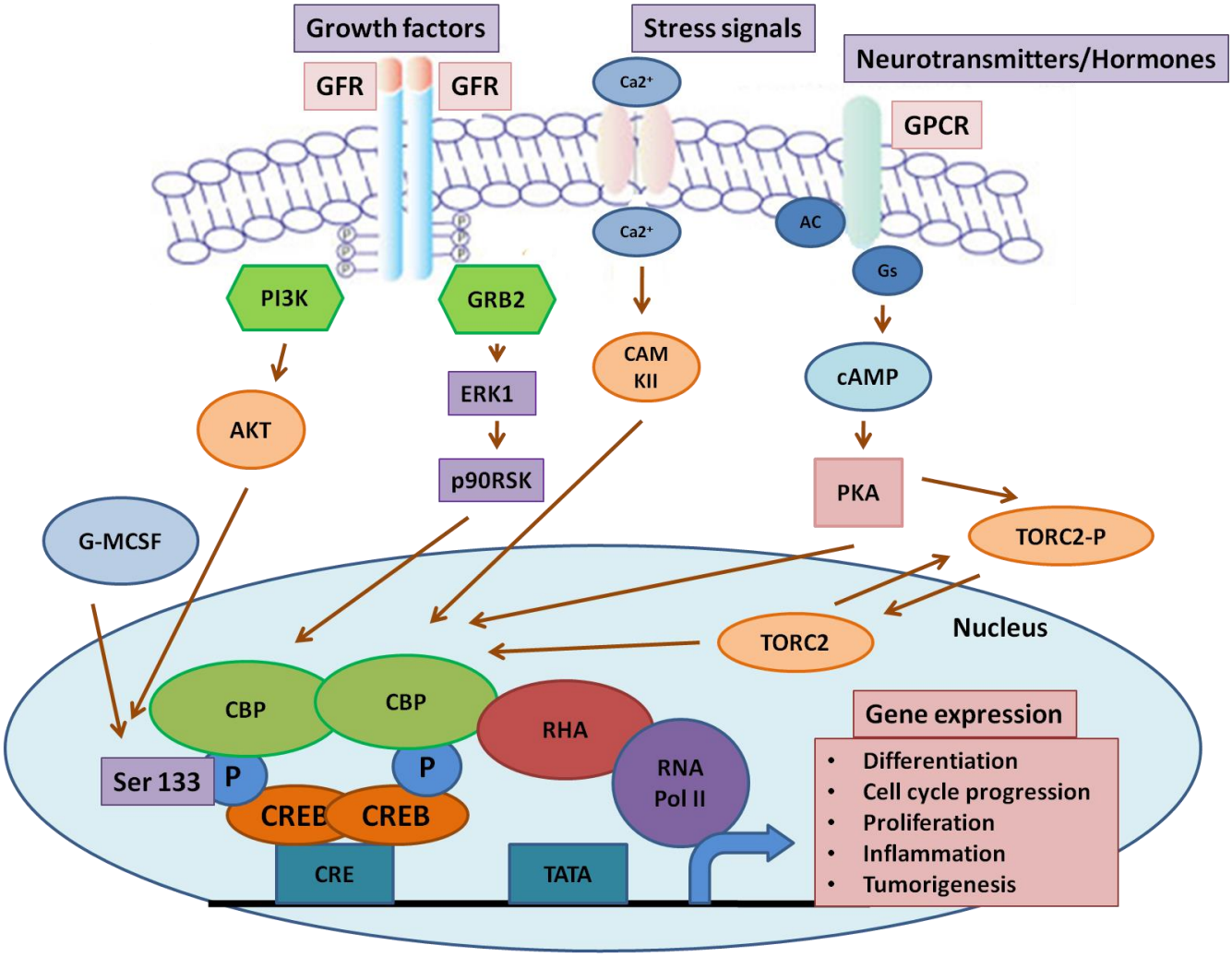

Figure 6: Activation of CREB. CREB can be phosphorylated by a variety of kinases in response to mitogen, calcium and stress dependent signals. Phosphorylation on Ser-133 promotes CREB to recruit transcriptional co-activators that induce transcription of a variety of intermediate early response genes [285-288].

1.10.2 CREB target genes

The broad array of CREB functions was revealed by genome-wide analysis occupying approximately 4,000 *in vivo* promoter sites. It plays an important role in controlling cell cycle regulators such as Ras, 14-3-3, cyclins and heat-shock proteins [289, 290]. Consistent with this, CREB is involved in a variety of cellular functions, including cell proliferation, survival, apoptosis, differentiation, metabolism, glucose homeostasis, hematopoiesis, immune response, and neuronal activities such as memory and learning [291, 292].

Regulation of transcription factors such as c-fos and MEIS1, which contain CREB binding motif on their promoters is modulated by phosphorylation of CREB at Ser-133 [293-295]. CRE binding sites are critical for c-fos transcription [293]. CREB can induce MEIS1 expression in normal and malignant hematopoietic cells [294]. The importance of CREB in metabolism has been suggested as numerous CRE containing genes were found to function in metabolic regulation [296]. Moreover, genes regulating immune response including IL-2 and IL-6, also possess consensus sites for CREB binding and can be modulated by CREB [297].

1.10.2.a Cell cycle and proliferation regulators

CREB has an impact on cell proliferation as it is capable of binding and regulating the promoter regions of cell cycle genes such as cyclin A, D1 and D2 [298, 299]. Both PI3K and CREB can regulate cyclin D2 promoter activity [299]. Phosphorylation of CREB at Ser-133 is critical for IL-2 induced cyclin D2 transactivation and the CREB-binding site in cyclin D2 promoter is important for its activity.

1.10.2.b Growth factors and signaling modulators

The proliferation and maturation of myeloid progenitor cells is stimulated with both GM-CSF and IL-3 as each of them can activate signaling pathways involving a CREB binding site of the early growth response-1 gene (egr-1) promoter [300]. GM-CSF induces CREB phosphorylation and egr-1 transcription by activating pp90RSK through a MEK-dependent signaling pathway in myeloid cell line (TF-1) [301].

1.10.2.c Cell survival regulation

The role of CREB in cell survival has been described in a number of tissues. Neurotrophins such as nerve growth factor (NGF) induces phosphorylation of CREB at Ser-133 which in turn induces genes that confer specificity to neurotrophin signals and promote the survival and differentiation of neurons [302]. Moreover, NGF and other neurotrophins activate Bcl-2 in a CREB-dependent fashion and overexpression of pro-survival factors like Bcl-2 reduces the death-promoting effects [303].

1.10.3 CREB and cancer

CREB signaling is associated with cancer development and poor clinical outcome in leukemogenesis, breast cancer and melanoma. CREB induces the transcription of aromatase in breast adipose mesenchymal cells. Increased levels of aromatase lead to increased estrogen levels, which have been implicated in breast cancer. Aromatase inhibitors, such as exemestane and anastrazole are currently used to treat breast cancer [304]. As an example of positive feedback regulation, estrogen causes CREB to bind and activate the cyclin D1 promoter [305]. The activation of CREB may further contribute to carcinogenesis by activating cyclin D1, which causes cells to progress through the cell cycle [305]. In MCF7 cells, dominant negative CREB

has been shown to block the transcription of Bcl-2 which implicates CREB as being proto-oncogenic as Bcl-2 blocks apoptosis [306].

1.11 Research hypothesis

As reviewed above, the tumor microenvironment plays crucial and versatile roles in tumor progression. Therapeutic targeting of the tumor stroma therefore holds great promise for improved cancer management. However, the success of such therapies highly depends on careful identification and characterization of the multiple players and molecular processes involved in the various steps of tumor progression. The research hypothesis for this PhD dissertation is that "Macrophage induced oxidative and nitrosative stress act as mediators in promoting growth and progression of breast cancer".

1.12 Objectives of the present study

The objectives of the present study are:

- To study the role of macrophages and inflammatory mediators in growth and migration of breast cancer cell lines.
- To identify the soluble factors secreted by macrophages responsible for tumor growth promotion.
- To understand the relationship between inflammatory response, DNA damage and survival factor signaling pathways in benign and malignant breast cancer.

CHAPTER 2

MATERIALS AND METHODS

The studies reported in this dissertation include (i) *in vitro* experiments carried out to assess the role of macrophages in growth and migration of breast cancer cells using conditioned medium (MϕCM) (ii) identification of constituents of macrophage conditioned medium (iii) evaluation of markers selected on the basis of *in vitro* study in benign fibroadenoma and invasive ductal carcinoma patient samples using immunohistochemistry. The common methodologies employed in (i) and (ii) include techniques like ELISA, clonogenic assay, real time PCR etc. Apart from this, methodologies like flow cytometry and 2D PAGE and MALDI analysis were exclusively used in (i) and (ii) respectively. Tissue microarray was constructed using the patient samples and antibody labelling was carried out for immunohistochemistry for (iii). The various methods followed through the course of the study are described in detail in this chapter.

2.1 Techniques employed in *in vitro* cell culture.

2.1.1 Cell culture

The breast adenocarcinoma cell lines used in this study MCF7 and MDA-MB-231 are derived from epithelial tissue cancers of mammary gland origin. MCF7 breast cancer cell line was derived from an *in situ* carcinoma, i.e. the cancerous cells that had not yet invaded surrounding tissues. It is hormone responsive, as it expresses estrogen and progesterone receptors. MDA-MB-231 breast cancer line was derived from a metastatic carcinoma and is not hormone sensitive; so, blocking estrogen receptor in these cells will not inhibit the growth. This cell line also expresses epidermal growth factor (EGF), an oncogene. In comparision to MCF7 cells, MDA-MB-231 cells grow faster and are more resistant to drug therapies.

Human breast adenocarcinoma cell lines - MCF7 (ATCC Number HTB-22, isolated in 1970 from a 69-year-old Caucasian woman and established in 1973 by Herbert Soule and co-

workers) and MDA-MB-231 (ATCC Number HTB-26, established in 1973 by Cailleau *et al.*) were obtained from National Centre for Cell Sciences, Pune, India. These cell lines were maintained in Dulbecco's Modified Eagle's medium (DMEM) (high glucose- 4mM L-glutamine, 4.5 g/L glucose and 3.7g/L sodium bicarbonate in 25 mM HEPES buffer with sodium pyruvate) supplemented with 10% fetal bovine serum (FBS), 100 units/ml of penicillin and 100 µg/ml of streptomycin (complete medium). Cells were passaged 2-3 times a week on attaining confluence by treatment with trypsin-EDTA (0.25% porcine trypsin, 0.02% EDTA) solution. The resulting single cell suspension was diluted 1:2 or 1:3, re-suspended in complete medium and was incubated in a humidified atmosphere at 37°C in 5% CO_2 or used for further experiments.

A monocyte cell line U937 (ATCC Number CRL-1953, established by Sundström and Nillson in 1975) of human histiocytic lymphoma origin was also obtained from National Centre for Cell Sciences, Pune, India. The cell line was maintained in RPMI 1640 medium (4mM L-glutamine, 2 g/L glucose and 2 g/L sodium bicarbonate in 25 mM HEPES buffer) supplemented with 10 % FBS in humidified incubators at 37°C with 5 % CO_2 atmosphere. The cells were sub-cultured at a cell density between 1 X 10^5 to 2 X 10^6 cells/ ml. Cell viability was estimated regularly by trypan blue dye exclusion.

Table 8: Cell lines used in the *in vitro* study

Cell Line	MCF 7	MDA-MB- 231	U937
Origin:	Human breast cancer cell line	Human breast cancer cell line	Human monocytic leukemia cell line
Ethnicity:	Caucasian	Caucasian	Caucasian
Gender:	Female	Female	Male
Age:	69 years	51 years	37 years
Isolation date:	1970	1973	1975
Morphology:	Epithelial cell type	Epithelial cell type	Myeloid cell type
Derived from metastatic site:	Pleural effusion	Pleural effusion	Pleural effusion
Estrogen receptor:	Positive	Negative	
Her2/ ERBB2:	Positive	Negative	
Antigen Expression:	Negative	epidermal growth factor (EGF), transforming growth factor alpha (TGF alpha)	
p53 status:	Wild type	Mutant	Mutant

Cell lines were cryopreserved using 10% dimethyl sulfoxide (DMSO) and stored in liquid nitrogen. The cells were revived by thawing the frozen stocks and washing twice with about 30 ml of medium, to remove all traces of DMSO, prior to re-suspension in DMEM with 20 % FBS,

100 U/ml penicillin and 100 µg/ml streptomycin in T25 flasks. Cells were maintained in humidified incubators with 5 % CO_2 at 37^0C. For cryopreservation, about 3 X 10^6 cells were suspended in 1 ml of freezing mixture (45 % DMEM, 45 % FBS and 10% DMSO) in freezing vials. The freezing vials were stored at -80^0C for about 48 hrs and subsequently stored in liquid nitrogen at -196^0C.

2.1.2 Collection of conditioned media from U937 cells

For the preparation of monocyte conditioned medium (MCM), U937 cells were plated in a density of 2 X 10^5 cells/ml in 24 well plates in complete media for 24 hr at 37^0C. After 24 hr, culture supernatant was collected. U937 cells were differentiated to macrophages with 160 nM phorbol 12-myristate 13-acetate (PMA) treatment for 48 h [307, 308]. The adherent cells (Mϕ) were washed with phosphate buffer saline (PBS) to remove PMA and were further cultured in serum containing growth medium for another 24 hr. The culture supernatants were used as macrophage conditioned medium (MϕCM). The conditioned media were filtered using 0.22 µm membranes and stored at -20^0C. MCF7 and MDA-MB-231 cells were treated with 10% of MCM and MϕCM in the entire study.

2.1.3 Clonogenic assay

Clonogenic assay or colony formation assay is an *in vitro* cell survival assay based on the ability of a single cell to grow into a colony [309]. The colony is defined to consist of at least 50 cells. The assay essentially tests every cell in the population for its ability to undergo "unlimited" division. Only a fraction of seeded cells retain the capacity to produce colonies. Before or after treatment, cells are seeded out in appropriate dilutions to form colonies in 1-3 weeks.

To measure colony forming ability of cells, MCF7 and MDA-MB-231 cells were seeded at a density of 10^3 cells/ml in 6 well plates in complete medium. Twenty four hr later, cells were incubated with MCM or MϕCM for a period of 6 days. Once colonies were formed, cells were washed with PBS and fixed with methanol: acetone (7:3) at -20^0C. Fixed colonies were stained with crystal violet (0.5% w/v). The stained colonies were counted using Gelcount™ cell counter (Oxford Optronix) and data were analyzed by Gelcount™ software. Each experiment was carried out in triplicates/group and was repeated three times. Cells not treated with any supernatant served as controls.

For antibody neutralization experiments, MϕCM was pre-treated with 1μg of anti-TNF-α, IL-1β, IL-6 alone or in combination for 3 hr at 37^0C. The treated CM was filtered through 0.22 μM filter prior to treatment of MCF7 cells.

2.1.4 Assay for apoptosis

Cell-cycle analysis employs flow cytometry to distinguish cells in different phases of the cell cycle. Before analysis, the cells are permeabilised and treated with a fluorescent dye, usually propidium iodide (PI) that stains DNA quantitatively as it binds stoichiometrically to nucleic acids and the fluorescence emission is proportional to DNA (and RNA, which has to be removed if DNA is to be measured) content of a cell. In 1991, Nicolette *et al.* reported that apoptotic cells, but not necrotic ones, have reduced DNA staining with a variety of fluorochromes. Therefore, the presence of cells with DNA content lower than that of G_1-cells (hypodiploid or sub-G_1 peaks) has been considered a marker of cell death by apoptosis. When apoptotic cells are stained with PI and analyzed in a flow cytometer, they display a broad

hypodiploid (sub-G1) peak, which can be easily discriminated from the narrow peak of cells with normal (diploid) DNA content in the red fluorescence channels.

MCF7 and MDA-MB-231 cells were seeded at a density of 10^4 cells/ml in 6 well plates in complete medium. Twenty four hr later, cells were treated with MCM or MϕCM and incubated for a period of 5 days. The cells were subsequently trypsinized, washed twice with cold PBS and fixed in ice cold ethanol (70 %) at -20°C O/N. Cells were washed with PBS and re-suspended in 50 µg/ml propidium iodide and 50 µg/ml RNase A at 37^0C for 30 min. Twenty thousand cells were acquired in a Partec CyFlow® Space flow cytometer using FloMax 2.1™ software and data were analysed using FCS Express™ software. Cells with less than G1 DNA content were enumerated as apoptotic cells.

2.1.5 Immunofluorescence analysis

Immunofluorescence is a powerful technique that utilizes fluorescent dye conjugated antibodies to detect specific antigens and allows visualization of target molecule distribution throughout the sample.

MCF7 and MDA-MB-231 cells (10^4/ml) grown on sterile glass coverslips were incubated with MCM or MϕCM for 5 days. For antibody neutralization experiments, MϕCM was pre-treated with 1µg of anti-TNF-α, IL-1β, IL-6 alone or in combination for 3 hr at 37^0C. The treated CM was filtered through 0.22 µM filter prior to treatment of MCF7 cells. For treatment with inhibitors, the cells were treated with MCM or MϕCM alone or in presence of pharmacological inhibitors of signaling, N-acetyl cysteine (NAC) (5 mM, antioxidant), 1400W (10 µM, a specific iNOS inhibitor) or CGK733 (2 µM, a selective inhibitor of ATR and ATM kinases). After treatment for 5 days, the cells were permeabilized with methanol: acetone (7:3) for 20 min at -

20°C for intracellular labeling of proteins. After 30 min of treatment with blocking buffer (10% FBS in PBS), cells were incubated with primary antibodies (1 µg/10^6 cells) directed against pCREB, CREB, pATM, γ-H2AX or vimentin for 1 hr at room temperature (RT). The cells were then stained with Alexa Fluor 488 conjugated secondary antibody for 30 min. Cells labeled only with the secondary antibody served as a negative control. After three PBS washes, the coverslips were mounted on glass slides with anti-fade mountant containing 4-, 6-diamidino-2 phenylindole (DAPI). Images were acquired using a Nikon Eclipse Ti™ inverted microscope equipped with a Nikon digital camera using NIS elements™ software. The fluorescence intensity of the cells was quantitated using Image J software in a minimum of 50 cells.

2.1.6. Intracellular labeling for flow cytometry

MCF7 and MDA-MB-231 cells (10^4/ml) were incubated with MCM or MϕCM for 5 days. For measuring intracellular TGF-β1 expression in MCF7 cells following MϕCM treatment, the cells were incubated with Golgi plug™ (a protein transport inhibitor) for 4 hr prior to harvesting for flow cytometric analysis. Cells were harvested using trypsin and fixed with 1 ml of 70% ethanol in -20°C O/N. Cells were further washed with PBS and non-specific binding was blocked with blocking buffer (5% FBS in PBS) for 30 min. The cells were incubated with primary antibodies (1 µg/10^6 cells) directed against anti-pan-TGF-β1, γ-H2AX, Bax, Bcl2 or iNOS intracellular antigens diluted in blocking buffer for 1 hr at RT. After three washes with PBS, the cells were incubated with Alexa Fluor 488 conjugated secondary antibody for 30 min. Cells labeled only with secondary antibody served as a negative control. Twenty thousand cells were acquired in a Partec CyFlow® Space flow cytometer using FloMax 2.1™ software and data were analysed using FCS Express™ software.

2.1.7 Detection of reactive oxygen and nitrogen species (ROS and RNS)

The cell permeant reagent 2',7' –dichlorofluorescin diacetate (DCFDA), is a fluorogenic dye that measures hydroxyl, peroxyl and other reactive oxygen species (ROS) activity within the cell. After diffusion into the cell, DCFDA is deacetylated by cellular esterases to a non-fluorescent compound, which is later oxidized by ROS into 2', 7' –dichlorofluorescein (DCF). DCF is a highly fluorescent compound which can be detected with maximum excitation and emission spectra of 488 nm and 525 nm respectively [310].

4-amino-5- methylamino-2',7'-difluorofluorescein diacetate (DAF-FMDA) permeates into living cells and is rapidly transformed into DAF-FM by cytosolic esterases, which is then oxidized by NO to a benzotriazole product accompanied by increased fluorescence detected with maximum excitation and emission spectra of 488 nm and 525 nm respectively [311].

MCF7 and MDA-MB-231 cells were seeded at a density of 10^4 cells/ml in a 6 well plate in complete medium. Twenty four hr later, cells were incubated with MCM or MϕCM for 24 hr, 48 hr and 5 days. Cells were treated with 20 µM DCF DA for detection of ROS and 10 µM DAF-FM for detection of RNS for 30 min at 37°C. Cells were subsequently harvested using trypsin, washed with PBS and acquired in flow cytometer and data were analyzed by FCS Express™ software.

2.1.8 Detection of changes in mitochondrial membrane potential (ΔΨm)

Mitochondrial membrane potential, Δψm, is an important parameter of mitochondrial function. 5,5',6,6'-tetrachloro-1,1',3,3'-tetraethylbenzimidazolocarbocyanine iodide (JC-1) is a lipophilic, cationic dye that can selectively enter into mitochondria and reversibly change color from green to red as the membrane potential increases. In healthy cells with high mitochondrial

Δψm, JC-1 spontaneously forms complexes known as J-aggregates with intense red fluorescence (measured in FL2 channel). On the other hand, in apoptotic or unhealthy cells with low Δψm, JC-1 remains in the monomeric form, which shows only green fluorescence (measured in FL1 channel) [312].

To study the effect of MϕCM on mitochondrial membrane potential, MCF7 and MDA-MB-231, cells were plated at density of 10^4cells/ml and were treated for 5 days. The cells were washed with PBS and labeled with 1 µM JC-1 for 30 min at 37°C. The cells were subsequently harvested, acquired in Cyflow Space flow cytometer and the data were analyzed by FCS Express™ software. Change in mitochondrial membrane potential (FL2/FL1 ratio) was quantified.

2.1.9 Western blotting

Western Blotting (also called immunoblotting) is a technique used for analysis of individual proteins in a protein mixture. The technique has three elements: (1) separation by size, (2) transfer to a solid support and (3) marking target protein using a appropriate primary and secondary antibody to visualize [313, 314]. The changes in expression of pro and anti-apoptotic proteins (Bcl2 family), MAPK signaling proteins and DNA damage markers in MCF7 and MDA-MB-231 cells treated with MϕCM were studied with western blotting.

The cells were lysed in 100 µl of 1X gel loading buffer supplemented with phosphatase inhibitor, 1 mM sodium orthovanadate and protease inhibitor cocktail. The cells were incubated on ice for 30 min and then heated at 98^0C for 10 min and the lysates were then stored at -20^0C.

The proteins were separated in 8-12 % SDS PAGE gel using Tris- glycine electrophoresis buffer. A pre-stained molecular weight marker was included in every gel. The separated proteins

were transferred to polyvinylidene fluoride (PVDF) membrane using wet blotting technique using a Tris-glycine transfer buffer. Following transfer, proteins on the membrane were stained with ponceau S stain to check for the efficiency of transfer. The membrane was blocked in 5% skim milk in PBS with 0.05% Tween 20 (PBST) for 1 hr at RT and then probed with primary antibody for 3 hr at RT or O/N at 4^0C. The primary antibody dilutions used were 1:10,000 for γ-H2AX, 1:5000 for ERK2, 1:5,000 for Bax and Bcl2 and 1:1000 for all the other antibodies in 4% BSA with 0.01% sodium azide in PBST. The membranes were washed thrice with PBST for 15 min each and probed with HRP-conjugated anti-mouse or rabbit IgG antibody (in 5% non-fat milk in PBST). The bands were developed on X ray film using chemilumescent substrate. The quantitation of protein bands was performed using Image J software.

2.1.10 Generation of ATM KD cells

RNA interference (RNAi) is the process of sequence specific, post-transcriptional gene silencing in animals and plants, induced by double- stranded RNA (dsRNA) that triggers the degradation of complementary mRNA. In eukaryotic organisms, *in vivo* or *in vitro* generated long double-stranded RNAs are cleaved into 21 -23 nucleotide long short interfering RNAs (siRNA) by a RNAse III like enzyme activity called DICER [315]. The siRNA is then taken up by the RNA-induced silencing complex (RISC), which anneals one of the siRNA strands to the complementary region of the mRNA and finally cleaves the mRNA [316].

The expression of ATM was downregulated using RNA silencing approaches. For this purpose, 2 X 10^5 cells were seeded in 35 mm dish in antibiotic free medium with 10% FBS. The commercially available 19-25 nt scrambled or ATM specific siRNA (h), designed to knock down gene expression was reconstituted in 330 µL of siRNA diluents (1 µg RNA contain 20-80

picomols and 8 µL of reconstituted siRNA contain 1 µg RNA). The cells were transfected with 1 µg of double-stranded RNA oligonucleotides targeting ATM using X-treme GENE transfection reagent. X-treme GENE siRNA transfection reagent (µL): siRNA (µg) ratio was 10:1. After 72 h of culture, cell lysates were prepared 15 min following exposure to 5 Gy γ radiation. The down regulation of ATM was confirmed using immunoflouresence.

2.1.11 *In vitro* scratch assay- wound healing

The mobility of breast cancer cells in presence of MCM and MϕCM was assessed by wound healing assay. MCF7 and MDA-MB-231 cells ($2X10^4$cells/ ml) were grown in medium containing MCM or MϕCM for 5 days. After formation of a confluent monolayer, wounds were created using a sterile pipette tip and the cells were incubated with serum free media. The cells were stained with calcein AM and images of the wound were acquired using a Nikon Eclipse Ti™ microscope equipped with a Nikon digital camera as 0 hr micrograph. The ability of cells to migrate into the wound area was assessed by comparing micrographs at 0 and 24 hr along the wounded area. The number of cells in the wounded area was enumerated using CellProfiler™ image analysis software (Broad Institute).

2.1.12 Migration assay

Migration of MCF7 and MDA-MB-231 cells was studied using polycarbonate inserts of 8.0 µm pore size PET track- etched membrane placed in the wells of tissue culture plate [317]. The cells (10^5/100 µL) were seeded in the top chamber of each transwell and allowed to migrate for 72 hr. The bottom chamber contained MCM or MϕCM alone or along with NAC (5 mM), 1400W (10 µM) or CGK733 (2 µM) or in combination. For antibody neutralization experiments, MϕCM was pre- treated with 1µg of anti-TNF-α, IL-1β, IL-6 alone or in combination for 3 hr at

37^0C. The treated CM was filtered through 0.22 μM filter prior to treatment of MCF7 cells. The cells on the upper side of the membrane were removed with a cotton swab. The membranes were fixed in methanol: acetone (7:3) for 20 min at -20^0C and stained with crystal violet for 5 min. Images were acquired using a Nikon Eclipse Ti™ inverted microscope equipped with a Nikon digital camera using NIS elements™ software. The number of cells that migrated to the lower surface of the membrane was counted using CellProfiler™ image analysis software.

2.2.13 Estimation of mRNA levels by real time PCR

The expression of TGF-β1, TGF-β2, TGF-β3, TGF-βRI, TGF-βRII, IL-6, EGFR, ICAM-1, ezrin, radixin and moesin genes in MCM and MϕCM treated MCF7 cells was assessed using real-time PCR.

Total RNA was isolated from one million cells (MCM and MϕCM treated MCF7 cells) using RNA isolation kit (HiPurA™ Total RNA Miniprep Purification Spin Kit, HiMedia, India). RNA purification procedure using miniprep spin columns comprises of three steps viz, adsorption of RNA to the membrane, removal of residual contaminants and elution of pure RNA. RNA concentration was determined by measuring its absorbance at wavelength of A260nm/A280nm (Picodrop™ spectrophotometer). A260nm/A280nm ratio gives an estimate of the purity of the RNA. Pure RNA solutions have an optical density ratio of 2.0. Optical density values less than 1.5 indicates ethanol or protein contamination. The RNA sample then was stored at -80ºC for future use.

Reverse transcription leads to synthesis of complementary strand of DNA from RNA. It is followed by polymerase chain reaction (PCR) and the two processes together are known as RT- PCR. One microgram of total RNA was reverse transcribed to cDNA in a reaction

containing random hexanucleotide primers, dNTPs and reverse transriptase using first strand cDNA synthesis kit (Roche, Germany). The reaction mixture was incubated at 25°C for 10 min and then 50ºC for 1hr to commence cDNA synthesis followed by incubation at 85ºC for 5 minutes to inactivate RNase. The cDNA was diluted to 1:10 in PCR water (distilled, deionised and UV- treated H_2O) and the samples were stored at -20ºC until required or used for PCR amplification.

Real time quantitative polymerase chain reaction (QPCR) was developed in1992 which allows quantification of DNA, cDNA, or RNA templates as the products accumulates with each cycle of amplification. It is based on the detection of a fluorescent reporter molecule that increases as PCR product accumulates with each cycle of amplification (the level of fluorescence detected is directly proportional to the PCR product yield). The level of fluorescence is continuously monitored through the software and hence the term 'real-time'. Fluorescent reporter molecules include dyes that bind double-stranded DNA (i.e. SYBR® Green I) or sequence–specific probes (i.e. Molecular Beacons®, Amplifluor® probes, Scorpions® probes or TaqMan® Probes). SYBR Green I binds to all double–stranded DNA and is monitored by measuring the increase in fluorescence throughout the cycle.

Equal amount of cDNA (0.5 µl) was used for PCR amplification of GAPDH as housekeeping gene and other target genes using 2.5 pmoles of gene specific primers (table 11). Real-time PCR was carried out in Light Cycler 480 (Roche, Germany). All reactions were performed with SYBR green I in PCR mix and in triplicates.

Table 9: List of primers used in the study

S. No.	Gene	Primer Sequence	Reference
1.	GAPDH	Forward: 5′-ATGACATCAAGAAGGTGGTG-3′ Reverse: 5′-CATACCAGGAAATGAGCTTG-3′	[318]
2.	TGF-β1	Forward: 5′-GGCCCTGCCCCTACATTT -3′ Reverse: 5′-CCGGGTTATGCTGGTTGTACA-3′	[319]
3.	TGF-β2	Forward: 5′-TCAAGAGGGATCTAGGGTGGAA -3′ Reverse: 5′-GGCAGCTCCAGCACAGAA -3′	[319]
4.	TGF-β3	Forward: 5′-CAGCTCTAAGCGGAATGAGCAG -3′ Reverse: 5′-TATAGCGCTGTTTGGCAATGTG -3′	[319]
5.	TGF-βRI	Forward: 5′-AAGTCATCACCTGGCCTTGGT-3′ Reverse: 5′-TGCGGTTGTGGCAGATATAGAC-3′	[319]
6.	TGF-βRII	Forward: 5′-AATATCCTCTGAAGAACGACCTAA-3′ Reverse: 5′-TCCCACCTGCCCACTGTTA-3′	[319]
7.	IL-6	Forward: 5′-TCTCCACAAGCGCCTTCG-3′ Reverse: 5′-CTCAGGGCTGAGATGCCG-3′	[320]
8.	EGFR	Forward: 5′-GTGACCGTTTGGGAGTTGATGA-3′ Reverse: 5′-GGCTGAGGGAGGCGTTCTC-3′	[321]
9.	ICAM-1	Forward: 5′-CTGCAGACAGTGACCATC-3′ Reverse: 5′-GTCCAGTTTCCCGGACAA-3′	[322]

10.	Ezrin	Forward: 5′-GTTTTCCCCAGTTGTAATAGTGCC -3′ Reverse: 5′-TCCGTAATTCAATCAGTCCTGC-3′	[323]
11.	Radixin	Forward: 5′-CGAGGAAGAACGTGTAACCGAA -3′ Reverse: 5′-TCTTGGTTTCATCTCTGGCTTG -3′	[323]
12.	Moesin	Forward: 5′-TGTAAACCAGAGAGCTGCTGG -3′ Reverse: 5′-GAAGAGCACACATGAGACAGAGAA -3′	[323]

The data obtained by QPCR was analyzed using software tool, REST© (relative expression software tool). The two groups were compared, with up to 16 data points in a sample and 16 in a control group, for reference and up to four target genes. The average fold changes were calculated by differences in threshold cycles (Ct) between pairs of samples compared. The mathematical model used was based on the PCR efficiencies and the mean crossing point deviation between the sample and control group.

2.2 Techniques employed in characterization of conditioned medium.

2.2.1 Enzyme-linked immunosorbent assay (ELISA)

ELISA uses a solid-phase enzyme immunoassay (EIA) to detect the presence of antigen, in a liquid sample [324]. The pro inflammatory cytokines present in the conditioned medium were quantitated using commercially available cytokine sandwich ELISA kits.

For this assay, capture antibody (2 μg/ml) diluted in bicarbonate-coating buffer (1:250) was added to the wells of enhanced protein binding 96 well - ELISA plates. The plates were sealed to prevent evaporation and incubated O/N at 4°C. The unbound capture antibody was

aspirated and wells were washed 3 times with buffer (PBS with 0.05% Tween 20, PBST). The non-specific binding was treated blocked with buffer containing 10% FBS (blocking buffer) and incubated at RT for 1 hr. The wells were washed thrice with PBST. Replicates of standards/ samples diluted in blocking buffer were added to the wells and incubated at RT for 2 hr. The wells were subsequently washed again with PBST. For detection, biotinylated anti-cytokine detection antibody (1 µg/ml) diluted in blocking buffer was added to each well for 1hr at RT followed by PBST washes. Streptavidin-HRP conjugate (1 µg/ml) was added to each well and incubated for 30 min at RT followed by thorough washes with PBST. TMB substrate was added to each well and incubated for 20-30 min at RT in dark. The reaction was stopped using 0.2M sulfuric acid. The absorbance of the plate was measured within 30 min in a microtitre plate reader set at 450 nm with wave length correction parameter set at 540 nm. Standard curves were generated from mean ± S.E.M. of O.D. absorbance values of recombinant cytokine standards. The amount of cytokine in each well was estimated from the standard curve for the cytokines.

Table 10: Standard range of cytokine ELISA

S.No	Cytokine	Standard range
1.	TNF-α	7.8 pg/ml -500 pg/ml
2.	IL-1β	3.9 pg/ml -250 pg/ml
3.	IL-6	4.7 pg/ml -300 pg/ml
4.	TGF-β1	62.5 pg/ml -4000 pg/ml
5.	IFN-γ	4.7 pg/ml -300 pg/ml

2.2.2 Collection of CM for 1D and 2D sodium dodecyl sulfate polyacrylamide gel electrophoresis (SDS-PAGE)

Serum free conditioned media were generated from monocytes and macrophages for secretome analysis since the presence of FBS proteins will mask the low abundance secreted proteins. U937 cells were plated in density of 1 X 10^6 cells/ml in T-75 flask in serum free media for 24 hr at 37°C. Monocytes were differentiated to macrophages as described before and were further cultured in serum free medium for 24 hr at 37°C. The culture supernatants were filtered using 0.22 µm membranes and were stored at -196°C in presence of protease (PS) and phosphatase inhibitors (PIC) till further processing. Around 40 ml of culture supernatant was concentrated 40 fold by two methods: (1) ammonium sulphate precipitation and (2) membrane ultracentrifugation with centricon tubes (10 kD cut off)

Ammonium sulfate ($(NH_4)_2SO_4$) precipitation is a classic first step to fractionate proteins by causing perturbations in the solvent with respect to ionic strength (Green and Hughes, 1955). It is performed to remove components in cell culture supernatant that may interfere with downstream purification methods. The major advantage to this method is that it causes the reversible precipitation of the protein and is non-denaturing to the protein structure. In brief, the CM was subjected to 10% ammonium sulfate (w/v) cut by slowly adding solid $(NH_4)_2SO_4$ while gently stirring at 4°C for 30 min. The CM was centrifuged at 4000 g for 15 min and supernatant was subjected to further 80% ammonium sulfate (w/v) cut with gentle stirring at 4°C for 1hr in which the protein of interest is "salted out". The CM was then centrifuged at 4000 g for 15 min in which precipitate was collected and the remaining supernatant that may contain additional "contaminating" proteins was discarded. The precipitate was dissolved in 1mM Tris (pH 8) and unwanted small molecules such as salts, reducing agents etc were removed by dialysis (10

kD cut off) O/N at 4°C. The samples were then concentrated to 1 ml by centricon tube ultrafiltration.

The CM was also concentrated by centricon tube ultrafiltration method. The process of ultrafiltration uses semi-permeable membranes and pressure to separate molecular species on the basis of size and shape. The centricon consist of a sample filter unit (10 kD cut off) and a filtration collection tube. The sample was loaded in the filter unit, placed in the collection tube and concentrated by ultrafiltration at 4000 g for 15 min. The concentrated samples were then washed with 1mM Tris for buffer exchange. The samples were stored at -80°C in presence of PIC&PS.

2.2.3 Protein estimation by Lowry method

The protein content in concentrated CM was estimated by Lowry's method (1951). The method combines the reactions of copper ions with the peptide bonds under alkaline conditions (the Biuret test) with the oxidation of aromatic protein residues. For estimation of proteins, 500 µl of diluted proteins (10 µl unknown protein sample in 490 µl water and 2-25 µg standards) were mixed with 500 µl Folin-Ciocalteau's reagent to make a total volume of 1 ml. The samples were incubated in dark for 10 min. Two fifty µl of Folin-Ciocalteau's reagent was then added in each tube and samples were incubated for 30 min in dark. Absorbance was measured at 750 nm and the concentration of the unknown protein samples was estimated using the standard graph prepared using bovine serum albumin.

2.2.4 One- dimensional SDS-PAGE gel electrophoresis

SDS-PAGE is used to separate proteins with relative molecular mass [325]. Twenty five μg of concentrated protein samples were separated on 10% SDS-PAGE gels as described earlier. The gel was washed with D/W and stained with Coomassie Brilliant Blue-250 (0.1% w/v) for 20 min with gentle agitation. This was compatible with downstream processing such as mass spectrometry analysis after protein digestion. The gel was placed in destaining solution (80% water, 10% methanol & 10% glacial acetic acid). The destaining solution was replenished several times until background of the gel was fully destained. Images of Coomassie Brilliant Blue-stained gels were acquired by Dyversity-6 gel imager (Syngene, UK) using GeneSnap^{TM} software (Syngene, UK).

2.2.5 Silver staining of SDS-PAGE gel

Silver staining is used to detect proteins after electrophoretic separation on polyacrylamide gels and has excellent sensitivity (detection of protein in nanogram range) [326]. Ten μg of concentrated protein samples were separated on 10% SDS-PAGE gels as described earlier.

The gel was washed in D/W and was treated with fixative solution (50% methanol, 12% acetic Acid, 0.5 ml 37% formaldehyde/L) for 1 hr or more. The gel was washed thrice with 50 % methanol for 20 min each. The gel was sensitized in 0.02% sodium thiosulfate for 1 min and washed thrice with water for 20 sec each. The gel was then impregnated with cold 0.2% silver nitrate solution (2g/L $AgNO_3$, 0.75 ml of 37% formaldehyde/L) for 20 min and rinsed twice with distilled water. The gel was treated with chilled 6% developing solution (60g/L Na_2CO_3, 0.5 ml 37% formaldehyde/L, 4 mg/L $Na_2S_2O_3.5H_2O$) till the bands appeared. The gel was then washed

with water and the reaction was terminated with stop solution (50% methanol and 12% acetic acid). The gel was stored in 1% acetic acid till further processing. Images of silver stained gels were acquired by Dyversity-6 gel imager (Syngene, UK) using GeneSnap^{TM} software (Syngene, UK).

2.2.6 Two - dimensional gel electrophoresis

Proteome analysis is a direct measure of protein in terms of their presence and relative abundance. One of the greatest challenges of proteome analysis is the reproducible fractionation of the complex protein mixtures while retaining the qualitative and quantitative relationships. Currently, 2-D PAGE is the only method that can handle this task. The mixture of proteins is separated by two properties viz. isoelectric point and protein mass [327]. Proteomic analysis was carried out in collaboration with Dr. Bhakti Basu, Molecular Biology Division, BARC. The different steps for 2-D is given below:

Sample Preparation: The concentrated CM samples were further reduced to 2 µL in a speed vac concentrator were incubated with 98 µL of 2D rehydration buffer (8 M urea, 1 M thiourea, 2% CHAPS, 15 mM DTT, 2% IPG buffer, traces of bromphenol blue) for 30 min at RT. Equal amount of samples were loaded on rehydration/equilibriation trays along the back edge of the tray channels. The IPG strips were gently placed using the forceps onto the samples without introduction of bubbles. The "+ terminal" & "pH 4-10 marked side" was positioned at the left side of the tray. The strips were overlaid with 2-3 ml of mineral oil to prevent evaporation during rehydration process. This method allows even distribution of the samples along the length of the strip. The tray was covered and left on the leveled bench O/N for rehydration and loading of protein samples on the IPG strips.

Isoelectric Focusing: One-dimensional protein separation was performed with the Protean Isoelectric Focusing Cell (Bio-Rad, India) at 20^0C. The rehydration IPG strips were placed in a clean and dry Protean IEF focusing tray of the same size and paper wicks were placed at both ends of the channels corresponding to wire electrodes. The paper wicks were wet with 8 µL of nanopure water. The IPG strips were carefully lifted using forceps and mineral oil was drained by holding the strips vertically for about 7-8 sec. The strip was transferred to the corresponding channel in the focusing tray and was covered with 2-3 ml of fresh mineral oil. The lid was placed on the tray which was placed into the Protean IEF cell. The run parameters for 11 cm strip at 20^0 C with a max current of 50 µA per strip was 8000 V with maximum volt-hour set at 30000 V-hr in rapid ramp. After completion of electrophoresis run IPG strips were stored at -80^0 C.

IPG Equilibration: The frozen strips stored at -80°C were thawed for 10-15 min at RT. The strips were incubated with equilibration buffer I (6 M urea, 50 mM Tris, pH 6.8, 30% glycerol, 4% SDS, 20 mM DTT) for 15 min with gentle shaking. The equilibration buffer I was decanted and strips were further incubated with equilibration buffer II (6 M urea, 50 mM Tris, pH 6.8, 30% glycerol, 4% SDS and 4.5% iodoacetamide) for 15 min with gentle shaking. The equilibration buffer II was decanted. The strips were washed with running buffer for 10 min.

SDS-PAGE: SDS resolving gel (12%) was prepared as described in Annexure. The strip was laid on top of the resolving gel with 1 strip/gel and the prestained molecular weight marker was loaded onto the last well of the gel. The agarose solution with bromophenol blue (BPB) was overlaid on the IPG well of the gel. The gel was run in 1X tris/glycine/SDS running buffer and migration of BPB was monitored to check the progress of electrophoresis.

Staining of the gel: The gel was stained with Coomassie Brilliant blue and destained as described in 2.2.4. Images of Coomassie Brilliant Blue-stained gels were acquired by Dyversity-6 gel imager (Syngene, UK) using GeneSnap^{TM} software (Syngene, UK).

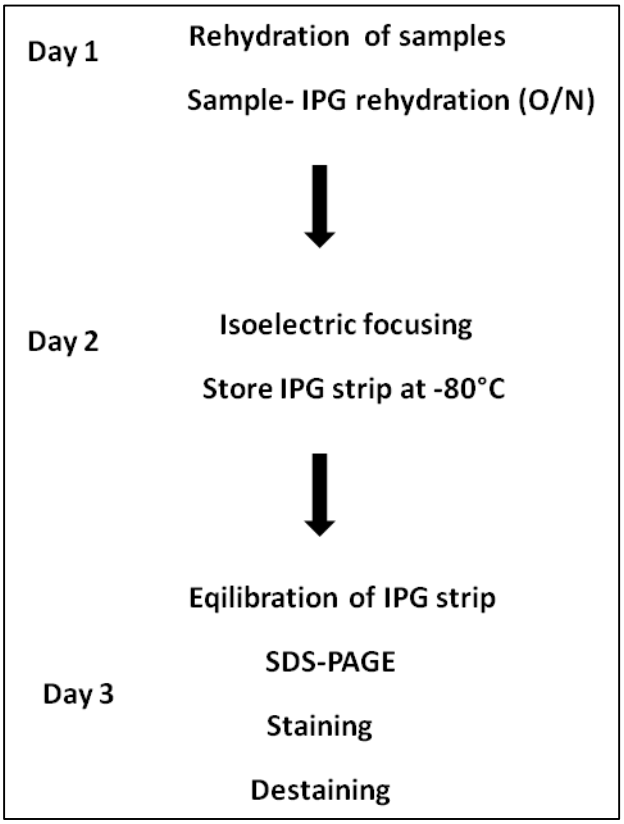

Figure 7: Procedure summary for 2-D SDS PAGE.

2.2.7 In gel trypsin digestion

In-gel proteolytic digestion of separated proteins is performed to cleave the protein of interest present within the polyacrylamide matrix. In-gel digestion is a multi step procedure including spot selection, spot excision, stain removal, reduction, alkylation, proteolytic cleavage and finally extraction of the peptides.

The proteins of interest separated in 1D or 2D PAGE were marked on the gel image. The gel was washed twice with distilled water for 10 min each. The spots of interest were excised from the gel into 1 mm cube pieces. The excised pieces were transferred to 1.5 ml microfuge tube. For destaining, the gel particles were washed with M/Q H_2O followed by treatment with 50 mM NH_4HCO_3/Acetonitrile (ACN) (1:1, v/v) for 15 min, rehydration in 50 mM NH_4HCO_3 for 5 min and addition of equal volume of ACN. The supernatant was removed after 15 min of incubation and 25 µL ACN was further added to cover the gel particle. The gel pieces were shrunk in presence of ACN and dried down in vacuum centrifugation.

For the reduction step, the gel particles were incubated in 10 mM DTT/ 50 mM NH_4HCO_3 at 56°C for 45 min. The samples were brought to RT and excess liquid was removed. The gel particles were alkylated by incubation with freshly prepared 55 mM iodoacetamide (IAA)/50 mM NH_4HCO_3 for 30 min at RT in dark. After removing IAA, gel particles were washed twice with 50 mM NH_4HCO_3/ ACN (1:1, v/v) for 15 min each and again with ACN for 15 min. The gel pieces were shrunk in presence of ACN and dried down in vacuum centrifuge.

The proteolytic cleavage of proteins in the gel particle was carried out with 20 ng of freshly prepared enzyme solution (in 25 mM NH_4HCO_3) at 4°C for 30 min. Four µL of 25 mM NH_4HCO_3 with 9% ACN was further added on the gel particle and was incubated at 37°C for O/N.

For peptide extraction, the gel particle was vortexed with 0.1 % trifluoroacetic acid (TFA) for 15 min. The extract was collected in a separate microfuge tube. Twenty-five µL of 0.1% TFA: ACN (1:1) was added to the gel particle and vortexed for 15 min. The extract was

collected and pooled in the tube. The gel particles were further vortexed with 25 µL ACN for 15 min. The extracts were pooled together and were reduced to 4-5 µL by vacuum centrifugation.

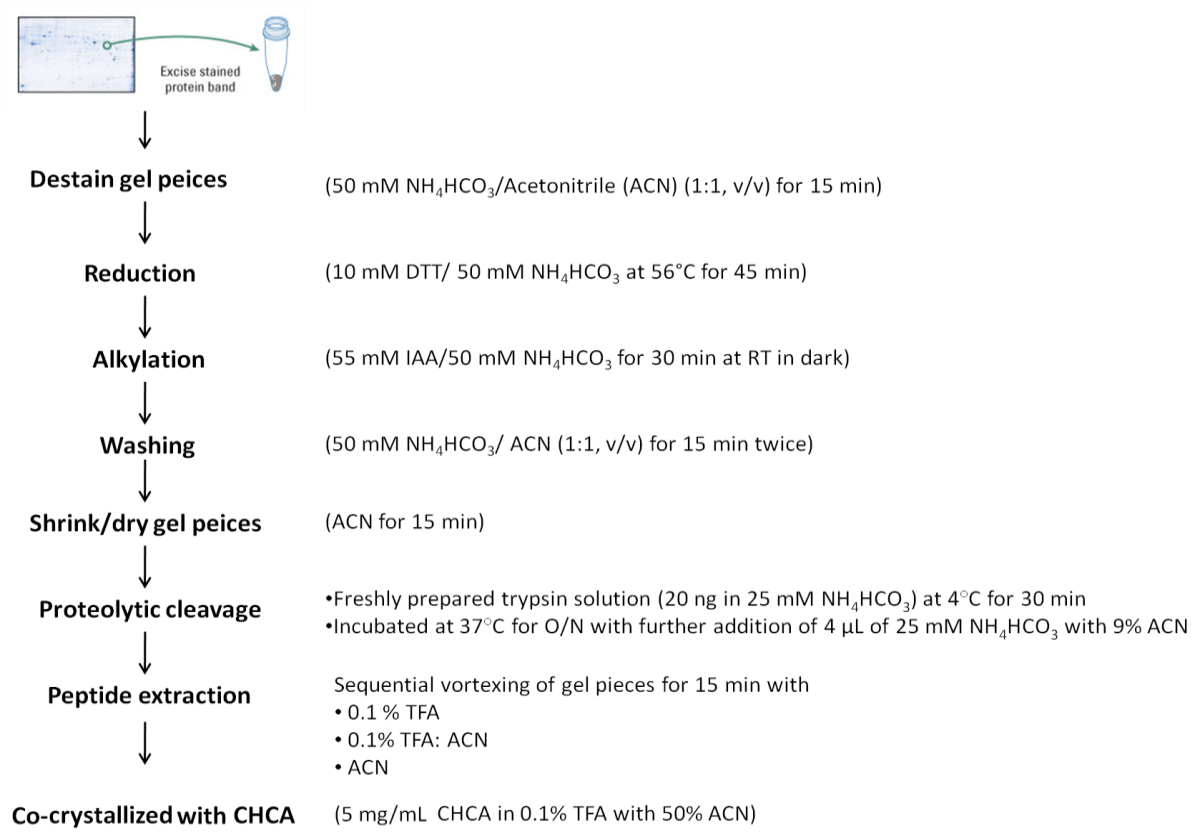

Figure 8: Procedure summary for in-gel trypsin digestion.

2.2.8 MALDI analysis

The eluted polypeptides were co-crystallized with α-cyano-4-hydroxycinnamic acid (CHCA) (5 mg/mL in 0.1% TFA with 50% ACN) matrix on the target plate (384-well Opti-TOF stainless steel plate) (Bruker Daltonics, Germany).The MALDI TOF/TOF UltraFlexIII mass spectrometer was externally calibrated using peptide calibration mix I (Bruker Daltonics). Peptide mass was calibrated with help of 13 externally spotted standard calibration mixture. The analysis was carried out in positive ion reflector mode and the mass spectra were acquired with

standard TOF-MS protocol in the mass range of 600–4500 Da. The laser was set to fire 150 times per spot. Peak list was generated using FlexAnalysis^{TM} software 3.0 (Bruker Daltonics). The mass spectra were imported into the database search engine (BioTools v3.1 connected to Mascot, Version 2.2.04, Matrix Science). Mascot searches were conducted using the NCBI non redundant database (released Jan 2012 or later) with the settings given in table 11.

Table 11: Parameters and settings for Mascot searches using NCBI database

Parameters	Settings
Number of missed cleavages permitted	One
Fixed modifications	Carbamidomethyl on cysteine
Variable modification	Oxidation on methionine residue
Peptide tolerance	100 ppm
Enzyme	Trypsin
Peptide charge	+1
Known contaminating peaks excluded	Matrix, keratin, trypsin, cytokeranine, coomassie and zinc finger

A Mascot score of >65 with a minimum of 10 peptide matches was considered to be a significant identification ($p < 0.05$).

2.2.9 Zymography

Zymography also referred to as substrate zymography, is an established technique for the routine detection and quantitation of various activities of proteases, such as gelatinase. This technique provides reliable identification of proteases based on the molecular mass of their inactive and active forms after gel electrophoresis [328]. It is applied to study matrix metallo proteases (MMPs) whose expression is enhanced during tumor invasion and metastasis. The CM protein samples were prepared in 2X sample loading buffer by incubation at RT for 10 min. Resolving polyacrylamide gel (8%) was prepared with either 3 mg/ml gelatin or 5 mg/ml casein as described in Annexure. The protein samples were loaded along with pre stained molecular weight marker. The gel was run with 1X tris/glycine/SDS running buffer and migration of BPB was monitored to check the progress of electrophoresis. The gel was washed in renaturing buffer (2.5% Triton X-100 in H_2O, freshly prepared) for 30 min at RT. The gel was placed in developing buffer for 30 min at RT was further incubated in fresh developing buffer for O/N at RT. The gel was then stained with fresh Coomassie Blue solution (5 %) for 1-3 hrs and destained as described earlier in 2.2.4. The area of protease activity appeared as a clear band against a dark blue background where the protease has digested the substrate (gelatin or casein). Images of zymograms were acquired by Dyversity-6 gel imager (Syngene, UK) using GeneSnap^{TM} software (Syngene, UK). The gel was dried for storage.

2.2.10 Preparation of exosome like vesicles

Exosomes are small vesicles secreted by most cell types in culture. Isolation of exosomes from cell culture medium was carried out with multiple ultracentrifugation steps [329].

Preparation of exosome free serum: The serum added to the cell culture medium was first depleted of exosomes by ultracentrifugation at 120 000 x g for 3 hr at 4 °C.

U937 cells were grown in exosome-free serum containing medium. MCM and MϕCM collected as described earlier in 2.1.2 were centrifuged at 16 500 x g for 20 min at 4 °C to remove cells and debris. The supernatant was filtered through a 0.22 μm filter to remove particles larger than 200 nm were centrifuged at 120000 x g for 100 min at 4 °C. The supernatant was discarded and the pellet contained exosomes. The exosome enriched pellet was further washed with PBS at 120000 x g for 100 min at 4°C.

2.2.11 Uptake of PKH-26 labeled exosomes

To study the uptake of the exosomes by cancer cells, they were labeled with PKH26 Red Fluorescent Cell Linker Kit (Sigma, USA). The kit uses a proprietary membrane labeling technology to stably incorporate a yellow-orange fluorescent dye (PKH-26) into the lipid region of the cell membrane. In brief, 1 ml of diluent C was added to the exosomes resuspended in minimum volume of PBS. PKH-26 dye (2μL) diluted in 1 ml of diluent C was added to the exosomes. The reagents were thoroughly mixed with pipette for 30 sec and the reaction was stopped with serum containing medium. The labeled exosomes were washed with PBS by centrifugation at 120000 x g for 100 min at 4°C and were filtered with 0.22 μm filter.

MCF7 cells were treated with PKH-26 labeled exosomes and incubated in complete medium O/N at 37°C. The cells were washed thoroughly and were observed under fluorescence microscope.

2.3 Techniques employed in clinical study

2.3.1 Sample collection

The breast cancer samples used in this study were archived samples from pathology unit of BARC hospital from March 2002 to Oct 2012, a retrospective study of 115 paraffin blocks of breast tissue. Ninety one samples of malignant IDC breast lesions and 24 samples of benign fibroadenoma were included in the study. Immunohistochemical studies of human tissue biopsies were approved by the BARC Medical Ethics Committee (BHMEC 5/08) and samples were processed anonymously. Formalin-fixed paraffin-embedded sample blocks were used in this study. This was carried out in collaboration with Dr. Susan Cherian, Head Pathology Unit, Medical Division, BARC Hospital. Hematoxylin and eosin (H&E) stained sections were re-examined by two pathologists. The clinical information regarding age, largest diameter of tumor, grade, stage, LN status, vessel space invasion and hormone receptor status were obtained from the available histological reports.

2.3.2 Preparation of Tissue Micro Array (TMA)

TMA was prepared using archived breast cancer biopsy samples. H & E labeled tissue samples were scanned by pathologists from BARC hospital (Dr. Susan Cherian and Dr. Nitin Chikhale) and areas were marked on slides having tumor mass with and without infiltrating cells. The 2 mm cores were lifted from the donor block for TMA preparation manually with biopsy syringe and were placed in the TMA recipient block. Three cores from each sample representing

tumor mass and infiltrating cells were taken out. The cores in the TMA were placed in asymmetric manner marked with proper orientation of samples. Each TMA contained 3 representing cores from 10-12 samples block and 10 such blocks were prepared.

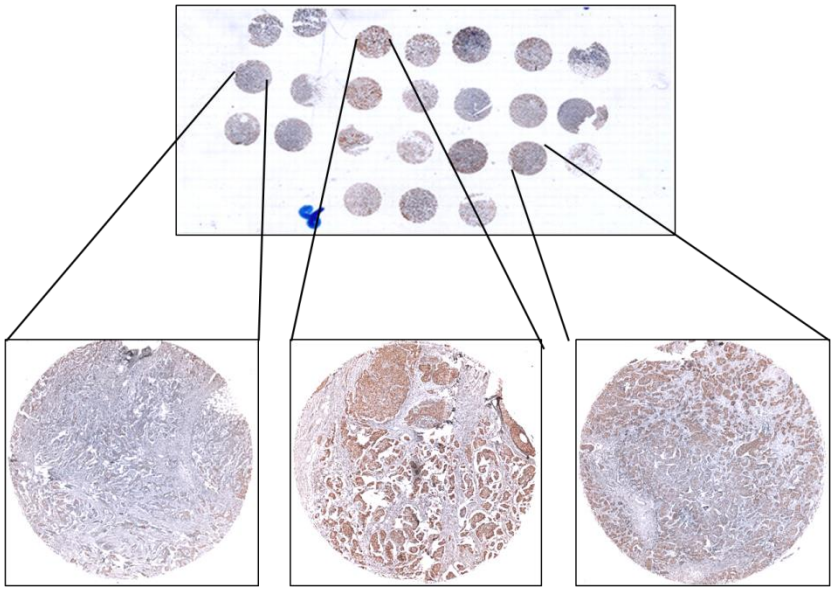

Figure 9: Representative TMA slide.

2.3.3 Preparation of sections on poly-L-lysine coated slide

The glass slides were treated with cleaning solution (10% NaOH solution in 96% ethanol) for 2 hr with gentle agitation. The slides were then rinsed four times with M/Q water. The slides were kept in freshly prepared poly-L-lysine solution (0.01% w/v) for 5-10 min in gentle orbital shaker. The slides were dried at 37^0C and then stored for 2 weeks for ageing before placing the sections. The paraffin embedded TMAs were sectioned in microtome and 5µm sections were mounted on poly-L-lysine coated slide. The mounted slides were incubated at 56°C in oven for O/N.

2.3.4 Immunohistochemistry

Immunohistochemistry (IHC) combines anatomical, immunological and biochemical techniques to identify discrete tissue components by the interaction of target antigens with specific antibodies tagged with a visible label (Albert Coons, 1941). IHC makes it possible to visualize the distribution and localization of specific cellular components within cells and in the proper tissue context.

Five µm sections were deparaffinized by three consecutive treatments in xylene for 5 min each and then rehydrated with decreasing grades of alcohol (100 %, 95% and 80% alcohol) for 5 min each. The slides were then washed with distilled water for 10 min. The endogenous peroxides were quenched with 3% H_2O_2 in methanol (peroxidase suppressor) for 20 min at RT. Antigen retrieval or unmasking of the epitopes was carried out in microwave oven for 20 min (10 min at 800 W power and remaining 10 min at 600W power) with sodium citrate buffer (pH 6). The slides were cooled down to RT and washed with 1X PBS. Reagents from vectastain elite ABC (Avidin-Biotin Complex) kit were used to perform immunohistochemistry of sections. The tissue sections were covered with blocking solution (1:100 horse serum) for 30 min at RT. The sections were treated with primary antibody in blocking solution (anti pCREB (1:200), anti CREB (1:250), anti γ-H2AX (1:100), anti p53 (1:50) and anti iNOS (1:100)) for 1 hr at RT. Negative control slides were treated with blocking solution for another 1 hr. The slides were then washed with 1X PBS for 5 min. The sections were covered with universal secondary antibody solution (1:50) for 30-40 min at RT and then washed with 1X PBS. The sections were incubated with ABC solution for 1 hr at RT and then washed with 1X PBS. Metal enhanced DAB reagent was used as the substrate of horseradish peroxidase (HRP) which deposits a specific brown stain. The slides were washed with distilled water for 5 min followed by counterstaining with

haemtoxylin for 30 sec and thorough washing with distilled water. The slides were then dehydrated with increasing concentration of alcohol (80%, 95% and 100%) and then cleared with xylene twice for 5 min each. The sections were then mounted with DPX mountant and covered with coverslips.

2.3.5 Image acquisition.

The images of stained tissues were taken with Metasystems Imager. Z2 Zeiss microscope enabled with Metaviewer^{TM} V2 software. The image of each slide (4 GB) generated was analysed using Vslide Metaviewer^{TM} software. (Dr. Kishore Amin's Lab, ACTREC).

2.3.6 Data analysis

For each section, one negative control was used which was treated exactly the same way except for the treatment with primary antibody. The slide's images were analyzed and the staining was independently evaluated by two different observers. Every sample (5-7 images/sample) was given a score in which the total intensity of staining (no staining = 0; low level = 1; medium staining = 2; strong staining = 3) and the percentage of stained cells (0% = 0; under 10% = 1; 11-50% = 2; 51-80% = 3; over 80% = 4) was multiplied. Using this system, the maximum score is 12 (with over 80% of the cells showing strong staining) [330]. Cellular localization (cytoplasm or nucleus or both) and tissue distribution (stroma, infiltrating cells) were determined by visual inspection of all the images. The nuclear staining in the tumor cells was counted for determining distribution of γ-H2AX, p53, CREB and pCREB and cytoplasmic staining was considered in iNOS labeled samples.

2.3.7 Bio-informatic analysis using Oncomine

ONCOMINE is a cancer microarray database with 700+ independent datasets and web-based data-mining platform aimed at facilitating discovery from genome-wide expression analyses. *ONCOMINE* (www.oncomine.org) was developed in Chinnaiyan lab at University of Michigan led by Compendia co-founder, Dan Rhodes. This database facilitates differential expression analysis comparing most major types of cancer with respective normal tissues as well as a variety of cancer subtypes. Clinical and pathology-based analyses are also available. Data can be queried and visualized for a selected gene across all analyses or for multiple genes in a selected analysis facilitating rapid interpretation of a gene's potential role in cancer.

2.3.8 Statistical analysis

All results are expressed as mean ± S.E.M. Statistical difference between means was assessed using independent Student's t test, with a 'p' value less than 0.05 considered significant.

For immunohistochemistry data analysis, descriptive data that included frequency (number of cases with score range 0-12), mean, median and standard deviation were determined for all the groups. Since the assessment of staining was done based on the scores, a nonparametric method, the Mann-Whitney test, was used for comparing the distributions of ranks in two unpaired groups. The nonparametric Spearman's rho correlation coefficient was used to analyze associations between pairs of markers. The chi square or Fisher's exact test was used to compare the expression of marker in different clinicopathological groups of IDC patients. For all the tests, a value of p less than or equal to 0.05 was considered statistically

significant. All the statistical analysis was performed using GraphPad™ Prism 6 software (Version 6.05) and Microsoft Excel software.

Table 12: Statistical tools employed in the study

S.No	Data to be analyzed	Statistical test used
1.	Expression of bio-marker in different clinico-pathological groups of IDC based on scores when all expected values are greater than 1.0 and at least 20% of the expected values are greater than 5	Chi- Square Test
2.	Expression of bio-marker in different clinico-pathological groups of IDC based on scores with small sample size and 2X2 contingency table where exact p value is calculated	Fisher's exact test
3.	Comparion of the distributions of scores in two unpaired groups	Mann-Whitney Test
4.	Comparion of the distributions of scores in more than two unpaired groups	Kruskal-Wallis Test
5.	Associations between pairs of markers	Spearman's Rho Correlation Coefficient

CHAPTER 3

RESULTS

Breast cancer is a multifaceted disease comprised of distinct biological subtypes with a varied spectrum of clinical, pathological and molecular features that have different prognostic and therapeutic implications. Consensus regarding the definitive prognostic/predictive marker is yet to be reached, but research is ongoing for understanding the role of all the different constituents of the tumor microenvironment. One important constituent that actively support cancer development and progression are the inflammatory components. But how the inflammation link operates in breast cancer is still an open question. Macrophages are the most important source of inflammation and focal macrophage infiltration is an important prognostic factor in breast invasive carcinoma and reduced survival is associated with high infiltration rates [331].

The results chapter is subdivided into three parts. Part I describes the findings of the role of macrophages in growth and migration of breast cancer cells *in vitro*. The breast cancer cell lines MCF7 and MDA-MB-231 were used as a model system to study the effects of macrophage conditioned medium. TGF-β1-ROS-ATM-CREB mediated signaling axis was identified to play a major role in macrophage mediated migration of human breast cancer MCF7 cells. In part II of the results chapter, the soluble cytokines present in the conditioned medium were identified using ELISA. The novel proteins present in macrophage conditioned medium were identified by 2-D electrophoresis and MALDI-TOF. Matrix metalloproteineases 1 and 9 were amongst the proteins identified from these studies and their expression was confirmed using gelatin zymography. In part III of the results chapter, the expression of some selected markers identified in the *in vitro* study was studied in invasive ductal carcinoma (IDC) and benign fibroadenoma tissue samples. The markers chosen for the immunohistochemistry studies were p53, γ-H2AX, iNOS, pCREB and CREB. Amongst the markers studied, iNOS and CREB expression was significantly higher in IDC as compared to fibroadenoma.

CHAPTER 3.1

Role of macrophages in growth and migration of breast cancer cell lines.

Interactions between tumor and immune cells and the soluble factors they secrete, influence the tumor cell survival and proliferation, integrity of the ECM, invasion, angiogenesis and metastasis. The macrophage – tumor interaction was studied by employing monocyte conditioned medium (MCM) and macrophage conditioned medium (MϕCM) treatment to epithelial breast cancer cell line, MCF7 and invasive breast cancer cell line, MDA-MB-231.

3.1.1. Differential modulation of growth pattern of breast cancer cells MCF7 and MDA- MB-231 by MϕCM

3.1.1.1 Changes in colony forming capacity

To assess the effect of macrophages on growth of breast cancer, MCF7 and MDA-MB-231 cells were treated with MCM or MϕCM. Treatment with MϕCM resulted in decreased colony forming ability of both breast cancer cell lines (Figure10a and 10c). There was greater than 2 fold decrease in the number of colonies in MCF7 cells and more than 3 fold decrease in the number of colonies in MDA-MB-231 cells ($P<0.01$; Figure 10b and 10d).

a.

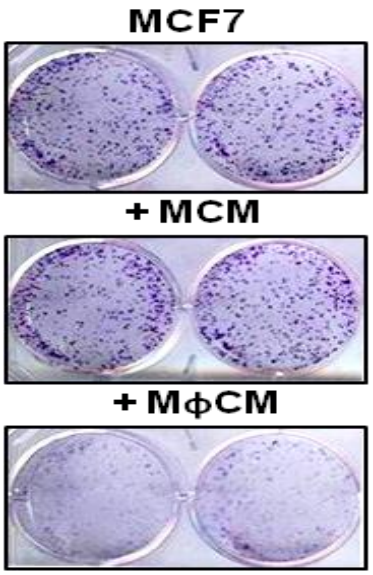

b.

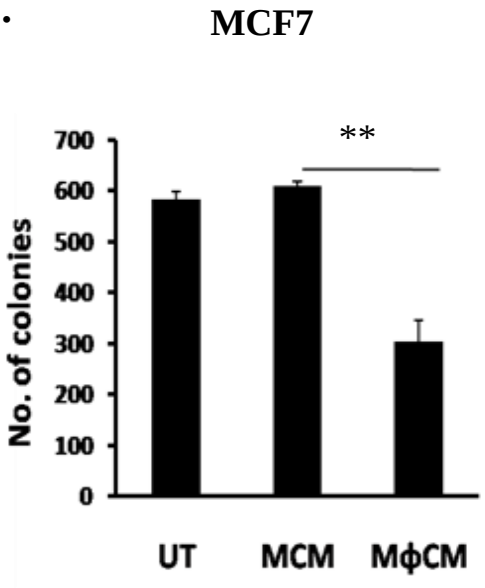

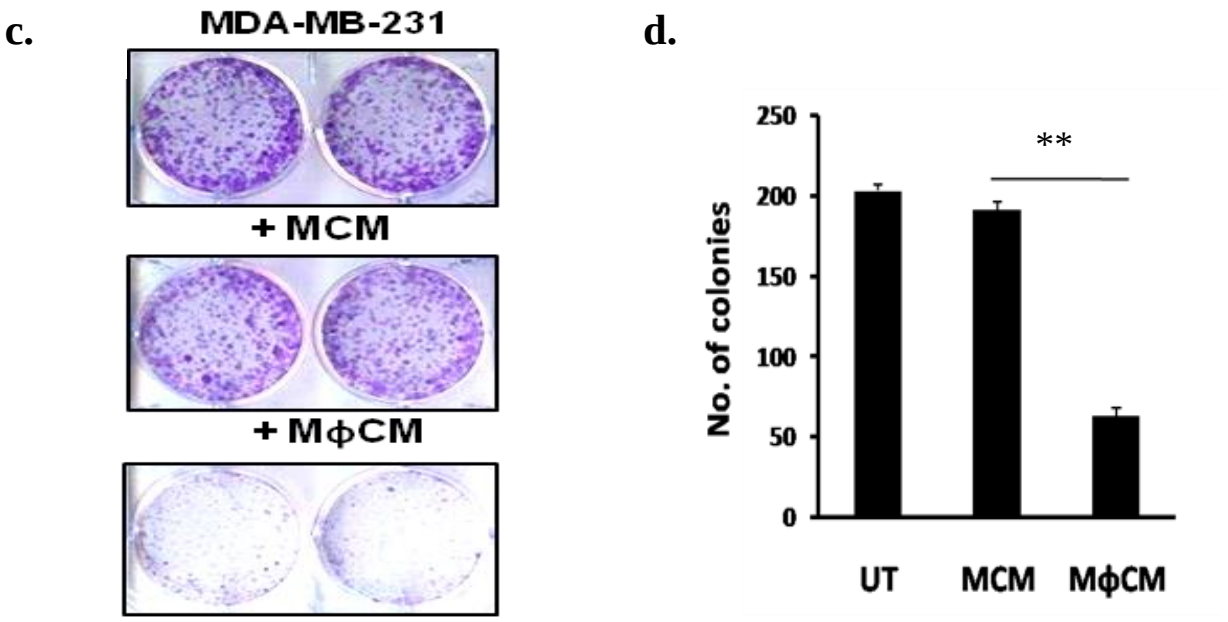

Figure 10: MϕCM decreases colony forming ability of breast cancer cells. MCF7 and MDA-MB-231 cells were grown for 6 days in presence of MCM or MϕCM. Once colonies were formed, cells were washed with PBS and fixed with cold methanol: acetone (7:3). Fixed colonies were stained with crystal violet. (a, c) Photomicrograph of the plate in duplicates. (b, d) Number of colonies were quantified in Oxford optronix gelcount^{TM} using Gelcount^{TM} software. Data from one representative experiment is shown. The experiment was repeated three times. **P<0.01.

3.1.1.2 Changes in morphology of breast cancer cells

When the colonies were observed microscopically, distinct changes in colony forming pattern were seen with MϕCM treatment. In MCF7 cells, though there was decrease in the number of colonies following MϕCM treatment, the smaller colonies had merged with each other forming a network. In contrast, colonies were compact and distinctly separated in MCM and untreated cells (Figure 11a). This was also accompanied by a decrease in number of cells

(Figure11b). These observations were also validated by the change in scatter properties of MCF7 cells treated with MϕCM. There were two distinct populations, viable cells with higher FSC and dead cells with lower FSC and SSC (Figure11c). Apoptotic cells are characterized by lower FSC and SSC [332].

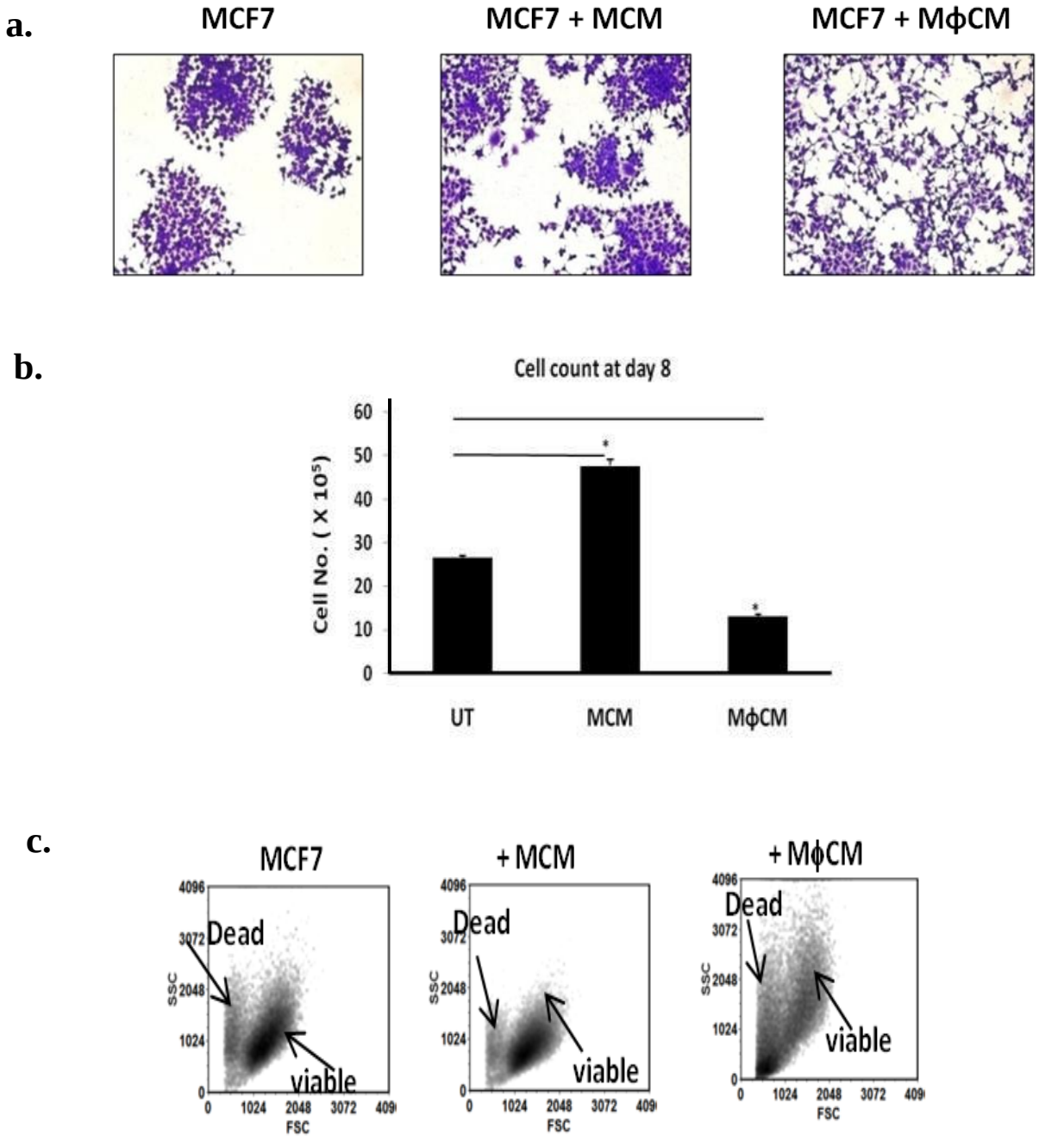

Figure 11: MϕCM induced distinct changes in MCF7 cells morphology. (a) Photomicrograph (10X) of MCF7 colonies showing alterations in morphology following MCM and MϕCM treatment. Images were acquired using a Nikon Eclipse Ti™ inverted microscope equipped with a Nikon digital camera using NIS elements™ software. (b) The cell number was ascertained on day 8 following treatment with conditioned media using haemtocytometer. (c) The forward and side scatter properties of the cells were analyzed by acquiring twenty thousand cells in Partec Cyflow space flow cytometer and analysed using FCS Express™ software. *P<0.05.

However, in MDA-MB-231, though the number of colonies was fewer, the cells were larger in size and had not merged with the neighboring colonies like MCF7 cells (Figure12a). The increased size was substantiated by the presence of population with increased FSC and SSC in MDA-MB-231 cells treated with MϕCM (Figure 12b).

a.

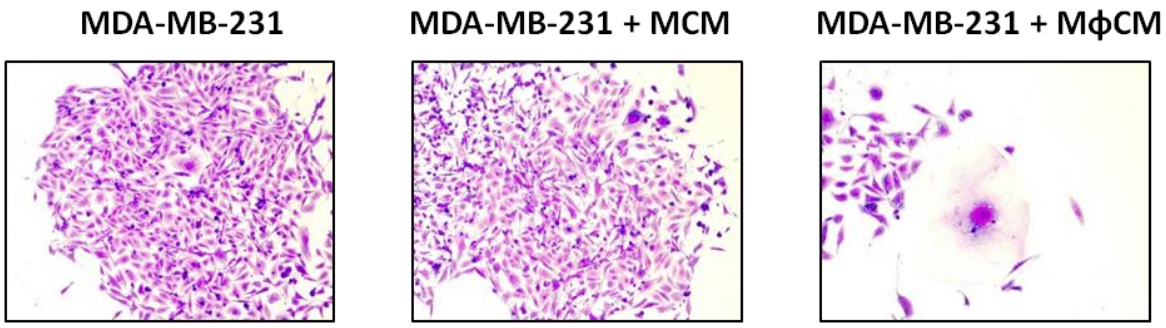

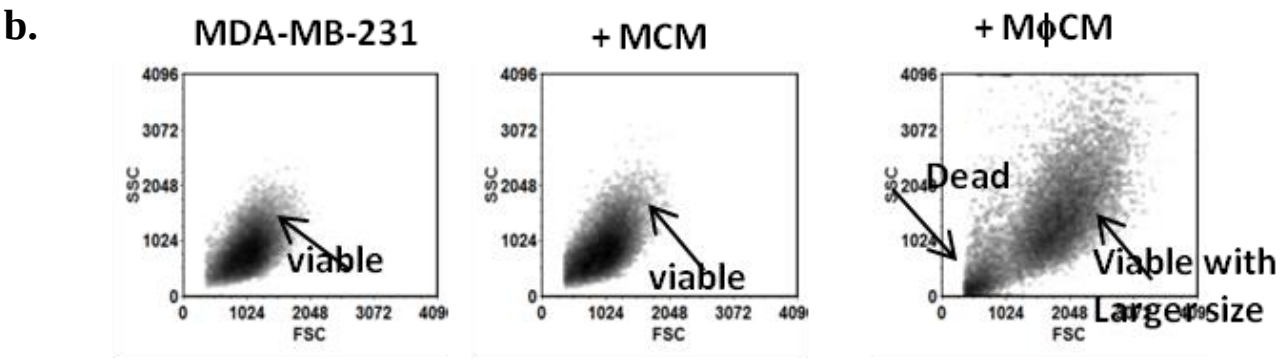

Figure 12: MϕCM induced distinct changes in MDA-MB-231 morphology. (a) Photomicrograph (10X) of MDA-MB-231 colonies showing alterations in morphology. Images were acquired using a Nikon Eclipse Ti™ inverted microscope equipped with a Nikon digital camera using NIS elements™ software. (b) The forward and side scatter properties of the cells were analyzed by acquiring twenty thousand cells in Partec Cyflow space flow cytometer and analysed using FCS Express™ software.

3.1.2 Effect of MϕCM on apoptosis

The role of apoptosis was studied in MCF7 and MDA-MB-231 cells after MCM and MϕCM treatment, since a decrease in cell number and clonogenic ability was observed. There was a marginal increase in cell death in MϕCM treated MCF7 cells, 24 hr after treatment which gradually increased up to three fold by 48 hr and remained high until 5 days of treatment ($P<0.05$; Figure 13a). In contrast, there was no increase in cells undergoing apoptosis in MDA-MB-231 cells even after 5 days of MϕCM treatment (Figure 13b).

a.

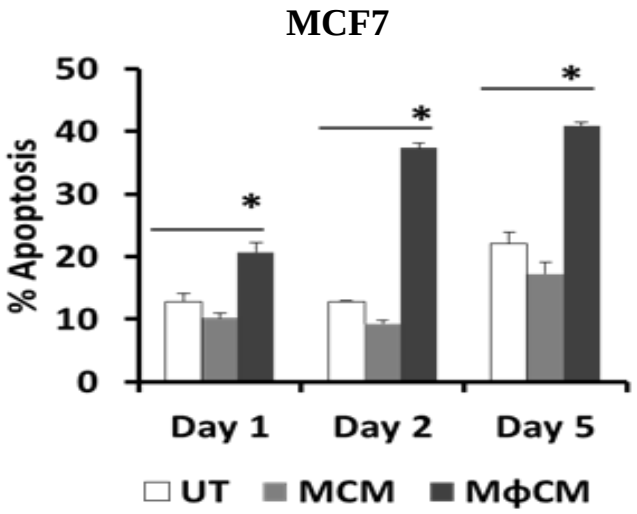

b.

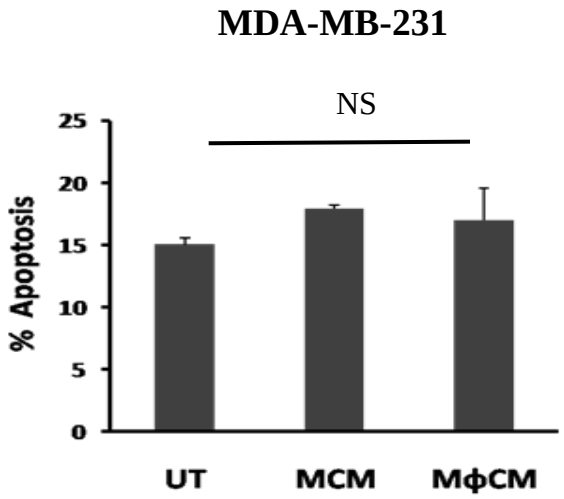

Figure 13: MϕCM increased MCF7 cell apoptosis. Cells were fixed and stained with propidium iodide on days 1-5 after treatment. Twenty thousand cells were acquired in Cyflow space flow cytometer and results were analysed using Cyflogic^{TM} software. Cells with less than G1 DNA content were enumerated as apoptotic cells. (a) Percent apoptosis in MCF7 cells. (b) Percent apoptosis in MDA-MB-231 cells. *P<0.05. NS- Not Significant

3.1. 3 Effect of MϕCM on mitochondrial membrane potential

Changes in mitochondrial membrane potential (ΔΨm) were further examined in these breast cancer cells treated with MCM and MϕCM since depolarization of the mitochondrial membrane is established to be part of the mitochondria-mediated apoptotic pathway [333]. ΔΨm was determined by flow cytometry using the fluorescent dye JC-1 and fluorescence was analyzed as ratio of FL-2 (585 nm) /FL-1 (525 nm). Mitochondrial membrane potential has a critical role in intrinsic pathway of apoptosis with initiating cascade of apoptosis linked to ΔΨm dissipation [334]. In MCF7 cells, the FL2/FL1 fluorescence ratio of JC-1 increased following treatment with MϕCM as compared to MCM treated and untreated cells ($P<0.01$; Figure 14). This intrinsic ratio (basal level between the two cell lines) was higher in MDA-MB-231 cells as compared to MCF7 cells and was not significantly altered following treatment with MϕCM (Figure14).

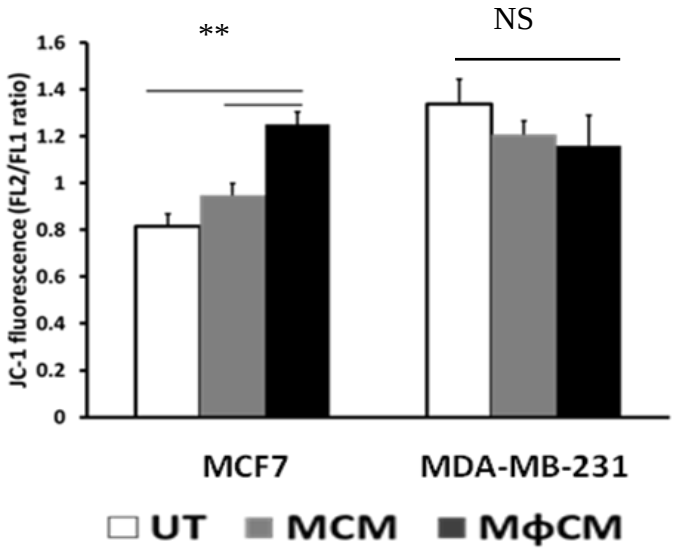

Figure 14: Effect of MϕCM on mitochondrial membrane potential in MCF7 and MDA-MB-231 cells. MCF7 and MDA-MB-231 cells were plated at a density of 10^4cells/ml and were treated with MCM or MϕCM for 5 days. The cells were labeled with 1 µM JC-1 for 30 min and then harvested. Twenty thousand cells were acquired in Cyflow Space flow cytometer and the data were analyzed by FCS Express™ software. A change in mitochondrial membrane potential was expressed as ratio of mean fluorescence intensity (MFI) (FL2)/MFI (FL1). **P<0.01; NS-Not significant

3.1.4 Effect of MϕCM on expression of pro-apoptotic and anti-apoptotic proteins

The expression of pro-apoptotic and anti-apoptotic proteins was evaluated in MCF7 and MDA-MB-231 cells treated with MϕCM. Differences in the basal level expression of these proteins were observed amongst the two cell lines, with MCF7 having higher expression of pro-apoptotic protein Bax whereas MDA-MB-231 containing a higher level of anti-apoptotic protein, Bcl-2 (Figure 15a). These results were confirmed by flow cytometric analysis of Bax and Bcl2 in both the cell lines (Figure 15 b-e). In MCF-7, the expression of Bcl-2 decreased following MϕCM treatment corresponding to the increase in apoptosis observed (Figure15 a, c). However, under the same conditions Bax levels also reduced (Figure 15 a, b). This was observed by western blot as well as flow cytometry. In MDA-MB-231 cells, MϕCM treatment resulted in a marginal decrease of Bax (Figure15 a, d), with an increase in Bcl-2 expression (Figure15 a, e).

a.

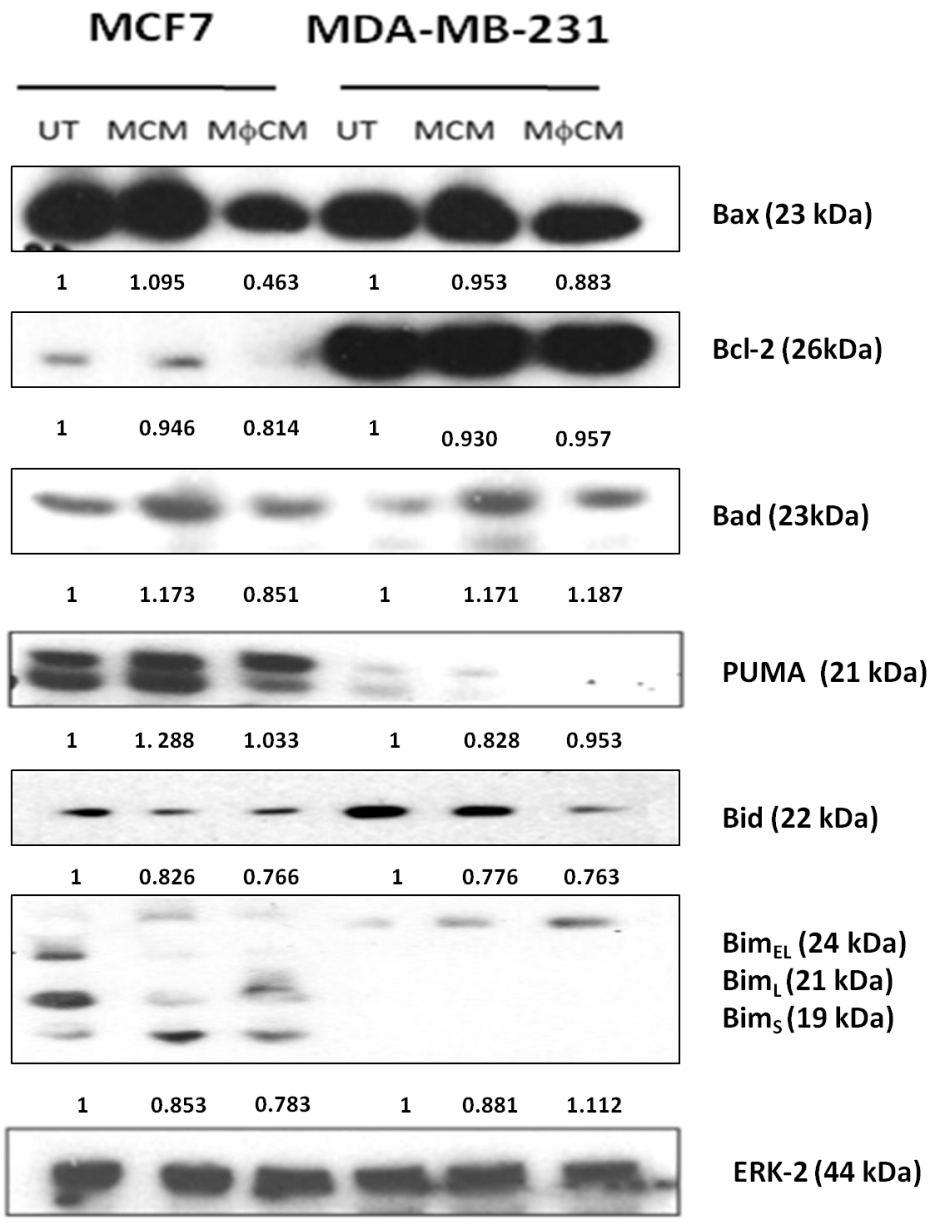
MCF7
MDA-MB-231
UT MCM MϕCM UT MCM MϕCM
Bax (23 kDa)
1 1.095 0.463 1 0.953 0.883
Bcl-2 (26kDa)
1 0.946 0.814 1 0.930 0.957
Bad (23kDa)
1 1.173 0.851 1 1.171 1.187
PUMA (21 kDa)
1 1. 288 1.033 1 0.828 0.953
Bid (22 kDa)
1 0.826 0.766 1 0.776 0.763
BimEL (24 kDa)
BimL (21 kDa)
BimS (19 kDa)
1 0.853 0.783 1 0.881 1.112
ERK-2 (44 kDa)

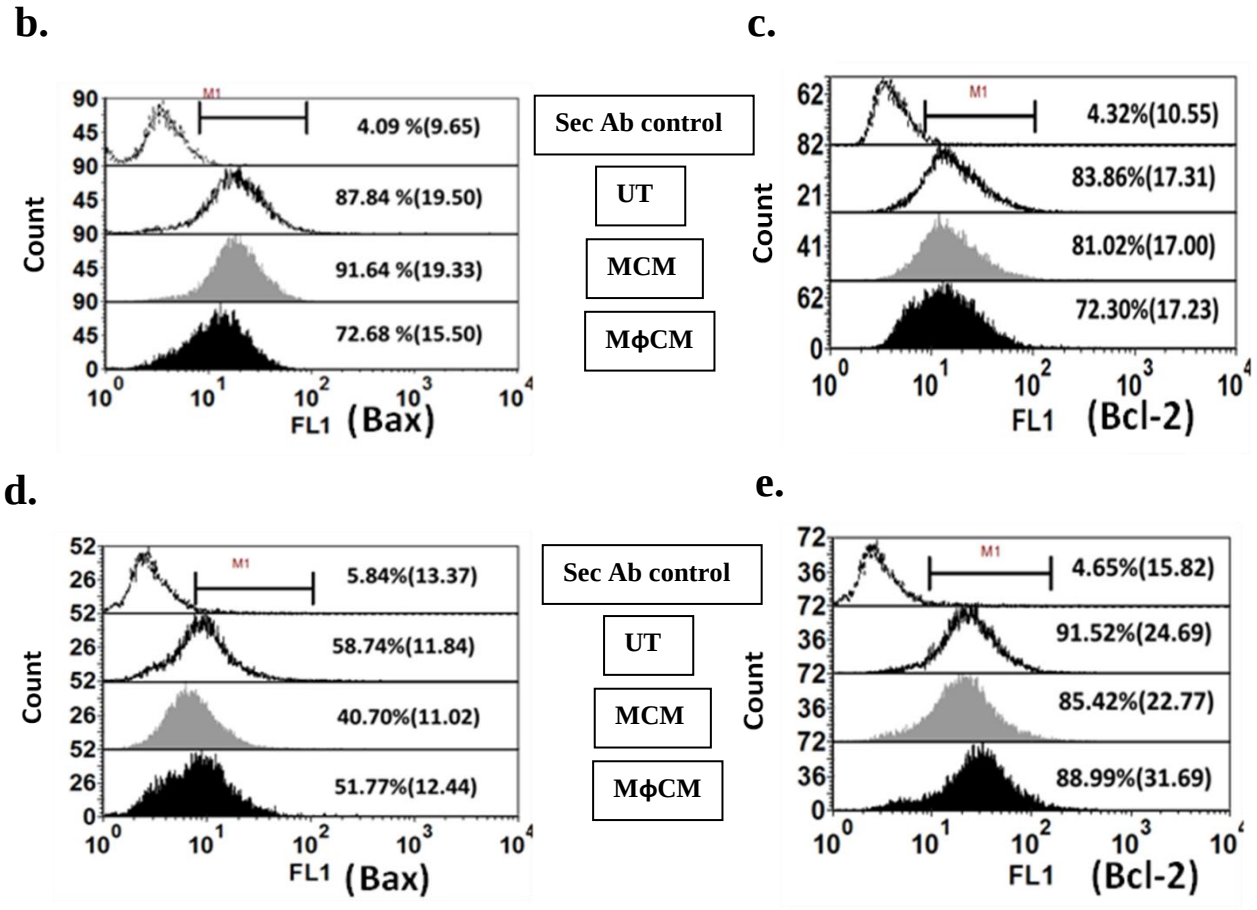

Figure 15: Effect of MϕCM on expression of pro- and anti- apoptotic proteins. (a) Western blot analysis of pro-apoptotic and anti-apoptotic proteins using specific antibodies. Cells were treated with MCM and MϕCM for 5 days and whole cell extract was prepared using lysis buffer. The numbers below the blots represent the ratio of expression of the specific gene to the loading control (ERK-2) quantified using ImageJ software for gel analysis. (b) MCF7 cells were treated with MCM or MϕCM for 5 days and labeled with anti-Bax antibody. Twenty thousand cells were acquired in Cyflow Space flow cytometer and the data were analyzed by FCS Express^{TM} software. Flow cytometric analysis of Bax expression in MCF7 cells. Flow cytometric analysis of (c) Bcl-2 expression in MCF-7 cells. (d) Bax expression in MDA-MB-231 cells (e) Bcl-2 expression in MDA-MB-231 cells. Numbers in histogram represent % positive cells. Mean fluorescence intensity is given in paranthesis.

3.1.5 Effect of MϕCM on activation of MAPKs in MCF7 cells

The changes in signal transduction induced in MCF7 cells by MϕCM treatment, were evaluated by studying the phosphorylation of SAPK, p38 and ERK-2 using specific antibodies. These MAPK proteins are activated by environmental stress, inflammatory cytokines as well as growth factors. MϕCM treatment in MCF7 did not cause appreciable change in phosphorylation of p38 but it resulted in activation of SAPK/JNK and ERK 1/2 (Figure 16).

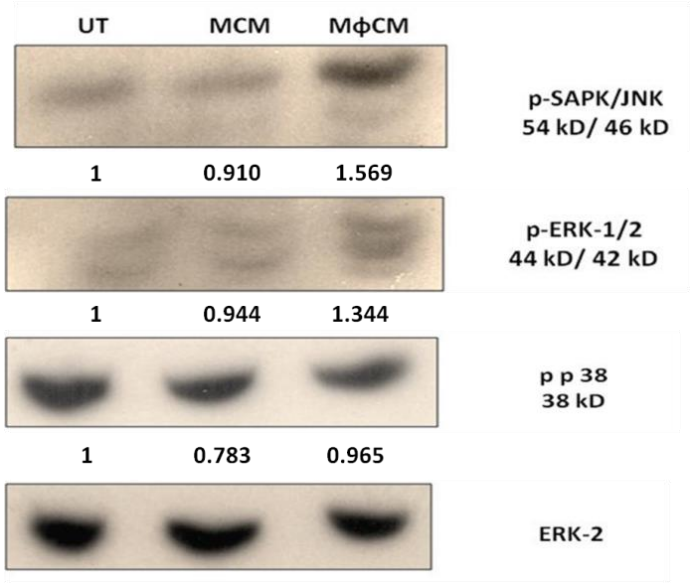

Figure 16: Effect of MϕCM on MAPKs phosphorylation in MCF7 cells. MCF7 cells were treated with MCM and MϕCM for 5 days. The cells were lysed and whole cell extracts were used for immunoblotting with antibodies against phospho-MAPKs. The numbers below the blots represent the ratio of expression of the specific gene to the loading control (ERK-2) quantified using ImageJ software for gel analysis.

3.1.6 MϕCM increased TGF-β1 and IL-6 secretion with up regulation of TGF-β1 and EGFR in MCF7 cells

A variety of cytokines and growth factors, such as tumor necrosis factor (TNF-α), transforming growth factor-β (TGF-β), hepatocyte growth factor (HGF), epidermal growth factor (EGF) etc., have been implicated in tumor-stroma cross-talk. The TGF-β-pathway is one of the major pathways altered in tumors, including breast cancer [335, 336]. TGF-β1 levels were estimated in supernatant of MCF7 cells treated with MCM and MϕCM. This was undetectable in the control cells as well as MCM treated cells. However there was a significant increase ($P<0.01$) in MCF7 cells treated with MϕCM (Figure 17a). This was confirmed by detection of intracellular accumulation of TGF-β1. There was no change in the intracellular levels of TGF-β1 between untreated and MϕCM treated MCF7 cells. Inhibition of protein secretion using Golgi plug™, did not alter the levels of TGF-β1 in untreated (32%) and MCM treated cells (33%). However, there was an increase in the percentage of cells expressing intracellular TGF-β1 (50%) in MϕCM treated cells (Figure 17b).

Expression of TGF-β1 and IL-6 transcripts was assessed in MCF7 cells treated with MCM and MϕCM by real-time PCR. The fold increase in cytokines transcripts was determined by calculating the ratio of normalized expression of these cytokines in MCF7 cells treated with MϕCM to that in MCM treated MCF7 cells. GAPDH was used as a reference gene. MϕCM treated MCF7 cells showed 4 fold increase in TGF-β1 mRNA and 6 fold increase in IL-6 mRNA as compared to MCM treated MCF7 cells (Figure 17c). This upregulation seems to be specific since there was no change in expression of TGF-β2 and TGF-β3 with MϕCM treatment. In parallel to increase in TGF-β1, an up regulation of receptors TGFβRII and EGFR was also

observed. There was 1.2 fold increase in TGFβRII expression and 1.7 fold increase in EGFR expression in MϕCM treated cell as compared to MCM treated MCF7 cells (Figure 17d).

a.

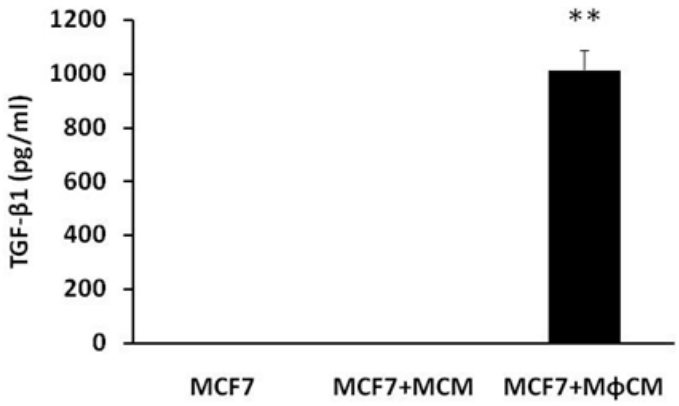

b.

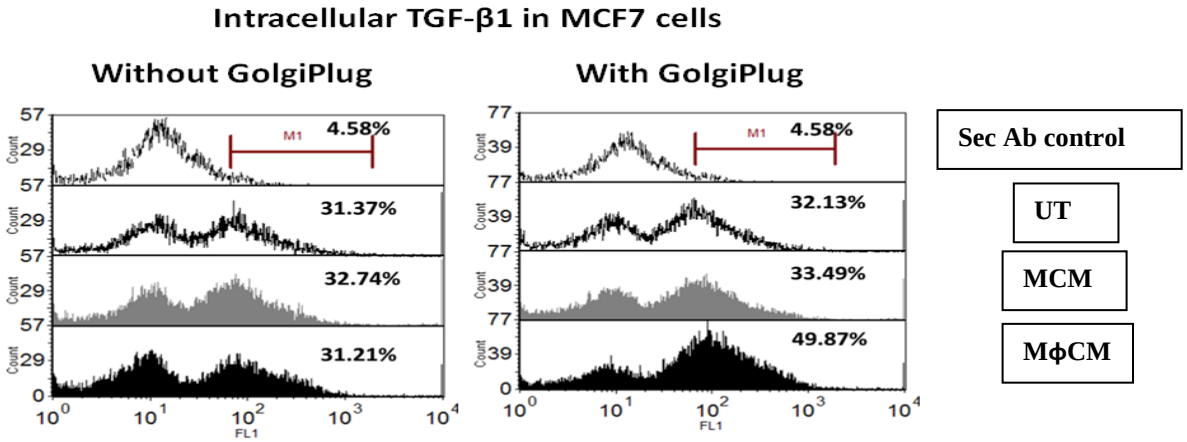

c.

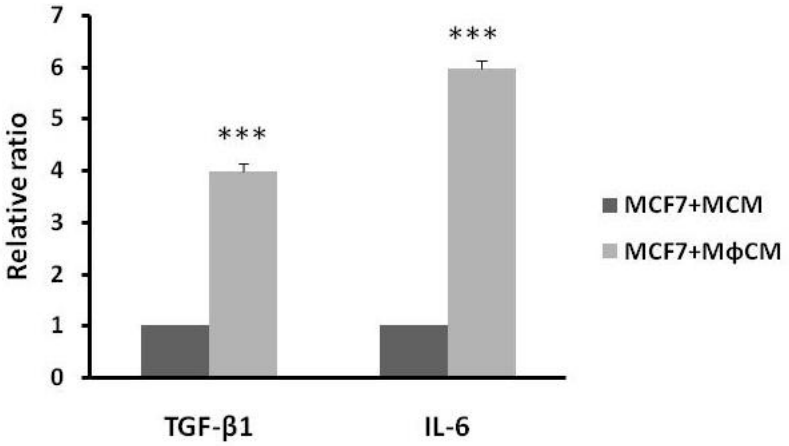

d.

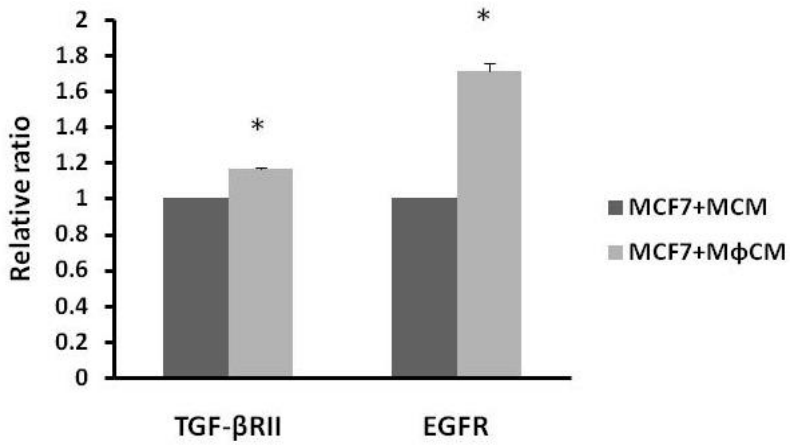

Figure 17: Secretion of TGF-β1 in MCF7 cells treated with MϕCM. (a) Secretion of TGF-β1 in the supernatant of MCF7 cells treated with MCM or MϕCM was assessed on day 5 by ELISA. (b) MCF7 cells were treated with MCM or MϕCM for 5 days and were labeled with anti-TGF-β1 antibody. Cells were acquired in Cyflow Space flow cytometer and data were analyzed by FCS Express™ software. (c) mRNA levels of TGF-β1 and IL-6 in MCM or MϕCM treated MCF7 cells were assessed by real-time PCR. (d) mRNA levels of TGFβRII and EGFR in MCM or MϕCM treated MCF7 cells were determined by real-time PCR. Ratios of these cytokines and receptors (relative to GAPDH) in MϕCM treated MCF7 cells in comparison to MCM treated MCF7 cells have been shown. Statistical analysis was carried out using REST software. *P<0.05; **P<0.01; ***P<0.001.

3.1.7 Increase in TGF-β1 is associated with increase in oxidative stress and DNA damage in MCF7 cells

As a multifunctional factor, TGF-β1 is involved in the regulation of many biological processes and induced concomitant apoptosis in some of the cells and significant increase in reactive oxygen species (ROS) and reactive nitrogen species (RNS) generation in the surviving cells. The oxidative and nitrosative stress as well as DNA damage response signaling was studied in breast cancer cells treated with MCM and MϕCM.

3.1.7.1 MϕCM increased ROS generation in MCF7 cells

TGF-β1 has been known to increase production of ROS in cancer cells [337]. ROS generation was therefore, estimated in breast cancer cells following treatment with MϕCM by using specific fluorescent dye, DCFDA. The cell permeable fluorogenic probe 2', 7'- DCFH-DA diffuses into cells and is deacetylated by cellular esterases to non-fluorescent 2', 7'- DCFH, which is rapidly oxidized to highly fluorescent DCF by ROS. The fluorescence intensity is proportional to the ROS levels within the cell cytosol. Treatment of MCF7 cells with MϕCM resulted in a gradual increase in ROS generation with 70% increase observed on day 5 ($P<0.01$; Figure18a-d). However, in parallel experiments conducted in MDA-MB-231 cells, there was no change in generation of ROS measured on day 5 (Figure 18e, f).

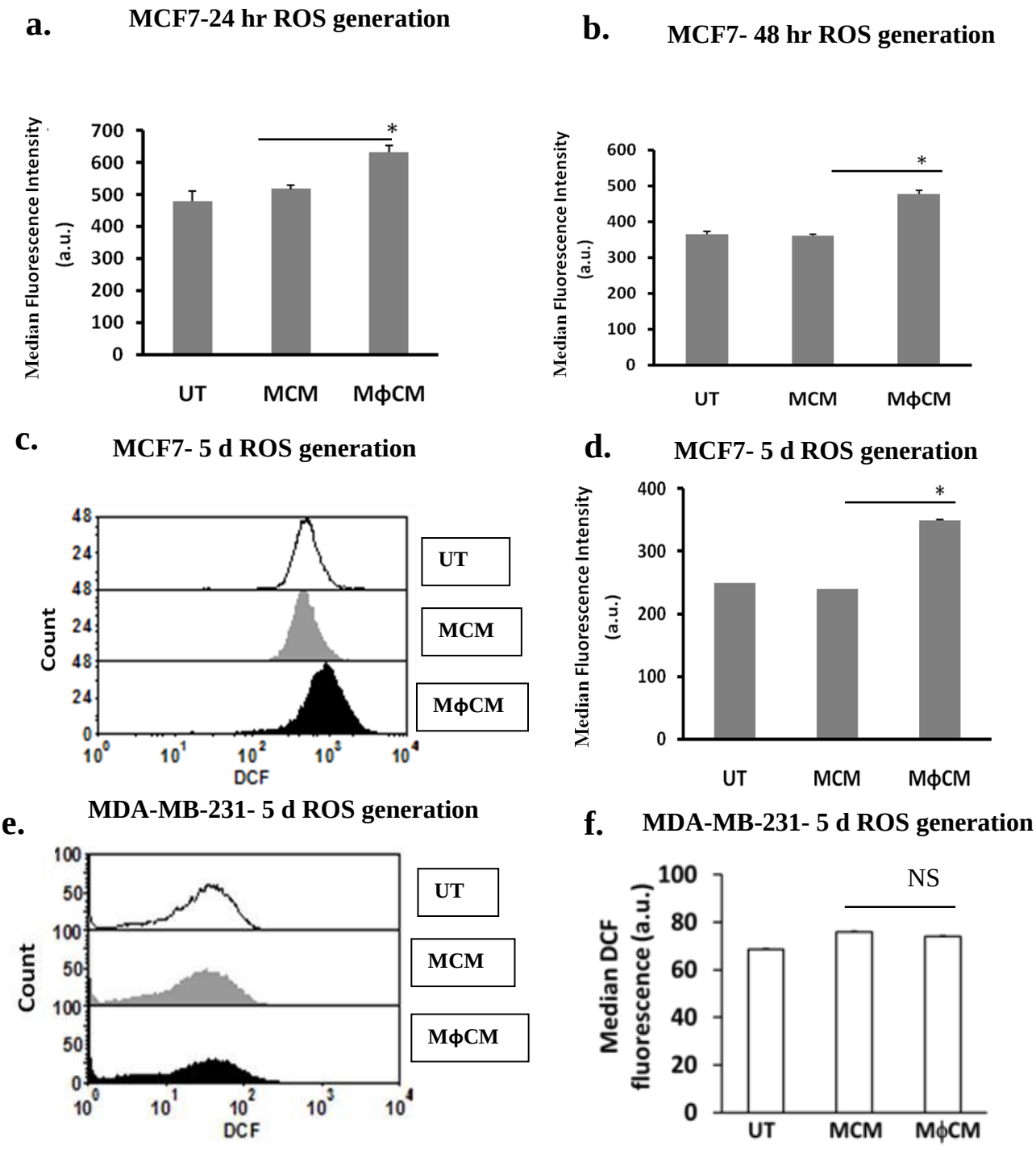

Figure 18: Estimation of ROS generation in breast cancer cells. Breast cancer cells MCF7 and MDA-MB-231 were incubated with 10% MCM or MϕCM for 24 hr, 48 hr and 5 days. Cells were labeled with DCFDA (20 µM) for 30 min and then were harvested. Twenty thousand cells

were acquired in Cyflow Space flow cytometer and the data were analyzed by FCS Express^{TM} software. DCF-DA fluorescence in MCF7 cells (a) 24 hr (b) 48 hr (c, d) 5 days after treatment. (e, f) DCF-DA fluorescence in MDA-MB-231 on day 5 after treatment. The experiment was repeated three times.* $P<0.05$. NS- Not significant

3.1.7.2 MϕCM increased iNOS expression and RNS generation in MCF7 cells

iNOS, presumably induced by inflammatory cytokines TNF-α, IL-1β and IFN-γ, produces larger amounts of NO which mediates its effect mainly due to conversion to reactive nitrogen species (RNS). NO reacts with the superoxide anion, yielding the potent oxidant peroxynitrite. RNS production in tumor cells is dependent upon the NO derived from iNOS. Treatment of MCF7 cells with MϕCM resulted in increased expression of iNOS. The iNOS positive MCF7 cells increased from 25% to 65% upon MϕCM treatment with MFI increasing from 155 to 369 (Figure 19a). RNS generation was estimated in breast cancer cells following treatment with MϕCM by using fluorescent probe DAF-FM. This dye is cell-permeant and passively diffuses across cellular membranes. Once inside cells, it is deacetylated by intracellular esterases to become non fluorescent DAF-FM which react with NO to form a fluorescent benzotriazole. The fluorescence intensity is proportional to RNS levels within the cell cytosol. When MCF7 cells were treated with MϕCM, there was a gradual increase in the generation of RNS corresponding to the increase in expression of iNOS. There was a 20% surge in RNS generation in 24 hr which further increased to more than 2 folds in 48hr and remained high until 5 days of treatment (Figure 19b-e). In MDA-MB-231 cells, there was no change observed in generation of RNS even after 5 days of MCM and MϕCM treatment (Figure19f, g).

a.

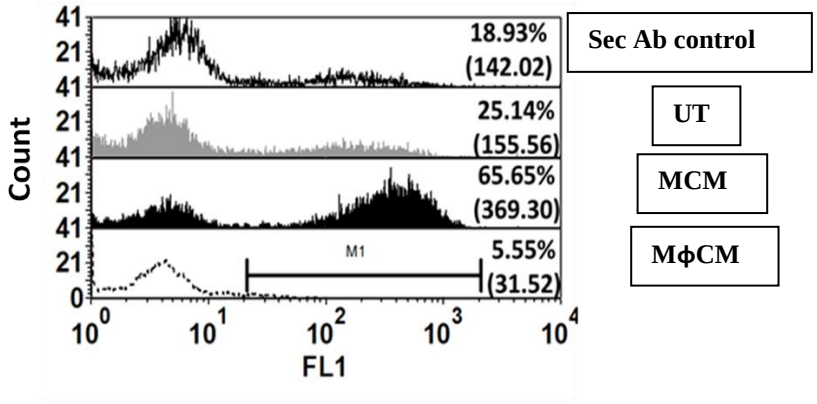

b. **MCF7- 24 hr RNS generation**

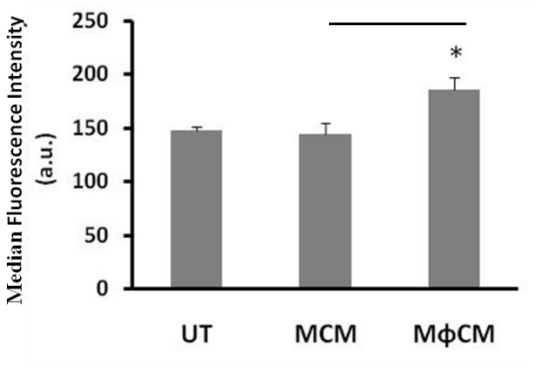

c. **MCF7- 48 hr RNS generation**

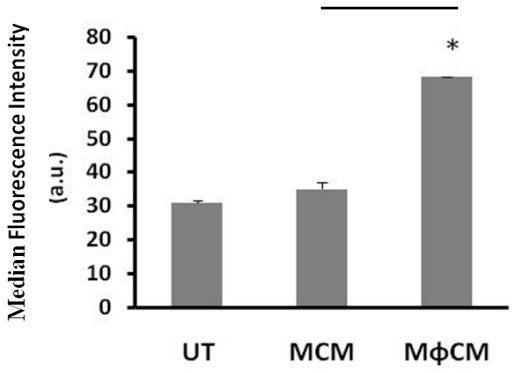

d. **MCF7-5 d RNS generation**

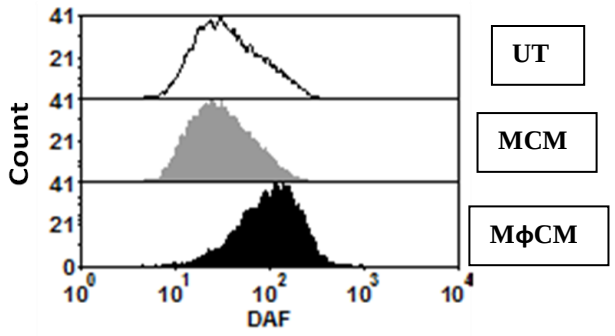

e. **MCF7- 5 d RNS generation**

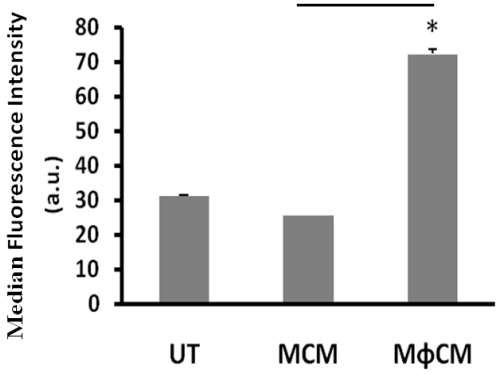

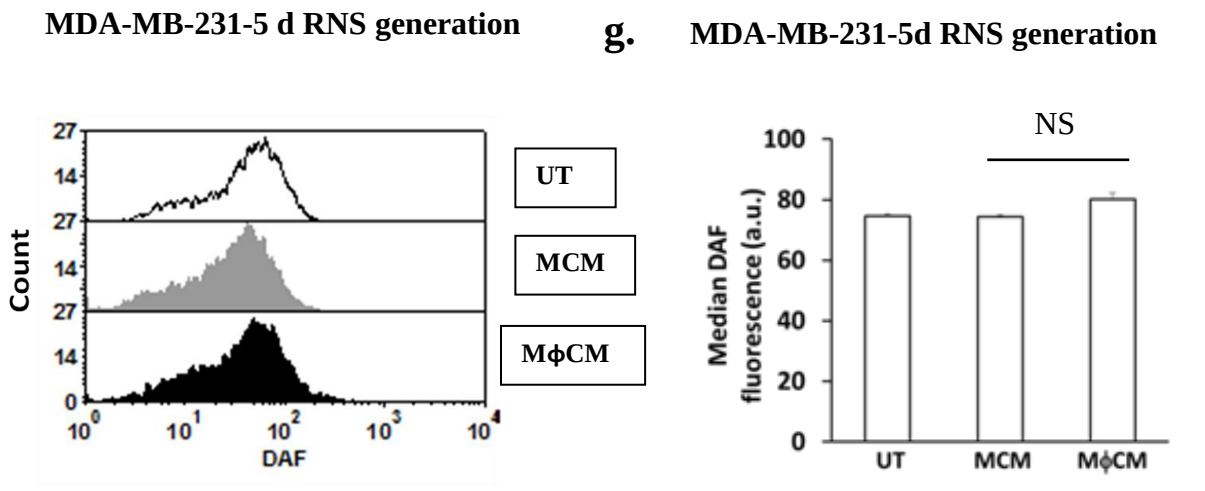

Figure 19: Estimation of iNOS expression and RNS generation in breast cancer cells. Breast cancer cells MCF7 and MDA-MB-231 were incubated with MCM or MϕCM for 5 days. (a) iNOS expression in MCF7 cells. The numbers in each histogram of figure.19a represent percentage positive cells and the median fluorescence intensity is given in parenthesis. Cells were labeled with 10 µM DAF FM for 30 min and the cells were harvested. Twenty thousand cells were acquired in Cyflow Space flow cytometer and the data were analyzed by FCS Express™ software. (b) DAF fluorescence in MCF7 cells at 24 hr (c) 48 hr (d, e) on day 5 after treatment. (f, g) DAF fluorescence in MDA-MB-231 on day 5 after treatment. Data from one representative experiment is shown. The experiment was repeated three times. *P<0.05. NS- Not significant.

3.1.8 MϕCM increased oxidative stress induced DNA damage response in MCF7 cells

Persistent increase in the level of ROS and RNS in cells leads to oxidative stress. Exposure of tumor cells to oxidative stress causes double-stranded DNA breaks (DSBs), triggering DNA damage response through activation of the ataxia telangiectasia mutated (ATM) kinase, which induces cell-cycle arrest and also promotes DNA repair to maintain chromosome stability. When activated, ATM undergoes auto phosphorylation at Ser1989 and phosphorylates the histone variant H2AX at Ser139 around DSBs, which also recruits other DNA repair proteins to sites of DNA damage. The phosphorylated histone H2AX (known as γ-H2AX) and the recruited DNA repair proteins form discrete nuclear foci at DSBs, providing surrogate markers to characterize the dynamic process of DNA repair [338].The DNA damage response was assessed in MCF7 cells by monitoring the expression of pATM, γ- H2AX as well as PARP. In the untreated and MCM treated MCF7 cells, there was no labeling for pATM or γ-H2AX. However, following MϕCM treatment, there was an increase in the expression of pATM (Figure 20a) as well as γ-H2AX foci (Figure 20b). A majority of the cells showed DNA damage and the foci were very intense in some of the cells indicating complex DNA damage. This was confirmed by western blot as well as flow cytometry (Figure 20c, d). MFI of γ- H2AX labelled MCF7 cells increased from 62.50 to 83.44 after treatment with MϕCM (Figure 20d) as compared to that of cells treated with MCM. When the expression of PARP was assessed by western blot, full-length PARP was present in all the treatment groups, whereas the cleaved PARP was seen only in MϕCM treated MCF7 cells (Figure 20e).

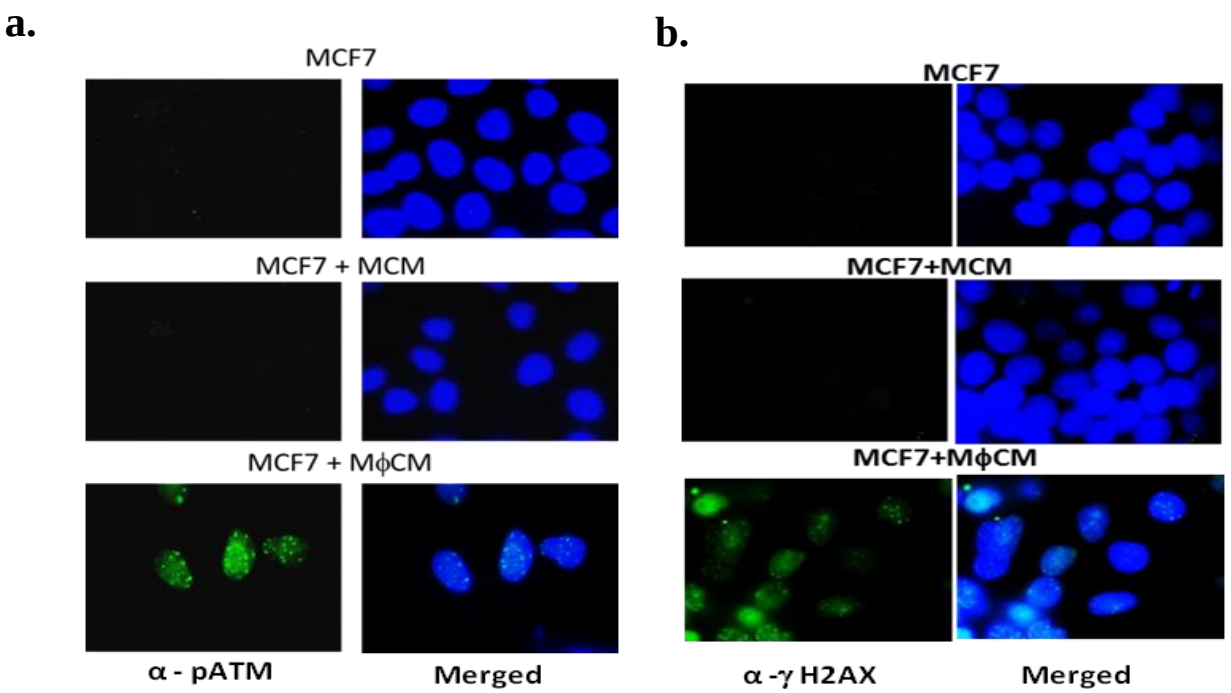
a.
MCF7
MCF7 + MCM
MCF7 + MϕCM
α - pATM
Merged
b.
MCF7
MCF7+MCM
MCF7+MϕCM
α -γ H2AX
Merged

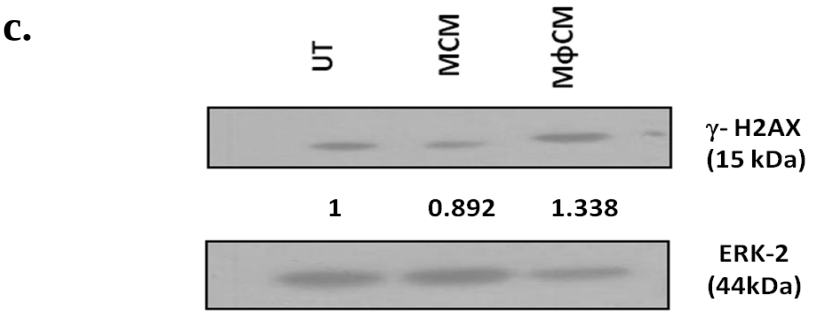
c.
UT
MCM
MϕCM
γ- H2AX
(15 kDa)
1
0.892
1.338
ERK-2
(44kDa)

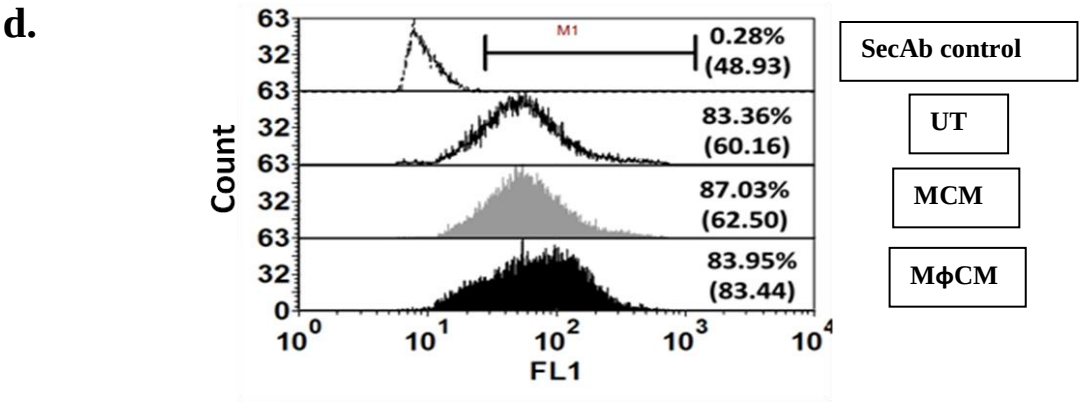
d.
Count
M1
0.28%
(48.93)
83.36%
(60.16)
87.03%
(62.50)
83.95%
(83.44)
FL1
SecAb control
UT
MCM
MϕCM

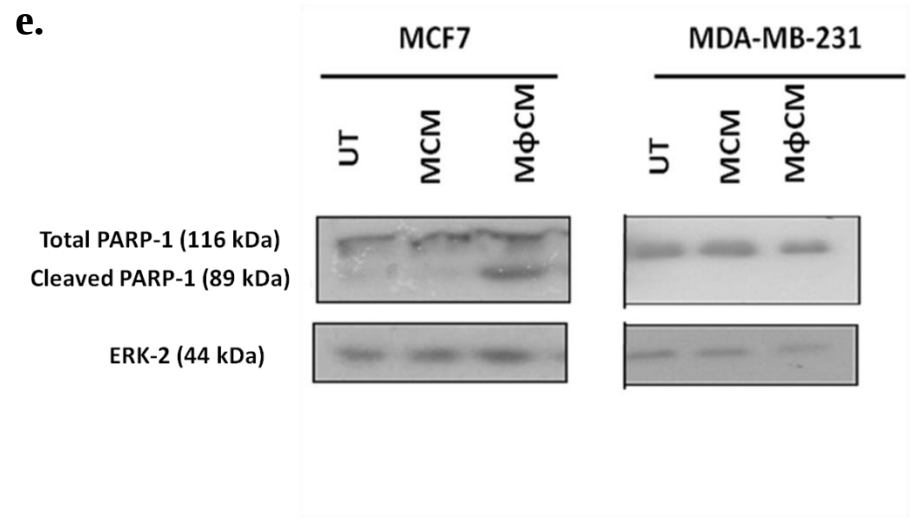

Figure 20: Oxidative stress increased DNA damage response in MCF7 cells. MCF7 cells (10^4 cells/ml) were grown on coverslips and treated with MCM or MϕCM for 5 days. The cells were labeled with (a) anti-phospho ATM and (b) anti-γ-H2AX primary antibody. The nuclei were counterstained with DAPI and visualized in a fluorescence microscope. Images were acquired using a Nikon Eclipse Ti™ inverted microscope equipped with a Nikon digital camera using NIS elements™ software. (c) Representative western blot of γ- H2AX in MCF7 whole-cell extracts. The expression of ERK-2 served as internal loading control. The numbers below the blots represent the ratio of expression of the specific gene to the loading control (ERK-2) quantified using ImageJ software for gel analysis. (d) Flow cytometric analysis of γ- H2AX expression in MCF7 cells. The numbers in each histogram represent percentage positive cells and the median fluorescence intensity is given in parenthesis.Twenty thousand cells were acquired in Cyflow Space flow cytometer and the data were analyzed by FCS Express™ software. (e) Western blot demonstrating PARP cleavage in MCF7 and MDA-MB-231 whole-cell extracts. The expression of ERK-2 served as internal loading control. The experiment was repeated three times.

3.1.9 MϕCM increased CREB phosphorylation in MCF7 cells

Deregulation of the response to ROS or DNA damage could result in activation of survival pathways leading to EMT [337, 339]. One of the important survival pathways that get activated is mediated by the transcription factor CREB. Hence the effect of MϕCM was assessed on the phosphorylation as well as expression of total CREB. The 43 kDa-basic/leucine zipper (bZip) transcription factor CREB plays important roles in cell differentiation, survival and cell proliferation [333]. There was a difference in the basal level of expression of pCREB (Figure 21a, 21c and 21b, 21d) between the two cell lines. There was no labelling in control MCF7 cells (Figure 21a and 21c) whereas control MDA-MB-231 cells were positive for pCREB (Figure 21b and 21d). However, upon treatment with MϕCM, MCF7 cells showed a dramatic increase in phosphorylation of CREB (Figure 21a, 21c). This was in contrast with MDA-MB-231 cells where the higher levels present in the untreated cells did not further change after treatment with MϕCM (Figure 21b, 21d).

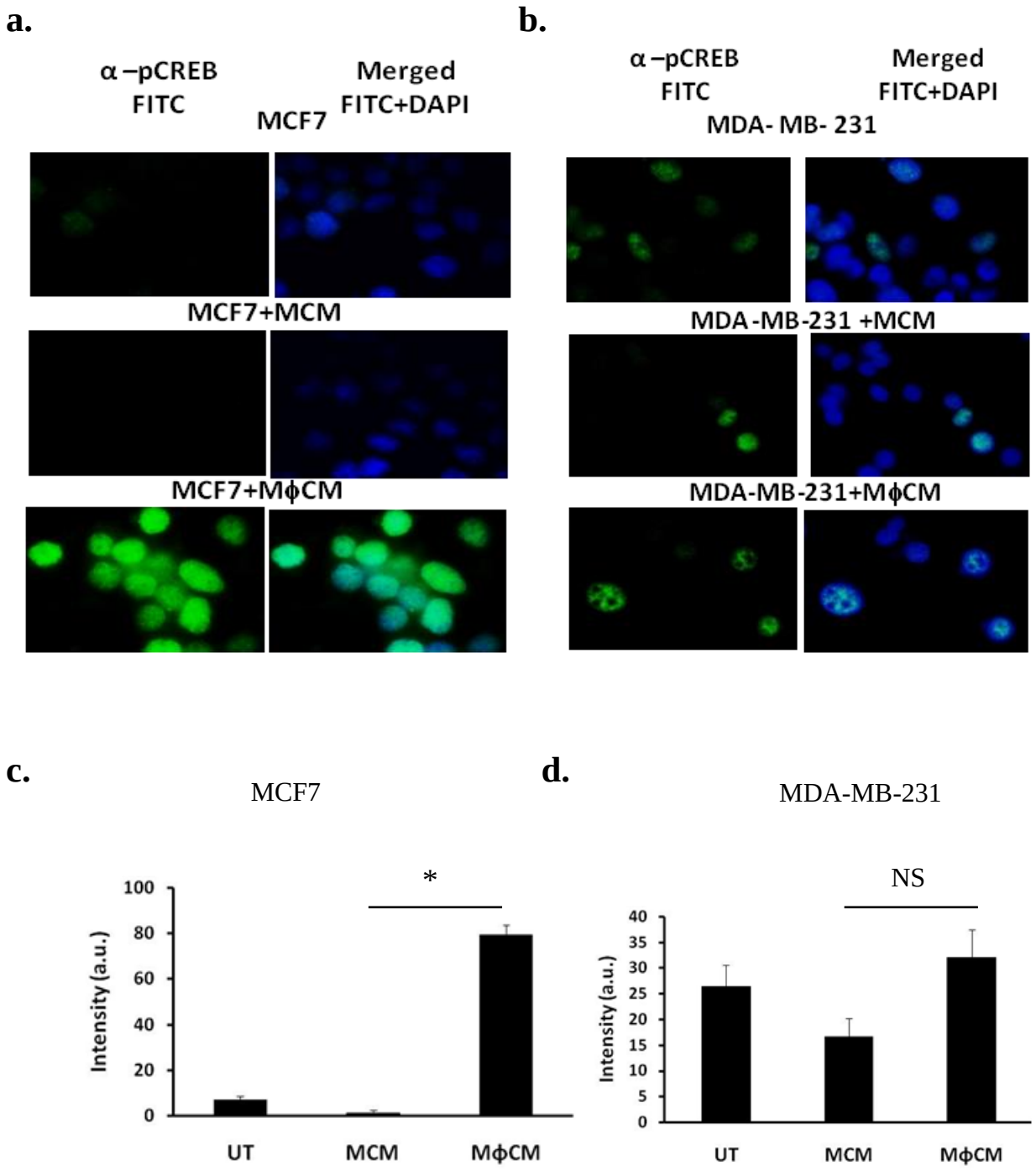

Figure 21: MϕCM induced phoshorylation of CREB in MCF7 cells. MCF7 and MDA-MB-231 cells were incubated with MCM or MϕCM for 5 days. The cells were labeled with pCREB antibody and visualized in a fluorescence microscope. Images were acquired using a Nikon Eclipse Ti™ inverted microscope equipped with a Nikon digital camera using NIS elements™

software. The intensity of pCREB labeling was quantified using Image J software in a minimum of 50 cells. Expression of (a, c) pCREB in MCF7, (b, d) pCREB in MDA-MB-231. Data from one representative experiment is shown. The experiment was repeated three times.*P<0.05. NS-Not significant

A difference in the basal level of expression of total CREB was also observed between the two cell lines (Figure 22a, 22c and 22b, 22d).There was no CREB labeling in control MCF7 cells (Figure 22a and 22c) whereas control MDA-MB-231 cells were positive for CREB (Figure 22b and 22d).However, upon treatment with MϕCM, MCF7 cells showed a significant increase in total CREB (P<0.05) (Figure 22a and 22c).

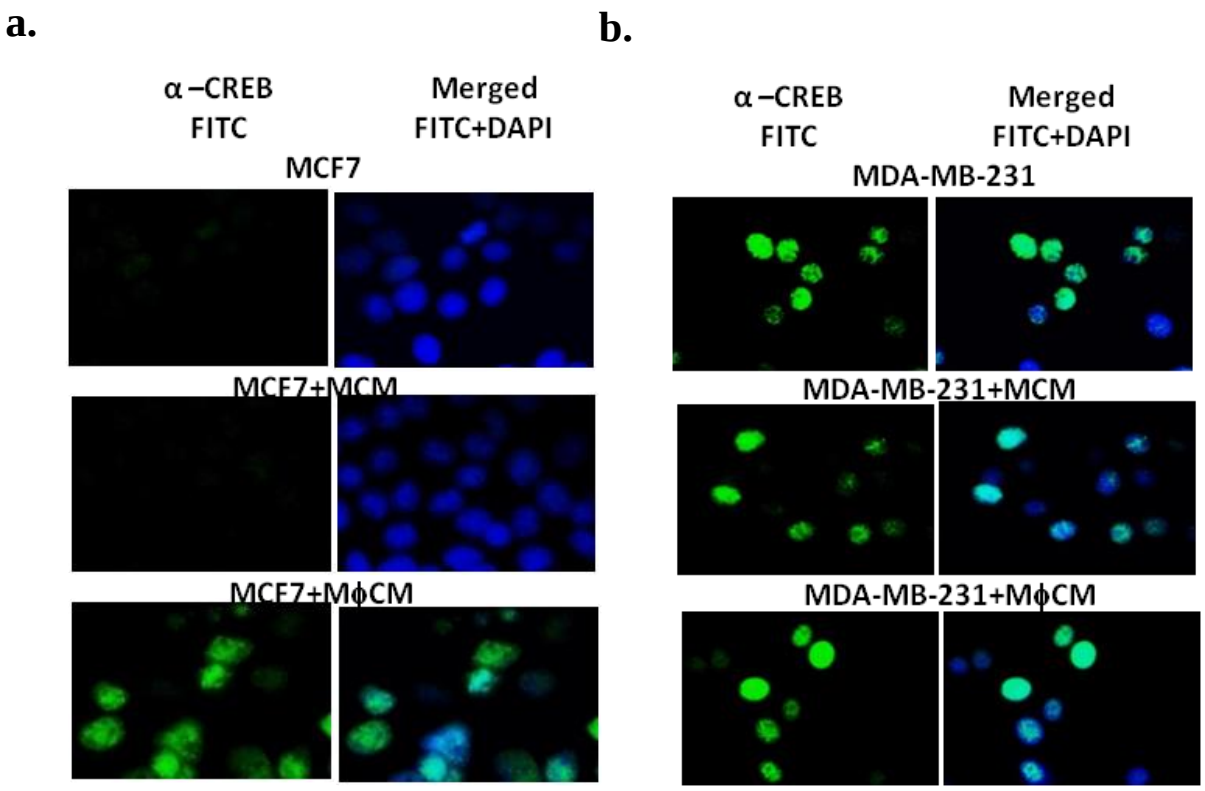

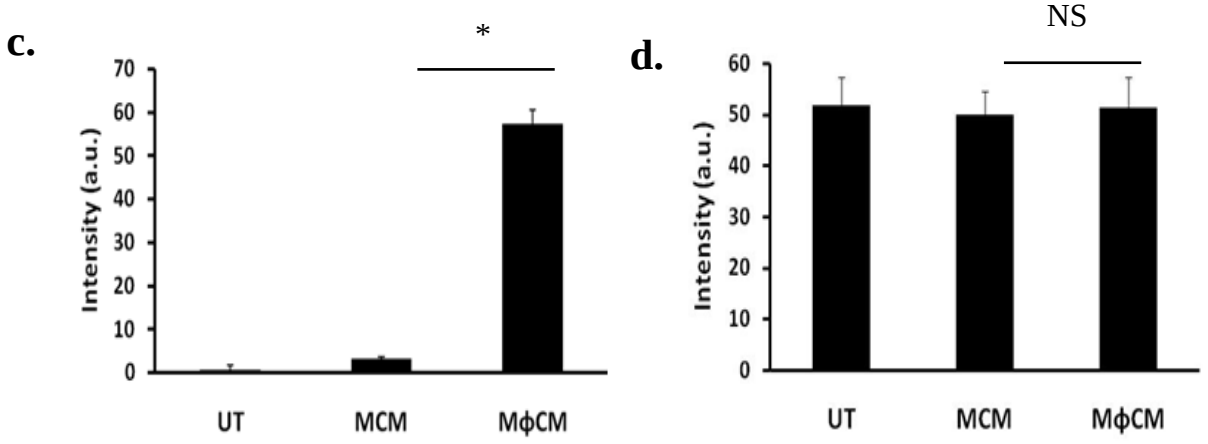

Figure 22: MϕCM induced expression of CREB in MCF7 cells. MCF7 and MDA-MB-231 cells were incubated with MCM or MϕCM for 5 days. The cells were labeled with the anti-CREB antibody and visualized in a fluorescence microscope. Images were acquired using a Nikon Eclipse Ti™ inverted microscope equipped with a Nikon digital camera using NIS elements™ software. The intensity of CREB labeling was quantified using Image J software in a minimum of 50 cells. Expression of CREB in (a, c) MCF7 and (b, d) MDA-MB-231. Data from one representative experiment are shown. The experiment was repeated three times. *P<0.05. NS- Not significant

3.1.10 MϕCM induced EMT responses in MCF7 cells

CREB binding proteins (CBP) mediate interactions between β-catenin and transforming growth factor-β signaling pathways and participate in regulation of EMT. Hence the effect of MϕCM treatment on vimentin expression and EMT response were studied in MCF7 cells.

3.1.10.1 MϕCM increased vimentin expression in MCF7 cells

The expression of TGF-β1 downstream protein vimentin, well known marker of EMT [340] was increased in MCF7 cells after treatment with MϕCM (Figure 23a) whereas in MDA-MB-231 cells, it was not affected though the basal expression was very high (Figure 23b).

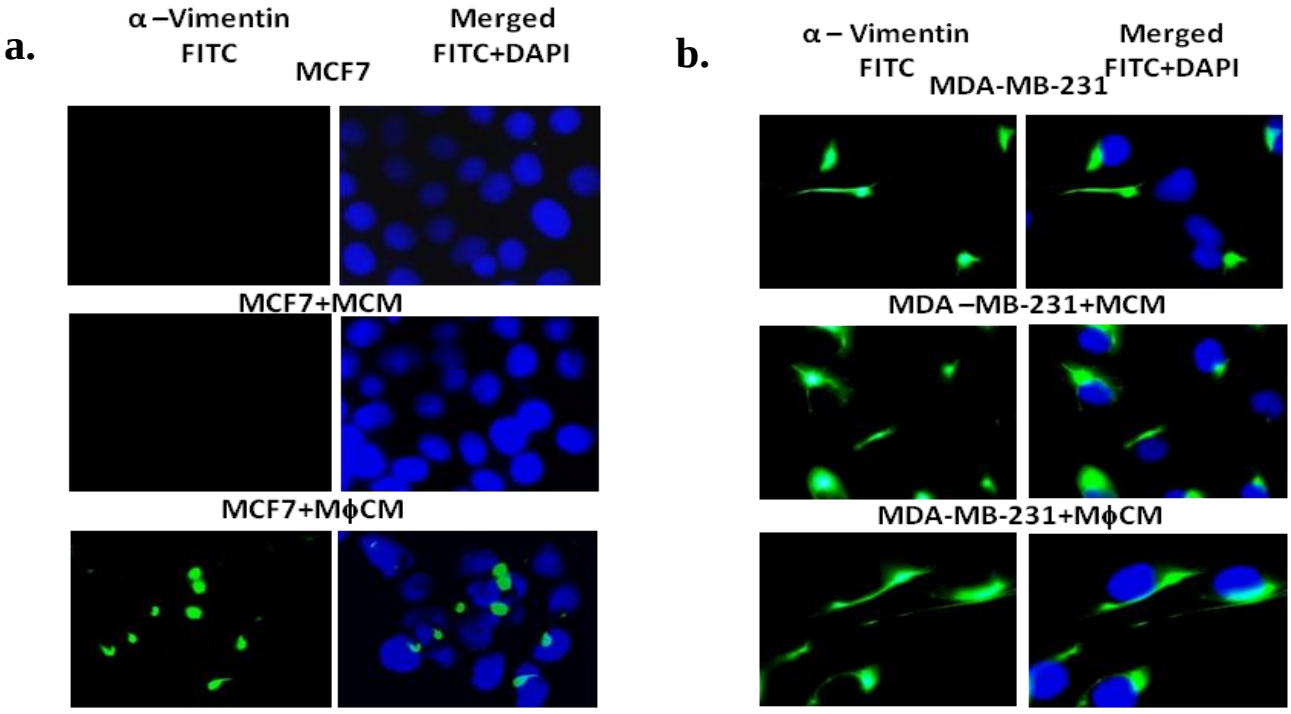

Figure 23. MϕCM induced expression of vimentin in MCF7 cells. MCF7 and MDA-MB-231 cells (10^4 cells/ml) were grown on coverslips and treated for 5 days. The cells were labeled with anti-vimentin primary antibody and alexa fluor 488 conjugated anti mouse IgG. The nuclei were counterstained with DAPI and visualized in a fluorescence microscope. Images were acquired using a Nikon Eclipse Ti™ inverted microscope equipped with a Nikon digital camera using NIS elements™ software. Vimentin expression in (a) MCF7 cells and (b) MDA-MB-231 cells.

3.1.10.2 MϕCM increased migration of MCF7 cells

EMT responses lead to changes in migratory properties of cells. These changes were evaluated using two well established *in vitro* model systems, the wound healing assay as well as transwell migration assay. MϕCM treatment resulted in increased closure of the wound area (Figure 24a, b) as well as migration through the transwell in MCF7 cells (Figure 24c, d). In MCF7 cells, there was a 4 fold augmentation in the cells moving into the wound area ($P<0.01$; Figure 24b) and 6 fold increase in the cells migrating through the transwell following MϕCM treatment ($P<0.01$; Figure 24d). However, in highly invasive MDA-MB-231 cells, the treatment did not further enhance cell migration (Figure 24e and 24f).

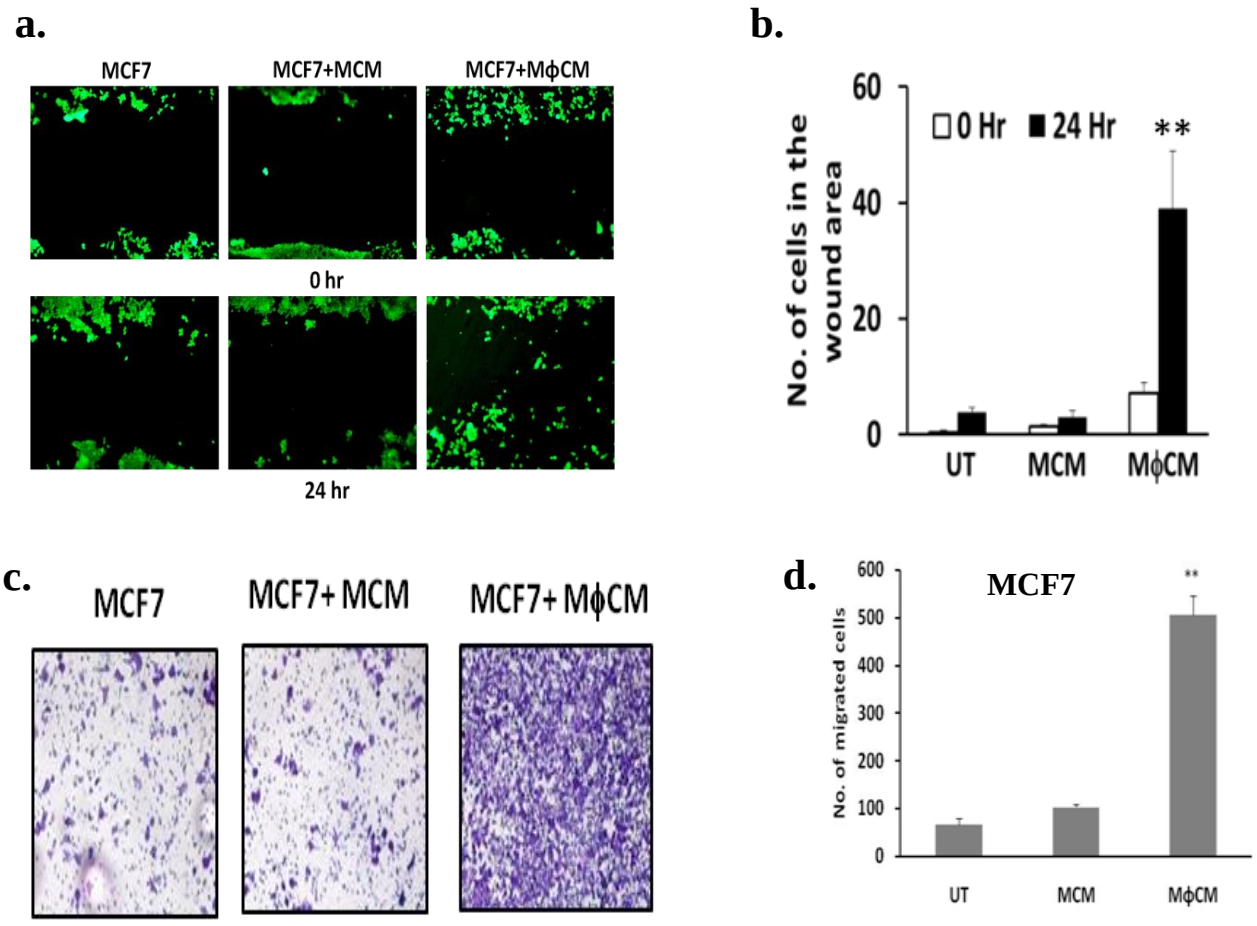

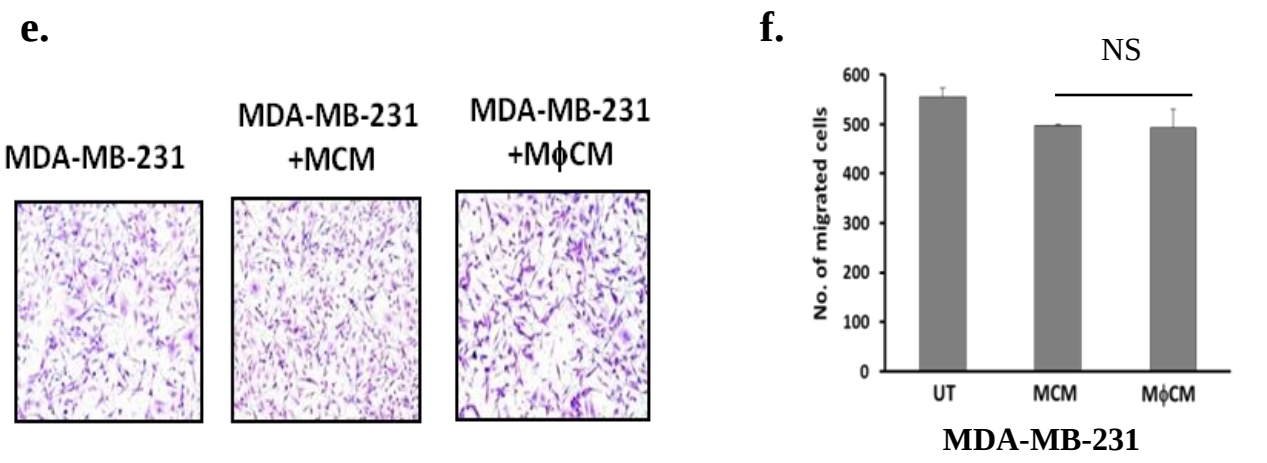

Figure 24: MϕCM induced EMT responses in MCF7 cells. (a) MCF7 cells were grown in presence of MCM or MϕCM for 5 days. After formation of a confluent monolayer, wounds were created using a sterile pipette tip and the cells were incubated with serum free media for 24 hr. The cells were stained with calcein AM and images of wound were acquired using a Nikon Eclipse Ti™ inverted microscope equipped with a Nikon digital camera using NIS elements™ software. (b)The number of cells in the wounded area calculated using CellProfiler™ image analysis software. Migration was assessed by plating cells in the top chamber of transwell inserts (8 µm) that were allowed to migrate for 72 hr. The bottom chamber contained MCM or MϕCM. The cells on the upper side of the membrane were removed with a cotton swab. The membranes were fixed in methanol: acetone (7:3) for 20 min and stained with crystal violet for 5 min (c) Photomicrograph of migrated MCF7 cells (d) The number of migrated MCF7 cells (e) Photomicrograph of migrated MDA-MB-231 and (f) The number of migrated MDA-MB-231 cells. Images from a representative experiment are shown. The migrated cells to the lower surface of the membrane were counted in ten randomly selected fields by light microscopy using CellProfiler™ software. **P<0.01. NS- Not significant.

3.1.11 Inhibition of ROS, RNS or DNA damage abrogated phosphorylation of CREB

The signaling pathways leading to MϕCM induced phosphorylation of CREB were delineated by assessing the ability of various ROS, RNS and DNA damage inhibitors to block this activation.

3.1.11.1 Effect of ROS, RNS and DNA damage inhibitors on phosphorylation of CREB in MCF7 cells

To characterize the signaling pathways leading to activation of survival factor, pCREB in MCF7, inhibitors of ROS, RNS or DNA damage response were employed. N-acetyl cysteine (NAC) was used to scavenge ROS. The NOS inhibitors, 1400W, a specific inhibitor of iNOS as well as L-N^G-monomethyl arginine (L NMMA) and N^G-nitro-L-arginine (L-NNA) were also used. CGK733, an inhibitor of ATM/ATR was used to inhibit DNA damage response. Pre-treatment with inhibitors of ROS, RNS or DNA damage substantially decreased phosphorylation of CREB induced by MϕCM treatment (Figure 25a, b). The intensity of pCREB expression in cells was quantitated using ImageJ software. There was a 70% decrease in the intensity of pCREB labeling on pre-treatment with 1400W ($P<0.01$), 3 fold decrease with NAC ($P<0.01$) and >2 fold reduction with CGK733 ($P<0.01$) (Figure 25b). Inhibition of iNOS with other inhibitors like NG-nitro-L-arginine (L-NNA), L-NG-monomethyl arginine citrate (L-NMMA) also resulted in diminished phosphorylation of CREB (Figure 25b).

a.

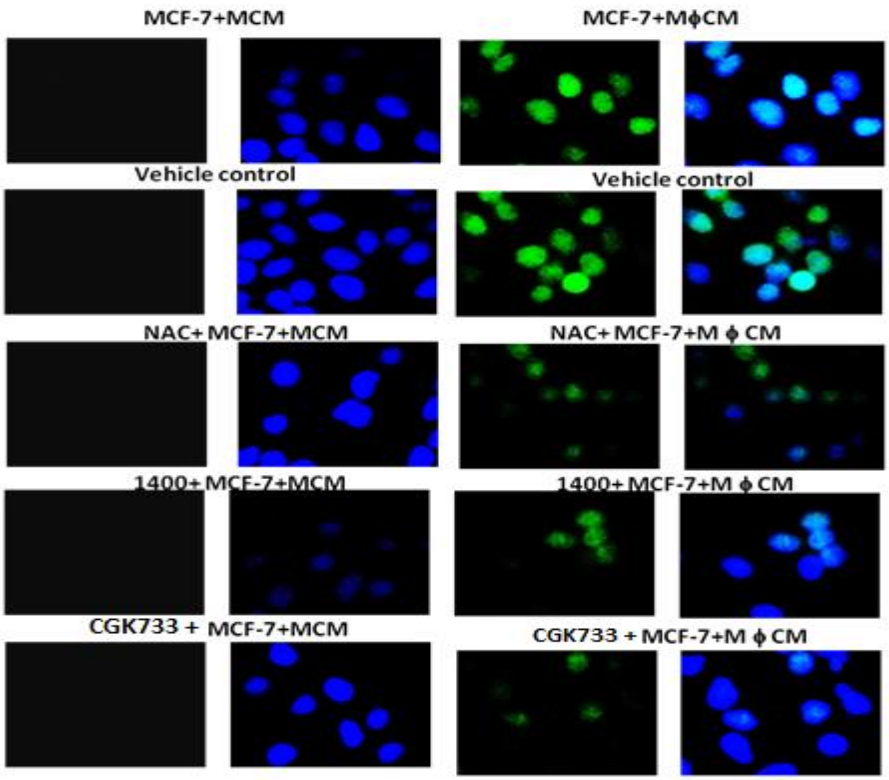
MCF-7+MCM
MCF-7+MϕCM
Vehicle control
Vehicle control
NAC+ MCF-7+MCM
NAC+ MCF-7+M ϕ CM
1400+ MCF-7+MCM
1400+ MCF-7+M ϕ CM
CGK733 + MCF-7+MCM
CGK733 + MCF-7+M ϕ CM

b.

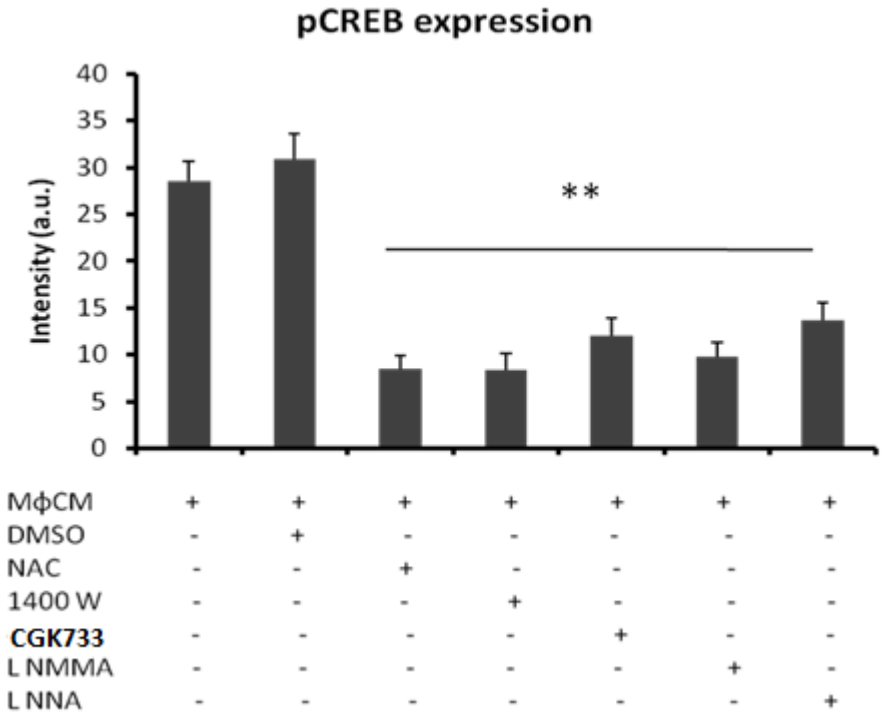
pCREB expression
Intensity (a.u.)
40
35
30
25
20
15
10
5
0
**
MϕCM + + + + + + +
DMSO - + - - - - -
NAC - - + - - - -
1400 W - - - + - - -
CGK733 - - - - + - -
L NMMA - - - - - + -
L NNA - - - - - - +

Figure 25: Inhibition of MϕCM induced phosphorylation of CREB in MCF7 cells by ROS, RNS and DNA damage inhibitors. MCF7 cells were pretreated with NAC (5 mM), 1400W (10 μM), CGK733 (2 μM), L NMMA (5 μM) or L NNA (5 μM) followed by 10% MCM or MϕCM for 5 days. The cells were labeled with pCREB antibody and visualized in a fluorescence microscope. (a) Images were acquired using a Nikon Eclipse Ti™ inverted microscope equipped with a Nikon digital camera using NIS elements™ software. Images from a representative experiment are shown. (b) The intensity of pCREB labeling was quantified using Image J software in a minimum of 50 cells. **P<0.01.

3.1.11.2 Effect of ATM knock down on pCREB expression in MCF7 cells

To validate the effects of CGK733 (ATM/ATR inhibitor) on abrogation of pCREB expression, ATM was transiently knocked down (ATM KD) with ATM siRNA. A non-targeting scrambled siRNA (scr control) was also used as control. The knockdown of ATM expression was validated using immunofluorescence (Figure 26a). There was a 40% decrease in pATM labeling in ATMKD cells 30 min after exposure to 5 Gy ionizing radiation as compared to the ATM scr cells (Figure 26a). A 30% decrease in phosphorylation of CREB was observed in ATM KD cells as compared to ATM scr cells in presence of MϕCM (P<0.01) (Figure 26b).

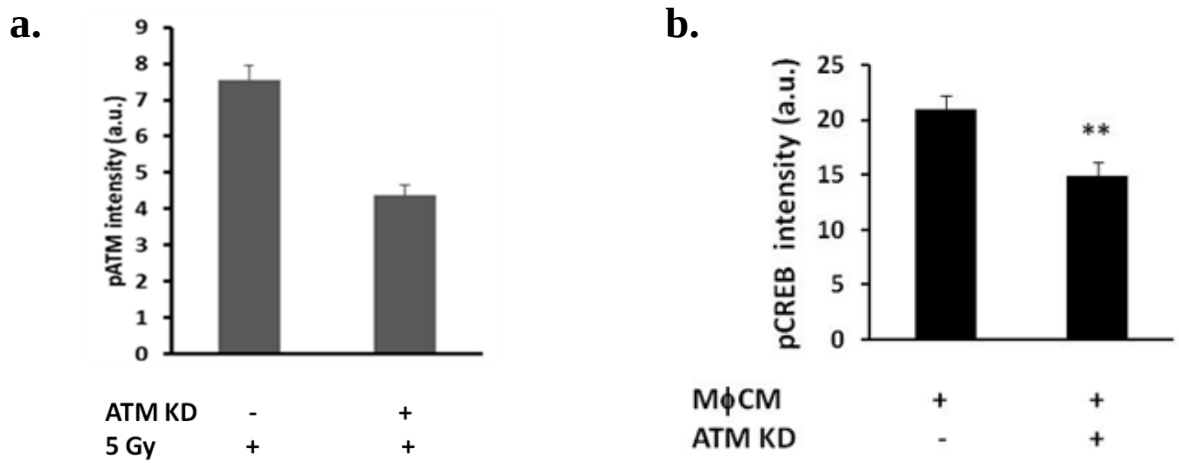

Figure 26: Inhibition of CREB phosphorylation in ATM-KD MCF7 cells. ATM was transiently knocked down in MCF7 cells using specific siRNA. (a) Validation of ATM KD by immunoflourescence labeling of pATM 30 min after exposure to 5Gy ionizing radiation (c) Control scr cells and ATM KD cells were treated with MϕCM for 5 days, labeled with pCREB antibody and visualized in a fluorescence microscope. (d) The intensity of pCREB expression was quantified using Image J software in a minimum of 50 cells. **P<0.01.

3.1.12 Inhibition of ROS, RNS or DNA damage abrogated migration in MCF7 cells

There was increased *in vitro* invasion of MCF7 cells with MϕCM treatment. To determine the association between CREB phosphorylation and migration of cells, the inhibitors of ROS, RNS generation and DNA damage response were used in a transwell assay. Inhibition of ROS, RNS or DNA damage pathways using these inhibitors abrogated the MϕCM induced migration in MCF7 cells. There was a 3 fold reduction in migration with NAC treatment, 25% decrease with 1400W treatment and 50 % reduction with CGK733 (P<0.01, Figure 27a). The pre treatment with combination of NAC and 1400W resulted in more than 3 fold decrease in migration (P<0.01, Figure 27a). A significant decrease in migration of ATM KD MCF7 cells

following MϕCM treatment as compared to the scrambled siRNA treated control cells was also observed (P<0.01, Figure 27b).

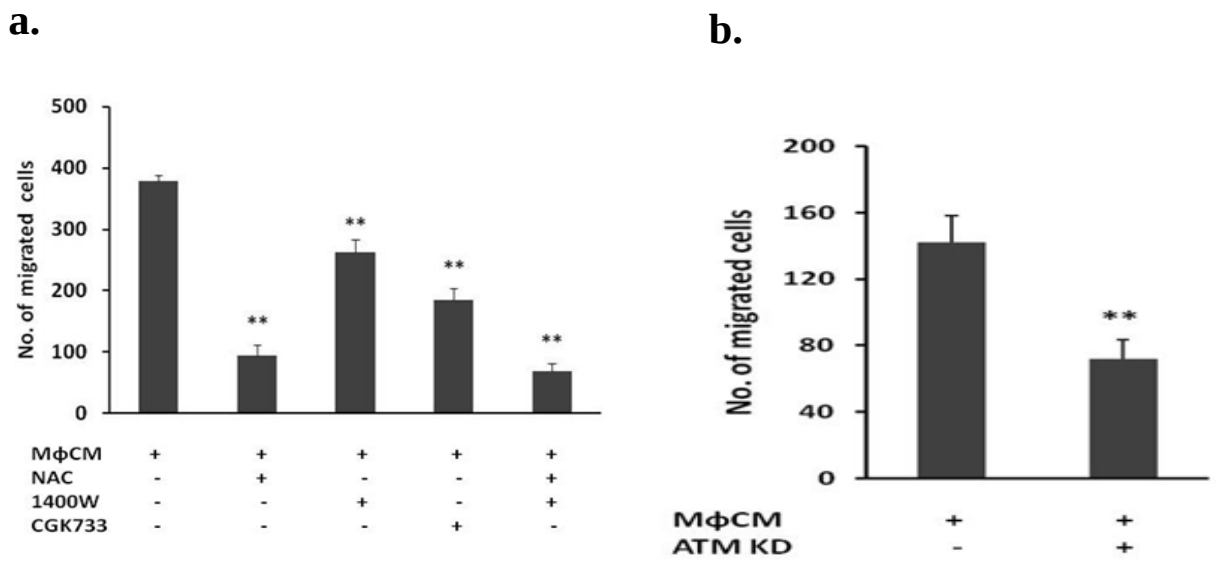

Figure 27: Abrogation of MϕCM induced migration of MCF7 cells by inhibitors of ROS, RNS and DNA damage. Migration of MCF7 was assessed by plating cells (10^5) in the top chamber of transwell inserts that were allowed to migrate for 72 hr. (a) The bottom chamber contained MCM or MϕCM supplemented with NAC (5 mM), 1400W (10 μM) or CGK733 (2 μM). The number of cells that migrated to the lower surface of the membrane was counted in ten randomly selected fields by light microscopy using CellProfiler™ software. (b) MϕCM induced migration in ATM scr and ATM KD cells. Data from one representative experiment is shown. The experiment was repeated three times. **P<0.01

CHAPTER 3.2

Characterization of monocyte and macrophage conditioned media

The tumor promoting activity of macrophages is attributed to its ability to express numerous mediators, such as growth factors, angiogenic molecules, ECM degrading enzymes, inflammatory cytokines and chemokines. Studies presented in this dissertation have demonstrated that MϕCM treatment resulted in differential growth patterns in breast cancer cell lines MCF7 and MDA-MB-231. MϕCM treatment induced TGF-β1 in MCF7 cells, which activated pCREB signaling, epithelial-mesenchymal-transition (EMT) responses and enhanced migration. This section describes the identification of soluble factors secreted by macrophages responsible for tumor growth promotion.

3.2.1 Protein profile of conditioned media

One dimensional separation of proteins:

MCM and MϕCM were collected from U937 cells and were concentrated 40 fold in presence of protease and phosphatase inhibitors. Differential expression of proteins was observed in 1D-SDS PAGE of MCM and MϕCM's concentrated proteins. An additional protein of around 90 kD was seen in MϕCM (Figure 28a).

Two dimensional separation of proteins:

In order to further characterize the proteins present in MϕCM, the conditioned media were subjected to 2D electrophoresis. The samples were prepared by ammonium sulphate precipitation or centricon filtration. The proteins concentrated by centricon filtration could not be absorbed on to the IPG strips during isoelectric focusing and hence proteins were not separated. Ionic contaminants or lipids are known to interfere with isoelectric focusing of proteins resulting in poor 2-D gel resolution and reproducibility. Hence the proteins were precipitated with

ammonium sulfate to remove lipids and other contaminants. Though in 1D PAGE, the number of differential proteins observed in MϕCM was higher, this difference was not very clearly seen in 2D gel electrophoresis (Figure 28a, b). A few proteins of 40-50 kD mass was seen upregulated in MCM as compared to MϕCM. Since, the IPG strip of pH range 3-10 was used, proteins with lower and higher pI that might not have absorbed onto the strip or the proteins might have formed multi protein complexes which could have also interfered with the 2D gel electrophoresis.

a.

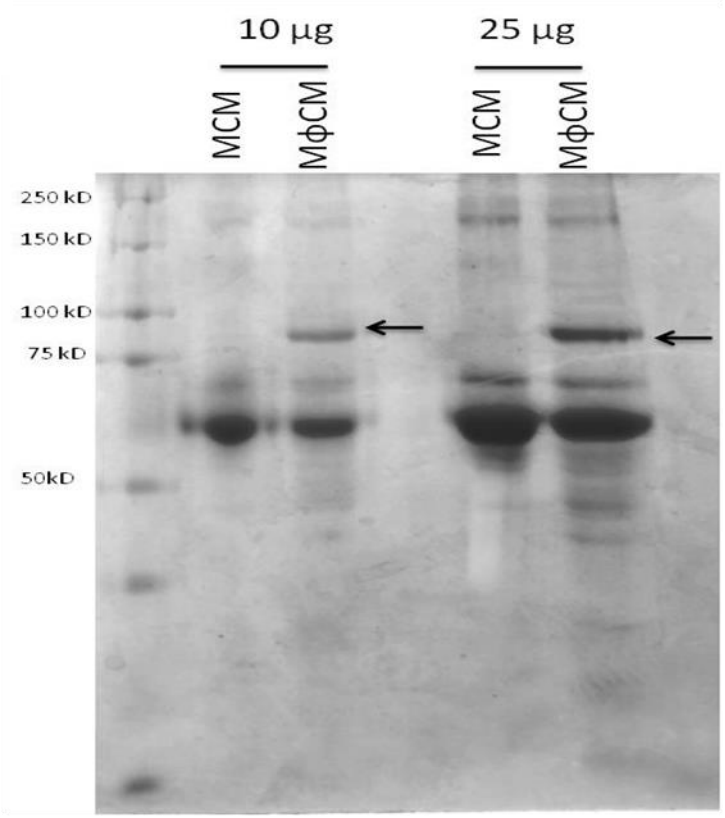

b.

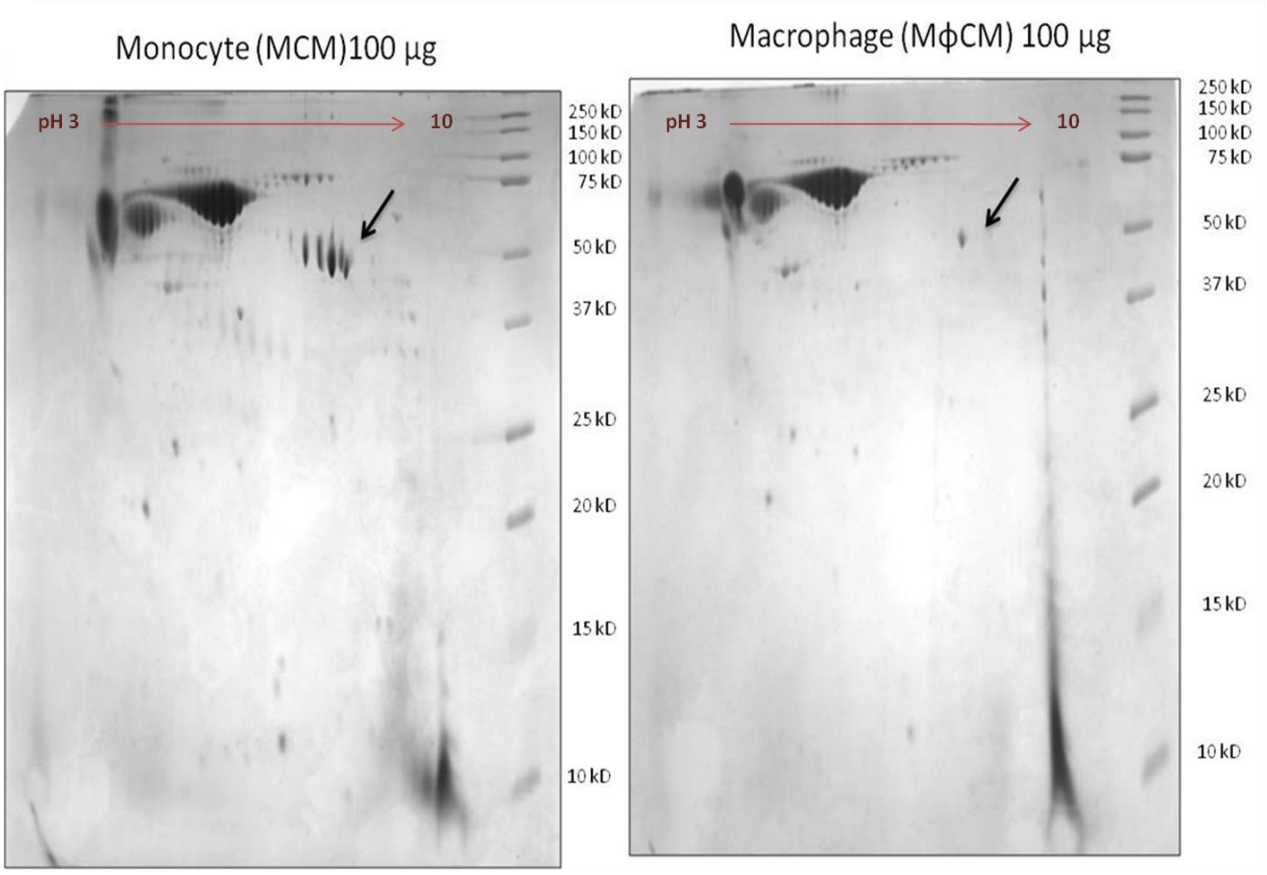

Figure 28: Protein profile of conditioned media. (a) MCM and MϕCM were collected and treated with protease and phosphatase inhibitors prior to protein concentration by ammonium sulphate precipitation followed by dialysis (cutoff 10 kD). Ten and twenty five µg of total proteins were run on 10% SDS PAGE and stained using Coomassie blue. (b) CM was further concentrated to 5 µl and then suspended in rehydration buffer consisting of urea, CHAPS and DTT for 1 hr. The rehydrated proteins were placed on IPG strip (11 cm; pH range 3-10) for O/N. The first dimensional iso-electric focusing (IEF) run was performed on strips and then further resolved on 10% SDS PAGE. Images of Coomassie Brilliant Blue-stained gels were acquired by Dyversity-6 gel imager (Syngene, UK) using GeneSnap^{TM} software (Syngene, UK).

3.2.2 MϕCM did not exert growth promoting effects through exosomes

The proteins in the conditioned media concentrated using centricon filters could not absorb onto IPG strips and thus did not separate in the electric field during IEF as opposed to proteins which were concentrated by ammonium sulphate precipitation. This indicated the presence of lipid components in the CM. Exosomes are small lipid membrane vesicles that are secreted *in vitro* by most cell types and they play roles as "intercellular messengers". To determine if exosomes were secreted by macrophages and were involved in the induction of EMT signals in breast cancer cells, they were purified from MCM and MϕCM. The exosomes were collected by ultracentrifugation and the supernatant obtained was termed as exosome free conditioned medium (EFCM). MCF7 cells were treated with PKH-26 labeled exosomes obtained from MCM and MϕCM. The uptake of exosomes could be visualised in both treatment, showing that the exosomes were present in both MCM and MϕCM and was taken up equally by MCF7 cells (Figure. 29a). The obtained exosomes were subjected to 1D PAGE to identify differential induction of proteins. The protein profile of exosomes secreted by monocytes and macrophages was similar with no differential pattern seen (Figure 29b). The ability of monocyte and macrophage's EFCM to interfere with the growth of breast cancer cells was assessed by colony forming assay. Treatment with EFMϕCM resulted in decrease in the colony forming ability of MCF7 and MDA-MB-231 cells. There was an increase in merging of colonies in MCF7 cells corroborating with the previous results of MCM and MϕCM (Figure 29c-f). These results confirmed that exosomes did not play a major role in the growth promoting effects exerted by MϕCM and the soluble mediators present in the CM rather than exosomes were responsible for the observed changes.

a.

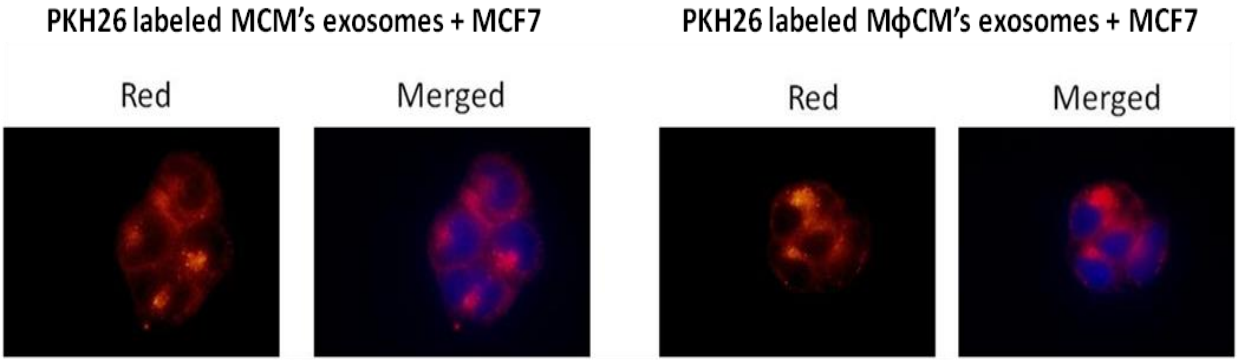
PKH26 labeled MCM's exosomes + MCF7
Red
Merged
PKH26 labeled MϕCM's exosomes + MCF7
Red
Merged

b.

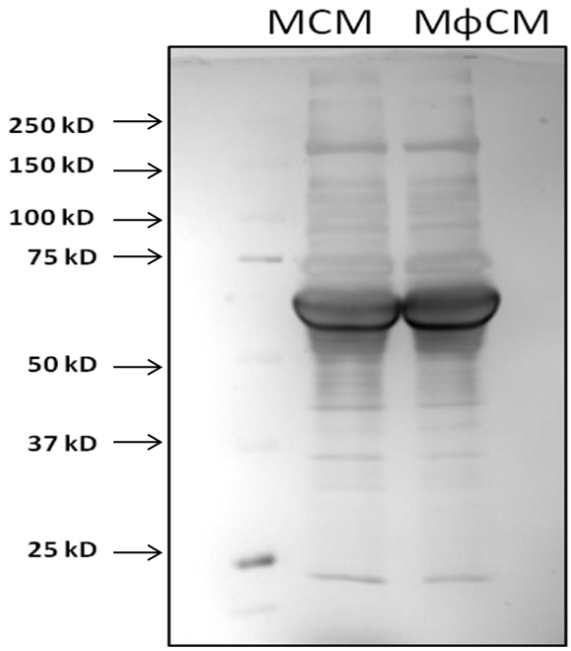
MCM
MϕCM
250 kD
150 kD
100 kD
75 kD
50 kD
37 kD
25 kD

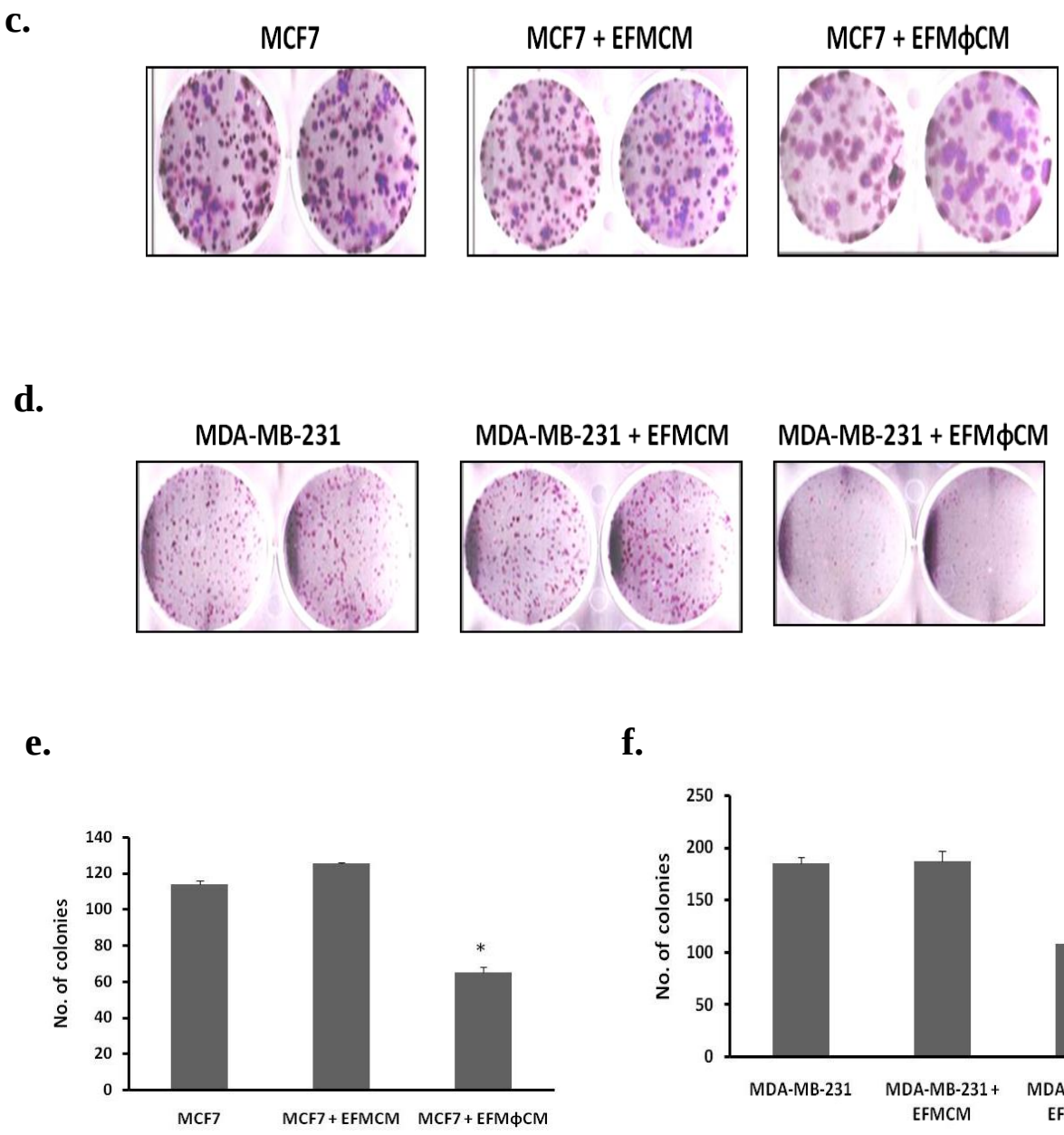

Figure 29: No role of exosomes in growth promoting effects of MϕCM. (a) Exosomes were prepared by culturing U937 cells in exosome free serum containing medium. The exosomes were isolated from CM by ultracentrifugation for 100 min at 12 0,000 x g. The resulting exosome pellet was stained with lipid labeling dye PKH-26. MCF7 cells were treated for 16 hr with the labeled exosomes and their uptake by cellswas visualized by fluorescence microscopy. Images were acquired using a Nikon Eclipse Ti inverted microscope equipped with a Nikon digital

camera using NIS elements^{TM} software. (b) Exosome proteins isolated from MCM and MϕCM (10 µg) were subjected to 1D SDS PAGE and the gel was silver stained. Images of silver-stained gels were acquired by Dyversity-6 gel imager (Syngene, UK) using GeneSnap^{TM} software (Syngene, UK). (c, d) Clonogenic assay was carried out by treating MCF7 and MDA-MB-231 cells with 10% EFCM for 7 days. Photomicrograph of the colonies in duplicates. (e, f) Histogram representing number of colonies quantified in Oxford optronix gelcount^{TM} using Gelcount^{TM} software. *P<0.05

3.2.3 Secretion of pro inflammatory cytokines by macrophages

The soluble mediators present in the conditioned media were estimated as exosomes did not have any role in MϕCM induced changes in MCF7 cells. Secretion of cytokines like TNF-α, IL-1β, IL-6, IFN- γ and TGF-β1 was assessed by ELISA. All cytokines were undetectable in MCM and pro-inflammatory cytokines TNF-α (300-700 pg/ml), IL-1 β (700-900 pg/ml) and IL-6 (400- 600 pg/ml) were induced several fold in MϕCM (Figure 30). IFN- γ and TGF-β1 were not present in MϕCM also (Figure 30).

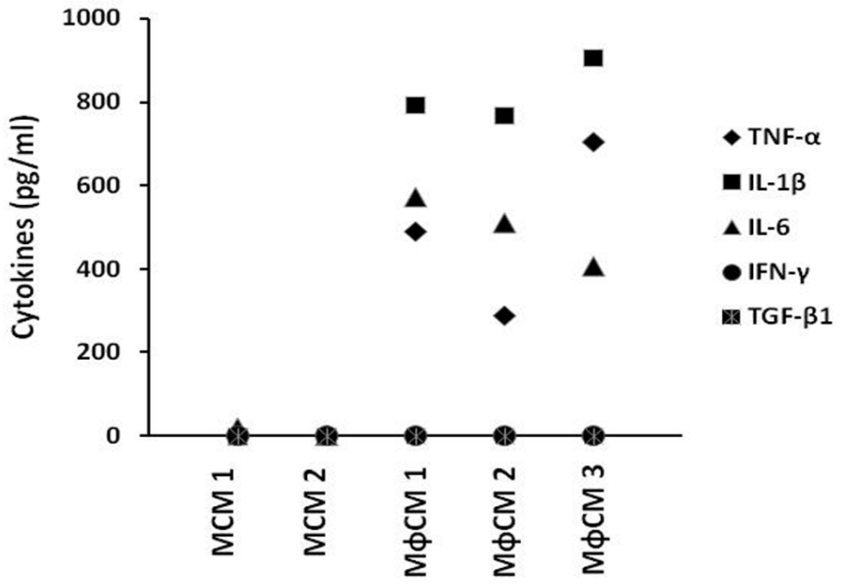

Figure 30: Estimation of cytokines in MCM and MϕCM. The cytokines TNF-α, IL-1β, IL-6, IFN-γ and TGF-β1 were estimated in MCM and MϕCM by ELISA. Cytokines were estimated in MϕCM independently collected from three different experiments.

3.2.4 Neutralization of pro-inflammatory cytokines abrogated MϕCM induced changes in colony morphology

To assess the role of the pro inflammatory cytokines TNF-α, IL-1β and IL-6 present in MϕCM in mediating alterations of growth pattern of MCF7 cells, these cytokines were neutralized using anti TNF-α, anti IL-1β and anti IL-6 antibodies for 4 hr prior to treatment to MCF7 cells. The neutralization of TNF-α, IL-1β and IL-6 abrogated the changes in colony morphology induced by MϕCM as well as reduction in colony numbers (Figure 31a, b). The scattering of cells and inability to form colonies in presence of MϕCM was inhibited and compact colonies were observed when any one of the pro-inflammatory cytokines were neutralized (Figure 31a).

a.

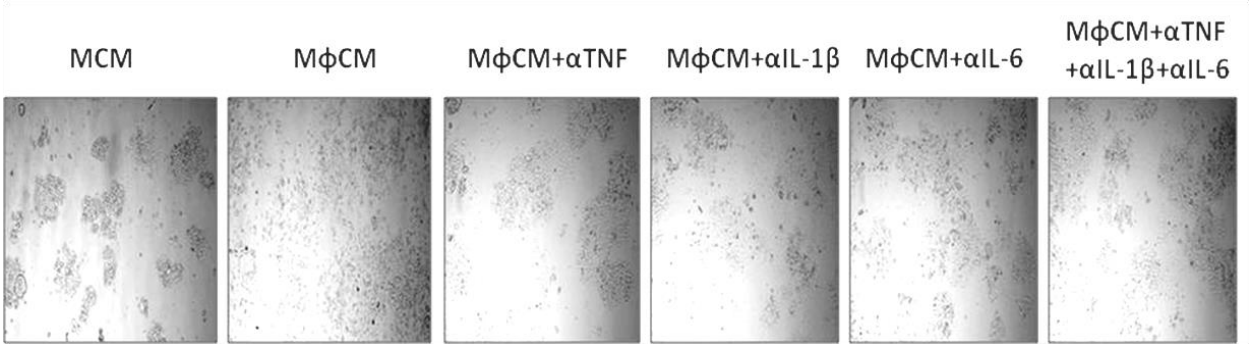
MCM
MϕCM
MϕCM+αTNF
MϕCM+αIL-1β
MϕCM+αIL-6
MϕCM+αTNF +αIL-1β+αIL-6

b.

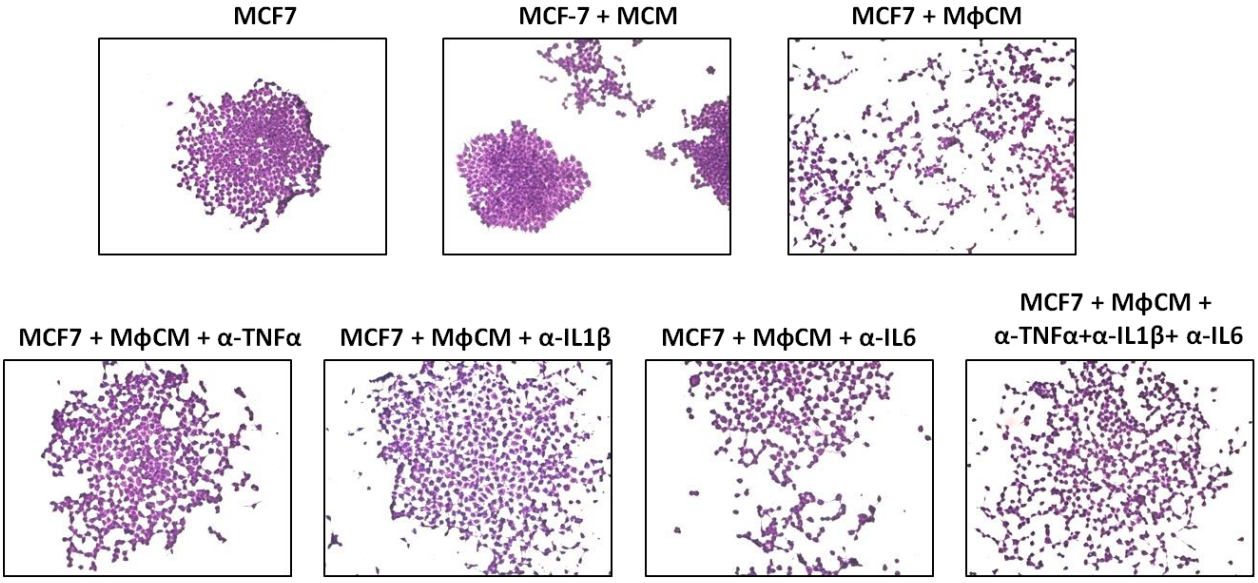
MCF7
MCF-7 + MCM
MCF7 + MϕCM
MCF7 + MϕCM + α-TNFα
MCF7 + MϕCM + α-IL1β
MCF7 + MϕCM + α-IL6
MCF7 + MϕCM + α-TNFα+α-IL1β+ α-IL6

c.

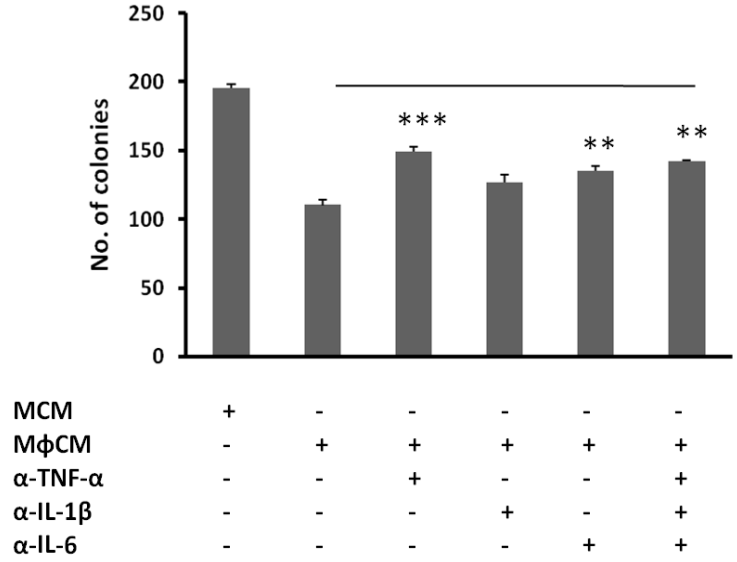
250
200
150
100
50
0
No. of colonies
***
**
**
MCM + - - - - -
MϕCM - + + + + +
α-TNF-α - - + - - +
α-IL-1β - - - + - +
α-IL-6 - - - - + +

Figure 31: Effect of neutralization of pro inflammatory cytokines on MϕCM treated MCF7 cells. MϕCM was treated with anti TNF-α, anti IL-1β or anti IL-6 antibodies (1μg) for 4 hr at 37°C prior to treatment of MCF7 cells for 6 days. The neutralizing antibodies were again supplemented on day 3. Colonies were fixed and stained with crystal violet. Images were acquired using a Nikon Eclipse Ti inverted microscope equipped with a Nikon digital camera using NIS elements^{TM} software. (a) Bright field images of the colonies (b) Crystal violet stained colonies (c) Number of colonies was quantified in Oxford optronix gelcount^{TM} using Gelcount^{TM} software. Data from one representative experiment is shown. **P<0.01***P<0.001.

3.2.5 Neutralization of pro-inflammatory cytokines abrogates MϕCM induced phosphorylation of CREB and migration in MCF7

The cytokines TNF-α, IL-1β and IL-6 were neutralized in MϕCM using the respective antibodies for 4 hr prior to treatment of MCF7 cells to assess their role in cytokine mediated activation of pCREB. Neutralization of the cytokines by pre-treatment of MϕCM with the respective antibodies alone or in combination resulted in abrogation of the increase in pCREB expression (Figure 32a; $p<0.01$), confirming the role of these pro-inflammatory cytokines in upregulation of pCREB. Neutralization of all three cytokines did not lead to any additive effect indicating the redundant function of these cytokines. Neutralization of the cytokines alone or in combination resulted in reduction in migration of MCF7 cells through transwell inserts as compared to MϕCM treated cells (Figure 32b, c; $p<0.01$)

a.

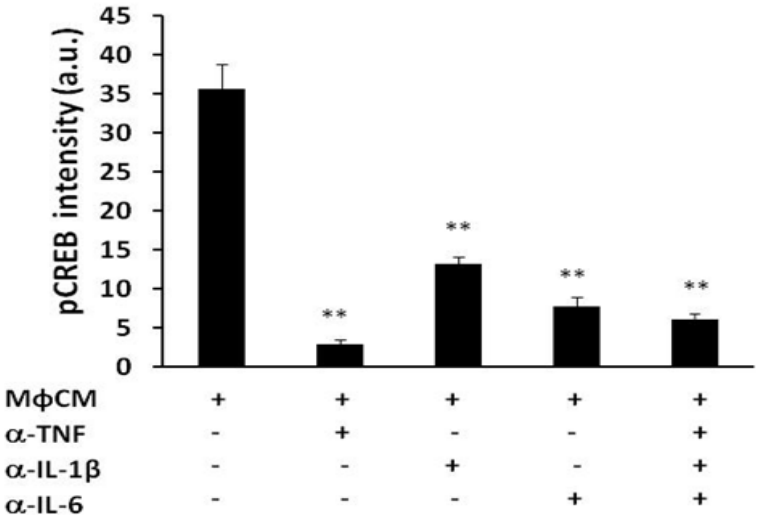
pCREB intensity (a.u.)
45
40
35
30
25
20
15
10
5
0
**
**
**
**
MϕCM + + + + +
α-TNF - + - - +
α-IL-1β - - + - +
α-IL-6 - - - + +

b.

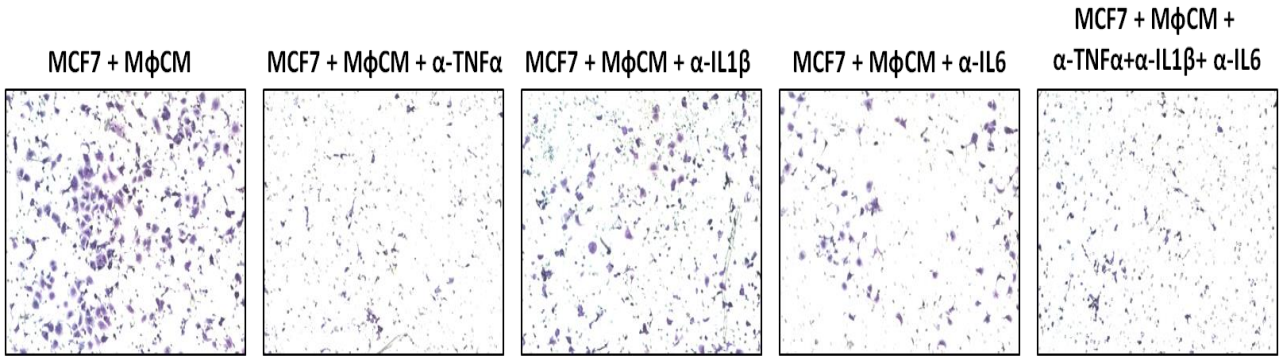
MCF7 + MϕCM
MCF7 + MϕCM + α-TNFα
MCF7 + MϕCM + α-IL1β
MCF7 + MϕCM + α-IL6
MCF7 + MϕCM + α-TNFα+α-IL1β+ α-IL6

c.

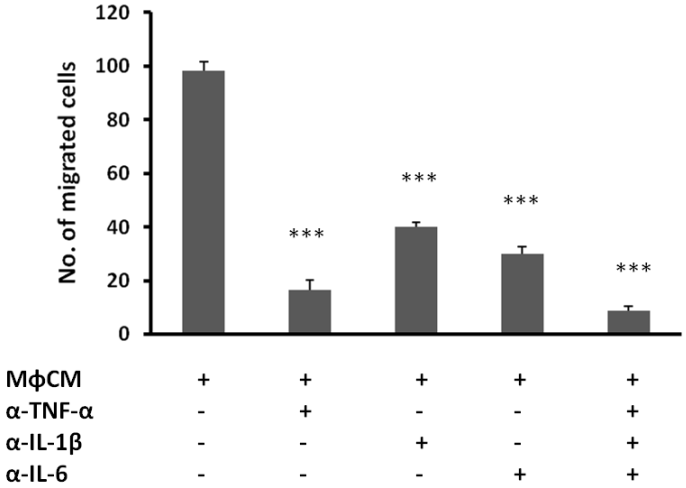
No. of migrated cells
120
100
80
60
40
20
0
***
***
***
***
MϕCM + + + + +
α-TNF-α - + - - +
α-IL-1β - - + - +
α-IL-6 - - - + +

Figure 32: Effect of neutralization of pro-inflammatory cytokines in MϕCM in pCREB expression. **(a)** MCF7 cells were grown on coverslips and treated with cytokine neutralized MϕCM for 5 days. The samples were labeled with pCREB antibody and counterstained with DAPI. Images were acquired using a Nikon Eclipse Ti inverted microscope equipped with a Nikon digital camera using NIS elements^{TM} software. The intensity of pCREB labeling was quantified using Image J software in a minimum of 50 cells **p<0.01. (b) Migration of MCF7 cells in presence of neutralizing antibodies and (c) the number of migrated MCF7 cells was assessed by plating cells in the top chamber of transwell inserts (8 μm) and allowed to migrate for 72 hr. Images from a representative experiment are shown. The migrated cells to the lower surface of the membrane were counted in ten randomly selected fields by light microscopy using CellProfiler^{TM} software. ***P<0.001.

3.2.6. MALDI-TOF analysis of differentially expressed proteins

Proteomic analysis of differentially expressed proteins, observed in one dimensional PAGE of MCM and MϕCM was carried out (Figure 33).

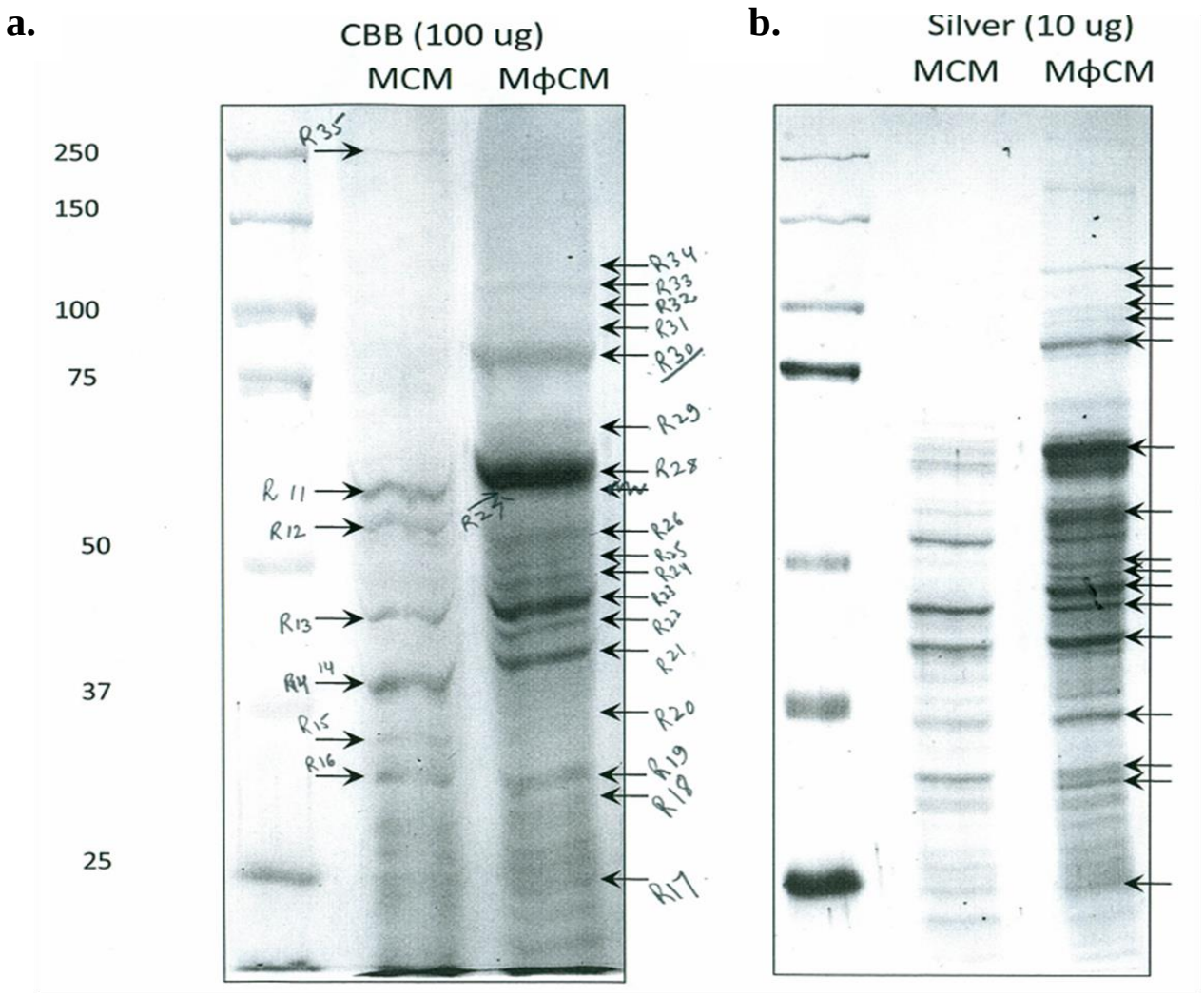

Figure 33: One dimensional PAGE of MCM and MϕCM proteins for MALDI-TOF analysis. MCM and MϕCM were collected and treated with protease and phosphatase inhibitors prior to protein concentration by ammonium sulphate precipitation followed by dialysis (cutoff 10 kD). Hundred and ten µg of total proteins were run on 10% SDS PAGE and stained using (a) coomassie blue and (b) silver staining respectively. Images of coomassie blue and silver stained gels were acquired by Dyversity-6 gel imager (Syngene, UK) using GeneSnap™ software (Syngene, UK).

The proteins present in MCM and MϕCM were identified with Peptide Mass Fingerprinting (PMF) through MALDI-TOF. Mascot searches were conducted using the NCBI non redundant database (released Jan 2012 or later) with the following settings: Number of missed cleavages permitted was one; fixed modifications such as carbamidomethyl on cysteine, variable modification of oxidation on methionine residue; peptide tolerance of 100 ppm, enzyme used as trypsin and a peptide charge setting as +1. A Mascot score of >65 with a minimum of 10 peptide matches was considered to be a significant identification ($p < 0.05$). A total of 25 proteins were identified from MCM and MϕCM by peptide mass fingerprinting by MALDI-TOF.

Seven proteins differentially expressed in MCM were selected for MALDI analysis (Figure 33). The R16 protein was not identified from the NCBI data base analysis. The six proteins that were identified by MALDI-TOF include moesin, plastin-2 isoform, glucose-6 phosphate isomerase, β-actin, aldolase A and ferritin light polypeptide. These proteins play the functional role in cell-cell recognition and signaling, cell motility and cytoskeleton regulation (Table 13).

Table 13: Differentially upregulated proteins identified in MCM

Spot no.	Protein	NCBI ID	Identification scores	No. of matched peptides	Mol. Wt. (kD)	Function
R11	Moesin	gi 119625804	161	28	66.6	Cell-cell recognition and signaling, cell movement
R12	Plastin-2 isoform 16	gi 114651551	221	32	70.8	Actin cytoskeleton regulator
R13	Glucose-6 phosphate isomerase isoform 1	gi 296080693	81	14	64.5	Glycolytic enzyme, endothelial cell motility
R14	Actin, beta, partial	gi 14250401	124	15	41.3	Cell motility, structure and integrity
R15	Aldolase A	gi 119600342	83	13	40.2	Cytoskeleton rearrangement, cell motility, membrane protein trafficking and recycling
R35	Ferritin light polypeptide	gi 171702853	86	6	10.3	Intracellular iron storage protein

Seventeen proteins differentially expressed in MϕCM were selected for MALDI analysis. Eleven upregulated MϕCM proteins were identiified by MALDI-TOF (Figure 33). Four proteins could not be identified in NCBI data base. The proteins identified include matrix metalloproteinase 1 (MMP-1) pre proprotein, annexin V, GAPDH, chitinase 3 like protein, plasminogen activator inhibitor2, myoferlin, plastin 2, CLK-3 isoform, metalloproteinase 9 (MMP-9) preproprotein and nitric oxide synthase. The majority of proteins play a functional role

in tissue remodeling, breakdown of extracellular matrix, membrane trafficking and cell migration (Table 14).

Table 14: Differentially upregulated proteins identified in MϕCM

Spot no.	Protein	NCBI ID	Identification scores	No. of matched peptides	Mol. Wt. (kD)	Function
R17	MMP 1 preproprotein variant	gi 62897673	76	11	46.6	Breakdown of extracellular matrix, tissue remodelling
R18	Annexin V mutant	gi 157831404	66	9	35.8	Membrane trafficking, membrane cytoskeleton anchorage, ion channel activity and regulation
R19	Glyceraldehyde-3-phosphate dehydrogenase isofom 2	gi 378404908	84	10	31.6	Glycolytic function, initiation signal for cellular apoptosis
R20	Chitinase3 like protein 1	gi 144226251	117	16	42.9	Inflammation and tissue remodelling
R21	Plasminogen activator inhibitor 2	gi 4505595	130	24	46.8	Maintainance of tissue homeostasis, invasion and remodeling of fetal and uterine tissue
R23	MMP 1 preproprotein variant	gi 62897673	160	20	46.6	Breakdown of extracellular matrix, tissue remodelling
R24	MMP 1 preproprotein variant	gi 62897673	136	17	46.6	Breakdown of extracellular matrix, tissue remodelling

R25	MMP 1 preproprotein variant	gi 62897673	68	12	46.6	Breakdown of extracellular matrix, tissue remodelling
R26	Myoferlin	gi 6731237	65	19	23.1	Regulator of EGFR activity in breast cancer, plasma membrane fusion, repair, endocytosis
R27	Plastin-2	gi 167614506	127	20	70.8	Actin binding protein, cell migration, PKA signaling
R28	Dual specificity protein kinase CLK-3 isoform	gi 194097436	72	16	74.2	Protein serine/ threonin/ tyrosine kinase activity, regulation of RNA splicing
R29	Dynamin 2 isoform 4 variant	gi 62088006	63	10	55.3	Membrane trafficking, cell signaling, cytokinesis, regulating actin assembly
R30	MMP 9 preproprotein variant	gi 74272287	162	22	79.4	Breakdown of extracellular matrix, angiogenesis, wound healing, cell migration, tissue remodelling .
R32	Nitric oxide synthase	gi 951319	48	11	16.2	Cellular signaling molecule

3.2.7 Validation of MMP-1 and MMP-9 in MϕCM

MALDI-TOF analysis of MϕCM proteins revealed the upregulation of MMP-1 pre proprotein and MMP-9 pre proprotein. These proteins play an important role in cancer cell migration and invasion. The expression of proteolytic enzymes like MMPs is studied through the functional assay ‘zymography’ by detecting the degradation of gelatin, casein or other substrates from various biological sources with one dimensional gel electrophoresis of proteins.

The clear band in the gel corresponding to the molecular weight of the MMP-1 in casein zymogram was observed (Figure 34a). In gelatin zymogram, the gelatinase activity of MMP-9 was seen as the clear band at 92 kD (Figure 34b). No band was observed with MCM proteins indicating the absence of proteinase activity (Figure 34).

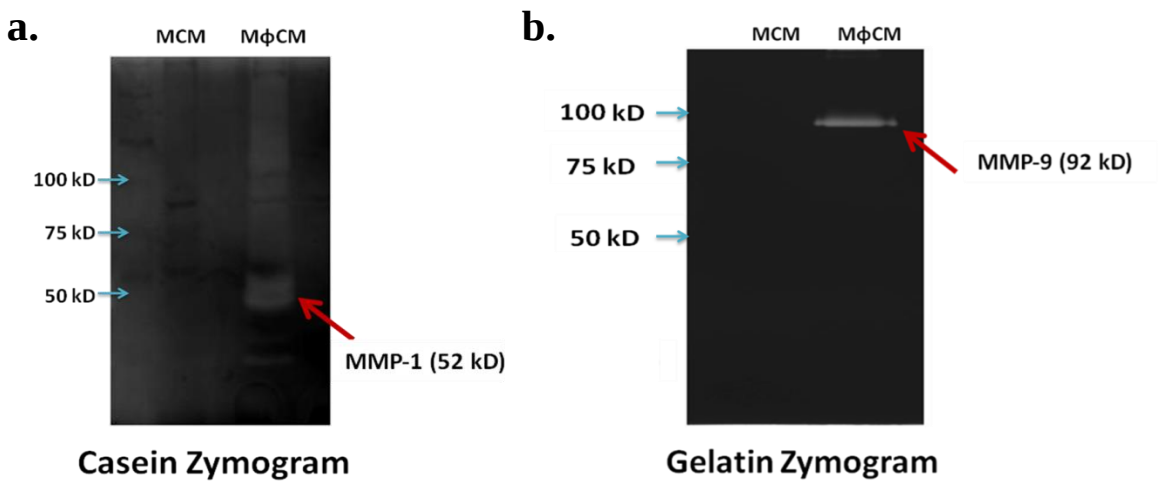

Figure 34: Expression of MMP-1 and MMP-9 in MϕCM. The conditioned media were collected and treated with protease and phosphatase inhibitors prior to protein concentration by ammonium sulphate precipitation followed by dialysis (cutoff 10 kD). Ten µg of MCM and MϕCM treated with non reducing sample buffer were run on 8% SDS PAGE consisting of (a) 50 mg/ml casein and (b) 30 mg/ml gelatin as substrate respectively. Images of coomassie blue stained zymograms were acquired by Dyversity-6 gel imager (Syngene, UK) using GeneSnap™ software (Syngene, UK).

3.2.8. MϕCM increases expression of ezrin, radixin and moesin (ERM) in MCF7 cells

MϕCM treatment resulted in increased cell migration and motility of MCF7 cells.The proteins identified by MALDI-TOF in MϕCM have a functional role in actin binding, regulation of cytoskeleton rearrangement, cell migration and invasion. Ezrin, radixin and moesin (ERM) proteins as well as ICAM-1 link cortical actin to the plasma membrane and coordinate cellular events that require cytoskeletal rearrangement, including cell division, migration and invasion. To determine if ERM proteins and ICAM-1 have any role in migration of MCF7 cells with MϕCM treatment, the transcript level of these proteins was estimated in these cells by real-time PCR. The relative expression of cytokines was determined by calculating the ratio of normalised expression of ERM mRNA in MϕCM treated MCF7 cells to that in MCM treated MCF7 cells. GAPDH was used as a reference gene. There was a 1.794, 1.761, 1.945 and 3.399 fold increase in radixin, ezrin, moesin and ICAM-1 expression respectively with MϕCM treatment in MCF7 cells as compared to MCM treatment (Figure 35).

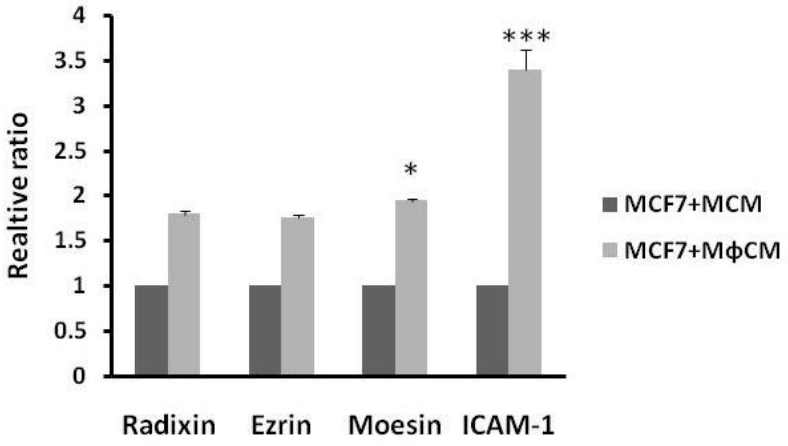

Figure 35: Expression of Radixin, ezrin, moesin and ICAM-1 in MϕCM treated MCF7. The mRNA levels of ERM proteins in MϕCM treated MCF7 was estimated by real-time PCR. Ratios of the normalized expression of these proteins were calculated in MϕCM treated cells to MCM treated MCF7 cells and significance analysis carried out using REST^{TM} software.*P<0.05***P<0.001

CHAPTER 3.3

Immunohistochemical evaluation of iNOS, p53, γ-H2AX, CREB and pCREB expression in benign fibroadenoma and invasive ductal carcinoma

Macrophage – tumor interaction was studied *in vitro* by employing MCM and MϕCM treatment to epithelial breast cancer cell line, MCF7 and invasive breast cancer cell line, MDA-MB-231. Differential effects of MϕCM were observed in these two cell lines differing in their invasive nature. The macrophage conditioned media contained various pro-inflammatory cytokines like TNF-α, IL-1β and IL-6. These cytokines in turn induced secretion of TGF-β1 in MCF7 cells. TGF-β1 caused apoptosis in some of the cells and significant increase in ROS and RNS generation in the surviving cells. This oxidative and nitrosative stress resulted in DNA damage response signaling as observed by expression of phosphorylated ATM and H2AX proteins. A significant increase in pCREB and total CREB labeling was observed in MϕCM treated MCF7 cells in contrast to MDA-MB-231 cells where basal level expression of CREB was higher and was unaffected by the treatments. There was a marked increase in vimentin expression (a EMT marker) as well as increase in migration of MCF7 cells treated with MϕCM.

Taking clues from this study, the expression of some of these proteins were evaluated in clinical samples (benign fibroadenoma and invasive ductal breast carcinomas (IDC). Expression of proteins iNOS, p53, γ-H2AX, CREB and pCREB were found to be crucial for increased migration in p53 positive MCF7 cells. The expressions of these chosen biomarkers were studied using specific antibodies by immunohistochemistry.

3.3.1 Patient's clinic-pathological characteristics

A retrospective study was performed on patient's biopsy samples enrolled from 2002 to 2012 in BARC Hospital, Mumbai which included 91 patients, diagnosed with invasive ductal breast carcinoma (IDC) after the pathology examination and 24 patients diagnosed with fibroadenoma (benign tumor). The research plan was approved by the Institutional Medical Ethics Committee (BHMEC 5/08). Data from patients with invasive ductal carcinoma of breast were classified according to age, tumor grade, tumor size, TNM stage, lymph node status as well as vessel space invasion.

3.3.1.1 Age

The age of IDC patients ranged from 28 to 77 years with a mean of 58.10±10.48 years. The peak age frequency was in the age category of 56-70 years at the time of diagnosis (Figure 36). The age of benign fibroadenoma patients ranged from 20-66 years.

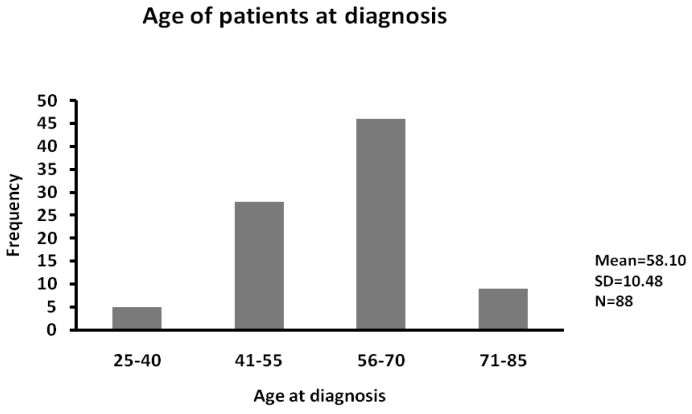

Figure 36: Bar chart showing the distribution of the IDC patients according to the age at the time of diagnosis.

3.3.1.2 Tumor grade

The invasive ductal carcinoma samples were graded according to the Nottingham modification of the Bloom and Richardson system. According to the grading of tumor, 16% IDC samples were grade I; 37% were grade II and 47% were grade III (Figure 37).

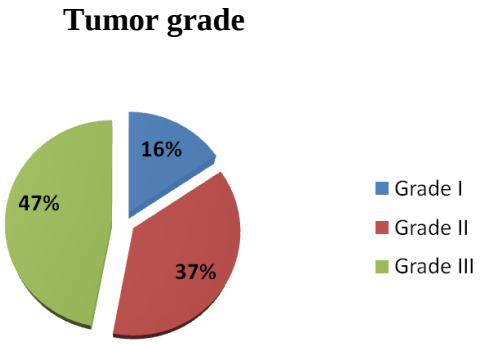

Figure 37: Distribution of infiltrative ductal carcinoma of breast according to Bloom Richardson grading system.

3.3.1.3 Tumor size

The tumor size was recorded from the initial pathology report. The tumor size ranged from 5 mm to 90 mm with a mean of 36 mm. The IDC samples were divided according to the tumor size into staging groups of T1 (tumor size <20 mm), T2 (tumor size 20-50 mm), T3 (tumor size >50 mm). Eight samples belonged to (8.79%) T1 group, 71 (78.02%) to T2 group and 12 samples (13.18%) toT3 group (Table 15).

Table 15: Distribution of IDC samples according to tumor size at the time of diagnosis

T size	Number (%)
T1 <20mm	8 (8.79%)
T2 20-50mm	71 (78.02%)
T3 >50mm	12 (13.18%)

3.3.1.4 TNM stage

The frequency of distribution of IDC patients according to pathological TNM staging were 5.8%, 58.1% and 36.1% for Stage I, Stage II and Stage III respectively (Table 16).

Table 16: Distribution of IDC samples according to TNM stages at the time of diagnosis

TNM tumor stage	Number (%)
Stage I	5 (5.8%)
Stage II	50 (58.1%)
Stage III	31 (36.1%)

3.3.1.5 Lymph node status

The histological examination of the axillary lymph nodes showed that 41% of cases had no lymph node invasion while 59% of cases had positive lymph node tumor invasion (Figure 38).

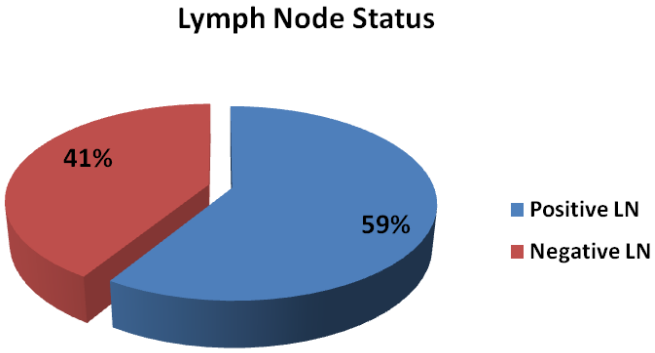

Figure 38: Distribution of infiltrative ductal carcinoma of breast samples according to the involvement of lymph nodes.

3.3.1.6 Vessel space invasion (VSI)

The presence or absence of vessel space invasion was reported in all 91 cancer samples. Vessel space invasion was present in 31 (28.2%) of the 91 IDC samples.

3.3.1.7 Correlation of pathological features

The relationship between each of the clinico-pathological features was compared as shown in table 17. In this study, the patient's tumor size correlated with the patient's age at diagnosis ($p<0.05$) and tumor stage ($p<0.05$), since the advanced stage patients had a larger tumor size. The stage of the tumor also correlated with LN metastasis positivity ($p<0.0001$). The

advanced stage samples were LN Mets positive. VSI positivity was associated with high grade tumors ($p<0.05$).

Table 17: Correlation between the clinico-pathological features

		Age	Tumor size	Grade	Stage	LN Mets	VSI
Age	**Chi-square, Df** **p-value** **Sig.**	. . . (a)	7.092, 2 0.0288 *	3.928,2 0.1403 ns	2.225, 2 0.3287 ns	0.9272, 1 0.7607 ns	0.5546, 1 0.4564 ns
T. Size	**Chi-square, Df** **p-value** **Sig.**	7.144, 2 0.0281 *	. . .(a)	2.276, 4 0.6851 ns	10.67, 4 0.0305 *	0.1962,2 0.9065 ns	2.9752, 2 0.2260 ns
Grade	**Chi-square, Df** **p-value** **Sig.**	5.026, 2 0.0810 ns	2.102, 4 0.7169 ns	. . .(a)	2.240, 4 0.6917 ns	0.8556, 2 0.6519 ns	6.406, 2 0.0406 *
Stage	**Chi-square, Df** **p-value** **Sig.**	1.726, 2 0.4219 ns	15.94, 4 0.0031 **	2.581, 4 0.6301 ns	. . .(a)	35.58, 2 <0.0001 ****	1.321, 20.5167 ns
LN Mets	**Chi-square, Df** **p-value** **Sig.**	0.1606, 1 0.6886 ns	1.675, 2 0.4329 ns	1.717, 2 0.4237 ns	35.58, 2 <0.0001 ****	. . .(a)	0.8426, 1 0.3587 ns
VSI	**Chi-square, Df** **p-value** **Sig.**	0.6141, 1 0.4333 ns	3.120, 2 0.2101 ns	6.208, 2 0.0449 *	1.373, 2 0.5034 ns	1.265, 1 0.2607 ns	. . .(a)

* The Chi-square statistic is significant at the 0.05 level. ** The Chi-square statistic is significant at the 0.01 level. **** The Chi-square statistic is significant at the <0.0001 level. (a): The Chi-square test is not performed for this sub-table because row and column variables are identical. (T.size = tumor size group, LN mets = Lymph Node Metastasis and VSI= vessel space involvement). Df- Degree of freedom.

3.3.2 Status of hormone receptor expression

3.3.2.1 Expression of estrogen and progesterone receptor (ER & PR)

The status of ER and PR was known in 88 IDC patient samples. Dual positive receptor expression was observed in 56.8% samples whereas dual negative receptor expression was observed in 32.95% samples. This is summarized in table 18.

Table 18: Expression of ER and PR status in IDC patients

Receptor Expression	Number (%)
ER^+	54 (61.36%)
ER^-	34 (38.63%)
PR^+	55 (62.5%)
PR^-	33 (37.5%)
ER^+/PR^+	50 (56.81%)
ER^+/PR^-	4 (4.54%)
ER^-/PR^+	5 (5.68%)
ER^-/PR^-	29 (32.95%)

3.3.2.2 Expression of Her-2/*neu* receptor

Her-2/*neu* receptor expression was studied in 86 IDC patients and was positive in 40.69% samples and negative in 59.3% samples. Expression of Her-2/*neu* and its co-expression with ER and PR are summarized in table 19. In this study, 8.53% of IDC samples constituted the triple positive ($ER^+/PR^+/Her\text{-}2^+$) as well as triple negative cancer ($ER^-/PR^-/Her\text{-}2^-$) population.

Table 19: Expression of Her-2/*neu* receptor and its coexpression with ER and PR in IDC samples

Receptor Expression	Number (%)
Her-2/neu^{+}	35 (40.69%)
Her-2/neu^{-}	51 (59.31%)
ER^{+}/PR^{+}/Her-2^{+}	7 (8.53%)
ER^{+}/PR^{+}/Her-2^{-}	44 (53.65%)
ER^{-}/PR^{-}/Her-2^{+}	24 (29.26%)
ER^{-}/PR^{-}/Her-2^{-}	7 (8.53%)

3.3.2.3 Correlation of clinico-pathological features with receptor status

The samples, earlier classified based on clinico-pathological features, were also classified based on the hormone receptor status as summarized in table 20. The relationship between hormone receptors and the clinico-pathological features of the IDC samples was compared as shown in table 21. The ER+ tumors were significantly related to low grade tumors ($p<0.01$) and smaller size tumors ($p<0.01$). The Fisher's exact analysis also demonstrated a significant relationship between ER+ and PR+ samples ($p<0.001$). An inverse correlation between ER+ and HER-2/neu+ tumors was seen ($p<0.001$). PR expression was significantly associated with low grade tumors ($p<0.01$). PR expression correlated significantly with ER ($p<0.001$) and negatively correlated to HER-2/neu expression in IDC samples ($p< 0.001$). A significant inverse relationship between HER-2/Neu expression with ER ($p<0.001$) and PR ($p<0.001$) status was observed.

Table 20: Distribution of patients with clinico-pathological characteristics as well as status of hormone receptor expression

		ER		PR		Her-2/*neu*	
		+	-	+	-	+	-
Age	≥ 50	15	5	15	5	6	14
	<50	38	26	39	25	27	37
T. Size	T1	6	0	6	0	1	5
	T2	40	32	41	31	32	40
	T3	8	2	8	2	3	7
Grade	I	9	3	10	2	5	7
	II	28	8	28	8	9	26
	III	17	20	16	20	19	17
Stage	I	4	0	4	0	1	3
	II	33	18	34	17	19	32
	III	15	13	15	13	13	15
LN Mets	Positive	28	20	29	19	20	28
	Negative	25	11	25	11	13	23
VSI	Positive	17	12	18	11	11	17
	Negative	37	22	37	22	25	35
ER	+			49	5	11	44
	-			5	26	24	7
PR	+	49	5			10	44
	-	4	26			23	7
Her-2/*neu*	+	9	44	10	23		
	-	44	7	44	7		

Table 21: Correlation between receptor status and pathological features

		ER	PR	Her-2/neu
Age	Fisher's exact test			
	p-value	0.2899	0.2958	0.4341
	Sig.	ns	ns	ns
T. Size	Chi-square test			
	p-value	0.0436	0.0535	0.3131
	Sig.	*	ns	ns
Grade	Chi-square test			
	p-value	0.0124	0.0042	0.0656
	Sig.	*	**	ns
Stage	Chi-square test			
	p-value	0.1770	0.1555	0.6013
	Sig.	ns	ns	ns
LN Mets	Fisher's exact test			
	p-value	0.3636	0.4916	0.6565
	Sig.	ns	ns	ns
VSI	Fisher's exact test			
	p-value	0.8167	1.000	1.000
	Sig.	ns	ns	ns
ER	Fisher's exact test			
	p-value	.	<0.0001	<0.0001
	Sig.	.(a)	****	****
PR	Fisher's exact test			
	p-value	<0.0001	.	<0.0001
	Sig.	****	.(a)	****
Her2/*Neu*	Fisher's exact test			
	p-value	<0.0001	<0.0001	.
	Sig.	****	****	.(a)

* The Chi-square/ Fisher's exact statistic is significant at the 0.05 level. ** The Chi-square/ Fisher's exact statistic is significant at the 0.01 level. **** The Chi-square/ Fisher's exact statistic is significant at the <0.0001 level. (a) The test is not performed for this sub-table because row and column variables are identical. (T. size = tumor size group, LN mets = Lymph Node Metastasis and VSI= vessel space involvement). Df- Degree of freedom

3.3.2.4 Immunohistochemistry data and statistical analysis of biomarkers

The "Remmele score" (IRS, immunoreactive score according to Remmele and Stegner, 1987) was used to score the expression of all markers in the samples. Two parameters were used in this score; intensity of immunoreactivity of the cytoplasmic staining and the proportion of the reactive tumor cells that are positive to biomarker. Every sample (5-7 images/sample) was given a score in which the total intensity of staining (no staining = 0; low level = 1; medium staining = 2; strong staining = 3) and the percentage of stained cells (0% = 0; under 10% = 1; 11-50% = 2; 51-80% = 3; over 80% = 4) was multiplied [330]. Using this system, the maximum score is 12 (with over 80% of the cells showing strong staining). Cellular localization (cytoplasm or nucleus or both) and tissue distribution (stroma, infiltrating cells) were determined by visual inspection of all the images. The nuclear staining in the tumor cells was counted for determining distribution of γ-H2AX, p53, CREB and pCREB and cytoplasmic staining was considered in iNOS labeled samples. Figure 39 shows representative fibroadenoma images with nuclear and cytoplasmic intensity 0, 1 and 2.

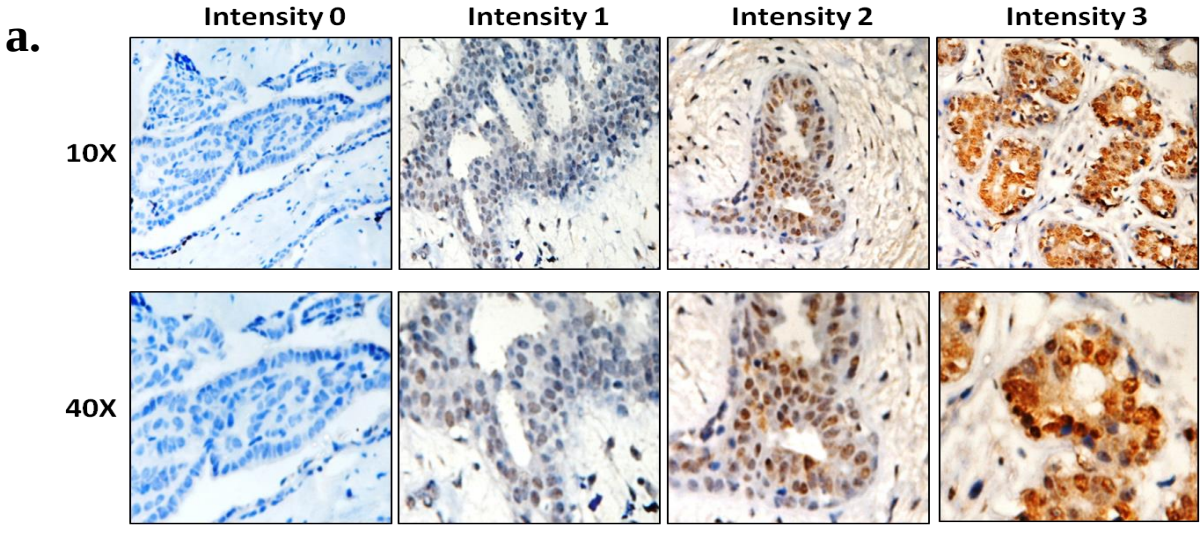

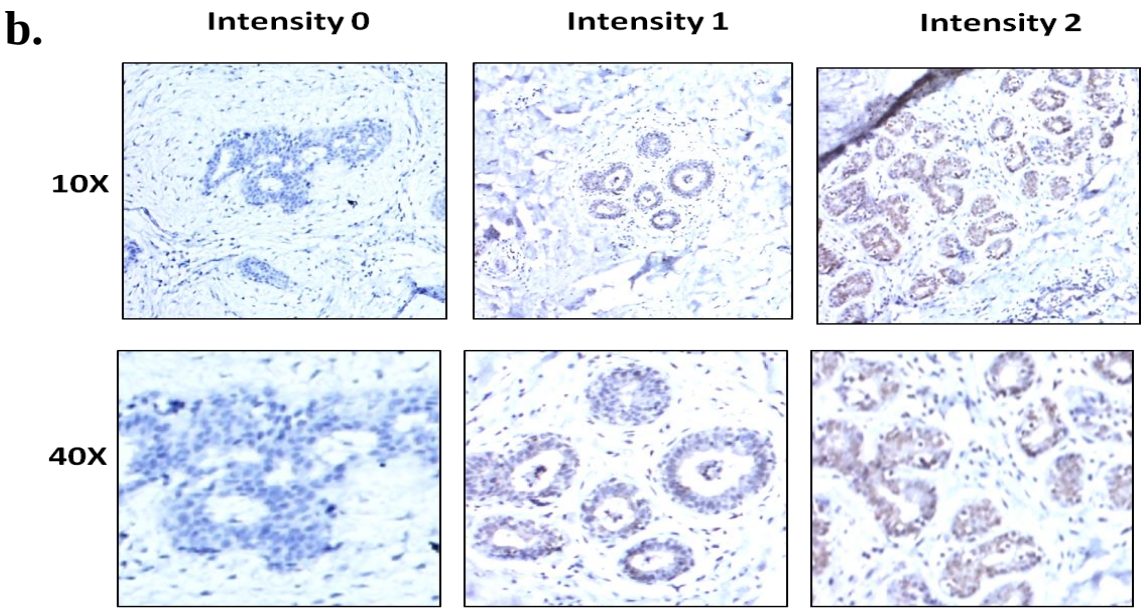

Figure 39: Representative images of benign fibroadenoma with different staining intensities (nuclear and cytoplasmic). (a) Representative fibroadenoma images with nuclear (p53) intensity 0, 1, 2 and 3. (b) Representative fibroadenoma images with cytoplasmic (iNOS) intensity 0, 1, and 2. The top panel represents the 10X image and bottom panel represents the 40 X image of the same field.

The descriptive data that included frequency (number of cases with score range 0-12), the mean, median and standard deviation were determined for all the groups. Since the assessment of staining was done based on the scores, a nonparametric method, the Mann-Whitney test, was used for pair wise comparisons and the Kruskal –Wallis test was used to study variance in more than 2 groups. The nonparametric Spearman's rho correlation coefficient was used to analyze associations between pairs of markers. The chi square test or Fisher's exact test was used to compare the expression of marker in different clinico-pathological groups of IDC patients. Chi-square calculations are valid when all expected values are greater than 1.0 and at least 20% of the expected values are greater than 5. With small sample size and 2X2 contingency table, Fisher's

exact test is considered instead of Chi-square test as it calculates an exact p value whereas latter calculates an approximation. For all the tests, a value of p less than or equal to 0.05 was considered statistically significant.

3.3.3 Expression of iNOS by immunohistochemistry

Several human cancers have been reported to express iNOS. An increased expression of iNOS in tumor cells was demonstrated for breast, ovarian [341], prostate [342], gastric [343], colorectal [344] and head and neck cancers [345], as well as in non-epithelial malignancies like sarcomas [346]. Tumoral iNOS expression has been associated with stage, histological differentiation, cell proliferation, induced angiogenesis, p53 expression or mutation and survival [345, 347]. This study was undertaken to investigate the expression of iNOS in benign fibroadenomas and invasive ductal carcinomas of the breast. The expression of iNOS was studied in 23 benign fibroadenoma and 91 IDC samples. The expression of iNOS was observed in stromal cells and also in a high proportion of tumor cells. Expression of iNOS in tumor cells was mostly cytoplasmic and sometimes nuclear. Figure 40 shows the representative images with iNOS intensity 1, 2 and 3.

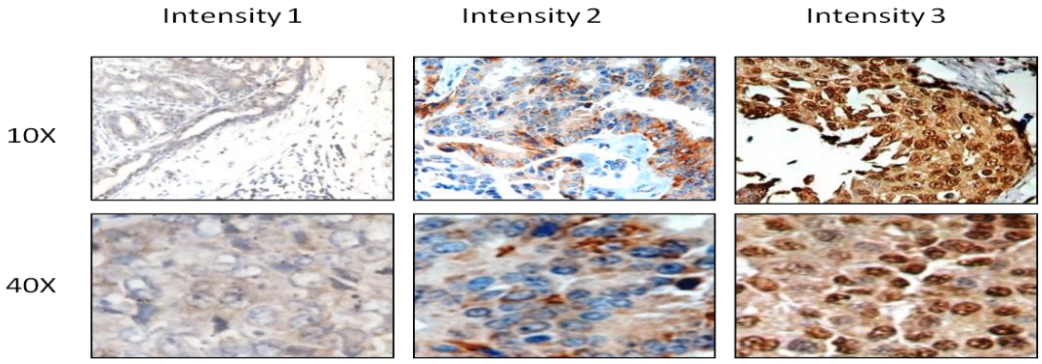

Figure 40: Representative images of iNOS expression with different staining intensities (intensity 1, intensity 2 and intensity 3). The top panel represents the 10X image and bottom panel represents the 40 X image of the same field.

3.3.3.1 iNOS expression in benign fibroadenoma and IDC samples

iNOS staining was observed in tumor cells as well as stromal cells (Figure 40). Occasional faint granular colouring was seen in inflammatory cells present in the samples. iNOS expression was studied in 23 benign fibroadenoma and 91 IDC samples. The median score in benign fibroadenoma sample was 6 (range 0-8) whereas the median iNOS score in malignant samples was 9.33 (range 4-12). The distribution of iNOS scores in benign fibroadenoma and IDC group differed significantly (Mann Whitney U score=310.5, p value <0.0001, two tailed) (Figure 41a). Bioinformatic analysis was carried out using Oncomine (www.oncomine.com, Oncomine Research Premium Edition) to assess transcript levels of iNOS in breast cancer database applying fold change ≥ 2 and $p \leq 0.01$ as thresholds. iNOS mRNA was significantly upregulated in invasive breast carcinoma (53 IDC samples) as compared to normal breast tissue (6 cases), (t-test=13.511, p value <0.0001, two tailed, fold change=2.53) [62] (Figure 41b). The data base constitutes of many studies which compare iNOS expression between different carcinoma subtypes. Data from some of the studies show the fold change of 1.064 (p=0.064) between normal and breast carcinoma [348], fold change of 1.803 (p=0.025) between breast adenocarcinoma and mucinous breast carcinoma [349] and fold change of 1.176 (p=0.037) in breast adenocarcinoma and ductal breast carcinoma [350].

The lower IHC scores (0-6) were classified as weak iNOS expression and higher scores (7-12) as strong iNOS expression in the tumor cells. iNOS score was low in 11 (12.6%) and high

in 76 (87.3%) malignant tumors. In benign fibroadenoma samples, 12 (52.17%) samples had weak iNOS expression and 11 (47.82%) samples had strong iNOS expression. The iNOS scores were significantly higher in malignant IDC as compared to the benign fibroadenoma group (Fisher's exact test, p=0.0001, two tailed) (Figure 41c).

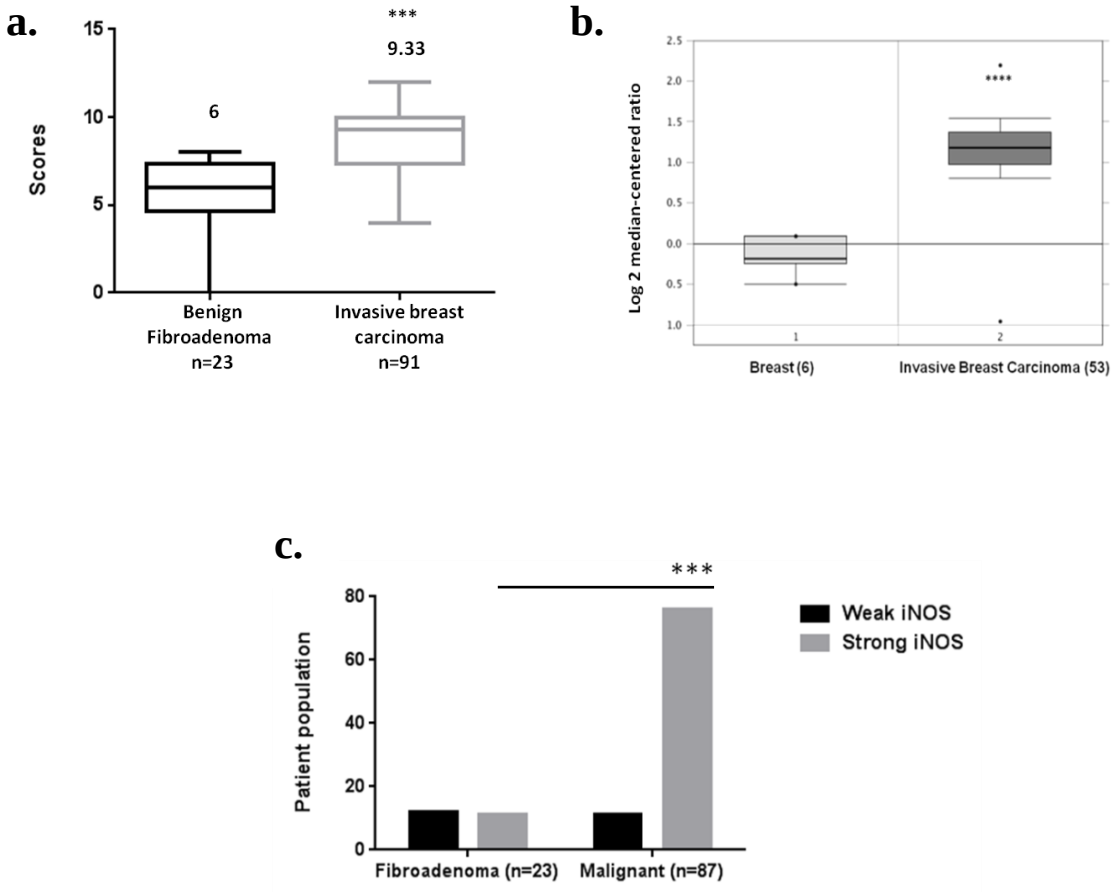

Figure 41: Expression of iNOS in benign fibroadenoma and invasive breast carcinoma (benign fibroadenoma=23 samples, IDC=91 samples). (a) Median iNOS score in benign fibroadenoma as compared to IDC group (Mann Whitney U score=310.5, p value <0.0001, two tailed). The bar represent the median value along with range of distribution of iNOS scores (b) Oncomine data set for transcript levels of iNOS in normal breast tissue and breast cancer samples (t-test=13.511, p value <0.0001, two tailed, fold change=2.53) [62]. (c) Proportion of

benign fibroadenoma and IDC patients with weak or strong iNOS expression (Fisher's exact test, p=0.0001, two tailed). *** The Mann Whitney U / Fisher's exact statistic is significant at the 0.001 level.

3.3.3.2 iNOS expression and its association with clinico-pathological features

The distribution of iNOS scores and the relationship with the clinico-pathological features of proportion of samples with weak or strong iNOS expression scores was analysed by chi square/ Fisher's exact analysis and is summarized in table 23. The distribution of iNOS score in malignant samples differing in clinico-pathological features was studied by non parametric one way ANOVA (Mann Whitney U test or Kruskal Wallis test) and is summarized in table 24.

Table 22: Distribution and correlation between the clinico-pathological features and iNOS scores.

Clinico-pathological characteristics		Patient's distribution		Clinico-pathological characteristics		iNOS Correlation
		Weak iNOS score	Strong iNOS score			
Age	≥ 50	1 (6.25%)	15 (93.75%)	Age	Fisher's exact test	
	<50	10 (14.49%)	59 (85.51%)		p-value	0.6812
					Sig.	ns
T. Size	T1	1 (14.29%)	6 (85.71%)	T. Size	Chi-square, Df	1.1233, 2
	T2	11 (15.49%)	60 (84.51%)		p-value	0.9402
	T3	1 (11.11%)	8 (88.89%)		Sig.	ns
Grade	I	2 (16.67%)	10 (83.33%)	Grade	Chi-square, Df	1.572, 2
	II	2 (6.67%)	28 (93.33%)		p-value	0.4556
	III	6 (16.22%)	31 (83.78%)		Sig.	ns
Stage	I & II	5 (9.25%)	49 (90.74%)	Stage	Fisher's exact test	
	III	6 (19.35%)	25 (80.65%)		p-value	0.1982
					Sig.	ns
LN Mets	Positive	9 (16.98%)	44 (83.02%)	LN Mets	Fisher's exact test	
	Negative	2 (5.88%)	32 (94.12%)		p-value	0.1894
					Sig.	ns
VSI	Positive	3 (11.11%)	24 (88.89%)	VSI	Fisher's exact test	
	Negative	8 (13.33%)	52 (86.67%)		p-value	1.000
					Sig.	ns
ER	+	5 (9.62%)	47 (90.38%)	ER	Fisher's exact test	
	-	4 (13.79%)	25 (86.21%)		p-value	0.7149
					Sig.	ns
PR	+	7 (13.21%)	46 (86.79%)	PR	Fisher's exact test	
	-	3 (10.71%)	25 (89.29%)		p-value	1.000
					Sig.	ns
Her-2/*neu*	+	5 (15.63%)	27 (84.38%)	Her2/*Neu*	Fisher's exact test	
	-	4 (8%)	46 (92%)		p-value	0.3020
					Sig.	ns

Table 23: Correlation between the clinico-pathological features and iNOS scores with Mann Whitney U or Kruskal Wallis analysis

Clinico-pathological features		Patients (N)	Median score	Mean score	Test	Test's score	P value
Age	**≤50**	16	8.667	8.666±0.544	Mann Whitney U	509	0.6311
	>50	69	9.333	8.855±0.218			
T. Siz	**T1**	7	9	8.8334±0.771	Kruskal-Wallis	0.377	0.828
	T2	71	9.333	8.836±0.231			
	T3	9	9.333	9.266±0.511			
Grade	**I**	12	9.333	8.512±0.466	Kruskal-Wallis	1.239	0.538
	II	30	9	9.253±0.365			
	III	37	9.333	8.705±0.304			
Stage	**I**	5	10	9±0.966	Kruskal-Wallis	0.789	0.673
	II	49	9.333	8.97±0.272			
	III	31	9.333	8.67±0.318			
LN Mets	**Positive**	53	9.333	8.761±0.263	Mann Whitney U	834	0.560
	Negative	34	9.333	8.962±0.306			
VSI	**Positive**	27	9.333	8.851±0.358	Mann Whitney U	736.5	0.851
	Negative	60	9.333	8.905±0.248			
ER	**+**	52	8.666	8.678±0.263	Mann Whitney U	631.5	0.226
	-	29	9.333	9.187±0.327			

PR	+	53	8.666	8.741±0.269	Mann Whitney U	659.5	0.412
	-	28	9.333	9.087±0.312			
Her2/*neu*	+	32	9.333	8.930±0.347	Mann Whitney U	725.5	0.572
	-	50	8.666	8.815±0.258			

There was no direct correlation between iNOS expression and age of IDC patients (p=0.6812, two tailed) (Table 22). A significant difference in iNOS scores distribution was not observed when scores of IDC patients were compared between age groups ≤50 and >50 (Mann Whitney U score=509, p value =0.631, two tailed). The median iNOS score was 8.66 and 9.33 for age groups ≤50 and >50 respectively (Table 23).

No significant relationship was observed between iNOS expression and tumor size (Chi square score=1.1233, p=0.9402, two tailed). The median iNOS scores of T1 tumor size was 9, T2 tumor size was 9.33 and T3 tumor size was 9.33. An insignificant difference in iNOS scores distribution was observed when scores of IDC patients were compared between different tumor size (Kruskal Wallis score=0.377, p value =0.828, two tailed) (Table 23).

There was no direct correlation between iNOS expression and tumor grade of IDC patients (Chi square score=1.572, p=0.4556, two tailed) (Table 22). When iNOS expression was compared in malignant patients with different tumor grades no significant difference was observed (Kruskal Wallis score=1.239, p value =0.538, two tailed). The median iNOS scores observed for Grade I, II and III patients were 9.33, 9 and 9.33 respectively (Table 23).

No significant correlation was observed between iNOS expression and tumor TNM staging of IDC patients (p=0.1982, two tailed) (Table 22). High expression of iNOS was seen in

80% of stage I patients, 91.8% of stage II patients and 80.6 % stage III patients. An insignificant difference in distribution of iNOS scores was observed between different TNM staging groups (Kruskal Wallis score=0.789, p value =0.673, two tailed) (Table 23). The median iNOS scores of Stage I tumor was 10, Stage II tumor was 9.33 and Stage III tumor was 9.33.

A direct correlation was not observed with iNOS expression and lymph node involvement (p=0.1894, two tailed) (Table 22). The median iNOS scores of patients with and without lymph node involvement was 9.33. When distribution of iNOS score was compared between malignant samples differing in lymph node status, an insignificant difference was observed, (Mann Whitney U score=834, p value =0.564, two tailed) (Table 23).

There was no direct correlation between iNOS expression and vessel space invasion in IDC samples (p=1.000, two tailed) (Table 22). An insignificant difference was observed when distribution of iNOS score was compared between malignant samples with different vessel space invasion (Mann Whitney U score=736.5, p value =0.851, two tailed).

There was no direct correlation between iNOS expression and ER receptor status of IDC patients (p=0.7149, two tailed). The median iNOS scores of patients with positive ER and negative ER status were 8.66 and 9.33 respectively. A direct correlation was not observed with iNOS expression and PR status (p=1.000, two tailed). When distribution of iNOS score was compared between malignant samples with different PR status an insignificant difference was observed (Mann Whitney U score=659.5, p value =0.412, two tailed).

No significant correlation was observed between iNOS expression and Her-2/neu status of IDC patients (p=0.3020, two tailed). High expression of iNOS was seen in 84.3% of Her-2/neu + patients and 92 % of Her-2/neu- patients. An insignificant difference in distribution of

iNOS scores was observed when IDC patients with different Her2/neu status were compared (Mann Whitney U score=725.5, p value =0.572, two tailed) (Table 23).

3.3.4 Expression of p53 by immunohistochemistry

The loss of normal p53 tumor suppressor gene function due to genetic alterations is a major factor behind human cancers. *TP53* is the gene most often mutated in human cancer, occurring in over 50% of the malignant tumors. Mutated p53 is unable to bind DNA and thus cannot function as a transcription factor. p53 can be inactivated in many ways resulting in possible over expression and alterations in the downstream target genes, complexing with other proteins, or abnormal degradation. The half life of wt p53 is short, with the protein degrading in 20-30 minutes. Genetic or other structural changes transform the wt p53 conformation, resulting in stabilization and accumulation in the cells and allowing its immunohistochemical detection [259, 351]. There have been reports of a positive prognostic value of p53 detected by immunohistochemistry. For instance, expression of mutant p53 protein was associated with early disease recurrence and early death in node negative breast cancer [352]. The accumulation of p53 was significantly associated with increased risk of progression to malignant breast cancer in women with benign breast disease [353]. Figure 42 shows the representative images with absence of p53 staining as well as p53 intensity 1, 2 and 3.

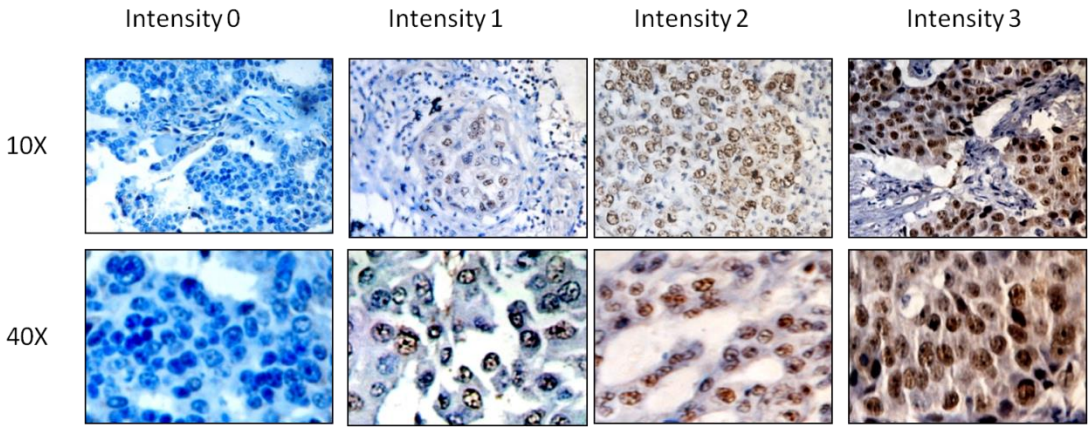

Figure 42: Representative images of p53 expression with different staining intensities (intensity 1, intensity 2 and intensity 3). The top panel represents the 10X image and bottom panel represents the 40 X image of the same field.

3.3.4.1 p53 expression in benign fibroadenoma and IDC samples

Heterogeneous nuclear p53 staining was observed in tumor cells (Figure 42). The p53 expression was studied in 22 benign fibroadenoma and 76 IDC samples. Seventeen out of 22 (77.27%) benign fibroadenoma and 57 out of 76 (75%) IDC samples were positive for p53 labeling. The median score in benign fibroadenoma samples was 1.75 (range 0-6) and that of IDC samples was 3 (range 0-12). The distribution of p53 score in benign fibroadenoma and IDC group did not differ significantly (Mann Whitney U score=638, p value 0.089, two tailed) (Figure 43a). Bioinformatic analysis was carried out using Oncomine (www.oncomine.com, Oncomine Research Premium Edition) to assess mRNA levels of p53 expression in breast cancer database applying fold change ≥ 2 and $p \leq 0.01$ as thresholds. p53 was significantly upregulated in invasive breast carcinoma (19 samples) as compared to normal breast tissue (3 samples), (t-test=2.434, p value=0.039, two tailed, fold change=2.321) [354] (Figure 43b). The data base also consisted of other studies comparing p53 expression amongst different carcinoma subtypes.

Some studies in the database show the fold change of 1.029 (p=0.007) between breast adenocarcinoma and medullary breast cancer [348], fold change of 1.126 (p=0.017) between breast adenocarcinoma and lobular breast carcinoma [349] and fold change of 1.256 (p=0.038) in normal and ductal breast carcinoma [350].

The lower IHC scores (0-6) were classified as weak and higher scores (7-12) as strong p53 expression in the tumor cells. The obtained p53 score was low in 50 (65.78%) and high in 26 (34.21%) malignant tumors. In benign fibroadenoma samples, 22 (100%) samples had weak p53 expression and none of the samples had strong p53 expression. The proportion of patients with strong p53 scores was significantly higer in IDC group as compared to fibroadenoma samples (Fisher's exact test, p=0.0006, two tailed) (Figure 43c).

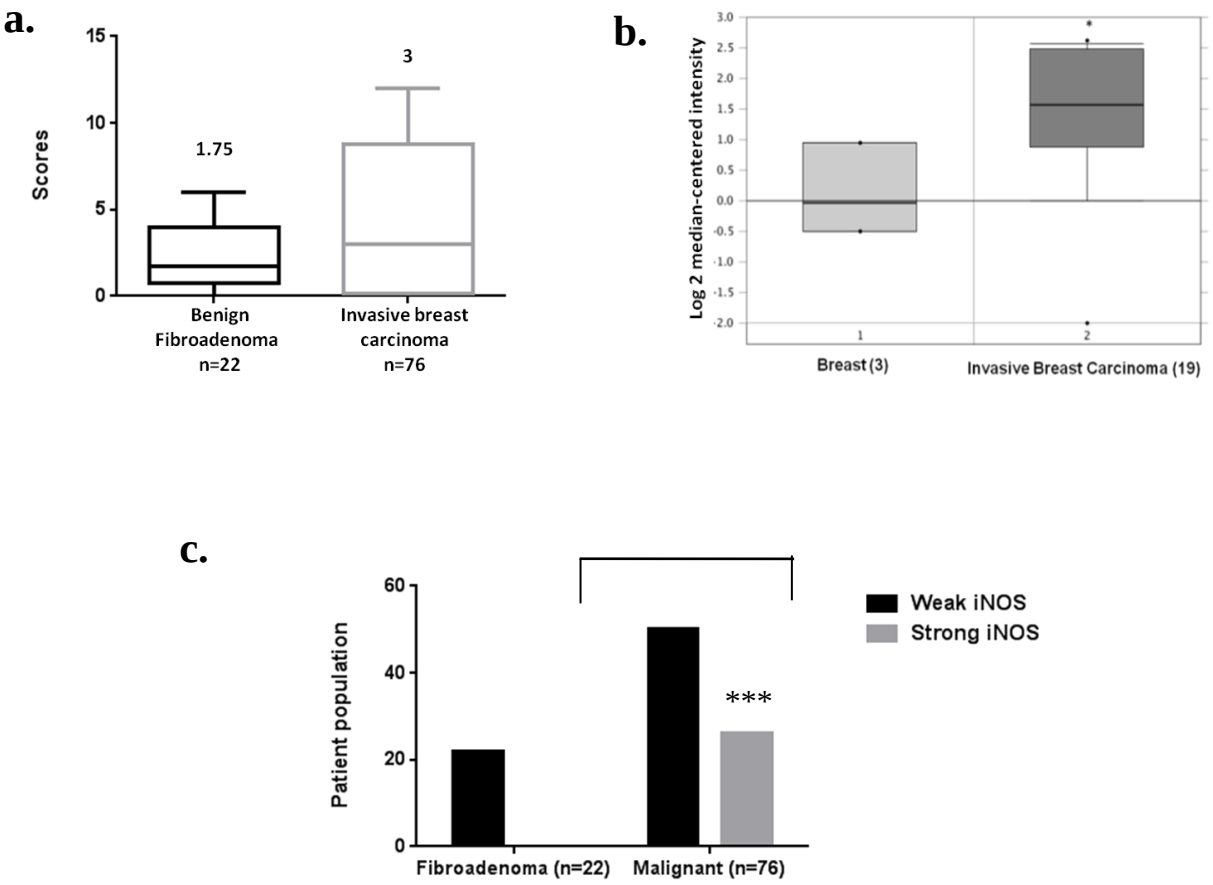

Figure 43: Expression of p53 in benign fibroadenoma and invasive breast carcinoma (benign fibroadenoma=22 samples, IDC =76 samples). (a) Median p53 scores distribution in benign fibroadenoma and IDC groups (Mann Whitney U score=638, p value = 0.089, two tailed). The bar represent median value along with the range of distribution of p53 scores (b) Oncomine data set for mRNA levels of p53 in normal breast tissue and breast cancer (t-test=2.434, p value=0.039, two tailed, fold change=2.321). (c) Proportion of fibroadenoma and IDC patients with weak or strong p53 (p=0.0006, two tailed) (Figure 44c). * The Mann Whitney U statistic is significant at the 0.05 level. *** The Fisher's exact test statistic is significant at the 0.001 level.

3.3.4.2 p53 expression and its association with clinicopathological features

The distribution of scores and relationship between the clinico-pathological features with proportion of samples with weak or strong p53 expression scores as analysed by chi square/ Fisher's exact analysis is summarized in table 24. The distribution of p53 score in IDC samples with different clinico-pathological features was studied with non parametric one way ANOVA (Mann Whitney U test or Kruskal Wallis test) and is summarized in table 25.

Table 24: Summary table showing the distribution and correlation between the clinico-pathological features and p53 scores

Clinico-pathological characteristics		Patient's distribution		Clinico-pathological characteristics		p53 Correlation
		Weak p53 score	Strong p53 score			
Age	25-40 41-55 56-70 70-85	2 (40%) 16 (66.67%) 27 (72.97%) 5 (62.5%)	3 (60%) 8 (33.33%) 10 (27.03%) 3 (37.50%)	Age	Chi-square, Df p-value Sig.	2.330, 3 0.5058 ns
T. Size	T1 T2 T3	6 (85.71%) 38 (65.52%) 6 (54.55%)	1 (14.29%) 20 (34.48%) 5 (45.45%)	T. Size	Chi-square, Df p-value Sig.	1.855, 2 0.3956 ns
Grade	I II III	9 (81.82%) 16 (61.54%) 15 (45.45%)	2 (18.18%) 10 (38.46%) 18 (54.55%)	Grade	Chi-square, Df p-value Sig.	4.356, 2 0.3599 ns
Stage	I II III	4 (80%) 29 (65.91%) 17 (65.38%)	1 (20%) 15 (34.09%) 9 (34.62%)	Stage	Chi-square, Df p-value Sig.	0.403, 2 0.8063 ns
LN Mets	Positive Negative	30 (68.18%) 21 (65.63%)	14 (31.82%) 11 (34.38%)	LN Mets	Fisher's exact test p-value Sig.	 1.000 ns
VSI	Positive Negative	16 (72.73%) 34 (64.15%)	6 (27.27%) 19 (35.85%)	VSI	Fisher's exact test p-value Sig.	 0.5940 ns
ER	+ -	31 (75.60%) 13 (50%)	10 (24.4%) 13 (50%)	ER	Fisher's exact test p-value Sig.	 0.0384 *
PR	+ -	35 (77.78%) 11 (44%)	10 (22.22%) 14 (56%)	PR	Fisher's exact test p-value Sig.	 0.0079 **
Her-2/*neu*	+ -	13 (46.43%) 33 (78.57%)	15 (53.57%) 9 (21.43%)	Her2/*Neu*	Fisher's exact test p-value Sig.	 0.0095 **

*****The Fisher's exact statistic is significant at the 0.05 level. ****** The Fisher's exact statistic is significant at the 0.01 level.

Table 25: Summary table showing the correlation between the clinico-pathological features and p53 scores distribution with Mann Whitney U or Kruskal Wallis analysis

Clinico-pathological features		Patients (N)	Median score	Mean score	Test	Test's score	P value
Age	**25-40**	5	10	7.3±2.165	Kruskal-Wallis	2.818	0.420
	41-55	24	3	4.645±0.837			
	56-70	37	4	4.445±0.739			
	71-85	8	1	3.875±1.716			
T. Size	**T1**	6	1.5	1.5±0.621	Kruskal-Wallis	3.136	0.2084
	T2	55	3	4.609±0.548			
	T3	11	6	5.909±1.404			
Grade	**I**	11	1	2.818±1.285	Kruskal-Wallis	4.743	0.0933
	II	26	3	4.076±0.824			
	III	33	6	5.742±0.774			
Stage	**I**	5	2	3±1.788	Kruskal-Wallis	0.760	0.683
	II	44	3	4.59±0.664			
	III	26	6	5.173±0.870			
LN Mets	**Positive**	44	3.5	4.659±0.641	Mann Whitney U	693	0.909
	Negative	32	2	4.578±0.814			
VSI	**Positive**	23	3	4.239±0.781	Mann Whitney U	542	0.796
	Negative	49	3	4.693±0.438			

ER	+	44	1.5	3.477±0.587	Mann Whitney U	349	0.0056
	-	26	7	6.326±0.813			**
PR	+	45	2	3.4±0.541	Mann Whitney U	344.5	0.006
	-	25	8	6.8±0.881			**
Her2/neu	+	28	8	6.392±0.758	Mann Whitney U	348.5	0.003
	-	42	1.5	3.297±0.595			**

****** The Mann Whitney U statistic is significant at the 0.01 level.

No direct correlation was observed between p53 expression and age of IDC patients (Chi square score=2.330, p=0.5068, two tailed) (Table 24). The median p53 scores of different group's viz. age 25-40, 41-55, 56-70 and above 70 were 10, 3, 4 and 1 respectively. Though p53 expression showed a decreasing trend with increase in patient's age, no significant difference in p53 scores was observed between the different age groups (Kruskal Wallis score= 2.818, p value = 0.420, two tailed) (Table 25).

There was no direct significant relationship between p53 expression and tumor size (Chi square score=1.855, p=0.3956, two tailed) (Table 24). An insignificant difference in distribution of p53 scores was observed between IDC samples of different tumor size groups (Kruskal Wallis score=3.136, p value =0.208, two tailed).

The median p53 scores of grade I tumors was 1, grade II tumors was 3 and grade III tumors was 6. Although the scores had increasing trend with higher tumor grade, this difference was not statistically significant (Kruskal Wallis score= 4.743, p value = 0.0933, two tailed) (Table 25). No direct correlation was observed between p53 expression and tumor grade of IDC patients (Chi square score= 4.781, p=0.0916, two tailed) (Table 24).

No correlation was observed between p53 expression and tumor TNM staging of IDC samples (Chi square score= 0.403, p=0.8063, two tailed) (Table 24). An insignificant difference in distribution of p53 scores between IDC samples of different TNM staging groups were compared (Kruskal Wallis score=0.760, p value =0.683, two tailed). However, the stage I patients had lowest p53 scores and stage III patients had highest p53 expression scores (Table 25).

No significant correlation was observed between p53 expression and lymph node involvement (p=1.000, two tailed) (Table 24). When distribution of p53 score was compared in malignant samples differing in lymph node status, an insignificant difference was observed (Mann Whitney U score=693, p value =0.909, two tailed).

There was no direct correlation between p53 expression and vessel space invasion in IDC samples (p=0.5940, two tailed) (Table 24). An insignificant difference was observed when distribution of p53 score was compared in malignant samples with different vessel space invasion (Mann Whitney U score=542, p value =0.796, two tailed) (Table 25).

There was a direct correlation between p53 expression and ER status of IDC samples (p=0.0384, two tailed) (Table 24). "Strong" p53 labeling was observed in 10 out of 43 patients with ER+ status and 13 out of 26 (50%) patients with ER- status. The median p53 scores of patients with positive ER status and negative ER status was 1.5 and 7 respectively. A significant difference in the distribution of p53 expression scores was observed with respect to ER+ and ER- status of IDC samples (Mann Whitney U score=349, p value =0.0056, two tailed) (Table 25; Figure 44a).

A direct correlation was observed with p53 expression and PR status (p=0.0079, two tailed) (Table 24). Strong p53 labeling was observed in 10 out of 45 patients with positive PR status and 14 out of 25 patients with negative PR status. The median p53 scores of patients with both PR+ and PR- status were 2 and 8 respectively. When distribution of p53 score was compared between malignant samples differing in PR status, a significant difference was observed as PR- samples had higher p53 expression (Mann Whitney U score=344.5, p value =0.006, two tailed) (Table 25; Figure 44b).

A significant correlation was observed between p53 expression and Her-2/neu status of IDC samples (p=0.0095, two tailed) (Table 24). "Strong" expression of p53 was seen in 53.5% of Her2/neu + patients and 21.4 % of Her2/neu- patients. A significant difference in distribution of p53 scores was observed when IDC patients with different Her2/neu status were compared (Mann Whitney U score=348.5, p value =0.003, two tailed). The median p53 scores of Her2/neu+ patient was 8 and Her2/neu- patients was 1.5 (Table 25; Figure 44c).

The median p53 scores of patients with $ER^+PR^+Her2^+$ was 1, $ER^+PR^+Her2^-$ was 1, $ER^-PR^-Her2^+$ was 9 and $ER^-PR^-Her2^-$ was 0.75. The p53 expression scores were highest in $ER^-PR^-Her2^+$ group whereas $ER^-PR^-Her2^-$ group showed lowest p53 expression (Figure 44d).

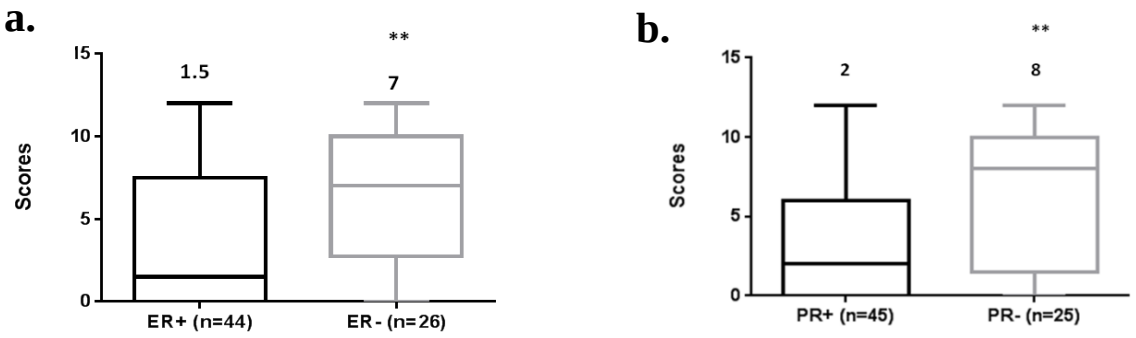

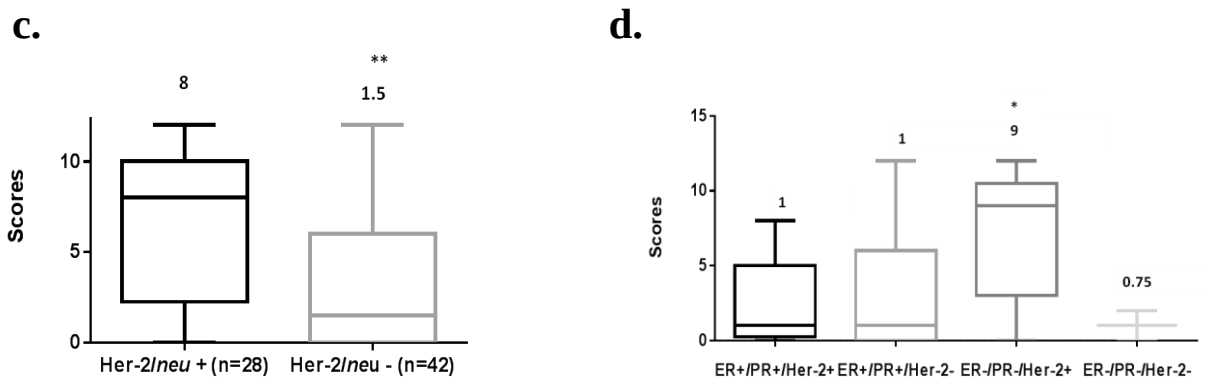

Figure 44: Expression of p53 in IDC patients of different receptor status. p53 score distribution is compared in IDC samples with different (a) ER status (Mann Whitney U score=349, p value =0.0056, two tailed). (b) PR status (Mann Whitney U score=344.5, p value =0.006, two tailed). (c) Her-2/neu status (Mann Whitney U score=348.5, p value =0.003, two tailed). (d) different ER, PR and Her2/neu receptor status. ***** The Mann-Whitney U statistic is significant at the 0.05 level. ****** The Mann-Whitney U statistic is significant at the <0.01 level.

3.3.5 Expression of γ-H2AX by immunohistochemistry

Histone H2AX phosphorylation on serine 139 (producing γ-H2AX) is a sensitive marker for DNA double-strand breaks (DSBs). DSBs may lead to cancer but, paradoxically, are also used to kill cancer cells. Detection of γ-H2AX to determine the extent of DSB induction may help to detect precancerous cells, cancers staging, for monitoring the effectiveness of cancer therapies and development of novel anticancer drugs. The nuclear labeling in tumor cells was studied for γ-H2AX expression. Figure 45 shows the representative images with absence of γ-H2AX staining as well as γ-H2AX intensity 1and 2.

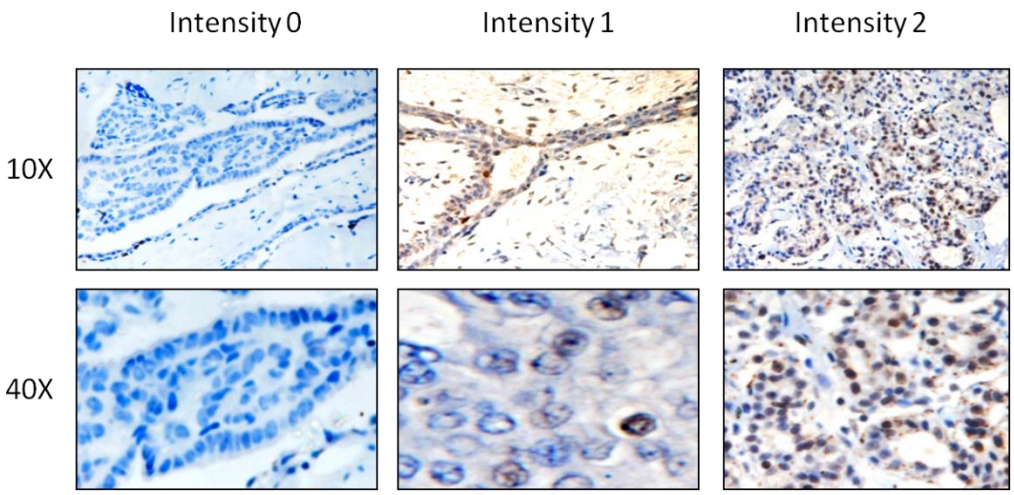

Figure 45: Representative images of γ-H2AX expression with different staining intensities (intensity 0, intensity 1 and intensity 2). The top panel represents the 10X image and bottom panel represents the 40 X image of the same field.

3.3.5.1 γ-H2AX expression in benign fibroadenoma and IDC samples

The nuclear γ-H2AX staining was observed in tumor cells (Figure 45). The γ-H2AX expression was studied in 22 benign fibroadenoma and 82 IDC samples. None of the fibroadenoma samples were negative for γ-H2AX expression whereas 19 out of 82 (23.17%) IDC samples were negative for γ-H2AX labeling. The median γ-H2AX score was same in both groups (4) but with different range in benign fibroadenoma (range 1-6) and IDC (range 0-12). The distribution of γ-H2AX score in benign fibroadenoma and IDC group did not differ significantly (Mann Whitney U score=887, p value= 0.9063, two tailed) (Figure 46a). Bioinformatic analysis was carried out using Oncomine (www.oncomine.com, Oncomine Research Premium Edition) to assess changes in transcript levels of histone variant H2AX in breast cancer database applying fold change ≥ 2 and p ≤ 0.01 as thresholds. H2AX mRNA was significantly upregulated in IDC data sets (1556 cases) as compared to normal breast tissue (144

cases), (t-test=28.241, p value< 0.0001, two tailed, fold change=1.481) [348] (Figure 46b). The data base also consisted of many studies comparing H2AX expression in different carcinoma subtypes. Some of the studies in the database show a fold change of 2.588 (p<0.0001) between normal and invasive breast carcinoma (TCGA Breast Statstics, 2010) and fold change of 1.226 (p=0.017) in adenocarcinoma and ductal breast carcinoma [355]. All these studies thus demonstrate that apart from post translational modifications of H2AX, which is monitored as γ-H2AX, this gene is upregulated at the transcriptional level also in many cancers.

The IHC lower scores (0-6) were classified as weak γ-H2AX expression and higher scores (7-12) as strong γ-H2AX expression in the tumor cells. The obtained γ-H2AX score was low in 68 (83%) samples and high in 14 (17%) malignant tumors. In fibroadenoma samples, 22 (100%) samples had weak γ-H2AX expression and none of the samples had strong γH2AX expression. The proportion of patients with strong γ-H2AX scores were significantly higher in IDC group as compared to benign fibroadenoma samples (Fisher's exact test, p=0.0374, two tailed) (Figure 46c).

a.

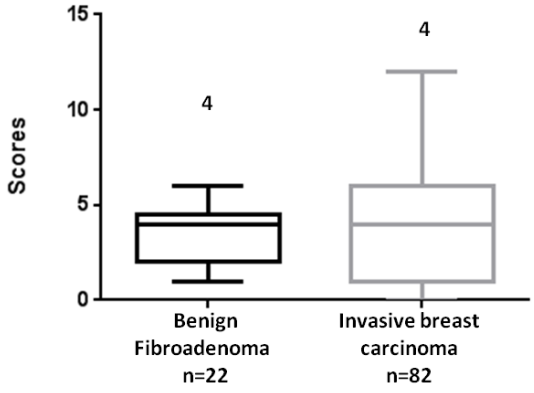

b.

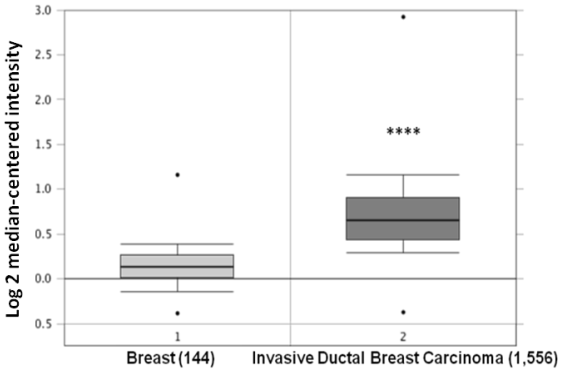

c.

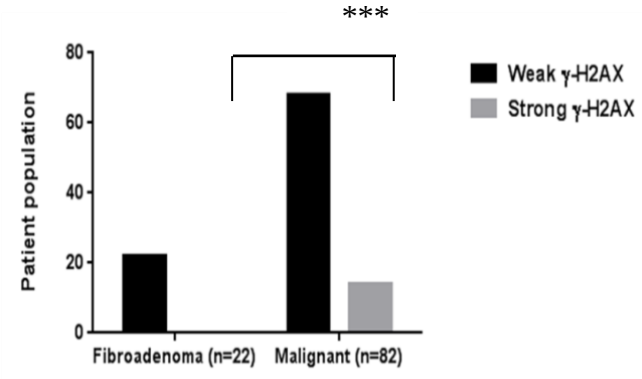

Figure 46: Expression of γ-H2AX in benign fibroadenoma and invasive ductal carcinoma samples (benign fibroadenoma=22 samples, IDC=82 samples). (a) Median γ-H2AX score along with range of distribution in benign fibroadenoma and IDC groups (Mann Whitney U score=887, p value= 0.9063, two tailed). (b) Oncomine data set for the mRNA levels of histone variant H2AX in breast cancer and normal samples (t-test=28.241, p value< 0.0001, two tailed, fold change=1.481) [348]. (c) Proportion of benign fibroadenoma and IDC patients with weak or strong γ-H2AX expression (p=0.0374, two tailed). *** The Fisher's exact statistic is significant at the 0.001 level.

3.3.5.2 γ-H2AX expression and its association with clinicopathological features

The distribution of scores and relationship between the proportion of patients with weak or strong γ-H2AX expression with the clinico-pathological features as analysed by chi square/ Fisher's exact analysis is summarized in table 26. The distribution of γ-H2AX score in IDC patient groups differing in clinico-pathological features studied with non parametric one way ANOVA (Mann Whitney U test or Kruskal Wallis test) is summarized in table 27.

Table 26: Summary table showing the distribution and correlation between the clinico-pathological features and γ-H2AX scores

Clinico-pathological characteristics		Patient's distribution		Clinico-pathological characteristics		γH2AX Correlation
		Weak γH2AX score	Strong γH2AX score			
Age	25-55 56-70 70-85	25 (86.20%) 32 (82.05%) 5 (62.5%)	4(13.79%) 7 (17.95%) 3 (37.5%)	Age	Chi-square, Df p-value Sig.	2.356, 2 0.3078 ns
T. Size	T1 T2 T3	4 (66.67%) 52 (83.87%) 7 (77.78%)	2 (33.33%) 10 (16.13%) 2 (22.22%)	T. Size	Chi-square, Df p-value Sig.	1.250, 2 0.5487 ns
Grade	I II III	5 (49.8%) 17 (68%) 19 (52.78%)	5.04 (50.2%) 8 (32%) 17 (47.22%)	Grade	Chi-square, Df p-value Sig.	1.687, 2 0.4301 ns
Stage	I & II III	38 (79.16%) 25 (89.29%)	10 (20.83%) 3(10.71%)	Stage	Fisher's exact test p-value Sig.	0.3507 ns
LN Mets	Positive Negative	38 (88.37%) 25 (75.76%)	5 (11.63%) 8 (24.24%)	LN Mets	Fisher's exact test p-value Sig.	0.2193 ns
VSI	Positive Negative	20 (86.96%) 43 (79.63%)	3 (13.04%) 11 (20.37%)	VSI	Fisher's exact test p-value Sig.	0.5346 ns
ER	+ -	37 (84.09%) 24 (88.89%)	7 (15.91%) 3 (11.11%)	ER	Fisher's exact test p-value Sig.	0.7317 ns
PR	+ -	40 (88.89%) 22 (84.62%)	5 (11.11%) 4 (15.38%)	PR	Fisher's exact test p-value Sig.	0.7156 ns
Her-2/*neu*	+ -	24 (82.76%) 37 (86.05%)	5 (17.24%) 6 (13.95%)	Her2/*Neu*	Fisher's exact test p-value Sig.	0.7468 ns

Table 27: Summary table showing the correlation between the clinico-pathological features and γ-H2AX scores distribution with Mann Whitney U or Kruskal Wallis analysis

Clinico-pathological features		Patients (N)	Median score	Mean score	Test	Test's score	P value
Age	**25-40**	5	3	3.4±0.812	Kruskal-Wallis	5.052	0.1681
	41-55	24	3.5	3.312±0.610			
	56-70	39	4	4.384±0.500			
	71-85	8	6	6.562±1.43			
T. Size	**T1**	6	4.5	5±1.511	Kruskal-Wallis	0.5447	0.7616
	T2	59	4	3.788±0.368			
	T3	9	4	4.111±1.101			
Grade	**I**	10	4.25	4.3±0.916	Kruskal-Wallis	3.697	0.157
	II	25	3	3.1±0.664			
	III	36	4	4.5±0.534			
Stage	**I**	5	6	5.8±1.959	Kruskal-Wallis	1.140	0.565
	II	43	4	3.872±0.490			
	III	28	4	4.214±0.594			
LN Mets	**Positive**	44	4	3.931±0.466	Mann Whitney U	687	0.687
	Negative	33	4	4.348±0.584			
VSI	**Positive**	24	4	3.812±0.527	Mann Whitney U	593.5	0.972
	Negative	50	4	3.98±0.438			

ER	+	45	4	4.066±0.452	Mann Whitney U	594.5	0.881
	-	27	4	3.611±0.503			
PR	+	45	4	3.722±0.382	Mann Whitney U	570	0.664
	-	27	4	4.185±0.645			
Her2/*neu*	+	29	3	3.551±0.643	Mann Whitney U	539	0.328
	-	43	4	4.127±0.363			

No direct correlation was observed between γ-H2AX expression and age of IDC patients (Chi square score=3.122, p=0.3732, two tailed) (Table 26). The median γ-H2AX scores of different groups viz. age 25-40, 41-55, 56-70 and above 70 were 3, 3.5, 4 and 6 respectively. Though an increasing trend in the γ-H2AX expression score was seen corresponding to an increase in patient's age, it was not found to be statistically significant (Kruskal Wallis score= 5.052, p value = 0.1681, two tailed) (Table 27).

There was no significant relationship between γ-H2AX expression and tumor size (Chi square score=1.250, p=0.5487, two tailed) (Table 26). An insignificant difference in distribution of γ-H2AX was observed when scores of IDC patients in different tumor size groups were compared (Kruskal Wallis score=5.447, p value =0.761, two tailed) (Table 27).

When distribution of γ-H2AX scores of patients with different tumor grades were compared, an insignificant difference was observed (Kruskal Wallis score= 3.697, p value = 0.157, two tailed) (Table 27). No direct correlation was observed between γ-H2AX expression and tumor grade of IDC patients (Chi square score= 1.687, p=0.430, two tailed) (Figure 50c) (Table 26).

No significant correlation was observed between γ-H2AX expression and TNM staging of patients (p=0.3507, two tailed) (Table 26). An insignificant difference was observed when γ-H2AX scores of IDC samples in different TNM staging groups were compared (Kruskal Wallis score=1.140, p value =0.565, two tailed). However, the stage I patients had the highest γ-H2AX expression (Table 27).

No significant correlation was observed with γ-H2AX expression and lymph node involvement (p=0.2193, two tailed) (Table 26). When distribution of γ-H2AX score was compared in malignant samples with different lymph node status an insignificant difference was observed (Mann Whitney U score=637, p value =0.687, two tailed) (Table 27). There was no direct correlation between γ-H2AX expression and vessel space invasion in IDC samples (p=0.5346, two tailed) (Table 26).

There was no direct correlation between γ-H2AX expression and ER status of IDC samples (p=0.7317, two tailed) (Table 26). A significant difference in the distribution of γ-H2AX expression scores was not observed with respect to ER+ and ER- status of IDC samples (Mann Whitney U score=594.5, p value =0.881, two tailed) (Table 27).

A direct correlation was not observed with γ-H2AX expression and PR status (p=0.7156, two tailed). A significant correlation was not observed between γ-H2AX expression and Her-2/neu status of IDC samples (p=0.7468, two tailed) (Table 26).

3.3.6 Expression of pCREB by immunohistochemistry

CREB functions as a regulator of the expression of several genes in response to hormones, ion fluxes, growth factors and stress signals [356]. Accumulating evidences show that CREB is overexpressed in several neoplastic cancers, functions as an important oncogene that promotes tumor cell growth and is involved in the proliferation, survival and metastasis of tumor cells [357]. Figure 47 shows the representative images with absence of pCREB staining as well as intensity 1, 2 and 3.

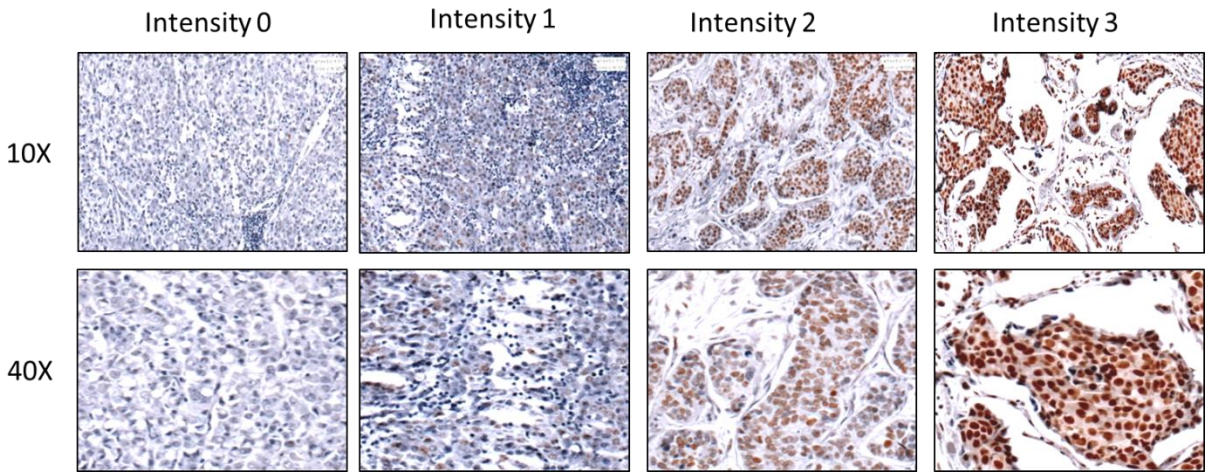

Figure 47: Representative images of pCREB expression with different staining intensities (intensity 1, intensity 2 and intensity 3). The top panel represents the 10X image and bottom panel represents the 40 X image of the same field.

3.3.6.1 pCREB expression in benign fibroadenoma and IDC samples

Heterogeneous nuclear pCREB staining was observed in tumor cells (Figure 47). pCREB expression was studied in 21 benign fibroadenoma samples and 85 IDC samples. All (100%) fibroadenoma samples were positive for pCREB expression whereas 77 out of 85 (90.2%) IDC samples were positive for pCREB labeling. None of the fibroadenoma samples were negative for

pCREB expression while 8 out of 85 (9.8%) IDC samples were negative for pCREB. The median pCREB score in benign fibroadenoma samples was 7.33 (range 1-9) and in IDC samples was 6.66 (range 0-12). The distribution of pCREB score in benign fibroadenoma and malignant group did not differ significantly (Mann Whitney U score=835, p value 0.651, two tailed) (Figure 48a).

The lower IHC scores (0-6) were classified as weak pCREB expression and higher scores (7-12) as strong pCREB expression in the tumor cells. The obtained pCREB score was low in 40 (47.05%) and high in 45 (52.95%) malignant tumors. In benign fibroadenoma samples, 8 (38%) samples had weak pCREB expression whereas 62% samples showed strong pCREB expression. Though the mean pCREB score in fibroadenoma patients was slightly higher than IDC patients, the highest pCREB score of 12 was seen in IDC samples where 10% samples had a score of 12. The proportion of patients with strong pCREB scores was not significantly higher in IDC group as compared to benign fibroadenoma samples (Fisher's exact test, p=0.6252, two tailed) (Figure 48b).

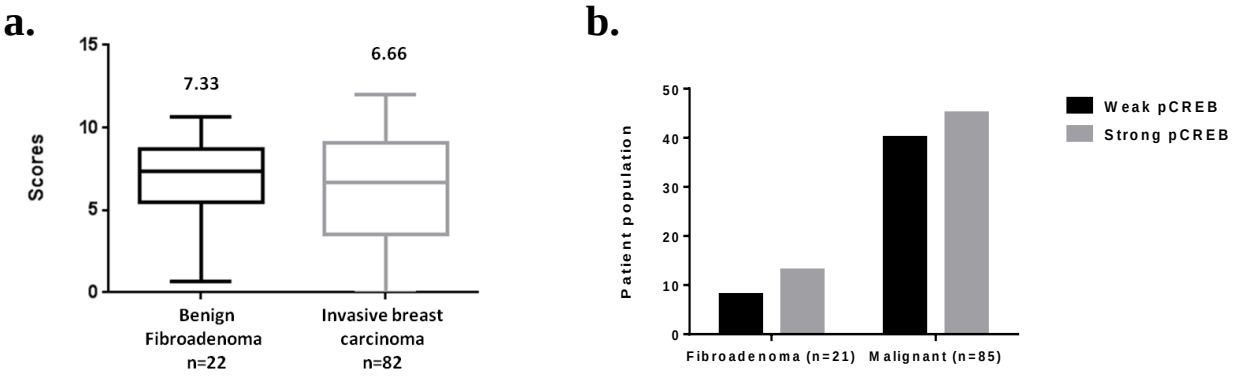

Figure 48: Expression of pCREB in benign fibroadenoma and invasive ductal carcinoma cases (benign fibroadenoma=21 samples, IDC =85 samples). (a) Median pCREB score distribution along with distribution of scores in benign fibroadenoma and malignant groups

(Mann Whitney U score=835, p value 0.651, two tailed). The bar represent median value along with the range of distribution of pCREB scores (b) Proportion of benign fibroadenoma and IDC patients with weak or strong pCREB expression (p=0.6252, two tailed).

3.3.6.2 pCREB expression and its association with clinico-pathological features

The distribution of scores and relationship of proportion of patients with weak or strong pCREB expression with the clinico-pathological features was analysed by chi square / Fisher's exact analysis and is summarized in table 28 and 29. The distribution of pCREB score in IDC patient groups differing in clinico-pathological features studied with non parametric one way ANOVA (Mann Whitney U test or Kruskal Wallis test) is summarized in table 30.

Table 28: Distribution and correlation between the TNM stage and pCREB

Tumor Stage	Patient's distribution			Chi Square Analysis	pCREB Correlation with tumor stage
	Weak pCREB score	Moderate pCREB score	Strong pCREB score		
I II III	0 (0%) 15 (34.09%) 5 (17.85%)	2 (40%) 13 (29.54%) 17 (60.71%)	3 (60%) 16 (36.36%) 6 (21.42%)	Chi-square, Df p-value Sig.	9.552, 4 0.0487 *

***** The Chi-square statistic is significant at the 0.05 level.

Table 29: Summary table showing the distribution and correlation between the clinico-pathological features and pCREB scores

Clinico-pathological characteristics		Patient's distribution		Clinico-pathological characteristics		pCREB Correlation
		Weak pCREB score	Strong pCREB score			
Age	25-40 41-55 56-70 70-85	3 (60%) 12 (48%) 20 (48.78%) 3 (37.5%)	2(40%) 13 (52%) 21 (51.22%) 5 (62.50%)	Age	Chi-square, Df p-value Sig.	0.654, 3 0.8846 ns
T. Size	T1 T2 T3	1(14.29%) 32 (49.23%) 6 (60%)	6 (85.71%) 33 (50.77%) 4 (40%)	T. Size	Chi-square, Df p-value Sig.	3.801, 2 0.1495 ns
Grade	I II III	5 (41.67%) 6 (21.43%) 10 (29.41%)	7 (58.33%) 22 (78.57%) 24 (70.59%)	Grade	Chi-square, Df p-value Sig.	1.726, 2 0.4219 ns
LN Mets	Positive Negative	23 (47.92%) 15 (46.88%)	25 (52.08%) 17 (53.13%)	LN Mets	Fisher's exact test p-value Sig.	 1.000 ns
VSI	Positive Negative	11(44%) 26 (47.27%)	14 (56%) 29 (52.73%)	VSI	Fisher's exact test p-value Sig.	 0.8136 ns
ER	+ -	23(47.92%) 13 (46.43%)	25 (52.08%) 15 (53.57%)	ER	Fisher's exact test p-value Sig.	 1.000 ns
PR	+ -	22 (46.81%) 14(51.85%)	25 (53.19%) 13 (48.15%)	PR	Fisher's exact test p-value Sig.	 0.8098 ns
Her-2/*neu*	+ -	14 (48.28%) 22 (46.81%)	15 (51.72%) 25 (53.19%)	Her2/*Neu*	Fisher's exact test p-value Sig.	 1.000 ns

Table 30: Summary table showing the correlation between the clinico-pathological features and pCREB scores distribution with Mann Whitney U or Kruskal Wallis analysis

Clinico-pathological features		Patients (N)	Median score	Mean score	Test	Test's score	P value
Age	**25-40**	5	6.11	6.022±1.904	Kruskal-Wallis	0.1658	0.9829
	41-55	25	7.22	6.239±0.663			
	56-70	41	6.66	6.331±0.606			
	71-85	8	7	6.774±1.150			
T. Size	**T1**	6	11.333	10.805±0.586	Kruskal-Wallis	11.59	0.003
	T2	62	6.388	6.111±0.415			**
	T3	10	3.527	4.888±1.348			
Grade	**I**	12	6.33	5.930±1.036	Kruskal-Wallis	2.412	0.299
	II	28	8	7.263±0.726			
	III	35	6.66	6.054±0.593			
Stage	**I**	5	9.166	8.788±1.498	Kruskal-Wallis	2.047	0.359
	II	46	7.111	6.267±0.599			
	III	29	6.666	6.394±0.556			
LN Mets	**Positive**	49	6.66	6.607±0.476	Mann Whitney U	749.5	0.741
	Negative	32	6.83	6.129±0.726			
VSI	**Positive**	25	6	6.434±0.658	Mann Whitney U	644	0.845
	Negative	53	6.66	6.259±0.248			

ER	+	48	6.66	6.684±0.535	Mann Whitney U	550.5	0.1922
	-	28	6.83	5.528±0.658			
PR	+	49	7.22	6.694±0.515	Mann Whitney U	533	0.164
	-	28	9.33	5.466±0.626			
Her2/*neu*	+	29	6.66	5.815±0.694	Mann Whitney U	607	0.428
	-	47	6.66	6.531±0.492			

****** The Kruskal-Wallis statistic is significant at the 0.01 level.

No correlation was observed between pCREB expression and age of IDC patients (Chi square score=0.654, p=0.8846, two tailed) (Table 29). There was no direct significant relationship between pCREB expression and tumor size (Chi square score=3.801, p=0.1495, two tailed) (Table 30). The median pCREB scores of T1 tumor size was 11.33, T2 tumor size was 6.38 and T3 tumor size was 3.52. A significant difference in distribution of pCREB scores was observed amongst different tumor size groups (Kruskal Wallis score=11.59, p value =0.003, two tailed) (Table 30). An inverse correlation between tumor size and pCREB was observed.

No direct correlation was observed between pCREB expression and tumor grade of IDC patients (Chi square score= 1.992, p=0.7372, two tailed) (Table 29). The median pCREB scores of grade I tumors was 1, grade II tumors was 3 and grade III tumors was 6. When distribution of pCREB scores of patients was compared between patients with different grades, an insignificant difference was observed (Kruskal Wallis score= 4.743, p value = 0.0933, two tailed) (Table 30). An inverse correlation was observed with pCREB expression and tumor TNM staging of IDC samples (Chi square score= 9.552, p=0.0487, two tailed) (Table 28). The median pCREB scores of stage I tumor was 9.16, stage II tumor was 7.11 and stage III tumor was 6.66. The highest pCREB expression was seen in stage I samples whereas stage III samples showed the lowest

pCREB expression. An insignificant difference was observed between pCREB score distribution of IDC samples of different TNM staging groups (Kruskal Wallis score=2.047, p value =0.359, two tailed) (Table 30).

No significant correlation was observed between pCREB expression and lymph node involvement (p=1.000, two tailed). There was no direct correlation between pCREB expression and vessel space invasion in IDC samples (p=0.8136, two tailed) (Table 29).

There was no direct correlation between pCREB expression and ER status of IDC samples (p=1.000, two tailed) (Table 29). A significant difference in the distribution of pCREB expression scores was not observed with respect to ER+ and ER- status of IDC samples (Mann Whitney U score=550.5, p value =0.1922, two tailed) (Table 30). A direct correlation was not observed with pCREB expression and PR status (p=0.8098, two tailed) (Table 29).

An insignificant correlation was observed between pCREB expression and Her-2/neu status of IDC samples (p=1.000, two tailed) (Table 29).

3.3.7 Expression of CREB by immunohistochemistry

The cyclic-AMP response element binding (CREB) protein has been shown to have an important role in cell survival, proliferation, growth and differentiation, in both normal and cancer cells. This molecule has been extensively studied in relation to stress response [358], memory [359] and in solid tumors, both benign and malignant [360]. CREB overexpression in transgenic animals imparts oncogenic properties to cells in various tissues and aberrant CREB expression is associated with tumors [361]. Sofi *et al* reported that the expression of CREB in tumor bearing breast adipose tissue is higher than the normal breast adipose tissue [356]. CREB is highly expressed and constitutively activated in patient glioma tissue and this activation

closely correlated with tumor grade [361]. Pathologically, CREB protein has been demonstrated to be upregulated in several human malignancies and act as an important oncogene [290]. Figure 49 shows the representative images with absence of CREB staining as well as CREB intensity 1, 2 and 3.

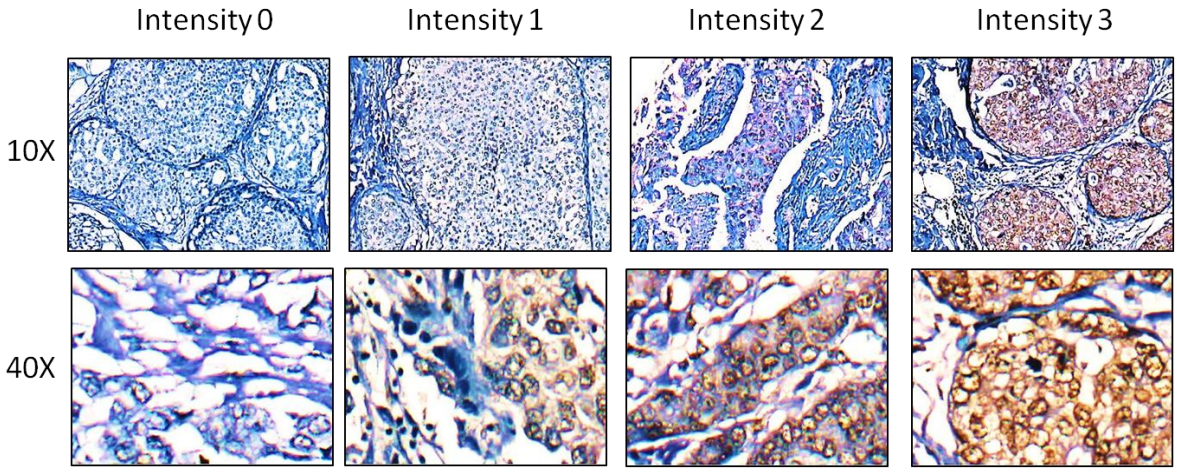

Figure 49: Representative images of CREB expression with different staining intensities (intensity 1, intensity 2 and intensity 3). The top panel represents the 10X image and bottom panel represents the 40 X image of the same field.

3.3.7.1 CREB expression in benign fibroadenoma and IDC samples

Nuclear staining of CREB was mostly restricted to tumor cells (Figure 49). A faint nuclear staining was seen in inflammatory cells present in the samples. CREB expression was studied in 22 benign fibroadenoma and 80 IDC samples. The median CREB score of fibroadenoma was 2 (range 0-8) and those of malignant IDC was 4 (range 0-12). CREB score distribution in benign fibroadenoma and IDC group differed significantly (Mann Whitney U score=641, p value = 0.0499, two tailed) (Figure 50a). Bioinformatic analysis was also carried

out using Oncomine (www.oncomine.com, Oncomine Research Premium Edition) to assess mRNA levels of CREB in breast cancer database applying fold change ≥ 2 and p ≤ 0.01 as thresholds. CREB mRNA was significantly upregulated in invasive breast carcinoma (13 cases) in data sets as compared to normal breast tissue (2 cases), (t-test=7.762, p value =0.004, two tailed, fold change=2.53) [354] (Figure 50b).

The lower IHC scores (0-6) were classified as weak CREB expression and higher scores (7-12) as strong CREB expression in the tumor cells. CREB score was low in 62 (75.6%) and high in 20 (24.4%) malignant tumors. In benign fibroadenoma samples, 20 (90.9%) samples had weak CREB expression and 2 (8.9%) samples had strong CREB expression. The CREB scores were not significantly higher in malignant IDC group as compared to benign fibroadenoma samples Fisher's exact test, p=0.1493, two tailed) (Figure 50c).

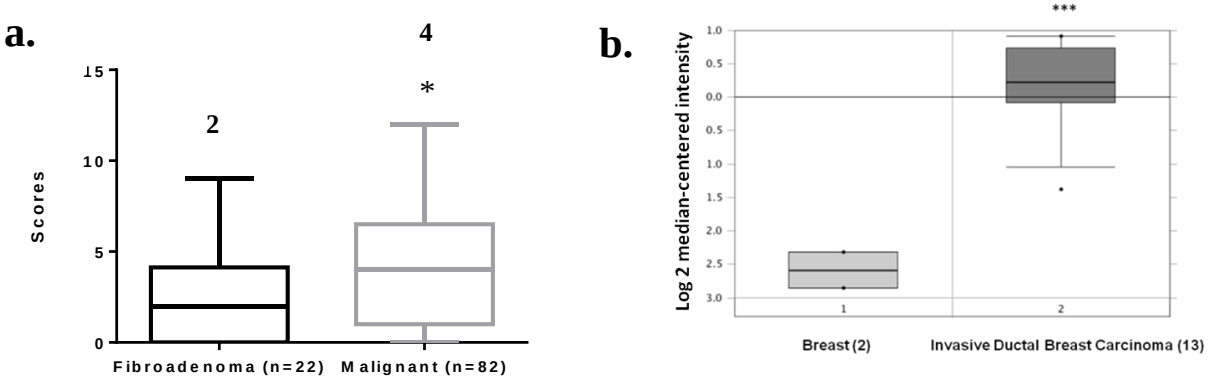

c.

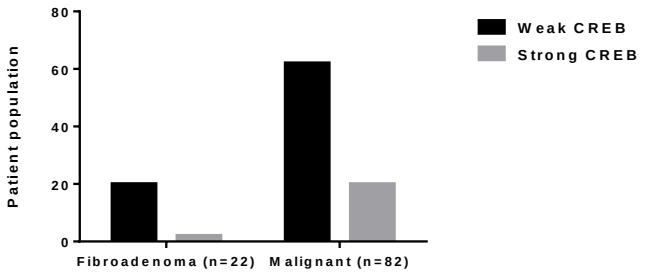

Figure 50: Expression of CREB in benign fibroadenoma and invasive ductal carcinoma samples (benign fibroadenoma=22 samples, IDC=82 samples). (a) Median CREB score in benign fibroadenoma and IDC samples (Mann Whitney U score=641, p value = 0.0499, two tailed). The bar represents the median value along with the range of distribution of CREB scores. (b) Oncomine data set for the expression of CREB mRNA in normal breast tissue and breast cancer samples (t-test=7.762, p value =0.004, two tailed, fold change=2.53) [354]. (c) Proportion of benign fibroadenoma and malignant patients with weak and strong CREB expression (p=0.1493, two tailed). * The Mann Whitney U statistic is significant at the 0.05 level. *** The Mann Whitney U statistic is significant at the 0.001 level.

3.3.7.2 CREB expression and its association with clinicopathological features

The distribution of scores and relationship between proportion of patients with weak or strong CREB expression scores with the clinico-pathological features as analysed by chi square/ Fisher's exact analysis is summarized in table 31. The distribution of CREB score in malignant patient groups differing in clinico-pathological features was studied by non parametric one way ANOVA (Mann Whitney U test or Kruskal Wallis test) and is summarized in table 32.

Table 31: Summary table showing the distribution and correlation between the clinico-pathological features and CREB scores

Clinico-pathological characteristics		Patient's distribution		Clinico-pathological characteristics		CREB Correlation
		Weak CREB score	Strong CREB score			
Age	≥ 50	11 (68.75%)	5 (31.25%)	Age	Fisher's exact test	
	<50	49 (77.78%)	14 (22.22%)		p-value	0.5164
					Sig.	ns
T. Size	T1	2 (40%)	3 (60%)	T. Size	Chi-square, Df	3.870, 2
	T2	49 (79.03%)	13 (20.97%)		p-value	0.1445
	T3	6 (75%)	2 (25%)		Sig.	ns
Grade	I	7 (70%)	3 (30%)	Grade	Chi-square, Df	0.291, 2
	II	20 (74.07%)	7 (25.93%)		p-value	0.8642
	III	28 (77.78%)	8 (22.22%)		Sig.	ns
Stage	I & II	38(77.55%)	11 (22.44%)	Stage	Fisher's exact test	
	III	22 (75.86%)	7 (24.14%)		p-value	1.000
					Sig.	ns
LN Mets	Positive	38 (79.17%)	10 (20.83%)	LN Mets	Fisher's exact test	
	Negative	22 (70.97%)	9 (20.03%)		p-value	0.4303
					Sig.	ns
VSI	Positive	21 (84%)	4 (16%)	VSI	Fisher's exact test	
	Negative	36 (72%)	14 (28%)		p-value	0.3902
					Sig.	ns
ER	+	33 (73.33%)	12 (26.67%)	ER	Fisher's exact test	
	-	23 (82.14%)	5 (17.86%)		p-value	0.5700
					Sig.	ns
PR	+	34 (75.56%)	11 (24.44%)	PR	Fisher's exact test	
	-	22 (78.57%)	6 (21.43%)		p-value	1.000
					Sig.	ns
Her-2/*neu*	+	21 (75%)	7 (25%)	Her2/*Neu*	Fisher's exact test	
	-	35 (77.78%)	10 (22.22%)		p-value	0.7837
					Sig.	ns

Table 32: Summary table showing the correlation between the clinico-pathological features and CREB scores distribution with Mann Whitney U or Kruskal Wallis analysis

Clinico-pathological features		Patients (N)	Median score	Mean score	Test	Test's score	P value
Age	**≤50**	16	4	4.343±0.783	Mann Whitney U	461	0.602
	>50	63	4	3.936±0.396			
T. Size	**T1**	5	8	6.9±1.048	Kruskal-Wallis	6.854	0.0325
	T2	62	3	3.572±0.386			*
	T3	8	5.25	5.562±1.061			
Grade	**I**	10	2.5	3.8±0.994	Kruskal-Wallis	0.516	0.772
	II	30	3	3.8±0.568			
	III	36	4	4.25±0.515			
Stage	**I**	4	5	5±1.549	Kruskal-Wallis	3.386	0.184
	II	45	3	3.5±0.467			
	III	29	4.5	4.568±0.556			
LN Mets	**Positive**	48	4	4.010±0.425	Mann Whitney U	718	0.795
	Negative	31	4	4.032±0.603			
VSI	**Positive**	25	4	4.1±0.582	Mann Whitney U	592	0.712
	Negative	50	3	3.96±0.455			
ER	**+**	45	3	3.844±0.468	Mann Whitney U	596	0.701
	-	28	4	4.035±0.547			

PR	+	45	3	3.7±0.4624	Mann Whitney U	552	0.3760
	-	28	4	4.267±0.565			
Her2/*neu*	+	28	4	4.07±0.583	Mann Whitney U	608	0.8047
	-	45	3	3.822±0.446			

***** The Kruskal-Wallis statistic is significant at the 0.05 level.

There was no direct correlation between CREB expression and age of IDC patients (Chi square score=0.7833, p=0.3761, two tailed) (Table 31). A significant difference in distribution of CREB scores was not observed between IDC patients of age group ≤50 and those in age group >50 (Mann Whitney U score=461, p value =0.602, two tailed) (Table 32).

No significant relationship was observed between CREB expression and tumor size (Chi square score=3.870, p=0.1445, two tailed) (Table 31). A significant difference in distribution of CREB scores was observed when different tumor groups were compared (Kruskal Wallis score=6.854, p value =0.0325, two tailed). The median CREB scores of T1 tumor size was 8, T2 tumor size was 3 and T3 tumor size was 5.25 (Table 32).

There was no correlation between CREB expression and tumor grade of IDC patients (Chi square score=0.291, p=0.8642, two tailed) (Table 31). The median CREB scores observed for grade I tumors was 2.5, grade II tumors was 3 and grade III tumors was 4.

No significant correlation was observed between CREB expression and tumor TNM staging of IDC patients (p=1.000, two tailed) (Table 31). An insignificant difference in distribution of CREB was observed when CREB scores of IDC patients in different TNM staging groups were compared (Kruskal Wallis score=3.386, p value =0.184, two tailed) (Table 32).

A direct correlation was not observed with CREB expression and lymph node involvement (p=0.4303, two tailed) (Table 31). When distribution of CREB score was compared between malignant samples with different lymph node status, an insignificant difference was observed (Mann Whitney U score=718, p value =0.795, two tailed) (Table 32). There was no correlation between CREB expression and vessel space invasion in IDC samples (p=0.3902, two tailed) (Table 31).

There was no correlation between CREB expression and ER status of IDC patients (p=0.5700, two tailed) (Table 31). A direct correlation was not observed with CREB expression and PR status (p=1.000, two tailed) (Table 31). When distribution of CREB score was compared between malignant samples with different PR status an insignificant difference was observed (Mann Whitney U score=552, p value =0.376, two tailed) (Table 32).

No significant correlation was observed between CREB expression and Her-2/neu status of IDC patients (p=0.7837, two tailed) (Table 31).

3.3.8 Corelation between expression of markers in IDC samples

The correlation between expression of different markers in IDC samples was studied. High coincidental expression of iNOS and p53 protein was observed (spearsman r coefficient=0.3461, p=0.0025) indicating that the greater the iNOS expression, the higher the p53 expression (Figure 51a). A significant correlation between p53 expression and CREB expression in IDC samples was also observed (spearsman r coefficient =0.2670, p=0.0277) (Figure 51b).

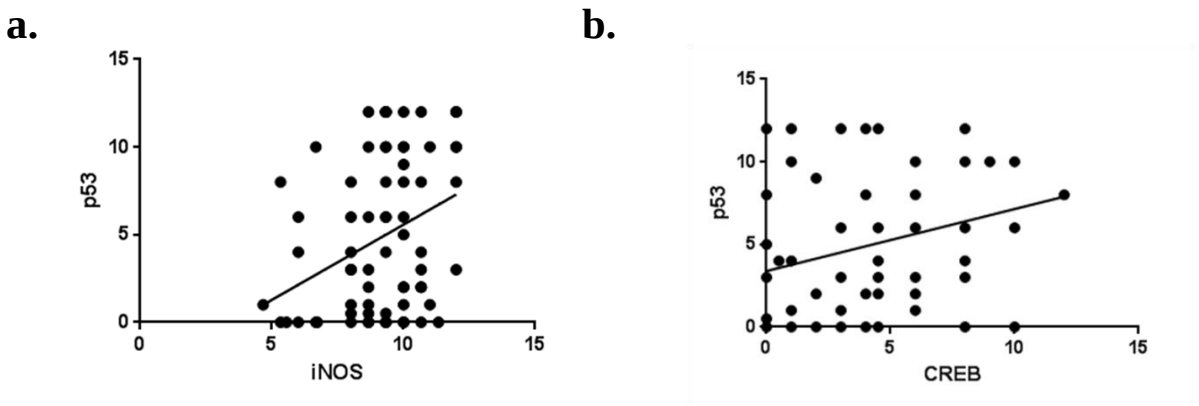

Figure 51: Correlation between the expression of markers. (a) Positive correlation between iNOS and p53 expression was seen in IDC samples (spearsman r coefficient=0.3461, p=0.0025). (b) p53 and CREB expression in IDC samples was positively correlated (spearsman r coefficient =0.2670, p=0.0277).

CHAPTER 4

DISCUSSION AND CONCLUSIONS

4.1 Discussion

Breast cancer accounts for 23% of all newly occurring cancers in women worldwide and represents 13.7% of all cancer deaths. It is the most frequent cancer in both developed and developing regions as well as the most frequent cause of cancer death [1].

Though lot of effort has gone into uncovering the genetic drivers responsible for breast cancer initiation and progression [362], the important role of tumor microenvironment is increasingly being recognized. The tumor microenvironment consists of different cell types that interact with each other and influence tumor initiation, growth and metastasis. In breast cancer, the tumor–stroma interactions are dynamic networks which take place between epithelial cells and the microenvironment consisting of stromal cells that include fibroblasts, innate and adaptive immune cells, adipocytes, vasculature and specialized mesenchymal cells [363, 364]. Immune cells represent a major component of the tumor microenvironment and consist of monocytes/macrophages, neutrophils, eosinophils, mast cells and lymphocytes [124]. Tumor-infiltrating immune cells were originally regarded as cytotoxic to the tumor cells; however, current findings support that such tumor-associated leukocytes have a dual role and can either contribute to cancer initiation, proliferation, metastasis due to immune tolerance, or can result in tumor suppression [365, 366]. The tumor associated macrophages (TAMs) represent the largest population of these immune cells and have been ascribed a dual role depending on the phenotype and secreted factors [124]. A vast amount of secretome including cytokines and growth factors is released both by the cancer and cells in the tumor microenvironment. The ECM in tumor microenvironment contains the secretome, constituted by proteins, receptors, proteoglycans and adhesive molecules as well as a milieu of secreted proteins including cytokines, chemokines, growth factors, angiogenesis factors and proteases at its surroundings [364, 367].

In the present studies, the TGF-β1-ROS-ATM-CREB pathway responsible for the increased migration of tumor cells was identified by studying the *in vitro* interaction of macrophage secretome and the tumor cells. This was achieved by employing MCM and MϕCM treatment to tumorigenic but noninvasive epithelial breast cancer cell line, MCF7 and invasive breast cancer cell line, MDA-MB-231. These two cell lines differ in their invasive nature as well as in several aspects including the p53 status, caspase 3 expression and estrogen receptor status [368]. Though both cell lines showed decreased clonogenic ability with MϕCM treatment, the mechanism behind this and other effects related to migration turned out to be dramatically different. Smaller merging colonies resulting in increased migration in one cell line (MCF7) and large multinucleated cells resembling senescent phenotype in the other (MDA-MB-231).

Cellular senescence is one of the many links between aging and cancer [369]. Though senescent cells fail to proliferate, they remain metabolically active and may secrete cytokines including IL-6, IL-8, IL-1α and IL-1β [370, 371]. Though a senescent phenotype was induced by MϕCM in invasive MDA-MB-231 cells, increased secretion of pro-inflammatory cytokines was not observed. But since only a limited number of cytokines were assessed, secretion of other factors leading to this phenotype cannot be ruled out. In contrast, the present study has identified that the network of secreted cytokines are the major players in the interaction of macrophages with MCF7 cells resulting in EMT responses.

The next quest was to identify this cytokine network between macrophages and tumor cells responsible for the observed changes. Pro-inflammatory cytokines like TNF-α, IL-1β and IL-6 were detected in the MϕCM. Though TGF-β1 was not secreted by both monocytes and macrophages, the interaction of other pro-inflammatory cytokines with cancer cells resulted in TGF-β1 secretion. Interestingly, the pro-inflammatory cytokine cocktail present in

MϕCM increased apoptosis only in MCF7 cells as opposed to MDA-MB-231 (ER/PR negative cell line). TNF-α has been shown to decrease ER dependent gene expression and cell survival [372] (Lu et al 2006) and induce apoptosis in MCF-7 cells [373, 374]. On the other hand, MDA-MB-231 cells express higher levels of anti-apoptotic proteins as demonstrated by these studies as well as by others [375, 376]. The Bcl-2 family of proteins comprises a number of related proteins whose expression has been shown to regulate apoptosis [377]. This family includes antiapoptotic members (Bcl-2, Mcl-1 and Bcl-XL) and proapoptotic members (Bax, Bid, Bad *etc*) whose individual expression and heterodimerization with each other regulate the sensitivity of cells to apoptosis. Bcl-2 overexpression inhibit apoptosis, whereas, a predominance of Bax over Bcl-2 accelerates cell death upon apoptotic stimuli [378]. This differential effect observed between the two cell lines could thus be combination of these factors like status of ER expression as well as the balance in pro and anti apoptotic proteins which alters their response to pro-inflammatory cytokines.

Though apoptosis was increased in MCF7 cells with MϕCM treatment, involvement of pro-apoptotic proteins Bax, Bad, truncated Bid, Bim and Puma were ruled out. Since Bax levels did not change, TNF-α induced apoptosis could have been through a RIP dependent mechanism [379]. In addition, PARP cleavage was also observed in these cells. Though MCF7 cells are caspase 3 deficient, TGF-β1 has been known to induce PARP cleavage as an independent event dissociated with cell apoptosis [380]. MϕCM induced apoptosis in MCF7 cells might be inititated by TNF-α itself through a RIP dependent mechanism or could be the effect of the induced TGF-β1. Both cytokines together also could have increased the susceptibility of MCF7 cells to undergo aoptosis.

Induction of various cytokines by TNF-α has been reported in different cell types: TGF-β1 in lung fibroblasts [381], IL-6 and TGF-β2 in breast cancer cells [382], IL-8 in endothelial cells [383], IL-1 and IL-6 in cardiac fibroblasts [384]. In the current study, there was no detectable secretion of TGF-β1 in the supernatant of MCF7 although about 30% of MCF7 cells were positive for intracellular TGF-β1. However, with MϕCM treatment of MCF7 cells, there was increased secretion of TGF-β1 as well as intracellular accumulation in presence of Golgi plug™. This upregulation seems to be at the transcriptional level as observed by an increase in mRNA of TGF-β1 and TGF-βRII and specific to TGF-β1 as there was no increase in mRNA of TGF-β2, TGF-β3 and TGF- βRI. The levels of TGF-β1, TGF-β2, TGF- βRI, TGF- βRII mRNA have been correlated with increasing invasive ability of a panel of breast cancer cell lines, with MCF7 having the lowest levels [385]. TNF-α produced by the activated macrophages accelerated TGF-β1 driven EMT in colon carcinoma [386] and enhanced recruitment of TAMs generated EMT-promoting microenvironment by increasing expression of TGF-β, PDGF and EGF in the mouse MMTV-PyMT mammary tumor model (in which the expression of the Polyoma Virus Middle T antigen oncogene is driven by the Mouse Mammary Tumor Virus promoter) [120].

TGF-β shows powerful cytostatic activity in normal mammary epithelial cells (MECs), but this ability is frequently inactivated in malignant MECs and leads to the acquisition of oncogenic activity in developing and progressing mammary tumors [153, 387]. This switch in TGF-β function is referred to as the "TGF-β Paradox". This is supported by a variety of genetic and epigenetic events that ultimately underlie the adverse prognosis associated with elevated TGF-β production in developing mammary carcinomas [388].

Induction of TGF-β1 by MCF7 cells was associated with the downstream events of increase in oxidative stress, DNA damage and CREB mediated survival signaling. This paradox of increased apoptosis in a group of cells and redox, DNA damage mediated survival

signaling in the remaining cells seems to be characteristic of TGF-β1. This has also been demonstrated in hepatocytes [389] and the choice of cells to undergo apoptosis or EMT responses depended on the cell cycle stage. TGF-β1 induced apoptosis in cells synchronized at G2/M phase and EMT responses in unsynchronized cells and cells at G1/S phase of the cell cycle [385]. Data from the present studies further confirm that apoptosis as well as EMT responses can be observed at the same time in a population of breast cancer cells, though changes in specific cell cycle stages were not studied. The gene expression signatures associated with the TGF-β signaling has been linked to the acquisition of EMT and stem cell-like phenotypes by breast cancer cells [390, 391].

A significant increase in EGF receptors was also observed along with TGF-βRII in MCF7 cells following MϕCM treatment. Activation of these receptors resulted in activation of SAPK/JNK and ERK 1/2 MAP kinase as compared to untreated cells and those treated with MCM. However an appreciable change in phosphorylation of p38 was not observed with MϕCM treatment of MCF7 cells. TGF-β1 signals through complexes of type II (TRII) and type I (TRI) receptors. Upon ligand binding, TRII receptors phosphorylate and activate the TRI receptors, which then activate regulatory Smads such as Smad2 and Smad3 via phosphorylation [145]. Phosphorylated Smads form complexes with regulatory Smads, translocate into the nucleus and regulate the transcription of TGF-β1 target genes. Smad4 cooperates with other transcription factors, such as FoxH1, Mixer, Runx-related proteins and E2F, as well as transcriptional co-activators (e.g., p300 and CBP) and co-repressors (e.g., SKI and SnoN, pro-oncoproteins) in the regulation of target genes [392, 393]. TGF-β1 signaling also activates signal transducers other than Smads, such as ERK1/2 MAP kinases, p38 MAP kinase (p38 MAPK), PI3 kinase and Rho-like GTPases [394, 395]. Synergistic signaling by EGF and TGF-β1 could have resulted in enhanced SAPK/JNK and ERK1/2 phosphorylation. The combined effect of these two ligands on activation of ERK1/2 and subsequently MMP-

9 function resulting in increased cell migration has been demonstrated [396]. Thus the present studies clearly demonstrate macrophage mediated upregulation of TGF- β1 signaling in MCF7 cells.

In addition to activation of MAPK pathways, there was an increase in redox signaling in MCF7 cells as demonstrated by augmentation in ROS and RNS generation. Increased ROS and RNS production was observed only in MCF7 cells and not in MDA-MB-231 cells following MϕCM treatment again showing that this could be specific downstream effect of TGF- β1. ROS and RNS play important roles in regulation of cell survival. ROS include radical species such as superoxide (O_2^-) and hydroxyl radical ($HO^\bullet$), along with non-radical species such as hydrogen peroxide (H_2O_2). ROS arise as a by-product of mitochondrial oxidative phosphorylation, oxygen metabolism and NADPH/NADPH oxidase (NOX) [397, 398]. RNS include nitric oxide ($NO^\bullet$) and peroxynitrite ($ONOO^-$) and are generated through specific nitric oxide synthase isoenzymes (reviewed in [399]).

In general, moderate levels of ROS/RNS function as signals to promote cell proliferation and survival, whereas severe increase of ROS/RNS induces cell death. The high metabolic rate of cancer cells drives their intracellular ROS up to an intermediate level, resulting in a shift in redox balance. ROS can also activate STAT3, MAPK and PI3K signaling pathways triggerring secretion of other growth factors that can induce cell proliferation, aggressiveness phenotype and apoptosis inhibition in the estrogen-responsive breast cells. [400].

Boudreau and colleagues have demonstrated that in both normal and metastatic breast epithelial cells, TGF-β treatment resulted in NOX-dependent superoxide production in the plasma membrane [175]. In contrast, studies have also demonstrated that expression of iNOS and secretion of NO antagonized TGF-β1 induced apoptosis and EMT in hepatocytes [401].

This again highlights the differences in TGF-β1 mediated signaling in normal and malignant cells (hepatocytes vs breast adenocarcinoma).

This oxidative stress resulted in DNA damage response signaling only in MCF7 cells as compared to MDA-MB-231 cells. The generation of ROS and RNS elevates the probability of oxidative DNA lesions. ATM is regarded as the major regulator of the cellular response to DNA double strand breaks (DSBs). Furthermore, ATM can also be activated directly by oxidative stress independent of DSBs by a mechanism distinct from MRN/DSB-dependent activation [402]. The observed ATM activation following MϕCM treatment could thus be directly activated by oxidative stress in a MRN independent pathway or as a result of MRN dependent DNA damage response. The basal level expression of ATM was higher in MDA-MB-231 cells which remained unchanged with the treatments. Phosphorylation of histone H2AX is performed by kinases of the PI3K family DNA-PK and ATM [403]. In the untreated and MCM treated MCF7 cells, there was no labeling of γ-H2AX. However, following MϕCM treatment, there was an increased formation of intense γ-H2AX-foci intense foci indicating complex DNA damage. γ-H2AX as well as other components of the DNA repair pathways are detectable in close vicinity to the DSBs soon after DNA damage [404]. The associated conformational changes of these proteins in turn recruit transducer and effector proteins responsible for the DNA damage response signaling. The earliest event in this process is histone poly (ADPribosylation), in which the poly (ADP-ribose) polymerases (PARP1, PARP2 and PARP3) catalyze the formation of poly (ADP-ribose) (PAR) and their covalent linkage to lysines in core histone proteins [405, 406]. PARP cleavage, a characteristic feature of apoptosis was observed only in MϕCM treated MCF7 cells. This again highlights the dichotomy of responses observed following TGF-β1 induction. PARP cleavage is typically associated with apoptosis, whereas pATM or γ-H2AX could result in DNA damage response and survival. This co-existence of PARP cleavage with pATM and γ-

H2AX could be similar to the parallel induction of apoptosis as well as EMT responses in different groups of cells by TGF-β1.

Along with redox signaling and DNA damage responses, MCF7 cells treated with MϕCM also displayed higher FL2/FL1 ratio of mitochondrial membrane potential. This basal level ratio was higher in MDA-MB-231 cells which did not further change on MϕCM treatment indicating membrane hyperpolarization. Subpopulations of cells with significant stable variations in intrinsic ΔΨm have been described within primary mammary tumor and in both primary and metastatic colonic tumor [407]. This hyperpolarization could be due to mitochondrial biogenesis which has been reported to increase in response to DNA damage. DNA topoisomerase II-targeting anticancer drugs like doxorubicin, mitoxantrone and etoposide, known inducers of DNA damage, also upregulate the abundance of mitochondria [408]. ROS may perturb mitochondrial homeostasis through two opposing effects. First, ROS can damage mitochondria leading to the production of more ROS and more defective mitochondria via a vicious cycle. Second, ROS can also induce mitochondrial biogenesis through a DNA damage/ATM/AMPK pathway and therefore ameliorate the ROS-mediated vicious cycle. The results presented in this dissertation support the second phenomenon. Cells with increased mitochondrial membrane potential as well as those with increased nitric oxide exhibited phenotypic properties consistent with promotion of tumor cell survival and expansion including secretion of angiogenic factors [200, 407]. These results strongly suggest that the increased ΔΨm could play an important role in the increased invasion observed in MCF7 cells following treatment with MϕCM. These changes of hyperpolarization instead of hypopolarization (characteristic of apoptotic cells) of mitochondrial membrane potential along with no changes observed in expression of Bax/Bcl-2 family members not only confirms Bax independent cell death mechanism but reaffirms the dichotomy of responses in the cells.

In response to DNA damage or extracellular signals, expression of several transcription factors like CREB, NF-κB, c-fos and c-jun allows the cells to overcome stressful or deleterious environment [264-267]. In the present studies, DNA damage response along with MAPK signaling was observed in MϕCM treated MCF7 cells. This resulted in significant increase in pCREB and total CREB in these cells in contrast to MDA- MB- 231 cells where basal level expression of CREB was higher and was unaffected by macrophage treatment. CREB (cyclic AMP (cAMP) response element binding protein) belongs to the basic/leucine zipper (bZIP) superfamily of transcription factors, which include CREB and the closely related factors CREM (cAMP response element modulator) and ATF-1 (activating transcription factor 1) [409]. Studies have shown that CREB, a 43 kDa bZip transcription factor plays an important role in cell differentiation, survival, proliferation, development, cell cycle progression and glucose metabolism [288, 303, 410, 411]. Canonical activation of CREB occurs in response to cAMP, which induces PKA-dependent Ser-133 phosphorylation [412]. The phosphorylation of CREB on Ser-133 promotes recruitment of additional proteins or co-activators like CBP [277] and p300 [413]. In addition to its regulation by metabolic and growth signals, CREB is also a target of the DNA damage response [266, 414]. CREB is activated by cAMP, growth factors, hormones, retinoids, cytokines and prostaglandins via multiple signaling pathways, including the cAMP/protein kinase A, PI3K/Akt, extracellular signal-regulated kinase (ERK)/p90 ribosomal S6 kinase and p38/mitogen- and stress-activated protein kinase pathways [274, 276]. cAMP may as well support the metastatic activity of TGF-β1 on triple-negative breast cancers. Triple-negative breast cancers from which MDA-MB-231 cells were derived, show higher metastatic potential, where the TGF-β/Smad3 pathway is more active [415].

Increased CREB stability as a result of phosphorylation of CREB on ser-133 has been reported [416]. We also observed increased total CREB expression in MCF7 cells following

MϕCM treatment whereas the basal levels were high in MDA-MB-231 cells. These results implicate the stabilization of total CREB due to phosphorylation on ser-133. These data also confirm earlier report on differences between these two cell lines in terms of total CREB expression [417].

The term epithelial to mesenchymal transition (EMT) describes a multi-step event during which cells lose numerous epithelial characteristics and gain the properties typical for mesenchymal cells. Transitions in cell phenotype from epithelial to mesenchymal (EMT) or mesenchymal to epithelial (MET), play a crucial role during embryonic development and tumorigenesis and require complex changes in gene expression, cell architecture and migratory and invasive behavior. Studies on human and mouse tumors suggest that the same molecular processes that drive developmental EMT are reactivated in the tumor cell to drive tumor progression towards invasive metastatic carcinomas [418].

A marked increase in vimentin expression as well as *in vitro* migration was found in MCF7 cells treated with MϕCM whereas MDA-MB-231, a highly invasive cell line had higher basal level expression of vimentin which did not futher increase with the treatment. A rapid increase in expression of mesenchymal markers vimentin and fibronectin has been demonstrated after TGF-β treatment of HMECs [418]. One of the essential molecules for formation and maintenance of the epithelial phenotype is the adhesion molecule E-cadherin (encoded by Cdh1) which is typically located at cell-cell adhesion junctions. Loss of E-cadherin is consistently observed during EMT and is currently regarded as a hallmark of EMT [419]. At the same time, up regulation of Snail, Slug, vimentin and fibronectin leads to acquisition of motility and invasive properties and allows the cells to migrate through the extracellular matrix and form metastases at distant sites [420]. EMT regulators like the transcription factors SNAIL/SLUG and TWIST, the homeobox protein SIX1 along with

interconnecting signaling pathways including Wnt, TGF-β and other growth factors are implicated in mammary development and in breast cancer [421, 422].

The results discussed so far thus implicate that the pro-inflammatory cytokine cocktail found in MϕCM induce a TGF-β1/ROS/ATM/CREB signaling axis in MCF7 cells. This effect seems to be differential and not observed in MDA-MB-231 cells probably due to a difference in estrogen receptor status or due to higher expression of anti-apoptotic proteins. To confirm if indeed this is the signaling pathway induced by macrophages resulting in EMT responses and increased migration, multiple approaches were followed. (1) Neutralization of pro-inflammatory cytokines TNF-α, IL-1β and IL-6 in MϕCM (2) Use of ROS scavenging agents like NAC or specific inhibitors of iNOS or ATM (3) Use of ATM knock down cells. The ability of all these agents to block this pathway was tested in two endpoints assays. These were (1) MϕCM induced pCREB expression (2) MϕCM induced increased migration in MCF7 cells. All three treatments of antibody neutralization, inhibitor treatment as well as ATM KD were very effective in decreasing MϕCM induced CREB phosphorylation as well as increased migration confirming that this indeed is the pathway activated by macrophages that resulted in EMT responses in MCF7 cells.

The growth and progression of breast tumor cells depend not only on their malignant potential, but also on the multidirectional interactions of secreted substances (secretome), including extracelluar matrix (ECM), produced by all the cell types including tumor, stroma, endothelial cells and immune cells within the local microenvironment. A permissive tumor microenvironment is required for successful progression and metastasis of tumor cells [423]. The mixture of multiple proteins and peptides released either from tumor or host cells constitute the secretome and are crucial for the communication between the tumor cells and their microenvironment [424]. The identification of proteins or peptides released into the

medium of tumor cells or immune cells cultured *in vitro* is the most common method for determining a secretome. However, the secretory pattern of cells *in vitro* might be different from the *in vivo* secretome. In the present study, the MCM and MϕCM were employed to study the tumor-immune cell interaction.

Apart from the pro-inflammatory cytokines detected by ELISA, attempts were made to identify other key players in MϕCM. This was carried out by 1D and 2D electrophoresis of MCM and MϕCM in which a differential pattern of secreted proteins was observed. When these proteins in CM were concentrated by ultrafiltration, they did not absorb onto IPG strips and remained immobile in the electric field during IEF in contrast to proteins that were concentrated by ammonium sulphate precipitation. This indicated the presence of lipid components in the CM when they were concentrated by ultrafiltration. Cancer cells and TME are known to communicate with each other not only via direct contact (by adhesion factors) but also by secreted paracrine factors (released factors) such as secreted proteins (cytokines and pro-angiogenic factors), nucleic acids and extracellular vesicles (EVs) [425]. Among the released factors, EVs represent a new paradigm of intercellular communications [426]. EVs have a size range of 50 to 1000 nm and are further categorized into microvesicles/apoptotic bodies, membrane particles, exosome like vesicles and exosomes based on their size, origin and molecular composition [427]. Exosomes are multivesicular body-derived vesicles of 50 to100 nm in diameter and were first described as such by Johnstone *et al*., in 1987 [428]. These vesicles contain a wide range of functional proteins, mRNAs and miRNAs and are actively secreted via exocytosis from almost all cell types including dendritic cells, lymphocytes and tumor cells [429]. Though exosmoes were purified from both MCM and MϕCM, they did not play any role in the MϕCM induced effects observed in MCF7 cells. This was confirmed by two ways: (1) Similar uptake of labeled exosomes obtained from both MCM and MϕCM by MCF7 cells; (2) The effect of EFMϕCM treatment in clonogenic assay

was similar to MϕCM. These results conclusively demonstrated that only soluble factors and not exosomes that played a major role in macrophage induced EMT responses of MCF7 cells in this study.

In addition to proinflammatory cytokines in MϕCM, MALDI/TOF analysis identified six upregulated proteins in MCM and eleven upregulated proteins in MϕCM. The proteins identified in MCM were moesin, plastin-2 isoform 16, glucose-6 phosphate isomerase isoform 1, actin, aldolase A and ferritin light polypeptide and they play a functional role in cell-cell recognition and signaling, cell motility and cytoskeleton regulation.

The proteins identified in secretome of macrophages were matrix metalloproteinase 1 (MMP-1) preproprotein, annexin V, GAPDH, chitinase 3 like protein, plasminogen activator inhibitor 2, myoferlin, plastin 2, CLK-3 isoform, metalloproteinase 9 (MMP-9) preproprotein and nitric oxide synthase. The majority of these proteins play a functional role of tissue remodeling, breakdown of extracellular matrix, membrane trafficking and cell migration. Even though many secreted proteins still remain to be determined, the biological activities of the proteins identified so far have provided us with a glimpse of the biological processes that can be initiated by proteins present in the tumor microenvironment.

The functional activity of MMP-1 and MMP-9 proteins identified in macrophage secretome was confirmed through zymography. A clear band was observed in MϕCM corresponding to the molecular weight of the MMP-1 and MMP-9. MMPs are a family of structural and functionally related endopeptidases. They are secreted as inactive zymogens and are activated by other activated MMPs or serine proteases outside the cell (e.g trypsin, plasmin, kallikrein) [430]. Increased expression and activity of MMP-2 and -9 in tumors has been associated with the degradation of basement membranes, an essential step in tumor invasion and with the tumor grade [431] as well as reduced survival in breast cancer patients

[432]. Studies have also demonstrated a basal level difference in expression of MMP-1, MMP-3 and MMP-13 in breast cancer cell lines. The highly invasive MDA-MB-231 cell line with a higher level of MMP-1, MMP-3 and MMP-13 expression may play a key role in the invasiveness of these cells through basement membranes [433].

Apart from MMPs, the other proteins identified by MALDI-TOF in MϕCM also had functional role in actin binding, regulation of cytoskeleton rearrangement and cell migration and invasion. Chitinase-3-like protein 1 (CHI3L1) identified in MϕCM, also known as YKL-40, is a glycoprotein secreted by activated macrophages, chondrocytes, neutrophils and synovial cells. It plays a role in the process of inflammation and tissue remodeling and has been linked to activation of the Akt pro-survival (anti-apoptotic) signaling pathway and promotion of angiogenesis through VEGF-dependent and independent pathways [434]. Elevated level of YKL-40 has been suggested as a biomarker of disease severity as it correlated strongly with stage and outcome of various types of cancer [435].

Another protein PAI-1 present in MϕCM, is a physiological inhibitor of urokinase-type plasminogen activator (uPA), a serine protease involved in the promotion of cellular de-adhesion, migration/invasion and activation of plasmin from plasminogen [436, 437]. Increased levels of this protease are associated with a poor prognosis of breast cancer [438].

Myoferlin, also present in MϕCM is a member of the ferlin family of proteins that participate in plasma membrane fusion, repair and endocytosis, vesicle trafficking and cell motility [439, 440]. Myoferlin also participates in the stabilization of several receptor tyrosine kinases [441].

L-plastin was differentially upregulated in MϕCM. A number of experiments performed with macrophages and polymorphonuclear neutrophils (PMN) point to a role for

L-plastin in regulating integrin mediated adhesion [442, 443]. From many *in vitro* and *in vivo* studies, there are indications that L-plastin plays a role in tumor cell motility [444].

The protein Dynamin was identified in exclusively upregulated in MϕCM. A large GTPase dynamin, is required for endocytic vesicle formation and regulates the actin cytoskeleton [445]. This has been suggested to be a novel antimitotic drug target for the treatment of cancer because the methyl ammonium bromide (MiTMAB) dynamin inhibitors exclusively block the abscission phase of cytokinesis, inhibits cell proliferation and reduce viability [446].

Since all identified proteins point toward cytoskeletal reorganization, the expression of some proteins with such functions like ezrin, radixin and moesin were studied in MCF7 cells treated with MϕCM. A significant increase in cytoskeleton associated proteins ezrin, radixin and moesin expression was observed in MCF7 cells with MϕCM treatment as compared to MCM treatment. Similar MϕCM induced upregulation of these proteins has also been reported in [447]. ERM (ezrin, moesin and radixin) belongs to a larger protein family, known as FERM (4.1 protein, Ezrin, Radixin, Moesin) [448, 449]. These proteins are cytoskeleton associated and have traditionally been known as molecules involved in maintaining the integrity and morphology of cells. They are also involved in the regulation of the migration of the cells and organizing the ruffling of the membrane. They have also been suggested to be candidate molecules in directional cell movement including that of cancer cells [450]. Ezrin has been shown to co-operate with c-Src in mammary cancer cells and regulate cell-cell contact and migration [451]. Moesin acts as a potential epithelial-mesenchymal transition (EMT) marker in breast and pancreatic cancer, and the expression level of moesin is linked to tumor size, invasion, and differentiation of oral squamous cell

carcinoma [452]. The expression level of radixin is found to be significantly increased in colon tumor tissues [453].

Though *in vitro* studies employing either conditioned media or co-culture can give a glimpse of the interaction that occur in the tumor microenvironment, the ultimate test of the hypothesis is validation of these markers in clinical samples. So taking clues from the *in vitro* study, expression of a set of chosen markers were validated in benign and malignant breast cancer. Pathologists have known for decades that breast cancer cannot be described as a single disease and heterogeneity based on tumor morphology, location, grade and lymph node metastasis, expression of hormone and growth factor receptors is well documented. However, in addition to heterogeneity between tumors, it is becoming increasingly appreciated that a high degree of molecular and morphological heterogeneity exists even within tumors, further complicating the development of therapeutic strategies and our understanding of disease progression. Through the use of gene expression profiling and other genomics approaches, the complexity and heterogeneity of breast cancer has been confirmed and emerging evidence has indicated that the tumor microenvironment plays a pivotal role in driving tumor heterogeneity.

ONCOMINE, a cancer microarray database and web-based data-mining platform aimed at facilitating discovery from genome-wide expression analyses. Differential expression analyses comparing breast cancer with respective normal tissues as well as a variety of cancer subtypes and clinical-based and pathology-based analyses was studied for iNOS, p53, H2AX and CREB. The data base constitutes of many studies which compare markers expression between different carcinoma subtypes. iNOS and p53 mRNA was significantly upregulated in invasive breast carcinoma as compared to normal breast tissue. Studies in the database for H2AX expression show a fold change of 2.588 ($p<0.0001$) between normal and invasive breast carcinoma (TCGA Breast Statstics, 2010) and fold

change of 1.226 (p=0.017) in adenocarcinoma and ductal breast carcinoma. CREB mRNA was significantly upregulated in invasive breast carcinoma in data sets as compared to normal breast tissue.

In the present study, the expression of iNOS, p53, γ-H2AX, pCREB and CREB were found to be crucial for increased migration in ER/PR positive MCF7 cells. Hence these markers were chosen for IHC analysis. CD68, a macrophage marker also was studied in these samples. However the labeling with the antibody clone (KP-1) seemed to be non specific and hence was not included in further analysis.

Invasive ductal carcinoma not otherwise specified (IDC NOS) was found to be the most common type in Indian population (88%) followed by infiltrating lobular carcinoma (3.7%), colloid carcinoma (1.1%) and ductal carcinoma *in situ* (DCIS) (1.1%) and metaplastic types (0.9%) [454]. In the present studies, 24 benign fibroadenoma samples and 91 IDC samples were studied for expression of these markers.

The incidence of breast cancer has been consistently increasing and it is estimated that it has risen by 50% between 1965 and 1985 [455]. The rise in incidence of 0.5-2% per annum has been seen across all regions of India and in all age groups but more so in the younger age groups (<45 years). More than 80% of Indian patients are reported to be younger than 60 years of age [6]. In this study, the age of IDC patients ranged from 28-77 years with a mean of 58.10±10.48 years. The demographics recorded show that patients in the study group were largely representative of overall population of breast cancer patients. The peak age frequency was in the age category of 56-70 years at the time of diagnosis. In Indian population, the average age of breast cancer patients is reported to be 50–53 years in various population-based studies [456]. While the majority of breast cancer patients in western countries are postmenopausal and in their 60s and 70s, the picture is quite different in India

with pre-menopausal patients constituting about 50% of all patients [457]. In this study, 37.5% patients were below 55 yrs age and 62.5% patients were above 55 yrs age.

The majority of breast cancers diagnosed in the study were grade III cancers (47%) with grade I and grade II cancers representing 16% and 37% of the cases. Reports also suggest that in Indian population the majority of patients are detected with grade III disease [458]. Grade of cancer is an important prognostic factor and is used as one of the components of the Nottingham Prognostic Index (NPI).

The tumor size was recorded in each case and there was a wide range from 5 mm to 90 mm with a mean of 36 mm. The cancers were divided into size groups according to the TNM staging system. The majority of tumors in the group were T2 cancers (20-50 mm). Though the average tumor size in Indian population is reported to be 54 mm and this presentation is similar in many other developing countries [459]. In this study, the patient's tumor size significantly correlated with the patient's age at diagnosis ($p=0.0288$) and tumor stage ($p=0.0031$), as patients detected with advanced stage had larger tumor size.

The frequency of distribution of IDC patients according to pathological TNM staging was 5.8%, 58.1% and 36.1% for Stage I, Stage II and Stage III respectively. This was consistent with data from Indian breast cancer patients where in Stage I: 1–8%; Stage II: 23–58%; Stage III: 29–52 % patients were recorded [460]. The data from the present studies also correlated with the Mumbai's breast cancer statistics which had reported around 7% patients with stage I, 57% patients with stage II and 28% patients with stage III cancer. In the present work, the patient's stage correlated with tumor size ($p=0.0305$) and LN metastasis positivity ($p<0.0001$). The advanced stage samples were LM Mets positive.

Though not used in the NPI, lympho-vascular vessel space invasion (VSI) is recognised as an independent prognostic indicator. The presence of VSI is important when

making decisions regarding adjuvant therapy. In this study, 28.2% of IDC samples were VSI positive. The patient's data show that VSI positivity was associated with high grade tumors ($p=0.0406$).

Lymph node status is established as the single most significant prognostic factors in invasive breast cancers [461]. The lymph node status was positive in 59% of IDC samples in the study and it correlated well with the stage of the tumor. The pathological feature of this study group conformed to expectations and standards set by previous studies in breast cancer [462].

In this study group, 61.36% of the IDC samples were ER positive and 68% were PR positive. ER status has been established to be an important factor in breast cancer correlating to pathological features and overall survival. Estrogen (ER) and progesterone receptors (PR) are found positive in only 20-45% of Indian patients. ER-positive rates were reported to be lower in Indian patients than those in western countries as not all patients in India undergo hormonal receptor testing as evident from the study in Delhi which showed only 35.5% of patients had receptor testing [463]. At TMH Mumbai, the ER+ status was found in 33% and PR+ in 46% of patients [458]. Comparatively, in this study higher percentage of ER positive samples was noted. In the present dissertation, the ER positive tumors were significantly related to low grade tumors ($p=0.0124$) and smaller size tumors ($p=0.0436$). These results agree with previously published work [30, 464, 465] and it is now widely agreed that ER status is an independent prognostic marker of disease outcome. The results also demonstrated a significant relationship between ER positive and PR positive cancers ($p<0.0001$) confirming that progesterone receptors expression could be induced by estrogen [466]. As the PR gene transcription is regulated by estrogen, PR expression has been considered to be a marker of functioning ER [467]. PR expression was significantly associated with low grade tumors ($p=0.0042$).This study showed an inverse correlation between ER positive and Her2

positive tumors ($p<0.0001$). This was in concordance with the previous studies [468], though it is suggested that this relationship or predictive power of ER status or Her2 status is more apparent in the elderly patients [469]. When considering PR correlation with other receptors, it was clear that it was significantly associated with ER ($p<0.0001$) and like ER it was also negatively correlated to Her-2 ($p< 0.0001$).

In this study, it was seen that the majority of the tumors were ER/PR double positive (56.8%) or ER/PR double negative (32.95%). The other 2 groups, ER+ve/PR-ve (4.54%) and ER-ve/PR+ve (5.68%) were too small. In larger studies, it has been suggested that ER/PR double positive cancers are more responsive to hormonal therapy and hence have a better outcome when compared to ER+ve/PR-ve cancers. This again is based on the theory that PR represented a functioning ER signaling system [470].

It is generally accepted that Her2/neu over expression is a marker of increased tumor aggressiveness [471] and in many studies Her2/neu over-expression has been related to a poorer overall survival. In this study, Her2/neu was over expressed in 40.69% of the cases. As with the previous receptors, the correlation of Her2/neu expression with the other pathological features of the tumors was also studied and the over expression of Her2/neu was not significantly associated with any of the clinico-pathological feature. It is widely reported that Her2/neu over expression is inversely associated with ER/PR expression [472]. The results from the present study are in agreement with a significant inverse relationship between Her2/neu expression with ER ($p<0.0001$) and PR ($p<0.0001$) status.

ER, PR and Her-2/Neu receptor negative breast cancer (triple negative), is biologically aggressive cancer phenotype which is resistant to conventional cytotoxic chemotherapy treatment and is associated with reduced survival compared to other subtypes of breast cancer [473]. In this study, 8.53% samples were triple negative cancer.

In this dissertation, expression of iNOS, p53, γ-H2AX, pCREB and CREB was studied in benign fibroadenoma and IDC samples. iNOS was the first NOS isoform implicated in the macrophage-mediated tumor killing process and as a consequence this isoform has been at the center of attention for study of its expression in cancer. In this study, 23 benign fibroadenoma samples and 91 breast cancer samples were analyzed using IHC for the expression of iNOS. The samples were scored according to the cytoplasmic location of the iNOS. The significant outcome of the present study has been to identify differences between iNOS expression in benign fibroadenoma and malignant samples with varying stages and grades of breast tumors.

The iNOS scores were significantly higher in malignant samples as compared to benign fibroadenoma group (p=0.0001). Strong iNOS expression was seen in 47.82% of benign fibroadenoma samples as compared to 87.3% of malignant tumors. Differences in iNOS expression between benign and malignant samples suggest a role for NO in breast carcinogenesis. The present study has demonstrated increased expression of iNOS in malignant tumors as compared to benign samples. Expression of NOS has been reported in malignant tissue derived from gynecological, breast, central nervous system, gastric and colorectal tumors and its role in cancer progression is suggested [186, 187, 474]. Reports on the activity of NOS in breast cancer have been conflicting, with different or completely opposing findings being reported. Most authors reported the presence of NOS activity in carcinoma [186, 475-477]. Among these, some reported higher NOS activity in malignant than in benign breast tissue [186, 476, 477]. A positive correlation between NOS activity and tumour grade is also reported [186, 476, 477] whereas others have also reported the reverse [478]. These paradoxical results may be explained by the fact that at low concentrations, nitric oxide has a tumor promoting effect, whereas at higher concentrations, it has antitumour activity. Although Loibl *et al* had demonstrated that none of the benign lesions were positive

for iNOS, in the present study, the benign samples were iNOS positive although with low expression. These results draws parallel with an ovarian cancer study which showed that though a majority of malignant samples had NOS activity, iNOS was also detected at lower levels in non cancer samples [479].

A significant association of iNOS expression was not observed with other clinico pathological characteristics of IDC samples in this study. Previous reports indicated that elevated NOS2 expression may be linked to a high grade and poor prognosis in breast cancer [480, 481] and also to poor outcome in other human epithelial cancers. There was a statistically significant higher expression of iNOS in IDC as compared to the benign fibroadenoma samples. Although our hypothesis was that iNOS may be a marker to detect malignant disease and metastasis, these results with limited number of samples demonstrate that it would be useful to differentiate benign and malignant tumors. In this study, there was no association between iNOS positivity and hormone receptor expression. Larger sample size is needed to confirm any such association as there are chances that it can be missed in studies with smaller sample size.

NO has proangiogenic activities [207] and also promotes carcinogenesis through the inactivation of wild-type p53 function, by either causing loss of DNA-binding activity [482] and/or selecting for mutant p53 [483]. In the current study, p53 expression status in benign and malignant samples was evaluted. Although p53 antibody used in this study could not differentiate wild-type p53 from mutant p53, previous studies have indicated that p53 protein detected by immunohistochemistry is representative of mostly mutant p53 along with accumulation of p53 and is an indicator for a loss of p53 tumor suppressor function. The p53 accumulation is caused by both mutations and protein-protein interactions [484]. High coincidental expression of iNOS and p53 protein was observed (spearsman r coefficient=0.3461, p=0.0025). Rajnkova et al., reported that increased expression of iNOS

may promote gastric cancer progression by providing a selective growth advantage to tumor cells with non-functioning p53 [485]. Thus p53 protein accumulation may also be important event to enhance breast carcinogenesis. Mutations in the tumor suppressor gene p53 are present in 18%–25% of primary breast carcinomas [486]. p53 expression was studied in 22 benign fibroadenoma and 76 IDC samples. Similar % of samples from both groups were positive for p53 (77.27% of benign fibroadenoma and 75 % of IDC samples). The mean p53 score in in fibroadenoma samples was 2.227±0.349 and that of malignant samples was 4.625±0.502. Although p53 expression was higher in IDC samples, this was not found to be statistically significant. ·

Studies have reported that p53 mutation does not impact the outcome of early breast cancer and that the evidence is not strong enough for p53 status to be recommended as a routine marker in clinical practice [487]. In contrast to this, some studies have indicated that abnormal p53 immunohistochemical expression, or p53-positive status, was associated with more aggressive tumor features, a higher tumor grade, negative estrogen and progesterone receptor (ER/PR) status and the more aggressive basal subtype [488]. Breast tumors expressing high levels of p53 are more frequently ER-negative and PR-negative. They are also associated with a high proliferation rate, high histological and nuclear grades, aneuploidy and poorer survival. Consistent with earlier reports, in this study, higher p53 expression was seen along with negative estrogen (p=0.0384) and progesterone receptor (p=0.0079) status. A high p53 level is frequently observed in tumors over-expressing as Her-2/neu [489]. In accordance to this, higher p53 expression was seen in Her2/ neu positive samples (p=0.0095). The mean p53 scores of patients with $ER^{+}PR^{+}Her2^{+}$ was 2.3±3.27, $ER^{+}PR^{+}Her2^{-}$ was 3.15±4.06, $ER^{-}PR^{-}Her2^{+}$ was 7.25±4.39 and $ER^{-}PR^{-}Her2^{-}$ was 1±1. p53 expression scores were highest in $ER^{-}PR^{-}Her2^{+}$ group whereas $ER^{-}PR^{-}Her2^{-}$ group showed lowest p53 expression. A co-existence of HER2/neu over-expression and p53 protein accumulation has

been suggested to be a strong prognostic molecular marker in breast cancer [490]. Insignificant association of p53 expression with age, tumor size, grade, stage, LM mets and VSI was observed.

p53 is a key player in the tumor suppressive DNA damage response (DDR) and is mutationally inactivated in approximately 50% of human cancers. Cellular responses to DNA damage are mediated through highly conserved DNA damage checkpoint mechanisms that are important for tumor suppression by arresting cell cycle progression, or evoking cellular senescence and apoptosis [491]. As a result of DNA DSBs in eukaryotic cells, the serine amino acid at position 139 of the H2AX proteins is phosphorylated in response to DNA damage [232]. Detection of γ-H2AX foci has been used as a biomarker for aging and cancer, as a biodosimeter for drug effects and radiation exposure in chemo- and radiotherapy respectively [492, 493].The aim of the study was to assess the expression of γ-H2AX in a cohort of 23 benign fibroadenoma and 82 IDC patients and correlate its expression with clinico-pathological parameters.

Nuclear γ-H2AX staining was observed in tumor cells. All of the benign fibroadenoma samples were positive for γ-H2AX expression while 77% of IDC samples were positive for γ-H2AX labeling. Though the IDC samples showed higher mean γ-H2AX expression scores, it was statistically insignificant from γ-H2AX expression scores of benign fibroadenoma samples. Similar differences in expression of γ-H2AX has been observed in a study with benign nevus and malignant melanoma cases [494].

As DNA damage gradually accumulates during lifetime, both the likelihood of oncogenic transformation as well as tissue dysfunction and degeneration increases with age. The increasing trend in the γ-H2AX expression score was seen with increase in patient's age, although not differing statistically. The median γ-H2AX scores of different groups viz. age

25-40, 41-55, 56-70 and above 70 were 3, 3.5, 4 and 6 respectively. No direct significant association was observed with γ-H2AX expression and tumor size, grade, stage, LN Mets and VSI.

The γ-H2AX expression scores were highest in triple negative ($ER^-PR^-Her2^-$) group whereas triple positive ($ER^+PR^+Her2^+$) group showed lowest γ-H2AX expression. This was in accordance with reported data that triple negative breast cancers display more endogenous γ-H2AX expression [495] and that his subset of cancers has a higher incidence of aberrations in components of the DNA damage repair pathway [495, 496].

Studies have shown that CREB may act as a positive or negative transcription regulator in various human benign and malignant conditions [410, 497-499]. It has been reported that CREB may act as a positive transcription regulator of aromatase and hence increased estrogen synthesis in breast cancer cells [356]. However, despite the extensive work on aromatase, little information is available on the expression and role of CREB in human breast cancer. Kovach et al had reported that total CREB and phosphorylated CREB (pCREB) proteins were both significantly elevated in hepato cellular carcinoma versus normal liver [500]. In resting cells, CREB exists in an unphosphorylated state that is transcriptionally inactive but can bind to DNA. Upon activation, CREB becomes phosphorylated, which induces its transcriptional activity by promoting its interaction with the 256-kDa coactivator protein CREB binding protein (CBP).

The aim of this study was to investigate the correlation of pCREB and CREB expression between benign fiboadenoma and IDC together with clinico-pathological characteristics of IDC samples. In the current study, CREB expression was studied in 22 benign fibroadenoma and 82 IDC samples. The median pCREB score in benign fibroadenoma samples was 7.33 whereas median pCREB score in malignant samples was

6.66. The pCREB score distribution in benign fibroadenoma and malignant group did not differ significantly. The median score in benign fibroadenoma was 2 as compared to that of 4 in malignant samples. CREB score distribution in benign fibroadenoma and malignant group differed significantly (Mann Whitney U test, p value = 0.0499). A significant correlation between p53 expression and CREB expression in IDC samples was also observed (spearsman r coefficient =0.2670, p=0.0277).

Though an insignificant association was observed with tumor grade and patient's age with pCREB and CREB expression, a significant association with tumor size was seen with CREB. An inverse correlation was also observed with pCREB expression and tumor TNM staging of IDC samples (p=0.0487). The median pCREB scores of Stage I tumor was 9.16, Stage II tumor was 7.11 and Stage III tumor was 6.66. The highest pCREB expression was seen in Stage I samples whereas Stage III samples showed the lowest pCREB expression. An insignificant difference in CREB scores distribution was observed when CREB scores of IDC patients in different TNM staging groups were compared. The median CREB scores of Stage I tumor was 5, Stage II tumor was 3 and Stage III tumor was 4.5.

CREB and pCREB expression was not correlated with lymph node metastasis, VSI and hormone receptors levels in IDC samples. This may be attributed to the small sample size that has limited the ability to derive statistically significant results and correct for differences in subgroup characteristics.

The findings reported herein emphasize that macrophages can induce change in tumor cells resulting in increased migratory properties. Macrophage mediated pro-inflammatory cytokines induce TGF-β1 further driving the ROS/ATM/CREB signalling axis in tumor cells ultimately resulting in increased migration. This has been conclusively proven in this dissertation by blocking the pathway at every step which ultimately leads to abrogation of

MϕCM induced pCREB as well as migration. The effect of these macrophages seems to be differential since the highly invasive MDA-MB-231 cells already having a high basal level of this signaling axis seems to be tolerant to further induction.

The complexity of cell-cell interaction by soluble factors is further exemplified by the fact that apart from the pro-inflammatory cytokines that induce TGF-β1/ROS/ATM/CREB signaling axis, there are many proteins present in the secretome of the macrophages. One interesting fact that emerges from this study is the identification of proteins involved in breakdown of extracellular matrix, membrane trafficking, cytoskeletal re-organization and cell migration in macrophage secretome further strengthening our hypothesis that macrophages secreted factors result in increased migration of tumor cells.

The crucial players of this macrophage –tumor cell interaction identified from the *in vitro* study were also subjected to validation in clinical samples. The most significant result from this study is that iNOS and CREB expression were significantly correlated with the malignancy of disease. There was also a significant positive correlation of p53 with iNOS as well as CREB in malignant samples. Expression of pCREB was significantly but inversely associated with the staging of the IDC samples and p53 expression was significantly associated with expression of hormone receptors.

The findings reported in this dissertation emphasize the importance of soluble factors or cytokines in the tumor microenvironment. It also reiterates the role of cytokine signaling network between the macrophages and the tumor cells. The study provides framework for targeting the stromal factors for effective control of tumor growth and metastasis. The proteomic studies gives a glimpse into the complexity of the tumor microenvironment and have given an insight of the many different proteins present in the tumor microenvironment that could affect the behavior of the cancer cells apart from the major players. This

knowledge of the stromal factors can also lead to predictive prognostic assays as well as improvement of cancer therapeutics. The potential markes, iNOS and CREB were significantly overexpressed in malignant breast cancer as compared to the benign disease. It would be interesting if these markers can be used along with the existing set of diagnostic markers that can determine course of therapy as well as responsiveness to different drugs. As seen from the *in vitro* study, some of these markers are promising targets for cancer therapeutics. Additional data with survival status of patients as well as greater sample size can confirm if these markers can be used for prognosis as well.

4.2 Summary

Macrophages and tumor cells mutually influence each other's behaviour in majority of cancers, with the tumor cell attracting macrophages and sustaining their survival and they, in turn, producing a myriad of factors to promote or regulate tumor growth and angiogenesis. The main finding of this study is that the pro-inflammatory cytokine cocktail of TNF-α, IL-1β and IL-6 secreted by macrophages induce secretion of TGF-β1 in MCF7 cells. This results in dichotomy of responses with apoptosis in a fraction of cells and activation of MAPK pathway, increase in redox signalling and DNA damage response, in the remaining cells. All these events triggered CREB mediated survival signaling inducing EMT responses. Blocking of all the upstream events resulted in abrogation of MϕCM induced pCREB expression and migration further confirming our hypothesis. Interesting information that emerged from these studies is that some breast cancer cell types could be refractory to the effect of macrophage induced signaling that resulted in increased migration.

Apart from the proinflammatory cytokines, many other crucial players were identified in macrophage secretome that also could contribute to EMT changes in MCF7 cells. All these proteins play a functional role in tissue remodeling, breakdown of extracellular matrix, membrane trafficking and cell migration.

The significance of these markers identified from the *in vitro* study was also validated in clinical benign fibroadenoma and IDC samples. In IDC, the patient's tumor size correlated with the patient's age at diagnosis ($p<0.05$) and tumor stage ($p<0.01$). The stage of tumor correlated with tumor size ($p<0.01$) and LN metastasis positivity ($p<0.0001$). The patient's data also showed that VSI positivity was associated with high grade tumors ($p<0.05$).

ER+ tumors were significantly related to low grade tumors ($p<0.01$) and smaller size tumors ($p<0.01$). PR expression was significantly associated with low grade tumors ($p<0.01$). ER expression correlated significantly with PR ($p<0.0001$) and negatively correlated to HER-2/neu expression in IDC samples ($p< 0.0001$).

A statistically significant higher expression of iNOS and CREB was observed in IDC samples as compared to the benign fibroadenoma samples. A significant association of iNOS expression was not observed with other clinico pathological characteristics of IDC samples in this study. High coincidental expression of iNOS and p53 protein accumulation was observed (spearsman r coefficient=0.3461, p=0.0025). Although the p53 expression was higher in IDC samples, this was not found to be statistically significant. A higher p53 expression was seen along with negative ER (p=0.0384) and PR (p=0.0079) status. A higher p53 expression was seen in Her-2/ neu positive samples (p=0.0095).

Though the IDC samples showed higher mean γ-H2AX expression scores, it was statistically insignificant from γ-H2AX expression scores of benign fibroadenoma samples. No direct significant association was observed with γ-H2AX expression and tumor size, grade, stage, LN Mets and VSI.

The CREB score distribution in malignant and benign fibroadenoma group differed significantly (Mann Whitney U test, p=0.0499). A significant correlation between p53 expression and CREB expression in IDC samples was observed (spearsman r coefficient =0.2670, p=0.0277).

In summary, this comprehensive study of macrophage-tumor interactions may provide new diagnostic markers as well as unique therapeutic opportunities directed at the microenvironment to improve patient response to therapies and improve survival rates.

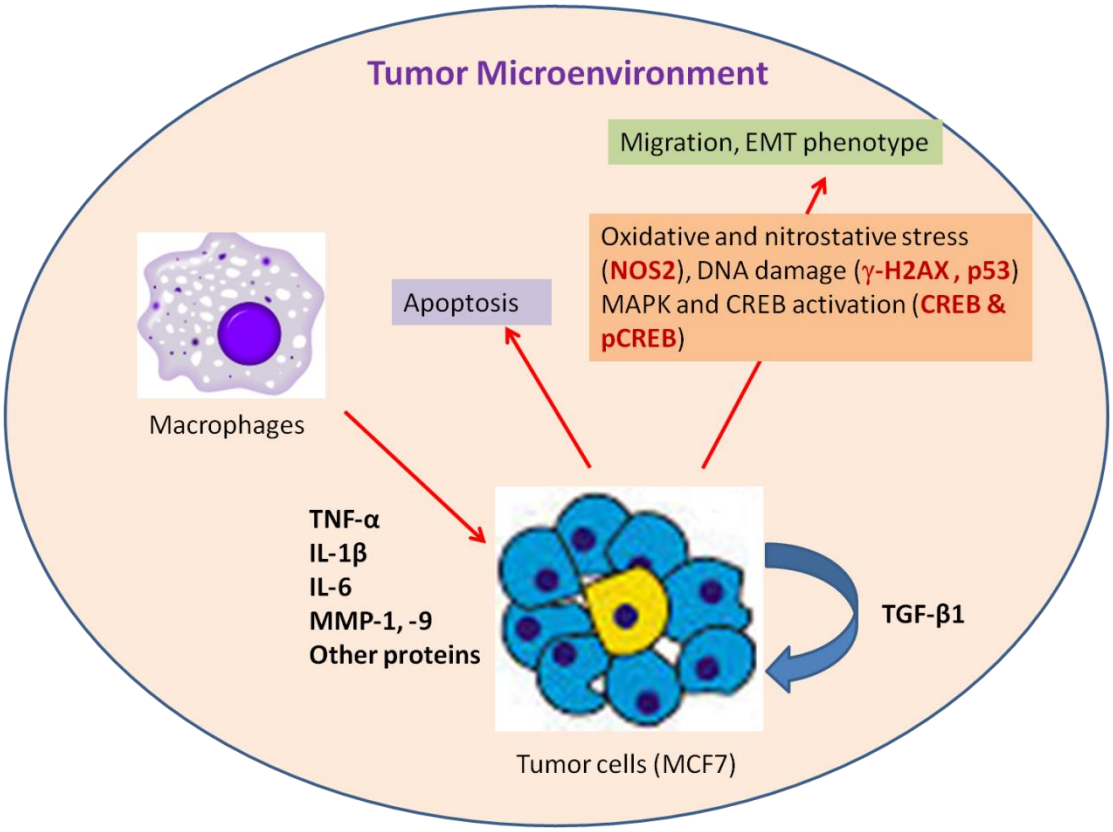

Figure 52: Schematic representation of the effect of MϕCM on MCF7 cells. Pro-inflammatory cytokines TNF-α, IL-1β and IL-6 along with MMP-1, -9 and other proteins secreted by macrophages induce secretion of TGF-β1 in MCF7 cells. This results in apoptosis in a fraction of cells. In the remaining cells, there is activation of ROS/ATM/CREB signalling axis resulting in EMT responses.

4.3. Conclusions

The major conclusions of the present dissertation are as follows:

- Macrophage conditioned medium (MϕCM) containing elevated levels of cytokines TNF-α, IL-1β and IL-6 had a differential effect on non-invasive (MCF7) and highly invasive (MDA-MB-231) breast cancer cell lines.
- MϕCM induced the secretion of TGF-β1 and IL-6 in MCF7 cells.
- MϕCM decreased colony numbers in both the cell lines but it was associated with increase in apoptosis, ROS and RNS generation only in MCF7 cells.
- MϕCM had a differential effect on mitochondrial membrane potential in MCF7 and MDA-MB-231 cell lines with hyperpolarization in the former and no significant effect on latter.
- Activation of MAPK pathway and upregulation of EGFR observed in MCF7 cells with MϕCM treatment.
- Increased phosporylation of ATM and H2AX as well as PARP cleavage following MϕCM treatment was observed in MCF7 cells and not in MDA-MB-231 cells.
- Increased phosphorylation of CREB and stabilization of total CREB protein was observed in MCF7 cells following treatment with MϕCM. In contrast, expression of pCREB was higher in MDA-MB-231 cells which did not change further with MϕCM treatment.
- Neutralization of TNF-α, IL-1β and IL-6 in MϕCM or pre-treatment with inhibitors of ROS, RNS or DNA damage as well as ATM knockdown abrogated the MϕCM induced expression of pCREB as well as migration through a transwell insert.

- Apart from pro-inflammatory cytokines, numerous proteins were identified by MALDI-TOF analysis which had a functional role of tissue remodeling, breakdown of extracellular matrix, membrane trafficking and cell migration.
- Bioinformatics analysis demonstrated transcript level upregulation of proteins like iNOS, p53, H2AX and CREB in invasive breast cancer as compared to normal breast tissue.
- In clinical samples, iNOS and CREB expression were significantly higher in IDC as compared to benign fibroadenoma.
- The expression of p53 was positively correlated with iNOS and CREB in IDC.
- p53 expression was associated with hormone receptors in IDC.
- pCREB expression in IDC was inversely associated with the staging of the tumor.
- iNOS and CREB can be potential diagnostic biomarker to detect invasive ductal carcinoma.

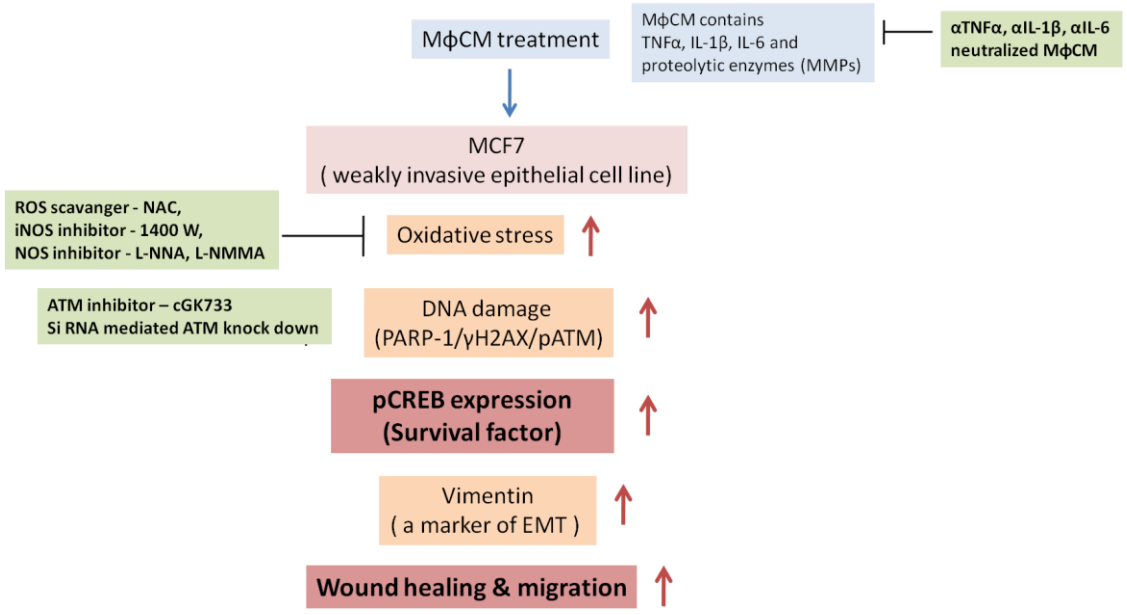

Figure 53: Summary chart of *in vitro* observations in MCF7 cells with MϕCM treatment.

4.4 Future directions

A logical extension of this work would require the following:

- Identification of the key players in the TGF-β1-ROS-ATM-CREB signaling pathway induced by MϕCM in MCF7 cells.
- Studying the interaction of SMAD pathway and TGF-β receptors with key transcription factors such as ATF2, Jun, JunB, JunD, Sp1, Sp3, Fos, Mixer, Runx *etc*.
- Study of the effect of TFG-β1 on the cell cycle regulation in the synchronized cells.
- Elucidation of the downstream mediators of CREB signaling by silencing CREB or by inhibition of its phosphorylation.
- To study the role of *in vitro* differentiated macrophages of M1 and M2 phenotypes from peripheral blood monocyte on MCF7 and MDA-MB-231 cell line.
- To further identify the macrophage mediated signaling pathway in tumor bearing mouse models and to study the CREB signaling under *in-vivo* conditions.
- The study of clinical markers such as chemokine receptors CXCR4; chemokine ligands CCL2 and 5; growth factors EGF, HGF, IGF and TGF-β; immunosuppressive Treg cells markers FOXP3 or micro RNA such as miR-497, miR-373 in light of their value as prognostic or predictive factors. To study their expression and its correlation with clinic-pathological parameters as well as 5 years survival data to identify their potential for integration into clinical practice.

5. REFERENCES

1. Ferlay J, Steliarova-Foucher E, Lortet-Tieulent J, Rosso S, Coebergh JW, Comber H, Forman D, Bray F: **Cancer incidence and mortality patterns in Europe: estimates for 40 countries in 2012**. *Eur J Cancer* 2013, **49**(6):1374-1403.
2. Agarwal G, Ramakant P: **Breast Cancer Care in India: The Current Scenario and the Challenges for the Future**. *Breast Care (Basel)* 2008, **3**(1):21-27.
3. Agarwal G, Ramakant P, Forgach ER, Rendón JC, Chaparro JM, Basurto CS, Margaritoni M: **Breast cancer care in developing countries**. *World J Surg* 2009, **33**(10):2069-2076.
4. Parkin DM, Bray F, Ferlay J, Pisani P: **Estimating the world cancer burden: Globocan 2000**. *Int J Cancer* 2001, **94**(2):153-156.
5. Parkin DM: **Global cancer statistics in the year 2000**. *Lancet Oncol* 2001, **2**(9):533-543.
6. Murthy NS, Agarwal UK, Chaudhry K, Saxena S: **A study on time trends in incidence of breast cancer - Indian scenario**. *Eur J Cancer Care (Engl)* 2007, **16**(2):185-186.
7. Bagchi S: **Breast cancer rises in India**. *CMAJ* 2008, **179**(1):27.
8. Chopra R: **The Indian scene**. *J Clin Oncol* 2001, **19**(18 Suppl):106S-111S.
9. Moore MA, Ariyaratne Y, Badar F, Bhurgri Y, Datta K, Mathew A, Gangadharan P, Nandakumar A, Pradhananga KK, Talukder MH *et al*: **Cancer epidemiology in South Asia - past, present and future**. *Asian Pac J Cancer Prev* 2010, **11 Suppl 2**:49-66.
10. Dhillon PK, Yeole BB, Dikshit R, Kurkure AP, Bray F: **Trends in breast, ovarian and cervical cancer incidence in Mumbai, India over a 30-year period, 1976-2005: an age-period-cohort analysis**. *Br J Cancer* 2011, **105**(5):723-730.
11. Yeole BB, Kurkure A, Advani S, Lizzy S: **An Assessment of Cancer Incidence Patterns in Parsi and Non Parsi Populations, Greater Mumbai**. *Asian Pac J Cancer Prev* 2001, **2**(4):293-298.
12. Lodha RS, Nandeshwar S, Pal DK, Shrivastav A, Lodha KM, Bhagat VK, Bankwar VV, Saxena DM: **Risk factors for breast cancer among women in Bhopal urban agglomerate: a case-control study**. *Asian Pac J Cancer Prev* 2011, **12**(8):2111-2115.
13. Bertos NR, Park M: **Breast cancer - one term, many entities?** *J Clin Invest* 2011, **121**(10):3789-3796.
14. Maller O, Martinson H, Schedin P: **Extracellular matrix composition reveals complex and dynamic stromal-epithelial interactions in the mammary gland**. *J Mammary Gland Biol Neoplasia* 2010, **15**(3):301-318.
15. Sakakura T, Nishizuka Y, Dawe CJ: **Mesenchyme-dependent morphogenesis and epithelium-specific cytodifferentiation in mouse mammary gland**. *Science* 1976, **194**(4272):1439-1441.
16. Howlett AR, Bissell MJ: **The influence of tissue microenvironment (stroma and extracellular matrix) on the development and function of mammary epithelium**. *Epithelial Cell Biol* 1993, **2**(2):79-89.
17. Hanahan D, Weinberg RA: **Hallmarks of cancer: the next generation**. *Cell* 2011, **144**(5):646-674.
18. Dvorak HF: **Tumors: wounds that do not heal. Similarities between tumor stroma generation and wound healing**. *N Engl J Med* 1986, **315**(26):1650-1659.
19. Espina V, Liotta LA: **What is the malignant nature of human ductal carcinoma in situ?** *Nat Rev Cancer* 2011, **11**(1):68-75.
20. Polyak K: **Breast cancer: origins and evolution**. *J Clin Invest* 2007, **117**(11):3155-3163.
21. Burstein HJ, Polyak K, Wong JS, Lester SC, Kaelin CM: **Ductal carcinoma in situ of the breast**. *N Engl J Med* 2004, **350**(14):1430-1441.
22. Place AE, Jin Huh S, Polyak K: **The microenvironment in breast cancer progression: biology and implications for treatment**. *Breast Cancer Res* 2011, **13**(6):227.
23. Schnitt SJ: **Breast cancer in the 21st century: neu opportunities and neu challenges**. *Mod Pathol* 2001, **14**(3):213-218.

24. Moelans CB, van der Groep P, Hoefnagel LD, van de Vijver MJ, Wesseling P, Wesseling J, van der Wall E, van Diest PJ: **Genomic evolution from primary breast carcinoma to distant metastasis: Few copy number changes of breast cancer related genes**. *Cancer Lett* 2014, **344**(1):138-146.
25. Elston CW, Ellis IO: **Pathological prognostic factors in breast cancer. I. The value of histological grade in breast cancer: experience from a large study with long-term follow-up**. *Histopathology* 1991, **19**(5):403-410.
26. Edge SB, Compton CC: **The American Joint Committee on Cancer: the 7th edition of the AJCC cancer staging manual and the future of TNM**. *Ann Surg Oncol* 2010, **17**(6):1471-1474.
27. Galea MH, Blamey RW, Elston CE, Ellis IO: **The Nottingham Prognostic Index in primary breast cancer**. *Breast Cancer Res Treat* 1992, **22**(3):207-219.
28. Fisher B, Jeong JH, Anderson S, Wolmark N: **Treatment of axillary lymph node-negative, estrogen receptor-negative breast cancer: updated findings from National Surgical Adjuvant Breast and Bowel Project clinical trials**. *J Natl Cancer Inst* 2004, **96**(24):1823-1831.
29. Winer EP: **Optimizing endocrine therapy for breast cancer**. *J Clin Oncol* 2005, **23**(8):1609-1610.
30. Fisher B, Redmond C, Fisher ER, Caplan R: **Relative worth of estrogen or progesterone receptor and pathologic characteristics of differentiation as indicators of prognosis in node negative breast cancer patients: findings from National Surgical Adjuvant Breast and Bowel Project Protocol B-06**. *J Clin Oncol* 1988, **6**(7):1076-1087.
31. Cheang MC, Treaba DO, Speers CH, Olivotto IA, Bajdik CD, Chia SK, Goldstein LC, Gelmon KA, Huntsman D, Gilks CB *et al*: **Immunohistochemical detection using the new rabbit monoclonal antibody SP1 of estrogen receptor in breast cancer is superior to mouse monoclonal antibody 1D5 in predicting survival**. *J Clin Oncol* 2006, **24**(36):5637-5644.
32. Cianfrocca M, Goldstein LJ: **Prognostic and predictive factors in early-stage breast cancer**. *Oncologist* 2004, **9**(6):606-616.
33. Borg A, Tandon AK, Sigurdsson H, Clark GM, Fernö M, Fuqua SA, Killander D, McGuire WL: **HER-2/neu amplification predicts poor survival in node-positive breast cancer**. *Cancer Res* 1990, **50**(14):4332-4337.
34. Slamon DJ, Leyland-Jones B, Shak S, Fuchs H, Paton V, Bajamonde A, Fleming T, Eiermann W, Wolter J, Pegram M *et al*: **Use of chemotherapy plus a monoclonal antibody against HER2 for metastatic breast cancer that overexpresses HER2**. *N Engl J Med* 2001, **344**(11):783-792.
35. Urruticoechea A, Smith IE, Dowsett M: **Proliferation marker Ki-67 in early breast cancer**. *J Clin Oncol* 2005, **23**(28):7212-7220.
36. Keam B, Im SA, Kim HJ, Oh DY, Kim JH, Lee SH, Chie EK, Han W, Kim DW, Moon WK *et al*: **Prognostic impact of clinicopathologic parameters in stage II/III breast cancer treated with neoadjuvant docetaxel and doxorubicin chemotherapy: paradoxical features of the triple negative breast cancer**. *BMC Cancer* 2007, **7**:203.
37. Jones RL, Salter J, A'Hern R, Nerurkar A, Parton M, Reis-Filho JS, Smith IE, Dowsett M: **Relationship between oestrogen receptor status and proliferation in predicting response and long-term outcome to neoadjuvant chemotherapy for breast cancer**. *Breast Cancer Res Treat* 2010, **119**(2):315-323.
38. Hu M, Polyak K: **Microenvironmental regulation of cancer development**. *Curr Opin Genet Dev* 2008, **18**(1):27-34.
39. Xing F, Saidou J, Watabe K: **Cancer associated fibroblasts (CAFs) in tumor microenvironment**. *Front Biosci (Landmark Ed)* 2010, **15**:166-179.
40. Orimo A, Gupta PB, Sgroi DC, Arenzana-Seisdedos F, Delaunay T, Naeem R, Carey VJ, Richardson AL, Weinberg RA: **Stromal fibroblasts present in invasive human breast carcinomas promote tumor growth and angiogenesis through elevated SDF-1/CXCL12 secretion**. *Cell* 2005, **121**(3):335-348.

41. Tyan SW, Kuo WH, Huang CK, Pan CC, Shew JY, Chang KJ, Lee EY, Lee WH: **Breast cancer cells induce cancer-associated fibroblasts to secrete hepatocyte growth factor to enhance breast tumorigenesis**. *PLoS One* 2011, **6**(1):e15313.
42. Jedeszko C, Victor BC, Podgorski I, Sloane BF: **Fibroblast hepatocyte growth factor promotes invasion of human mammary ductal carcinoma in situ**. *Cancer Res* 2009, **69**(23):9148-9155.
43. Worthley DL, Ruszkiewicz A, Davies R, Moore S, Nivison-Smith I, Bik To L, Browett P, Western R, Durrant S, So J *et al*: **Human gastrointestinal neoplasia-associated myofibroblasts can develop from bone marrow-derived cells following allogeneic stem cell transplantation**. *Stem Cells* 2009, **27**(6):1463-1468.
44. Elkabets M, Gifford AM, Scheel C, Nilsson B, Reinhardt F, Bray MA, Carpenter AE, Jirström K, Magnusson K, Ebert BL *et al*: **Human tumors instigate granulin-expressing hematopoietic cells that promote malignancy by activating stromal fibroblasts in mice**. *J Clin Invest* 2011, **121**(2):784-799.
45. Chabottaux V, Noel A: **Breast cancer progression: insights into multifaceted matrix metalloproteinases**. *Clin Exp Metastasis* 2007, **24**(8):647-656.
46. Barker HE, Chang J, Cox TR, Lang G, Bird D, Nicolau M, Evans HR, Gartland A, Erler JT: **LOXL2-mediated matrix remodeling in metastasis and mammary gland involution**. *Cancer Res* 2011, **71**(5):1561-1572.
47. McDaniel SM, Rumer KK, Biroc SL, Metz RP, Singh M, Porter W, Schedin P: **Remodeling of the mammary microenvironment after lactation promotes breast tumor cell metastasis**. *Am J Pathol* 2006, **168**(2):608-620.
48. Man YG, Sang QX: **The significance of focal myoepithelial cell layer disruptions in human breast tumor invasion: a paradigm shift from the "protease-centered" hypothesis**. *Exp Cell Res* 2004, **301**(2):103-118.
49. Dewan MZ, Terunuma H, Takada M, Tanaka Y, Abe H, Sata T, Toi M, Yamamoto N: **Role of natural killer cells in hormone-independent rapid tumor formation and spontaneous metastasis of breast cancer cells in vivo**. *Breast Cancer Res Treat* 2007, **104**(3):267-275.
50. de Kruijf EM, Sajet A, van Nes JG, Natanov R, Putter H, Smit VT, Liefers GJ, van den Elsen PJ, van de Velde CJ, Kuppen PJ: **HLA-E and HLA-G expression in classical HLA class I-negative tumors is of prognostic value for clinical outcome of early breast cancer patients**. *J Immunol* 2010, **185**(12):7452-7459.
51. de Kruijf EM, Sajet A, van Nes JG, Putter H, Smit VT, Eagle RA, Jafferji I, Trowsdale J, Liefers GJ, van de Velde CJ *et al*: **NKG2D ligand tumor expression and association with clinical outcome in early breast cancer patients: an observational study**. *BMC Cancer* 2012, **12**:24.
52. Banchereau J, Palucka AK: **Dendritic cells as therapeutic vaccines against cancer**. *Nat Rev Immunol* 2005, **5**(4):296-306.
53. Koido S, Hara E, Homma S, Torii A, Toyama Y, Kawahara H, Watanabe M, Yanaga K, Fujise K, Tajiri H *et al*: **Dendritic cells fused with allogeneic colorectal cancer cell line present multiple colorectal cancer-specific antigens and induce antitumor immunity against autologous tumor cells**. *Clin Cancer Res* 2005, **11**(21):7891-7900.
54. Curiel TJ, Coukos G, Zou L, Alvarez X, Cheng P, Mottram P, Evdemon-Hogan M, Conejo-Garcia JR, Zhang L, Burow M *et al*: **Specific recruitment of regulatory T cells in ovarian carcinoma fosters immune privilege and predicts reduced survival**. *Nat Med* 2004, **10**(9):942-949.
55. Markiewski MM, DeAngelis RA, Benencia F, Ricklin-Lichtsteiner SK, Koutoulaki A, Gerard C, Coukos G, Lambris JD: **Modulation of the antitumor immune response by complement**. *Nat Immunol* 2008, **9**(11):1225-1235.

56. Aspord C, Pedroza-Gonzalez A, Gallegos M, Tindle S, Burton EC, Su D, Marches F, Banchereau J, Palucka AK: **Breast cancer instructs dendritic cells to prime interleukin 13-secreting CD4+ T cells that facilitate tumor development**. *J Exp Med* 2007, **204**(5):1037-1047.
57. Liu F, Lang R, Zhao J, Zhang X, Pringle GA, Fan Y, Yin D, Gu F, Yao Z, Fu L: **CD8$^+$ cytotoxic T cell and FOXP3$^+$ regulatory T cell infiltration in relation to breast cancer survival and molecular subtypes**. *Breast Cancer Res Treat* 2011, **130**(2):645-655.
58. Benevides L, Cardoso CR, Tiezzi DG, Marana HR, Andrade JM, Silva JS: **Enrichment of regulatory T cells in invasive breast tumor correlates with the upregulation of IL-17A expression and invasiveness of the tumor**. *Eur J Immunol* 2013, **43**(6):1518-1528.
59. Fridman WH, Pagès F, Sautès-Fridman C, Galon J: **The immune contexture in human tumours: impact on clinical outcome**. *Nat Rev Cancer* 2012, **12**(4):298-306.
60. Mlecnik B, Tosolini M, Kirilovsky A, Berger A, Bindea G, Meatchi T, Bruneval P, Trajanoski Z, Fridman WH, Pagès F *et al*: **Histopathologic-based prognostic factors of colorectal cancers are associated with the state of the local immune reaction**. *J Clin Oncol* 2011, **29**(6):610-618.
61. Mahmoud SM, Paish EC, Powe DG, Macmillan RD, Grainge MJ, Lee AH, Ellis IO, Green AR: **Tumor-infiltrating CD8+ lymphocytes predict clinical outcome in breast cancer**. *J Clin Oncol* 2011, **29**(15):1949-1955.
62. Finak G, Bertos N, Pepin F, Sadekova S, Souleimanova M, Zhao H, Chen H, Omeroglu G, Meterissian S, Omeroglu A *et al*: **Stromal gene expression predicts clinical outcome in breast cancer**. *Nat Med* 2008, **14**(5):518-527.
63. Schedin P, O'Brien J, Rudolph M, Stein T, Borges V: **Microenvironment of the involuting mammary gland mediates mammary cancer progression**. *J Mammary Gland Biol Neoplasia* 2007, **12**(1):71-82.
64. DeNardo DG, Barreto JB, Andreu P, Vasquez L, Tawfik D, Kolhatkar N, Coussens LM: **CD4(+) T cells regulate pulmonary metastasis of mammary carcinomas by enhancing protumor properties of macrophages**. *Cancer Cell* 2009, **16**(2):91-102.
65. Lin EY, Nguyen AV, Russell RG, Pollard JW: **Colony-stimulating factor 1 promotes progression of mammary tumors to malignancy**. *J Exp Med* 2001, **193**(6):727-740.
66. Aharinejad S, Paulus P, Sioud M, Hofmann M, Zins K, Schäfer R, Stanley ER, Abraham D: **Colony-stimulating factor-1 blockade by antisense oligonucleotides and small interfering RNAs suppresses growth of human mammary tumor xenografts in mice**. *Cancer Res* 2004, **64**(15):5378-5384.
67. Mantovani A, Pierotti MA: **Cancer and inflammation: a complex relationship**. *Cancer Lett* 2008, **267**(2):180-181.
68. Pollard PJ, Ratcliffe PJ: **Cancer. Puzzling patterns of predisposition**. *Science* 2009, **324**(5924):192-194.
69. Beck AH, Espinosa I, Edris B, Li R, Montgomery K, Zhu S, Varma S, Marinelli RJ, van de Rijn M, West RB: **The macrophage colony-stimulating factor 1 response signature in breast carcinoma**. *Clin Cancer Res* 2009, **15**(3):778-787.
70. Steidl C, Lee T, Shah SP, Farinha P, Han G, Nayar T, Delaney A, Jones SJ, Iqbal J, Weisenburger DD *et al*: **Tumor-associated macrophages and survival in classic Hodgkin's lymphoma**. *N Engl J Med* 2010, **362**(10):875-885.
71. Niino D, Komohara Y, Murayama T, Aoki R, Kimura Y, Hashikawa K, Kiyasu J, Takeuchi M, Suefuji N, Sugita Y *et al*: **Ratio of M2 macrophage expression is closely associated with poor prognosis for Angioimmunoblastic T-cell lymphoma (AITL)**. *Pathol Int* 2010, **60**(4):278-283.
72. Hammes LS, Tekmal RR, Naud P, Edelweiss MI, Kirma N, Valente PT, Syrjänen KJ, Cunha-Filho JS: **Macrophages, inflammation and risk of cervical intraepithelial neoplasia (CIN) progression--clinicopathological correlation**. *Gynecol Oncol* 2007, **105**(1):157-165.

73. Kamper P, Bendix K, Hamilton-Dutoit S, Honoré B, Nyengaard JR, d'Amore F: **Tumor-infiltrating macrophages correlate with adverse prognosis and Epstein-Barr virus status in classical Hodgkin's lymphoma**. *Haematologica* 2011, **96**(2):269-276.
74. Bronkhorst IH, Ly LV, Jordanova ES, Vrolijk J, Versluis M, Luyten GP, Jager MJ: **Detection of M2-macrophages in uveal melanoma and relation with survival**. *Invest Ophthalmol Vis Sci* 2011, **52**(2):643-650.
75. Ohno S, Inagawa H, Dhar DK, Fujii T, Ueda S, Tachibana M, Suzuki N, Inoue M, Soma G, Nagasue N: **The degree of macrophage infiltration into the cancer cell nest is a significant predictor of survival in gastric cancer patients**. *Anticancer Res* 2003, **23**(6D):5015-5022.
76. Forssell J, Oberg A, Henriksson ML, Stenling R, Jung A, Palmqvist R: **High macrophage infiltration along the tumor front correlates with improved survival in colon cancer**. *Clin Cancer Res* 2007, **13**(5):1472-1479.
77. Sconocchia G, Zlobec I, Lugli A, Calabrese D, Iezzi G, Karamitopoulou E, Patsouris ES, Peros G, Horcic M, Tornillo L *et al*: **Tumor infiltration by FcγRIII (CD16)+ myeloid cells is associated with improved survival in patients with colorectal carcinoma**. *Int J Cancer* 2011, **128**(11):2663-2672.
78. Allavena P, Mantovani A: **Immunology in the clinic review series; focus on cancer: tumour-associated macrophages: undisputed stars of the inflammatory tumour microenvironment**. *Clin Exp Immunol* 2012, **167**(2):195-205.
79. Hanahan D, Weinberg RA: **The hallmarks of cancer**. *Cell* 2000, **100**(1):57-70.
80. Mallmann M, Schmidt S, Schultze J: **Macrophages in human cancer: Current and future aspects.** In., vol. 16. Atlas Genet Cytogenet Oncol Haematol.; 2012: 765-774.
81. Murray PJ, Wynn TA: **Protective and pathogenic functions of macrophage subsets**. *Nat Rev Immunol* 2011, **11**(11):723-737.
82. Gordon S, Taylor PR: **Monocyte and macrophage heterogeneity**. *Nat Rev Immunol* 2005, **5**(12):953-964.
83. Biswas SK, Mantovani A: **Macrophage plasticity and interaction with lymphocyte subsets: cancer as a paradigm**. *Nat Immunol* 2010, **11**(10):889-896.
84. Gordon S: **Alternative activation of macrophages**. *Nat Rev Immunol* 2003, **3**(1):23-35.
85. Gordon S, Martinez FO: **Alternative activation of macrophages: mechanism and functions**. *Immunity* 2010, **32**(5):593-604.
86. Stout RD, Watkins SK, Suttles J: **Functional plasticity of macrophages: in situ reprogramming of tumor-associated macrophages**. *J Leukoc Biol* 2009, **86**(5):1105-1109.
87. Mantovani A, Allavena P, Sica A, Balkwill F: **Cancer-related inflammation**. *Nature* 2008, **454**(7203):436-444.
88. Mantovani A: **Role of inflammatory cells and mediators in tumor invasion and metastasis**. *Cancer Metastasis Rev* 2010, **29**(2):241.
89. Coussens LM, Werb Z: **Inflammation and cancer**. *Nature* 2002, **420**(6917):860-867.
90. Lewis CE, Pollard JW: **Distinct role of macrophages in different tumor microenvironments**. *Cancer Res* 2006, **66**(2):605-612.
91. Movahedi K, Laoui D, Gysemans C, Baeten M, Stangé G, Van den Bossche J, Mack M, Pipeleers D, In't Veld P, De Baetselier P *et al*: **Different tumor microenvironments contain functionally distinct subsets of macrophages derived from Ly6C(high) monocytes**. *Cancer Res* 2010, **70**(14):5728-5739.
92. Duluc D, Delneste Y, Tan F, Moles MP, Grimaud L, Lenoir J, Preisser L, Anegon I, Catala L, Ifrah N *et al*: **Tumor-associated leukemia inhibitory factor and IL-6 skew monocyte differentiation into tumor-associated macrophage-like cells**. *Blood* 2007, **110**(13):4319-4330.
93. Heusinkveld M, de Vos van Steenwijk PJ, Goedemans R, Ramwadhdoebe TH, Gorter A, Welters MJ, van Hall T, van der Burg SH: **M2 macrophages induced by prostaglandin E2 and IL-6 from**

cervical carcinoma are switched to activated M1 macrophages by CD4+ Th1 cells. *J Immunol* 2011, **187**(3):1157-1165.

94. Kuang DM, Wu Y, Chen N, Cheng J, Zhuang SM, Zheng L: **Tumor-derived hyaluronan induces formation of immunosuppressive macrophages through transient early activation of monocytes**. *Blood* 2007, **110**(2):587-595.
95. Kim S, Joo YE: **Theaflavin Inhibits LPS-Induced IL-6, MCP-1, and ICAM-1 Expression in Bone Marrow-Derived Macrophages Through the Blockade of NF-κB and MAPK Signaling Pathways**. *Chonnam Med J* 2011, **47**(2):104-110.
96. Biswas SK, Gangi L, Paul S, Schioppa T, Saccani A, Sironi M, Bottazzi B, Doni A, Vincenzo B, Pasqualini F *et al*: **A distinct and unique transcriptional program expressed by tumor-associated macrophages (defective NF-kappaB and enhanced IRF-3/STAT1 activation)**. *Blood* 2006, **107**(5):2112-2122.
97. Buddingh EP, Kuijjer ML, Duim RA, Bürger H, Agelopoulos K, Myklebost O, Serra M, Mertens F, Hogendoorn PC, Lankester AC *et al*: **Tumor-infiltrating macrophages are associated with metastasis suppression in high-grade osteosarcoma: a rationale for treatment with macrophage activating agents**. *Clin Cancer Res* 2011, **17**(8):2110-2119.
98. Zabuawala T, Taffany DA, Sharma SM, Merchant A, Adair B, Srinivasan R, Rosol TJ, Fernandez S, Huang K, Leone G *et al*: **An ets2-driven transcriptional program in tumor-associated macrophages promotes tumor metastasis**. *Cancer Res* 2010, **70**(4):1323-1333.
99. Ojalvo LS, Whittaker CA, Condeelis JS, Pollard JW: **Gene expression analysis of macrophages that facilitate tumor invasion supports a role for Wnt-signaling in mediating their activity in primary mammary tumors**. *J Immunol* 2010, **184**(2):702-712.
100. Lin WW, Karin M: **A cytokine-mediated link between innate immunity, inflammation, and cancer**. *J Clin Invest* 2007, **117**(5):1175-1183.
101. Joyce JA, Pollard JW: **Microenvironmental regulation of metastasis**. *Nat Rev Cancer* 2009, **9**(4):239-252.
102. Bromberg J, Wang TC: **Inflammation and cancer: IL-6 and STAT3 complete the link**. *Cancer Cell* 2009, **15**(2):79-80.
103. Grivennikov S, Karin E, Terzic J, Mucida D, Yu GY, Vallabhapurapu S, Scheller J, Rose-John S, Cheroutre H, Eckmann L *et al*: **IL-6 and Stat3 are required for survival of intestinal epithelial cells and development of colitis-associated cancer**. *Cancer Cell* 2009, **15**(2):103-113.
104. Osborne J, Moore PS, Chang Y: **KSHV-encoded viral IL-6 activates multiple human IL-6 signaling pathways**. *Hum Immunol* 1999, **60**(10):921-927.
105. Cozen W, Gill PS, Ingles SA, Masood R, Martínez-Maza O, Cockburn MG, Gauderman WJ, Pike MC, Bernstein L, Nathwani BN *et al*: **IL-6 levels and genotype are associated with risk of young adult Hodgkin lymphoma**. *Blood* 2004, **103**(8):3216-3221.
106. Berger FG: **The interleukin-6 gene: a susceptibility factor that may contribute to racial and ethnic disparities in breast cancer mortality**. *Breast Cancer Res Treat* 2004, **88**(3):281-285.
107. Bommert K, Bargou RC, Stühmer T: **Signalling and survival pathways in multiple myeloma**. *Eur J Cancer* 2006, **42**(11):1574-1580.
108. Stone RC, Feng D, Deng J, Singh S, Yang L, Fitzgerald-Bocarsly P, Eloranta ML, Rönnblom L, Barnes BJ: **Interferon regulatory factor 5 activation in monocytes of systemic lupus erythematosus patients is triggered by circulating autoantigens independent of type I interferons**. *Arthritis Rheum* 2012, **64**(3):788-798.
109. Derynck R, Akhurst RJ, Balmain A: **TGF-beta signaling in tumor suppression and cancer progression**. *Nat Genet* 2001, **29**(2):117-129.

110. Standiford TJ, Kuick R, Bhan U, Chen J, Newstead M, Keshamouni VG: **TGF-β-induced IRAK-M expression in tumor-associated macrophages regulates lung tumor growth**. *Oncogene* 2011, **30**(21):2475-2484.
111. Kryczek I, Wei S, Zou L, Zhu G, Mottram P, Xu H, Chen L, Zou W: **Cutting edge: induction of B7-H4 on APCs through IL-10: novel suppressive mode for regulatory T cells**. *J Immunol* 2006, **177**(1):40-44.
112. Kuang DM, Zhao Q, Peng C, Xu J, Zhang JP, Wu C, Zheng L: **Activated monocytes in peritumoral stroma of hepatocellular carcinoma foster immune privilege and disease progression through PD-L1**. *J Exp Med* 2009, **206**(6):1327-1337.
113. Liu J, Zhang N, Li Q, Zhang W, Ke F, Leng Q, Wang H, Chen J: **Tumor-associated macrophages recruit CCR6+ regulatory T cells and promote the development of colorectal cancer via enhancing CCL20 production in mice**. *PLoS One* 2011, **6**(4):e19495.
114. Hagemann T, Robinson SC, Schulz M, Trümper L, Balkwill FR, Binder C: **Enhanced invasiveness of breast cancer cell lines upon co-cultivation with macrophages is due to TNF-alpha dependent up-regulation of matrix metalloproteases**. *Carcinogenesis* 2004, **25**(8):1543-1549.
115. Vasiljeva O, Papazoglou A, Krüger A, Brodoefel H, Korovin M, Deussing J, Augustin N, Nielsen BS, Almholt K, Bogyo M *et al*: **Tumor cell-derived and macrophage-derived cathepsin B promotes progression and lung metastasis of mammary cancer**. *Cancer Res* 2006, **66**(10):5242-5250.
116. Wyckoff J, Wang W, Lin EY, Wang Y, Pixley F, Stanley ER, Graf T, Pollard JW, Segall J, Condeelis J: **A paracrine loop between tumor cells and macrophages is required for tumor cell migration in mammary tumors**. *Cancer Res* 2004, **64**(19):7022-7029.
117. Goswami S, Sahai E, Wyckoff JB, Cammer M, Cox D, Pixley FJ, Stanley ER, Segall JE, Condeelis JS: **Macrophages promote the invasion of breast carcinoma cells via a colony-stimulating factor-1/epidermal growth factor paracrine loop**. *Cancer Res* 2005, **65**(12):5278-5283.
118. Wyckoff JB, Wang Y, Lin EY, Li JF, Goswami S, Stanley ER, Segall JE, Pollard JW, Condeelis J: **Direct visualization of macrophage-assisted tumor cell intravasation in mammary tumors**. *Cancer Res* 2007, **67**(6):2649-2656.
119. Thiery JP: **Epithelial-mesenchymal transitions in tumour progression**. *Nat Rev Cancer* 2002, **2**(6):442-454.
120. Bonde AK, Tischler V, Kumar S, Soltermann A, Schwendener RA: **Intratumoral macrophages contribute to epithelial-mesenchymal transition in solid tumors**. *BMC Cancer* 2012, **12**:35.
121. Zhang B, Yao G, Zhang Y, Gao J, Yang B, Rao Z: **M2-polarized tumor-associated macrophages are associated with poor prognoses resulting from accelerated lymphangiogenesis in lung adenocarcinoma**. *Clinics (Sao Paulo)* 2011, **66**(11):1879-1886.
122. Utrera-Barillas D, Castro-Manrreza M, Castellanos E, Gutiérrez-Rodríguez M, Arciniega-Ruíz de Esparza O, García-Cebada J, Velazquez JR, Flores-Reséndiz D, Hernández-Hernández D, Benítez-Bribiesca L: **The role of macrophages and mast cells in lymphangiogenesis and angiogenesis in cervical carcinogenesis**. *Exp Mol Pathol* 2010, **89**(2):190-196.
123. Murdoch C, Muthana M, Coffelt SB, Lewis CE: **The role of myeloid cells in the promotion of tumour angiogenesis**. *Nat Rev Cancer* 2008, **8**(8):618-631.
124. Leek RD, Harris AL: **Tumor-associated macrophages in breast cancer**. *J Mammary Gland Biol Neoplasia* 2002, **7**(2):177-189.
125. Landskron G, De la Fuente M, Thuwajit P, Thuwajit C, Hermoso MA: **Chronic inflammation and cytokines in the tumor microenvironment**. *J Immunol Res* 2014, **2014**:149185.
126. Popa C, Netea MG, van Riel PL, van der Meer JW, Stalenhoef AF: **The role of TNF-alpha in chronic inflammatory conditions, intermediary metabolism, and cardiovascular risk**. *J Lipid Res* 2007, **48**(4):751-762.

127. Moore RJ, Owens DM, Stamp G, Arnott C, Burke F, East N, Holdsworth H, Turner L, Rollins B, Pasparakis M *et al*: **Mice deficient in tumor necrosis factor-alpha are resistant to skin carcinogenesis**. *Nat Med* 1999, **5**(7):828-831.
128. Szlosarek P, Charles KA, Balkwill FR: **Tumour necrosis factor-alpha as a tumour promoter**. *Eur J Cancer* 2006, **42**(6):745-750.
129. Chen G, Goeddel DV: **TNF-R1 signaling: a beautiful pathway**. *Science* 2002, **296**(5573):1634-1635.
130. Havell EA, Fiers W, North RJ: **The antitumor function of tumor necrosis factor (TNF), I. Therapeutic action of TNF against an established murine sarcoma is indirect, immunologically dependent, and limited by severe toxicity**. *J Exp Med* 1988, **167**(3):1067-1085.
131. Balkwill F: **TNF-alpha in promotion and progression of cancer**. *Cancer Metastasis Rev* 2006, **25**(3):409-416.
132. Woo CH, Eom YW, Yoo MH, You HJ, Han HJ, Song WK, Yoo YJ, Chun JS, Kim JH: **Tumor necrosis factor-alpha generates reactive oxygen species via a cytosolic phospholipase A2-linked cascade**. *J Biol Chem* 2000, **275**(41):32357-32362.
133. Hussain SP, Hofseth LJ, Harris CC: **Radical causes of cancer**. *Nat Rev Cancer* 2003, **3**(4):276-285.
134. Suganuma M, Watanabe T, Yamaguchi K, Takahashi A, Fujiki H: **Human gastric cancer development with TNF-α-inducing protein secreted from Helicobacter pylori**. *Cancer Lett* 2012, **322**(2):133-138.
135. Kwong J, Lee JY, Wong KK, Zhou X, Wong DT, Lo KW, Welch WR, Berkowitz RS, Mok SC: **Candidate tumor-suppressor gene DLEC1 is frequently downregulated by promoter hypermethylation and histone hypoacetylation in human epithelial ovarian cancer**. *Neoplasia* 2006, **8**(4):268-278.
136. Ohri CM, Shikotra A, Green RH, Waller DA, Bradding P: **Tumour necrosis factor-alpha expression in tumour islets confers a survival advantage in non-small cell lung cancer**. *BMC Cancer* 2010, **10**:323.
137. Lee SH, Hong HS, Liu ZX, Kim RH, Kang MK, Park NH, Shin KH: **TNFα enhances cancer stem cell-like phenotype via Notch-Hes1 activation in oral squamous cell carcinoma cells**. *Biochem Biophys Res Commun* 2012, **424**(1):58-64.
138. Heikkilä K, Harris R, Lowe G, Rumley A, Yarnell J, Gallacher J, Ben-Shlomo Y, Ebrahim S, Lawlor DA: **Associations of circulating C-reactive protein and interleukin-6 with cancer risk: findings from two prospective cohorts and a meta-analysis**. *Cancer Causes Control* 2009, **20**(1):15-26.
139. Hodge DR, Hurt EM, Farrar WL: **The role of IL-6 and STAT3 in inflammation and cancer**. *Eur J Cancer* 2005, **41**(16):2502-2512.
140. Gasche JA, Hoffmann J, Boland CR, Goel A: **Interleukin-6 promotes tumorigenesis by altering DNA methylation in oral cancer cells**. *Int J Cancer* 2011, **129**(5):1053-1063.
141. Kinoshita H, Hirata Y, Nakagawa H, Sakamoto K, Hayakawa Y, Takahashi R, Nakata W, Sakitani K, Serizawa T, Hikiba Y *et al*: **Interleukin-6 mediates epithelial-stromal interactions and promotes gastric tumorigenesis**. *PLoS One* 2013, **8**(4):e60914.
142. Chatterjee M, Stühmer T, Herrmann P, Bommert K, Dörken B, Bargou RC: **Combined disruption of both the MEK/ERK and the IL-6R/STAT3 pathways is required to induce apoptosis of multiple myeloma cells in the presence of bone marrow stromal cells**. *Blood* 2004, **104**(12):3712-3721.
143. Kim SY, Kang JW, Song X, Kim BK, Yoo YD, Kwon YT, Lee YJ: **Role of the IL-6-JAK1-STAT3-Oct-4 pathway in the conversion of non-stem cancer cells into cancer stem-like cells**. *Cell Signal* 2013, **25**(4):961-969.
144. Santibañez JF, Quintanilla M, Bernabeu C: **TGF-β/TGF-β receptor system and its role in physiological and pathological conditions**. *Clin Sci (Lond)* 2011, **121**(6):233-251.

145. Massagué J: **A very private TGF-beta receptor embrace**. *Mol Cell* 2008, **29**(2):149-150.
146. Matsuzaki K: **Smad phospho-isoforms direct context-dependent TGF-β signaling**. *Cytokine Growth Factor Rev* 2013, **24**(4):385-399.
147. Tang B, Vu M, Booker T, Santner SJ, Miller FR, Anver MR, Wakefield LM: **TGF-beta switches from tumor suppressor to prometastatic factor in a model of breast cancer progression**. *J Clin Invest* 2003, **112**(7):1116-1124.
148. Morrison CD, Parvani JG, Schiemann WP: **The relevance of the TGF-β Paradox to EMT-MET programs**. *Cancer Lett* 2013, **341**(1):30-40.
149. Malliri A, Yeudall WA, Nikolic M, Crouch DH, Parkinson EK, Ozanne B: **Sensitivity to transforming growth factor beta 1-induced growth arrest is common in human squamous cell carcinoma cell lines: c-MYC down-regulation and p21waf1 induction are important early events**. *Cell Growth Differ* 1996, **7**(10):1291-1304.
150. Guasch G, Schober M, Pasolli HA, Conn EB, Polak L, Fuchs E: **Loss of TGFbeta signaling destabilizes homeostasis and promotes squamous cell carcinomas in stratified epithelia**. *Cancer Cell* 2007, **12**(4):313-327.
151. Levy L, Hill CS: **Alterations in components of the TGF-beta superfamily signaling pathways in human cancer**. *Cytokine Growth Factor Rev* 2006, **17**(1-2):41-58.
152. Bierie B, Moses HL: **TGF-beta and cancer**. *Cytokine Growth Factor Rev* 2006, **17**(1-2):29-40.
153. Massagué J: **TGFbeta in Cancer**. *Cell* 2008, **134**(2):215-230.
154. Connolly EC, Freimuth J, Akhurst RJ: **Complexities of TGF-β targeted cancer therapy**. *Int J Biol Sci* 2012, **8**(7):964-978.
155. Sabat R, Grütz G, Warszawska K, Kirsch S, Witte E, Wolk K, Geginat J: **Biology of interleukin-10**. *Cytokine Growth Factor Rev* 2010, **21**(5):331-344.
156. Gastl GA, Abrams JS, Nanus DM, Oosterkamp R, Silver J, Liu F, Chen M, Albino AP, Bander NH: **Interleukin-10 production by human carcinoma cell lines and its relationship to interleukin-6 expression**. *Int J Cancer* 1993, **55**(1):96-101.
157. Costa NL, Valadares MC, Souza PP, Mendonça EF, Oliveira JC, Silva TA, Batista AC: **Tumor-associated macrophages and the profile of inflammatory cytokines in oral squamous cell carcinoma**. *Oral Oncol* 2013, **49**(3):216-223.
158. Finbloom DS, Larner AC, Nakagawa Y, Hoover DL: **Culture of human monocytes with granulocyte-macrophage colony-stimulating factor results in enhancement of IFN-gamma receptors but suppression of IFN-gamma-induced expression of the gene IP-10**. *J Immunol* 1993, **150**(6):2383-2390.
159. Schottelius AJ, Mayo MW, Sartor RB, Baldwin AS: **Interleukin-10 signaling blocks inhibitor of kappaB kinase activity and nuclear factor kappaB DNA binding**. *J Biol Chem* 1999, **274**(45):31868-31874.
160. Kundu N, Fulton AM: **Interleukin-10 inhibits tumor metastasis, downregulates MHC class I, and enhances NK lysis**. *Cell Immunol* 1997, **180**(1):55-61.
161. Hamidullah, Changkija B, Konwar R: **Role of interleukin-10 in breast cancer**. *Breast Cancer Res Treat* 2012, **133**(1):11-21.
162. Braun DA, Fribourg M, Sealfon SC: **Cytokine response is determined by duration of receptor and signal transducers and activators of transcription 3 (STAT3) activation**. *J Biol Chem* 2013, **288**(5):2986-2993.
163. Alas S, Bonavida B: **Rituximab inactivates signal transducer and activation of transcription 3 (STAT3) activity in B-non-Hodgkin's lymphoma through inhibition of the interleukin 10 autocrine/paracrine loop and results in down-regulation of Bcl-2 and sensitization to cytotoxic drugs**. *Cancer Res* 2001, **61**(13):5137-5144.

164. Lech-Maranda E, Bienvenu J, Michallet AS, Houot R, Robak T, Coiffier B, Salles G: **Elevated IL-10 plasma levels correlate with poor prognosis in diffuse large B-cell lymphoma**. *Eur Cytokine Netw* 2006, **17**(1):60-66.
165. Ogden CA, Pound JD, Batth BK, Owens S, Johannessen I, Wood K, Gregory CD: **Enhanced apoptotic cell clearance capacity and B cell survival factor production by IL-10-activated macrophages: implications for Burkitt's lymphoma**. *J Immunol* 2005, **174**(5):3015-3023.
166. Halliwell B: **Biochemistry of oxidative stress**. *Biochem Soc Trans* 2007, **35**(Pt 5):1147-1150.
167. Mencalha A, Victorino VJ, Cecchini R, Panis C: **Mapping oxidative changes in breast cancer: understanding the basic to reach the clinics**. *Anticancer Res* 2014, **34**(3):1127-1140.
168. Pani G, Giannoni E, Galeotti T, Chiarugi P: **Redox-based escape mechanism from death: the cancer lesson**. *Antioxid Redox Signal* 2009, **11**(11):2791-2806.
169. Martinez-Outschoorn UE, Balliet RM, Rivadeneira DB, Chiavarina B, Pavlides S, Wang C, Whitaker-Menezes D, Daumer KM, Lin Z, Witkiewicz AK *et al*: **Oxidative stress in cancer associated fibroblasts drives tumor-stroma co-evolution: A new paradigm for understanding tumor metabolism, the field effect and genomic instability in cancer cells**. *Cell Cycle* 2010, **9**(16):3256-3276.
170. Halliwell B: **Oxidative stress and cancer: have we moved forward?** *Biochem J* 2007, **401**(1):1-11.
171. Gauthier N, Lohm S, Touzery C, Chantôme A, Perette B, Reveneau S, Brunotte F, Juillerat-Jeanneret L, Jeannin JF: **Tumour-derived and host-derived nitric oxide differentially regulate breast carcinoma metastasis to the lungs**. *Carcinogenesis* 2004, **25**(9):1559-1565.
172. Glynn SA, Boersma BJ, Dorsey TH, Yi M, Yfantis HG, Ridnour LA, Martin DN, Switzer CH, Hudson RS, Wink DA *et al*: **Increased NOS2 predicts poor survival in estrogen receptor-negative breast cancer patients**. *J Clin Invest* 2010, **120**(11):3843-3854.
173. Cairns RA, Harris I, McCracken S, Mak TW: **Cancer cell metabolism**. *Cold Spring Harb Symp Quant Biol* 2011, **76**:299-311.
174. Choudhary S, Sood S, Donnell RL, Wang HC: **Intervention of human breast cell carcinogenesis chronically induced by 2-amino-1-methyl-6-phenylimidazo[4,5-b]pyridine**. *Carcinogenesis* 2012, **33**(4):876-885.
175. Boudreau HE, Casterline BW, Rada B, Korzeniowska A, Leto TL: **Nox4 involvement in TGF-beta and SMAD3-driven induction of the epithelial-to-mesenchymal transition and migration of breast epithelial cells**. *Free Radic Biol Med* 2012, **53**(7):1489-1499.
176. Okoh V, Deoraj A, Roy D: **Estrogen-induced reactive oxygen species-mediated signalings contribute to breast cancer**. *Biochim Biophys Acta* 2011, **1815**(1):115-133.
177. Penney RB, Roy D: **Thioredoxin-mediated redox regulation of resistance to endocrine therapy in breast cancer**. *Biochim Biophys Acta* 2013, **1836**(1):60-79.
178. Ostrakhovitch EA: **Redox environment and its meaning for breast cancer cells fate**. *Curr Cancer Drug Targets* 2011, **11**(4):479-495.
179. Vurusaner B, Poli G, Basaga H: **Tumor suppressor genes and ROS: complex networks of interactions**. *Free Radic Biol Med* 2012, **52**(1):7-18.
180. Diers AR, Vayalil PK, Oliva CR, Griguer CE, Darley-Usmar V, Hurst DR, Welch DR, Landar A: **Mitochondrial bioenergetics of metastatic breast cancer cells in response to dynamic changes in oxygen tension: effects of HIF-1α**. *PLoS One* 2013, **8**(6):e68348.
181. Cai Q, Lin T, Kamarajugadda S, Lu J: **Regulation of glycolysis and the Warburg effect by estrogen-related receptors**. *Oncogene* 2013, **32**(16):2079-2086.
182. Ignarro LJ, Buga GM, Wood KS, Byrns RE, Chaudhuri G: **Endothelium-derived relaxing factor produced and released from artery and vein is nitric oxide**. *Proc Natl Acad Sci U S A* 1987, **84**(24):9265-9269.

183. Palmer RM, Ferrige AG, Moncada S: **Nitric oxide release accounts for the biological activity of endothelium-derived relaxing factor**. *Nature* 1987, **327**(6122):524-526.
184. Choudhari SK, Chaudhary M, Bagde S, Gadbail AR, Joshi V: **Nitric oxide and cancer: a review**. *World J Surg Oncol* 2013, **11**:118.
185. Rosbe KW, Prazma J, Petrusz P, Mims W, Ball SS, Weissler MC: **Immunohistochemical characterization of nitric oxide synthase activity in squamous cell carcinoma of the head and neck**. *Otolaryngol Head Neck Surg* 1995, **113**(5):541-549.
186. Reveneau S, Arnould L, Jolimoy G, Hilpert S, Lejeune P, Saint-Giorgio V, Belichard C, Jeannin JF: **Nitric oxide synthase in human breast cancer is associated with tumor grade, proliferation rate, and expression of progesterone receptors**. *Lab Invest* 1999, **79**(10):1215-1225.
187. Taysi S, Uslu C, Akcay F, Sutbeyaz MY: **Malondialdehyde and nitric oxide levels in the plasma of patients with advanced laryngeal cancer**. *Surg Today* 2003, **33**(9):651-654.
188. Ying L, Hofseth LJ: **An emerging role for endothelial nitric oxide synthase in chronic inflammation and cancer**. *Cancer Res* 2007, **67**(4):1407-1410.
189. Shang ZJ, Li JR, Li ZB: **Effects of exogenous nitric oxide on oral squamous cell carcinoma: an in vitro study**. *J Oral Maxillofac Surg* 2002, **60**(8):905-910; discussion 910-901.
190. Harada K, Supriatno, Kawaguchi S, Tomitaro O, Yoshida H, Sato M: **Overexpression of iNOS gene suppresses the tumorigenicity and metastasis of oral cancer cells**. *In Vivo* 2004, **18**(4):449-455.
191. Moncada S, Palmer RM: **Biosynthesis and actions of nitric oxide**. *Semin Perinatol* 1991, **15**(1):16-19.
192. Ambs S, Merriam WG, Ogunfusika MO, Bennett WP, Ishibe N, Hussain SP, Tzeng EE, Geller DA, Billiar TR, Harris CC: **p53 and vascular endothelial growth factor regulate tumor growth of NOS2-expressing human carcinoma cells**. *Nat Med* 1998, **4**(12):1371-1376.
193. Kanner J, Harel S, Granit R: **Nitric oxide as an antioxidant**. *Arch Biochem Biophys* 1991, **289**(1):130-136.
194. Grisham MB, Jourd'Heuil D, Wink DA: **Nitric oxide. I. Physiological chemistry of nitric oxide and its metabolites:implications in inflammation**. *Am J Physiol* 1999, **276**(2 Pt 1):G315-321.
195. Wink DA, Vodovotz Y, Laval J, Laval F, Dewhirst MW, Mitchell JB: **The multifaceted roles of nitric oxide in cancer**. *Carcinogenesis* 1998, **19**(5):711-721.
196. Patel RP, McAndrew J, Sellak H, White CR, Jo H, Freeman BA, Darley-Usmar VM: **Biological aspects of reactive nitrogen species**. *Biochim Biophys Acta* 1999, **1411**(2-3):385-400.
197. Wink DA, Grisham MB, Mitchell JB, Ford PC: **Direct and indirect effects of nitric oxide in chemical reactions relevant to biology**. *Methods Enzymol* 1996, **268**:12-31.
198. Sun Y: **Free radicals, antioxidant enzymes, and carcinogenesis**. *Free Radic Biol Med* 1990, **8**(6):583-599.
199. Thomsen LL, Miles DW, Happerfield L, Bobrow LG, Knowles RG, Moncada S: **Nitric oxide synthase activity in human breast cancer**. *Br J Cancer* 1995, **72**(1):41-44.
200. Nakamura Y, Yasuoka H, Tsujimoto M, Yoshidome K, Nakahara M, Nakao K, Nakamura M, Kakudo K: **Nitric oxide in breast cancer: induction of vascular endothelial growth factor-C and correlation with metastasis and poor prognosis**. *Clin Cancer Res* 2006, **12**(4):1201-1207.
201. Switzer CH, Cheng RY, Ridnour LA, Glynn SA, Ambs S, Wink DA: **Ets-1 is a transcriptional mediator of oncogenic nitric oxide signaling in estrogen receptor-negative breast cancer**. *Breast Cancer Res* 2012, **14**(5):R125.
202. Alagöl H, Erdem E, Sancak B, Turkmen G, Camlibel M, Bugdayci G: **Nitric oxide biosynthesis and malondialdehyde levels in advanced breast cancer**. *Aust N Z J Surg* 1999, **69**(9):647-650.
203. Tschugguel W, Knogler W, Czerwenka K, Mildner M, Weninger W, Zeillinger R, Huber JC: **Presence of endothelial calcium-dependent nitric oxide synthase in breast apocrine metaplasia**. *Br J Cancer* 1996, **74**(9):1423-1426.

204. Zeillinger R, Tantscher E, Schneeberger C, Tschugguel W, Eder S, Sliutz G, Huber JC: **Simultaneous expression of nitric oxide synthase and estrogen receptor in human breast cancer cell lines**. *Breast Cancer Res Treat* 1996, **40**(2):205-207.
205. Pance A: **Nitric oxide and hormones in breast cancer: allies or enemies?** *Future Oncol* 2006, **2**(2):275-288.
206. Choi BM, Pae HO, Jang SI, Kim YM, Chung HT: **Nitric oxide as a pro-apoptotic as well as anti-apoptotic modulator**. *J Biochem Mol Biol* 2002, **35**(1):116-126.
207. Ziche M, Morbidelli L: **Nitric oxide and angiogenesis**. *J Neurooncol* 2000, **50**(1-2):139-148.
208. Lala PK: **Significance of nitric oxide in carcinogenesis, tumor progression and cancer therapy**. *Cancer Metastasis Rev* 1998, **17**(1):1-6.
209. Lepoivre M, Flaman JM, Henry Y: **Early loss of the tyrosyl radical in ribonucleotide reductase of adenocarcinoma cells producing nitric oxide**. *J Biol Chem* 1992, **267**(32):22994-23000.
210. Lechner M, Lirk P, Rieder J: **Inducible nitric oxide synthase (iNOS) in tumor biology: the two sides of the same coin**. *Semin Cancer Biol* 2005, **15**(4):277-289.
211. Aranda E, López-Pedrera C, De La Haba-Rodriguez JR, Rodriguez-Ariza A: **Nitric oxide and cancer: the emerging role of S-nitrosylation**. *Curr Mol Med* 2012, **12**(1):50-67.
212. Nowell PC: **The clonal evolution of tumor cell populations**. *Science* 1976, **194**(4260):23-28.
213. Negrini S, Gorgoulis VG, Halazonetis TD: **Genomic instability--an evolving hallmark of cancer**. *Nat Rev Mol Cell Biol* 2010, **11**(3):220-228.
214. Shah SN, Hile SE, Eckert KA: **Defective mismatch repair, microsatellite mutation bias, and variability in clinical cancer phenotypes**. *Cancer Res* 2010, **70**(2):431-435.
215. Rouse J, Jackson SP: **Interfaces between the detection, signaling, and repair of DNA damage**. *Science* 2002, **297**(5581):547-551.
216. Harrison JC, Haber JE: **Surviving the breakup: the DNA damage checkpoint**. *Annu Rev Genet* 2006, **40**:209-235.
217. Bartek J, Lukas J: **DNA damage checkpoints: from initiation to recovery or adaptation**. *Curr Opin Cell Biol* 2007, **19**(2):238-245.
218. Callegari AJ, Kelly TJ: **Shedding light on the DNA damage checkpoint**. *Cell Cycle* 2007, **6**(6):660-666.
219. Giglia-Mari G, Zotter A, Vermeulen W: **DNA damage response**. *Cold Spring Harb Perspect Biol* 2011, **3**(1):a000745.
220. Zhou BB, Elledge SJ: **The DNA damage response: putting checkpoints in perspective**. *Nature* 2000, **408**(6811):433-439.
221. Bernstein C, Bernstein H, Payne CM, Garewal H: **DNA repair/pro-apoptotic dual-role proteins in five major DNA repair pathways: fail-safe protection against carcinogenesis**. *Mutat Res* 2002, **511**(2):145-178.
222. Lee JH, Paull TT: **ATM activation by DNA double-strand breaks through the Mre11-Rad50-Nbs1 complex**. *Science* 2005, **308**(5721):551-554.
223. Abraham RT, Tibbetts RS: **Cell biology. Guiding ATM to broken DNA**. *Science* 2005, **308**(5721):510-511.
224. Matsuoka S, Ballif BA, Smogorzewska A, McDonald ER, Hurov KE, Luo J, Bakalarski CE, Zhao Z, Solimini N, Lerenthal Y *et al*: **ATM and ATR substrate analysis reveals extensive protein networks responsive to DNA damage**. *Science* 2007, **316**(5828):1160-1166.
225. Ahn J, Urist M, Prives C: **The Chk2 protein kinase**. *DNA Repair (Amst)* 2004, **3**(8-9):1039-1047.
226. Wakeman TP, Kim WJ, Callens S, Chiu A, Brown KD, Xu B: **The ATM-SMC1 pathway is essential for activation of the chromium[VI]-induced S-phase checkpoint**. *Mutat Res* 2004, **554**(1-2):241-251.

227. Chen Y, Sanchez Y: **Chk1 in the DNA damage response: conserved roles from yeasts to mammals**. *DNA Repair (Amst)* 2004, **3**(8-9):1025-1032.
228. Smits VA, Warmerdam DO, Martin Y, Freire R: **Mechanisms of ATR-mediated checkpoint signalling**. *Front Biosci (Landmark Ed)* 2010, **15**:840-853.
229. Burma S, Chen BP, Chen DJ: **Role of non-homologous end joining (NHEJ) in maintaining genomic integrity**. *DNA Repair (Amst)* 2006, **5**(9-10):1042-1048.
230. Burma S, Chen DJ: **Role of DNA-PK in the cellular response to DNA double-strand breaks**. *DNA Repair (Amst)* 2004, **3**(8-9):909-918.
231. Rogakou EP, Pilch DR, Orr AH, Ivanova VS, Bonner WM: **DNA double-stranded breaks induce histone H2AX phosphorylation on serine 139**. *J Biol Chem* 1998, **273**(10):5858-5868.
232. Redon C, Pilch D, Rogakou E, Sedelnikova O, Newrock K, Bonner W: **Histone H2A variants H2AX and H2AZ**. *Curr Opin Genet Dev* 2002, **12**(2):162-169.
233. Cheung P, Allis CD, Sassone-Corsi P: **Signaling to chromatin through histone modifications**. *Cell* 2000, **103**(2):263-271.
234. Chew YC, Camporeale G, Kothapalli N, Sarath G, Zempleni J: **Lysine residues in N-terminal and C-terminal regions of human histone H2A are targets for biotinylation by biotinidase**. *J Nutr Biochem* 2006, **17**(4):225-233.
235. Fernandez-Capetillo O, Allis CD, Nussenzweig A: **Phosphorylation of histone H2B at DNA double-strand breaks**. *J Exp Med* 2004, **199**(12):1671-1677.
236. Stiff T, Walker SA, Cerosaletti K, Goodarzi AA, Petermann E, Concannon P, O'Driscoll M, Jeggo PA: **ATR-dependent phosphorylation and activation of ATM in response to UV treatment or replication fork stalling**. *EMBO J* 2006, **25**(24):5775-5782.
237. Rogakou EP, Boon C, Redon C, Bonner WM: **Megabase chromatin domains involved in DNA double-strand breaks in vivo**. *J Cell Biol* 1999, **146**(5):905-916.
238. Pilch DR, Sedelnikova OA, Redon C, Celeste A, Nussenzweig A, Bonner WM: **Characteristics of gamma-H2AX foci at DNA double-strand breaks sites**. *Biochem Cell Biol* 2003, **81**(3):123-129.
239. Savic V, Yin B, Maas NL, Bredemeyer AL, Carpenter AC, Helmink BA, Yang-Iott KS, Sleckman BP, Bassing CH: **Formation of dynamic gamma-H2AX domains along broken DNA strands is distinctly regulated by ATM and MDC1 and dependent upon H2AX densities in chromatin**. *Mol Cell* 2009, **34**(3):298-310.
240. Sedelnikova OA, Pilch DR, Redon C, Bonner WM: **Histone H2AX in DNA damage and repair**. *Cancer Biol Ther* 2003, **2**(3):233-235.
241. Fernandez-Capetillo O, Celeste A, Nussenzweig A: **Focusing on foci: H2AX and the recruitment of DNA-damage response factors**. *Cell Cycle* 2003, **2**(5):426-427.
242. Bonner WM, Redon CE, Dickey JS, Nakamura AJ, Sedelnikova OA, Solier S, Pommier Y: **GammaH2AX and cancer**. *Nat Rev Cancer* 2008, **8**(12):957-967.
243. Sedelnikova OA, Horikawa I, Zimonjic DB, Popescu NC, Bonner WM, Barrett JC: **Senescing human cells and ageing mice accumulate DNA lesions with unrepairable double-strand breaks**. *Nat Cell Biol* 2004, **6**(2):168-170.
244. Sedelnikova OA, Bonner WM: **GammaH2AX in cancer cells: a potential biomarker for cancer diagnostics, prediction and recurrence**. *Cell Cycle* 2006, **5**(24):2909-2913.
245. Celeste A, Petersen S, Romanienko PJ, Fernandez-Capetillo O, Chen HT, Sedelnikova OA, Reina-San-Martin B, Coppola V, Meffre E, Difilippantonio MJ *et al*: **Genomic instability in mice lacking histone H2AX**. *Science* 2002, **296**(5569):922-927.
246. Reinhardt HC, Schumacher B: **The p53 network: cellular and systemic DNA damage responses in aging and cancer**. *Trends Genet* 2012, **28**(3):128-136.
247. Vogelstein B, Kinzler KW: **Achilles' heel of cancer?** *Nature* 2001, **412**(6850):865-866.

248. Milner BJ, Allan LA, Eccles DM, Kitchener HC, Leonard RC, Kelly KF, Parkin DE, Haites NE: **p53 mutation is a common genetic event in ovarian carcinoma**. *Cancer Res* 1993, **53**(9):2128-2132.
249. Vousden KH, Lu X: **Live or let die: the cell's response to p53**. *Nat Rev Cancer* 2002, **2**(8):594-604.
250. Jacks T, Remington L, Williams BO, Schmitt EM, Halachmi S, Bronson RT, Weinberg RA: **Tumor spectrum analysis in p53-mutant mice**. *Curr Biol* 1994, **4**(1):1-7.
251. Malkin D, Li FP, Strong LC, Fraumeni JF, Nelson CE, Kim DH, Kassel J, Gryka MA, Bischoff FZ, Tainsky MA: **Germ line p53 mutations in a familial syndrome of breast cancer, sarcomas, and other neoplasms**. *Science* 1990, **250**(4985):1233-1238.
252. Kastan MB, Bartek J: **Cell-cycle checkpoints and cancer**. *Nature* 2004, **432**(7015):316-323.
253. Soussi T, Béroud C: **Assessing TP53 status in human tumours to evaluate clinical outcome**. *Nat Rev Cancer* 2001, **1**(3):233-240.
254. Olivier M, Eeles R, Hollstein M, Khan MA, Harris CC, Hainaut P: **The IARC TP53 database: new online mutation analysis and recommendations to users**. *Hum Mutat* 2002, **19**(6):607-614.
255. Hamroun D, Kato S, Ishioka C, Claustres M, Béroud C, Soussi T: **The UMD TP53 database and website: update and revisions**. *Hum Mutat* 2006, **27**(1):14-20.
256. Teodoro JG, Evans SK, Green MR: **Inhibition of tumor angiogenesis by p53: a new role for the guardian of the genome**. *J Mol Med (Berl)* 2007, **85**(11):1175-1186.
257. Pharoah PD, Day NE, Caldas C: **Somatic mutations in the p53 gene and prognosis in breast cancer: a meta-analysis**. *Br J Cancer* 1999, **80**(12):1968-1973.
258. Lacroix M, Toillon RA, Leclercq G: **p53 and breast cancer, an update**. *Endocr Relat Cancer* 2006, **13**(2):293-325.
259. Vogelstein B, Lane D, Levine AJ: **Surfing the p53 network**. *Nature* 2000, **408**(6810):307-310.
260. Yu J, Tiwari S, Steiner P, Zhang L: **Differential apoptotic response to the proteasome inhibitor Bortezomib [VELCADE, PS-341] in Bax-deficient and p21-deficient colon cancer cells**. *Cancer Biol Ther* 2003, **2**(6):694-699.
261. Yu J, Zhang L: **No PUMA, no death: implications for p53-dependent apoptosis**. *Cancer Cell* 2003, **4**(4):248-249.
262. Martins CP, Brown-Swigart L, Evan GI: **Modeling the therapeutic efficacy of p53 restoration in tumors**. *Cell* 2006, **127**(7):1323-1334.
263. Xue W, Zender L, Miething C, Dickins RA, Hernando E, Krizhanovsky V, Cordon-Cardo C, Lowe SW: **Senescence and tumour clearance is triggered by p53 restoration in murine liver carcinomas**. *Nature* 2007, **445**(7128):656-660.
264. Kaina B, Haas S, Kappes H: **A general role for c-Fos in cellular protection against DNA-damaging carcinogens and cytostatic drugs**. *Cancer Res* 1997, **57**(13):2721-2731.
265. Potapova O, Basu S, Mercola D, Holbrook NJ: **Protective role for c-Jun in the cellular response to DNA damage**. *J Biol Chem* 2001, **276**(30):28546-28553.
266. Shi Y, Venkataraman SL, Dodson GE, Mabb AM, LeBlanc S, Tibbetts RS: **Direct regulation of CREB transcriptional activity by ATM in response to genotoxic stress**. *Proc Natl Acad Sci U S A* 2004, **101**(16):5898-5903.
267. Janssens S, Tschopp J: **Signals from within: the DNA-damage-induced NF-kappaB response**. *Cell Death Differ* 2006, **13**(5):773-784.
268. Oeckinghaus A, Ghosh S: **The NF-kappaB family of transcription factors and its regulation**. *Cold Spring Harb Perspect Biol* 2009, **1**(4):a000034.
269. Eckert RL, Adhikary G, Young CA, Jans R, Crish JF, Xu W, Rorke EA: **AP1 transcription factors in epidermal differentiation and skin cancer**. *J Skin Cancer* 2013, **2013**:537028.
270. Efimova T, LaCelle P, Welter JF, Eckert RL: **Regulation of human involucrin promoter activity by a protein kinase C, Ras, MEKK1, MEK3, p38/RK, AP1 signal transduction pathway**. *J Biol Chem* 1998, **273**(38):24387-24395.

271. Efimova T, Broome AM, Eckert RL: **A regulatory role for p38 delta MAPK in keratinocyte differentiation. Evidence for p38 delta-ERK1/2 complex formation**. *J Biol Chem* 2003, **278**(36):34277-34285.
272. Eckert LB, Repasky GA, Ulkü AS, McFall A, Zhou H, Sartor CI, Der CJ: **Involvement of Ras activation in human breast cancer cell signaling, invasion, and anoikis**. *Cancer Res* 2004, **64**(13):4585-4592.
273. Eckert RL, Efimova T, Balasubramanian S, Crish JF, Bone F, Dashti S: **p38 Mitogen-activated protein kinases on the body surface--a function for p38 delta**. *J Invest Dermatol* 2003, **120**(5):823-828.
274. Mayr B, Montminy M: **Transcriptional regulation by the phosphorylation-dependent factor CREB**. *Nat Rev Mol Cell Biol* 2001, **2**(8):599-609.
275. Sandoval S, Pigazzi M, Sakamoto KM: **CREB: A Key Regulator of Normal and Neoplastic Hematopoiesis**. *Adv Hematol* 2009, **2009**:634292.
276. Cho EC, Mitton B, Sakamoto KM: **CREB and leukemogenesis**. *Crit Rev Oncog* 2011, **16**(1-2):37-46.
277. Chrivia JC, Kwok RP, Lamb N, Hagiwara M, Montminy MR, Goodman RH: **Phosphorylated CREB binds specifically to the nuclear protein CBP**. *Nature* 1993, **365**(6449):855-859.
278. Kundu TK, Palhan VB, Wang Z, An W, Cole PA, Roeder RG: **Activator-dependent transcription from chromatin in vitro involving targeted histone acetylation by p300**. *Mol Cell* 2000, **6**(3):551-561.
279. Shaywitz AJ, Greenberg ME: **CREB: a stimulus-induced transcription factor activated by a diverse array of extracellular signals**. *Annu Rev Biochem* 1999, **68**:821-861.
280. Conkright MD, Canettieri G, Screaton R, Guzman E, Miraglia L, Hogenesch JB, Montminy M: **TORCs: transducers of regulated CREB activity**. *Mol Cell* 2003, **12**(2):413-423.
281. Johannessen M, Delghandi MP, Moens U: **What turns CREB on?** *Cell Signal* 2004, **16**(11):1211-1227.
282. Hunter T: **The age of crosstalk: phosphorylation, ubiquitination, and beyond**. *Mol Cell* 2007, **28**(5):730-738.
283. Montminy MR, Bilezikjian LM: **Binding of a nuclear protein to the cyclic-AMP response element of the somatostatin gene**. *Nature* 1987, **328**(6126):175-178.
284. Yamamoto KK, Gonzalez GA, Biggs WH, Montminy MR: **Phosphorylation-induced binding and transcriptional efficacy of nuclear factor CREB**. *Nature* 1988, **334**(6182):494-498.
285. Böhm M, Moellmann G, Cheng E, Alvarez-Franco M, Wagner S, Sassone-Corsi P, Halaban R: **Identification of p90RSK as the probable CREB-Ser133 kinase in human melanocytes**. *Cell Growth Differ* 1995, **6**(3):291-302.
286. Xing J, Ginty DD, Greenberg ME: **Coupling of the RAS-MAPK pathway to gene activation by RSK2, a growth factor-regulated CREB kinase**. *Science* 1996, **273**(5277):959-963.
287. Kwon EM, Raines MA, Blenis J, Sakamoto KM: **Granulocyte-macrophage colony-stimulating factor stimulation results in phosphorylation of cAMP response element-binding protein through activation of pp90RSK**. *Blood* 2000, **95**(8):2552-2558.
288. Mayr BM, Canettieri G, Montminy MR: **Distinct effects of cAMP and mitogenic signals on CREB-binding protein recruitment impart specificity to target gene activation via CREB**. *Proc Natl Acad Sci U S A* 2001, **98**(19):10936-10941.
289. Impey S, McCorkle SR, Cha-Molstad H, Dwyer JM, Yochum GS, Boss JM, McWeeney S, Dunn JJ, Mandel G, Goodman RH: **Defining the CREB regulon: a genome-wide analysis of transcription factor regulatory regions**. *Cell* 2004, **119**(7):1041-1054.
290. Zhang X, Odom DT, Koo SH, Conkright MD, Canettieri G, Best J, Chen H, Jenner R, Herbolsheimer E, Jacobsen E *et al*: **Genome-wide analysis of cAMP-response element binding protein**

occupancy, phosphorylation, and target gene activation in human tissues. *Proc Natl Acad Sci U S A* 2005, **102**(12):4459-4464.
291. Siu YT, Jin DY: **CREB--a real culprit in oncogenesis**. *FEBS J* 2007, **274**(13):3224-3232.
292. Xiao X, Li BX, Mitton B, Ikeda A, Sakamoto KM: **Targeting CREB for cancer therapy: friend or foe**. *Curr Cancer Drug Targets* 2010, **10**(4):384-391.
293. Ahn S, Olive M, Aggarwal S, Krylov D, Ginty DD, Vinson C: **A dominant-negative inhibitor of CREB reveals that it is a general mediator of stimulus-dependent transcription of c-fos**. *Mol Cell Biol* 1998, **18**(2):967-977.
294. Esparza SD, Chang J, Shankar DB, Zhang B, Nelson SF, Sakamoto KM: **CREB regulates Meis1 expression in normal and malignant hematopoietic cells**. *Leukemia* 2008, **22**(3):665-667.
295. Wang Z, Iwasaki M, Ficara F, Lin C, Matheny C, Wong SH, Smith KS, Cleary ML: **GSK-3 promotes conditional association of CREB and its coactivators with MEIS1 to facilitate HOX-mediated transcription and oncogenesis**. *Cancer Cell* 2010, **17**(6):597-608.
296. Altarejos JY, Montminy M: **CREB and the CRTC co-activators: sensors for hormonal and metabolic signals**. *Nat Rev Mol Cell Biol* 2011, **12**(3):141-151.
297. Wen AY, Sakamoto KM, Miller LS: **The role of the transcription factor CREB in immune function**. *J Immunol* 2010, **185**(11):6413-6419.
298. Desdouets C, Matesic G, Molina CA, Foulkes NS, Sassone-Corsi P, Brechot C, Sobczak-Thepot J: **Cell cycle regulation of cyclin A gene expression by the cyclic AMP-responsive transcription factors CREB and CREM**. *Mol Cell Biol* 1995, **15**(6):3301-3309.
299. White PC, Shore AM, Clement M, McLaren J, Soeiro I, Lam EW, Brennan P: **Regulation of cyclin D2 and the cyclin D2 promoter by protein kinase A and CREB in lymphocytes**. *Oncogene* 2006, **25**(15):2170-2180.
300. Sakamoto KM, Fraser JK, Lee HJ, Lehman E, Gasson JC: **Granulocyte-macrophage colony-stimulating factor and interleukin-3 signaling pathways converge on the CREB-binding site in the human egr-1 promoter**. *Mol Cell Biol* 1994, **14**(9):5975-5985.
301. Shankar DB, Cheng JC, Kinjo K, Federman N, Moore TB, Gill A, Rao NP, Landaw EM, Sakamoto KM: **The role of CREB as a proto-oncogene in hematopoiesis and in acute myeloid leukemia**. *Cancer Cell* 2005, **7**(4):351-362.
302. Bonni A, Ginty DD, Dudek H, Greenberg ME: **Serine 133-phosphorylated CREB induces transcription via a cooperative mechanism that may confer specificity to neurotrophin signals**. *Mol Cell Neurosci* 1995, **6**(2):168-183.
303. Riccio A, Ahn S, Davenport CM, Blendy JA, Ginty DD: **Mediation by a CREB family transcription factor of NGF-dependent survival of sympathetic neurons**. *Science* 1999, **286**(5448):2358-2361.
304. Nabholtz JM, Gligorov J: **The emerging role of aromatase inhibitors in the adjuvant management of breast cancer**. *Rev Recent Clin Trials* 2006, **1**(3):237-249.
305. Castro-Rivera E, Samudio I, Safe S: **Estrogen regulation of cyclin D1 gene expression in ZR-75 breast cancer cells involves multiple enhancer elements**. *J Biol Chem* 2001, **276**(33):30853-30861.
306. Dong L, Wang W, Wang F, Stoner M, Reed JC, Harigai M, Samudio I, Kladde MP, Vyhlidal C, Safe S: **Mechanisms of transcriptional activation of bcl-2 gene expression by 17beta-estradiol in breast cancer cells**. *J Biol Chem* 1999, **274**(45):32099-32107.
307. Rovera G, Santoli D, Damsky C: **Human promyelocytic leukemia cells in culture differentiate into macrophage-like cells when treated with a phorbol diester**. *Proc Natl Acad Sci U S A* 1979, **76**(6):2779-2783.
308. Tsuchiya S, Kobayashi Y, Goto Y, Okumura H, Nakae S, Konno T, Tada K: **Induction of maturation in cultured human monocytic leukemia cells by a phorbol diester**. *Cancer Res* 1982, **42**(4):1530-1536.

309. PUCK TT, MARCUS PI, CIECIURA SJ: **Clonal growth of mammalian cells in vitro; growth characteristics of colonies from single HeLa cells with and without a feeder layer**. *J Exp Med* 1956, **103**(2):273-283.
310. Zhu H, Bannenberg GL, Moldéus P, Shertzer HG: **Oxidation pathways for the intracellular probe 2',7'-dichlorofluorescein**. *Arch Toxicol* 1994, **68**(9):582-587.
311. Kojima H, Nakatsubo N, Kikuchi K, Urano Y, Higuchi T, Tanaka J, Kudo Y, Nagano T: **Direct evidence of NO production in rat hippocampus and cortex using a new fluorescent indicator: DAF-2 DA**. *Neuroreport* 1998, **9**(15):3345-3348.
312. Smiley ST, Reers M, Mottola-Hartshorn C, Lin M, Chen A, Smith TW, Steele GD, Chen LB: **Intracellular heterogeneity in mitochondrial membrane potentials revealed by a J-aggregate-forming lipophilic cation JC-1**. *Proc Natl Acad Sci U S A* 1991, **88**(9):3671-3675.
313. Towbin H, Staehelin T, Gordon J: **Electrophoretic transfer of proteins from polyacrylamide gels to nitrocellulose sheets: procedure and some applications**. *Proc Natl Acad Sci U S A* 1979, **76**(9):4350-4354.
314. Burnette WN: **"Western blotting": electrophoretic transfer of proteins from sodium dodecyl sulfate--polyacrylamide gels to unmodified nitrocellulose and radiographic detection with antibody and radioiodinated protein A**. *Anal Biochem* 1981, **112**(2):195-203.
315. Bernstein E, Caudy AA, Hammond SM, Hannon GJ: **Role for a bidentate ribonuclease in the initiation step of RNA interference**. *Nature* 2001, **409**(6818):363-366.
316. Hammond SM, Bernstein E, Beach D, Hannon GJ: **An RNA-directed nuclease mediates post-transcriptional gene silencing in Drosophila cells**. *Nature* 2000, **404**(6775):293-296.
317. BOYDEN S: **The chemotactic effect of mixtures of antibody and antigen on polymorphonuclear leucocytes**. *J Exp Med* 1962, **115**:453-466.
318. Muccioli GG, Xu C, Odah E, Cudaback E, Cisneros JA, Lambert DM, López Rodríguez ML, Bajjalieh S, Stella N: **Identification of a novel endocannabinoid-hydrolyzing enzyme expressed by microglial cells**. *J Neurosci* 2007, **27**(11):2883-2889.
319. Gomes LR, Terra LF, Wailemann RA, Labriola L, Sogayar MC: **TGF-β1 modulates the homeostasis between MMPs and MMP inhibitors through p38 MAPK and ERK1/2 in highly invasive breast cancer cells**. *BMC Cancer* 2012, **12**:26.
320. Verhoog NJ, Du Toit A, Avenant C, Hapgood JP: **Glucocorticoid-independent repression of tumor necrosis factor (TNF) alpha-stimulated interleukin (IL)-6 expression by the glucocorticoid receptor: a potential mechanism for protection against an excessive inflammatory response**. *J Biol Chem* 2011, **286**(22):19297-19310.
321. Ariazi EA, Clark GM, Mertz JE: **Estrogen-related receptor alpha and estrogen-related receptor gamma associate with unfavorable and favorable biomarkers, respectively, in human breast cancer**. *Cancer Res* 2002, **62**(22):6510-6518.
322. Li W, Yan XT, Sun YN, Ngan TT, Shim SH, Kim YH: **Anti-Inflammatory and PPAR Transactivational Effects of Oleanane-Type Triterpenoid Saponins from the Roots of Pulsatilla koreana**. *Biomol Ther (Seoul)* 2014, **22**(4):334-340.
323. Tokunou M, Niki T, Saitoh Y, Imamura H, Sakamoto M, Hirohashi S: **Altered expression of the ERM proteins in lung adenocarcinoma**. *Lab Invest* 2000, **80**(11):1643-1650.
324. Engvall E, Perlmann P: **Enzyme-linked immunosorbent assay (ELISA). Quantitative assay of immunoglobulin G**. *Immunochemistry* 1971, **8**(9):871-874.
325. Laemmli UK: **Cleavage of structural proteins during the assembly of the head of bacteriophage T4**. *Nature* 1970, **227**(5259):680-685.
326. Merril CR, Dunau ML, Goldman D: **A rapid sensitive silver stain for polypeptides in polyacrylamide gels**. *Anal Biochem* 1981, **110**(1):201-207.

327. O'Farrell PH: **High resolution two-dimensional electrophoresis of proteins**. *J Biol Chem* 1975, **250**(10):4007-4021.
328. Granelli-Piperno A, Reich E: **A study of proteases and protease-inhibitor complexes in biological fluids**. *J Exp Med* 1978, **148**(1):223-234.
329. Théry C, Amigorena S, Raposo G, Clayton A: **Isolation and characterization of exosomes from cell culture supernatants and biological fluids**. *Curr Protoc Cell Biol* 2006, **Chapter 3**:Unit 3.22.
330. Remmele W, Stegner HE: **[Recommendation for uniform definition of an immunoreactive score (IRS) for immunohistochemical estrogen receptor detection (ER-ICA) in breast cancer tissue]**. *Pathologe* 1987, **8**(3):138-140.
331. Leek RD, Lewis CE, Whitehouse R, Greenall M, Clarke J, Harris AL: **Association of macrophage infiltration with angiogenesis and prognosis in invasive breast carcinoma**. *Cancer Res* 1996, **56**(20):4625-4629.
332. Chrest FJ, Buchholz MA, Kim YH, Kwon TK, Nordin AA: **Identification and quantitation of apoptotic cells following anti-CD3 activation of murine G0 T cells**. *Cytometry* 1993, **14**(8):883-890.
333. Fan CF, Mao XY, Wang EH: **Elevated p-CREB-2 (ser 245) expression is potentially associated with carcinogenesis and development of breast carcinoma**. *Mol Med Rep* 2012, **5**(2):357-362.
334. Ly JD, Grubb DR, Lawen A: **The mitochondrial membrane potential (deltapsi(m)) in apoptosis; an update**. *Apoptosis* 2003, **8**(2):115-128.
335. Wakefield LM, Roberts AB: **TGF-beta signaling: positive and negative effects on tumorigenesis**. *Curr Opin Genet Dev* 2002, **12**(1):22-29.
336. Roberts AB, Wakefield LM: **The two faces of transforming growth factor beta in carcinogenesis**. *Proc Natl Acad Sci U S A* 2003, **100**(15):8621-8623.
337. Rhyu DY, Yang Y, Ha H, Lee GT, Song JS, Uh ST, Lee HB: **Role of reactive oxygen species in TGF-beta1-induced mitogen-activated protein kinase activation and epithelial-mesenchymal transition in renal tubular epithelial cells**. *J Am Soc Nephrol* 2005, **16**(3):667-675.
338. Burma S, Chen BP, Murphy M, Kurimasa A, Chen DJ: **ATM phosphorylates histone H2AX in response to DNA double-strand breaks**. *J Biol Chem* 2001, **276**(45):42462-42467.
339. Chiba N, Comaills V, Shiotani B, Takahashi F, Shimada T, Tajima K, Winokur D, Hayashida T, Willers H, Brachtel E *et al*: **Homeobox B9 induces epithelial-to-mesenchymal transition-associated radioresistance by accelerating DNA damage responses**. *Proc Natl Acad Sci U S A* 2012, **109**(8):2760-2765.
340. Vuoriluoto K, Haugen H, Kiviluoto S, Mpindi JP, Nevo J, Gjerdrum C, Tiron C, Lorens JB, Ivaska J: **Vimentin regulates EMT induction by Slug and oncogenic H-Ras and migration by governing Axl expression in breast cancer**. *Oncogene* 2011, **30**(12):1436-1448.
341. Raspollini MR, Amunni G, Villanucci A, Boddi V, Baroni G, Taddei A, Taddei GL: **Expression of inducible nitric oxide synthase and cyclooxygenase-2 in ovarian cancer: correlation with clinical outcome**. *Gynecol Oncol* 2004, **92**(3):806-812.
342. Aaltoma SH, Lipponen PK, Kosma VM: **Inducible nitric oxide synthase (iNOS) expression and its prognostic value in prostate cancer**. *Anticancer Res* 2001, **21**(4B):3101-3106.
343. Song ZJ, Gong P, Wu YE: **Relationship between the expression of iNOS,VEGF,tumor angiogenesis and gastric cancer**. *World J Gastroenterol* 2002, **8**(4):591-595.
344. Cianchi F, Cortesini C, Fantappiè O, Messerini L, Schiavone N, Vannacci A, Nistri S, Sardi I, Baroni G, Marzocca C *et al*: **Inducible nitric oxide synthase expression in human colorectal cancer: correlation with tumor angiogenesis**. *Am J Pathol* 2003, **162**(3):793-801.
345. Gallo O, Masini E, Morbidelli L, Franchi A, Fini-Storchi I, Vergari WA, Ziche M: **Role of nitric oxide in angiogenesis and tumor progression in head and neck cancer**. *J Natl Cancer Inst* 1998, **90**(8):587-596.

346. Weninger W, Rendl M, Pammer J, Mildner M, Tschugguel W, Schneeberger C, Stürzl M, Tschachler E: **Nitric oxide synthases in Kaposi's sarcoma are expressed predominantly by vessels and tissue macrophages**. *Lab Invest* 1998, **78**(8):949-955.
347. Ropponen KM, Kellokoski JK, Lipponen PK, Eskelinen MJ, Alanne L, Alhava EM, Kosma VM: **Expression of inducible nitric oxide synthase in colorectal cancer and its association with prognosis**. *Scand J Gastroenterol* 2000, **35**(11):1204-1211.
348. Curtis C, Shah SP, Chin SF, Turashvili G, Rueda OM, Dunning MJ, Speed D, Lynch AG, Samarajiwa S, Yuan Y *et al*: **The genomic and transcriptomic architecture of 2,000 breast tumours reveals novel subgroups**. *Nature* 2012, **486**(7403):346-352.
349. Fackler MJ, Umbricht CB, Williams D, Argani P, Cruz LA, Merino VF, Teo WW, Zhang Z, Huang P, Visvananthan K *et al*: **Genome-wide methylation analysis identifies genes specific to breast cancer hormone receptor status and risk of recurrence**. *Cancer Res* 2011, **71**(19):6195-6207.
350. Ma XJ, Wang Z, Ryan PD, Isakoff SJ, Barmettler A, Fuller A, Muir B, Mohapatra G, Salunga R, Tuggle JT *et al*: **A two-gene expression ratio predicts clinical outcome in breast cancer patients treated with tamoxifen**. *Cancer Cell* 2004, **5**(6):607-616.
351. Levine AJ, Momand J, Finlay CA: **The p53 tumour suppressor gene**. *Nature* 1991, **351**(6326):453-456.
352. Allred DC, Clark GM, Elledge R, Fuqua SA, Brown RW, Chamness GC, Osborne CK, McGuire WL: **Association of p53 protein expression with tumor cell proliferation rate and clinical outcome in node-negative breast cancer**. *J Natl Cancer Inst* 1993, **85**(3):200-206.
353. Rohan TE, Li SQ, Hartwick R, Kandel RA: **p53 Alterations and protein accumulation in benign breast tissue and breast cancer risk: a cohort study**. *Cancer Epidemiol Biomarkers Prev* 2006, **15**(7):1316-1323.
354. Radvanyi L, Singh-Sandhu D, Gallichan S, Lovitt C, Pedyczak A, Mallo G, Gish K, Kwok K, Hanna W, Zubovits J *et al*: **The gene associated with trichorhinophalangeal syndrome in humans is overexpressed in breast cancer**. *Proc Natl Acad Sci U S A* 2005, **102**(31):11005-11010.
355. Desmedt C, Piette F, Loi S, Wang Y, Lallemand F, Haibe-Kains B, Viale G, Delorenzi M, Zhang Y, d'Assignies MS *et al*: **Strong time dependence of the 76-gene prognostic signature for node-negative breast cancer patients in the TRANSBIG multicenter independent validation series**. *Clin Cancer Res* 2007, **13**(11):3207-3214.
356. Sofi M, Young MJ, Papamakarios T, Simpson ER, Clyne CD: **Role of CRE-binding protein (CREB) in aromatase expression in breast adipose**. *Breast Cancer Res Treat* 2003, **79**(3):399-407.
357. Peng B, Hu S, Jun Q, Luo D, Zhang X, Zhao H, Li D: **MicroRNA-200b targets CREB1 and suppresses cell growth in human malignant glioma**. *Mol Cell Biochem* 2013, **379**(1-2):51-58.
358. Sabban EL, Liu X, Serova L, Gueorguiev V, Kvetnansky R: **Stress triggered changes in gene expression in adrenal medulla: transcriptional responses to acute and chronic stress**. *Cell Mol Neurobiol* 2006, **26**(4-6):845-856.
359. Wagatsuma A, Azami S, Sakura M, Hatakeyama D, Aonuma H, Ito E: **De Novo synthesis of CREB in a presynaptic neuron is required for synaptic enhancement involved in memory consolidation**. *J Neurosci Res* 2006, **84**(5):954-960.
360. Luciani P, Buci L, Conforti B, Tonacchera M, Agretti P, Elisei R, Vivaldi A, Cioppi F, Biliotti G, Manca G *et al*: **Expression of cAMP response element-binding protein and sodium iodide symporter in benign non-functioning and malignant thyroid tumours**. *Eur J Endocrinol* 2003, **148**(5):579-586.
361. Daniel P, Filiz G, Brown DV, Hollande F, Gonzales M, D'Abaco G, Papalexis N, Phillips WA, Malaterre J, Ramsay RG *et al*: **Selective CREB-dependent cyclin expression mediated by the PI3K and MAPK pathways supports glioma cell proliferation**. *Oncogenesis* 2014, **3**:e108.

362. Liu Y, Hu Z: **Identification of collaborative driver pathways in breast cancer**. *BMC Genomics* 2014, **15**:605.
363. Liotta LA, Kohn EC: **The microenvironment of the tumour-host interface**. *Nature* 2001, **411**(6835):375-379.
364. Wiseman BS, Werb Z: **Stromal effects on mammary gland development and breast cancer**. *Science* 2002, **296**(5570):1046-1049.
365. Condeelis J, Pollard JW: **Macrophages: obligate partners for tumor cell migration, invasion, and metastasis**. *Cell* 2006, **124**(2):263-266.
366. Luo Y, Zhou H, Krueger J, Kaplan C, Lee SH, Dolman C, Markowitz D, Wu W, Liu C, Reisfeld RA *et al*: **Targeting tumor-associated macrophages as a novel strategy against breast cancer**. *J Clin Invest* 2006, **116**(8):2132-2141.
367. Pupa SM, Ménard S, Forti S, Tagliabue E: **New insights into the role of extracellular matrix during tumor onset and progression**. *J Cell Physiol* 2002, **192**(3):259-267.
368. Jänicke RU: **MCF-7 breast carcinoma cells do not express caspase-3**. *Breast Cancer Res Treat* 2009, **117**(1):219-221.
369. DePinho RA: **The age of cancer**. *Nature* 2000, **408**(6809):248-254.
370. Kuilman T, Michaloglou C, Vredeveld LC, Douma S, van Doorn R, Desmet CJ, Aarden LA, Mooi WJ, Peeper DS: **Oncogene-induced senescence relayed by an interleukin-dependent inflammatory network**. *Cell* 2008, **133**(6):1019-1031.
371. Coppé JP, Patil CK, Rodier F, Sun Y, Muñoz DP, Goldstein J, Nelson PS, Desprez PY, Campisi J: **Senescence-associated secretory phenotypes reveal cell-nonautonomous functions of oncogenic RAS and the p53 tumor suppressor**. *PLoS Biol* 2008, **6**(12):2853-2868.
372. Lu D, Huang J, Basu A: **Protein kinase Cepsilon activates protein kinase B/Akt via DNA-PK to protect against tumor necrosis factor-alpha-induced cell death**. *J Biol Chem* 2006, **281**(32):22799-22807.
373. Chinnaiyan AM, Dixit VM: **Portrait of an executioner: the molecular mechanism of FAS/APO-1-induced apoptosis**. *Semin Immunol* 1997, **9**(1):69-76.
374. Cai Z, Capoulade C, Moyret-Lalle C, Amor-Gueret M, Feunteun J, Larsen AK, Paillerets BB, Chouaib S: **Resistance of MCF7 human breast carcinoma cells to TNF-induced cell death is associated with loss of p53 function**. *Oncogene* 1997, **15**(23):2817-2826.
375. Niu Z, Li X, Hu B, Li R, Wang L, Wu L, Wang X: **Small interfering RNA targeted to secretory clusterin blocks tumor growth, motility, and invasion in breast cancer**. *Acta Biochim Biophys Sin (Shanghai)* 2012, **44**(12):991-998.
376. Wang Y, Wang X, Zhao H, Liang B, Du Q: **Clusterin confers resistance to TNF-alpha-induced apoptosis in breast cancer cells through NF-kappaB activation and Bcl-2 overexpression**. *J Chemother* 2012, **24**(6):348-357.
377. Reed JC: **Regulation of apoptosis by bcl-2 family proteins and its role in cancer and chemoresistance**. *Curr Opin Oncol* 1995, **7**(6):541-546.
378. Williams GT, Smith CA: **Molecular regulation of apoptosis: genetic controls on cell death**. *Cell* 1993, **74**(5):777-779.
379. Lin Y, Devin A, Rodriguez Y, Liu ZG: **Cleavage of the death domain kinase RIP by caspase-8 prompts TNF-induced apoptosis**. *Genes Dev* 1999, **13**(19):2514-2526.
380. Yang Y, Zhao S, Song J: **Caspase-dependent apoptosis and -independent poly(ADP-ribose) polymerase cleavage induced by transforming growth factor beta1**. *Int J Biochem Cell Biol* 2004, **36**(2):223-234.
381. Sullivan DE, Ferris M, Pociask D, Brody AR: **Tumor necrosis factor-alpha induces transforming growth factor-beta1 expression in lung fibroblasts through the extracellular signal-regulated kinase pathway**. *Am J Respir Cell Mol Biol* 2005, **32**(4):342-349.

382. Suarez-Cuervo C, Harris KW, Kallman L, Väänänen HK, Selander KS: **Tumor necrosis factor-alpha induces interleukin-6 production via extracellular-regulated kinase 1 activation in breast cancer cells**. *Breast Cancer Res Treat* 2003, **80**(1):71-78.
383. Zhao RZ, Chen X, Yao Q, Chen C: **TNF-alpha induces interleukin-8 and endothelin-1 expression in human endothelial cells with different redox pathways**. *Biochem Biophys Res Commun* 2005, **327**(4):985-992.
384. Turner NA, Mughal RS, Warburton P, O'Regan DJ, Ball SG, Porter KE: **Mechanism of TNFalpha-induced IL-1alpha, IL-1beta and IL-6 expression in human cardiac fibroblasts: effects of statins and thiazolidinediones**. *Cardiovasc Res* 2007, **76**(1):81-90.
385. Yang Y, Pan X, Lei W, Wang J, Song J: **Transforming growth factor-beta1 induces epithelial-to-mesenchymal transition and apoptosis via a cell cycle-dependent mechanism**. *Oncogene* 2006, **25**(55):7235-7244.
386. Bates RC, Mercurio AM: **Tumor necrosis factor-alpha stimulates the epithelial-to-mesenchymal transition of human colonic organoids**. *Mol Biol Cell* 2003, **14**(5):1790-1800.
387. Tian M, Neil JR, Schiemann WP: **Transforming growth factor-β and the hallmarks of cancer**. *Cell Signal* 2011, **23**(6):951-962.
388. Tian M, Schiemann WP: **The TGF-beta paradox in human cancer: an update**. *Future Oncol* 2009, **5**(2):259-271.
389. Yang Y, Pan X, Lei W, Wang J, Shi J, Li F, Song J: **Regulation of transforming growth factor-beta 1-induced apoptosis and epithelial-to-mesenchymal transition by protein kinase A and signal transducers and activators of transcription 3**. *Cancer Res* 2006, **66**(17):8617-8624.
390. Taube JH, Herschkowitz JI, Komurov K, Zhou AY, Gupta S, Yang J, Hartwell K, Onder TT, Gupta PB, Evans KW *et al*: **Core epithelial-to-mesenchymal transition interactome gene-expression signature is associated with claudin-low and metaplastic breast cancer subtypes**. *Proc Natl Acad Sci U S A* 2010, **107**(35):15449-15454.
391. Shipitsin M, Campbell LL, Argani P, Weremowicz S, Bloushtain-Qimron N, Yao J, Nikolskaya T, Serebryiskaya T, Beroukhim R, Hu M *et al*: **Molecular definition of breast tumor heterogeneity**. *Cancer Cell* 2007, **11**(3):259-273.
392. Taylor MA, Parvani JG, Schiemann WP: **The pathophysiology of epithelial-mesenchymal transition induced by transforming growth factor-beta in normal and malignant mammary epithelial cells**. *J Mammary Gland Biol Neoplasia* 2010, **15**(2):169-190.
393. Shi Y, Massagué J: **Mechanisms of TGF-beta signaling from cell membrane to the nucleus**. *Cell* 2003, **113**(6):685-700.
394. Derynck R, Zhang YE: **Smad-dependent and Smad-independent pathways in TGF-beta family signalling**. *Nature* 2003, **425**(6958):577-584.
395. Liu T, Feng XH: **Regulation of TGF-beta signalling by protein phosphatases**. *Biochem J* 2010, **430**(2):191-198.
396. Tian YC, Chen YC, Chang CT, Hung CC, Wu MS, Phillips A, Yang CW: **Epidermal growth factor and transforming growth factor-beta1 enhance HK-2 cell migration through a synergistic increase of matrix metalloproteinase and sustained activation of ERK signaling pathway**. *Exp Cell Res* 2007, **313**(11):2367-2377.
397. Indo HP, Davidson M, Yen HC, Suenaga S, Tomita K, Nishii T, Higuchi M, Koga Y, Ozawa T, Majima HJ: **Evidence of ROS generation by mitochondria in cells with impaired electron transport chain and mitochondrial DNA damage**. *Mitochondrion* 2007, **7**(1-2):106-118.
398. Edderkaoui M, Hong P, Vaquero EC, Lee JK, Fischer L, Friess H, Buchler MW, Lerch MM, Pandol SJ, Gukovskaya AS: **Extracellular matrix stimulates reactive oxygen species production and increases pancreatic cancer cell survival through 5-lipoxygenase and NADPH oxidase**. *Am J Physiol Gastrointest Liver Physiol* 2005, **289**(6):G1137-1147.

399. Wiseman H, Halliwell B: **Damage to DNA by reactive oxygen and nitrogen species: role in inflammatory disease and progression to cancer**. *Biochem J* 1996, **313 (Pt 1)**:17-29.
400. McCormack D, Schneider J, McDonald D, McFadden D: **The antiproliferative effects of pterostilbene on breast cancer in vitro are via inhibition of constitutive and leptin-induced Janus kinase/signal transducer and activator of transcription activation**. *Am J Surg* 2011, **202**(5):541-544.
401. Pan X, Wang X, Lei W, Min L, Yang Y, Song J: **Nitric oxide suppresses transforming growth factor-beta1-induced epithelial-to-mesenchymal transition and apoptosis in mouse hepatocytes**. *Hepatology* 2009, **50**(5):1577-1587.
402. Guo Z, Kozlov S, Lavin MF, Person MD, Paull TT: **ATM activation by oxidative stress**. *Science* 2010, **330**(6003):517-521.
403. Durocher D, Jackson SP: **DNA-PK, ATM and ATR as sensors of DNA damage: variations on a theme?** *Curr Opin Cell Biol* 2001, **13**(2):225-231.
404. Löbrich M, Shibata A, Beucher A, Fisher A, Ensminger M, Goodarzi AA, Barton O, Jeggo PA: **gammaH2AX foci analysis for monitoring DNA double-strand break repair: strengths, limitations and optimization**. *Cell Cycle* 2010, **9**(4):662-669.
405. Thompson LH: **Recognition, signaling, and repair of DNA double-strand breaks produced by ionizing radiation in mammalian cells: the molecular choreography**. *Mutat Res* 2012, **751**(2):158-246.
406. Polo SE, Jackson SP: **Dynamics of DNA damage response proteins at DNA breaks: a focus on protein modifications**. *Genes Dev* 2011, **25**(5):409-433.
407. Houston MA, Augenlicht LH, Heerdt BG: **Stable differences in intrinsic mitochondrial membrane potential of tumor cell subpopulations reflect phenotypic heterogeneity**. *Int J Cell Biol* 2011, **2011**:978583.
408. Kluza J, Marchetti P, Gallego MA, Lancel S, Fournier C, Loyens A, Beauvillain JC, Bailly C: **Mitochondrial proliferation during apoptosis induced by anticancer agents: effects of doxorubicin and mitoxantrone on cancer and cardiac cells**. *Oncogene* 2004, **23**(42):7018-7030.
409. De Cesare D, Fimia GM, Sassone-Corsi P: **Signaling routes to CREM and CREB: plasticity in transcriptional activation**. *Trends Biochem Sci* 1999, **24**(7):281-285.
410. Shankar DB, Sakamoto KM: **The role of cyclic-AMP binding protein (CREB) in leukemia cell proliferation and acute leukemias**. *Leuk Lymphoma* 2004, **45**(2):265-270.
411. Conkright MD, Montminy M: **CREB: the unindicted cancer co-conspirator**. *Trends Cell Biol* 2005, **15**(9):457-459.
412. Montminy M: **Transcriptional regulation by cyclic AMP**. *Annu Rev Biochem* 1997, **66**:807-822.
413. Eckner R, Ewen ME, Newsome D, Gerdes M, DeCaprio JA, Lawrence JB, Livingston DM: **Molecular cloning and functional analysis of the adenovirus E1A-associated 300-kD protein (p300) reveals a protein with properties of a transcriptional adaptor**. *Genes Dev* 1994, **8**(8):869-884.
414. Shanware NP, Trinh AT, Williams LM, Tibbetts RS: **Coregulated ataxia telangiectasia-mutated and casein kinase sites modulate cAMP-response element-binding protein-coactivator interactions in response to DNA damage**. *J Biol Chem* 2007, **282**(9):6283-6291.
415. de Graauw M, van Miltenburg MH, Schmidt MK, Pont C, Lalai R, Kartopawiro J, Pardali E, Le Dévédec SE, Smit VT, van der Wal A *et al*: **Annexin A1 regulates TGF-beta signaling and promotes metastasis formation of basal-like breast cancer cells**. *Proc Natl Acad Sci U S A* 2010, **107**(14):6340-6345.
416. Sheng L, Zhou Y, Chen Z, Ren D, Cho KW, Jiang L, Shen H, Sasaki Y, Rui L: **NF-κB–inducing kinase (NIK) promotes hyperglycemia and glucose intolerance in obesity by augmenting glucagon action**. *Nat Med* 2012, **18**(6):943-949.

417. Son J, Lee JH, Kim HN, Ha H, Lee ZH: **cAMP-response-element-binding protein positively regulates breast cancer metastasis and subsequent bone destruction**. *Biochem Biophys Res Commun* 2010, **398**(2):309-314.
418. Lindley LE, Briegel KJ: **Molecular characterization of TGFbeta-induced epithelial-mesenchymal transition in normal finite lifespan human mammary epithelial cells**. *Biochem Biophys Res Commun* 2010, **399**(4):659-664.
419. Thiery JP, Acloque H, Huang RY, Nieto MA: **Epithelial-mesenchymal transitions in development and disease**. *Cell* 2009, **139**(5):871-890.
420. Polyak K, Weinberg RA: **Transitions between epithelial and mesenchymal states: acquisition of malignant and stem cell traits**. *Nat Rev Cancer* 2009, **9**(4):265-273.
421. Guarino M: **Epithelial-mesenchymal transition and tumour invasion**. *Int J Biochem Cell Biol* 2007, **39**(12):2153-2160.
422. Micalizzi DS, Farabaugh SM, Ford HL: **Epithelial-mesenchymal transition in cancer: parallels between normal development and tumor progression**. *J Mammary Gland Biol Neoplasia* 2010, **15**(2):117-134.
423. Vernon AE, Bakewell SJ, Chodosh LA: **Deciphering the molecular basis of breast cancer metastasis with mouse models**. *Rev Endocr Metab Disord* 2007, **8**(3):199-213.
424. Huang CM, Wang CC, Barnes S, Elmets CA: **In vivo detection of secreted proteins from wounded skin using capillary ultrafiltration probes and mass spectrometric proteomics**. *Proteomics* 2006, **6**(21):5805-5814.
425. Paltridge JL, Belle L, Khew-Goodall Y: **The secretome in cancer progression**. *Biochim Biophys Acta* 2013, **1834**(11):2233-2241.
426. Svensson KJ, Belting M: **Role of extracellular membrane vesicles in intercellular communication of the tumour microenvironment**. *Biochem Soc Trans* 2013, **41**(1):273-276.
427. György B, Szabó TG, Pásztói M, Pál Z, Misják P, Aradi B, László V, Pállinger E, Pap E, Kittel A *et al*: **Membrane vesicles, current state-of-the-art: emerging role of extracellular vesicles**. *Cell Mol Life Sci* 2011, **68**(16):2667-2688.
428. Johnstone RM, Adam M, Hammond JR, Orr L, Turbide C: **Vesicle formation during reticulocyte maturation. Association of plasma membrane activities with released vesicles (exosomes)**. *J Biol Chem* 1987, **262**(19):9412-9420.
429. Bang C, Thum T: **Exosomes: new players in cell-cell communication**. *Int J Biochem Cell Biol* 2012, **44**(11):2060-2064.
430. Page-McCaw A, Ewald AJ, Werb Z: **Matrix metalloproteinases and the regulation of tissue remodelling**. *Nat Rev Mol Cell Biol* 2007, **8**(3):221-233.
431. Li HC, Cao DC, Liu Y, Hou YF, Wu J, Lu JS, Di GH, Liu G, Li FM, Ou ZL *et al*: **Prognostic value of matrix metalloproteinases (MMP-2 and MMP-9) in patients with lymph node-negative breast carcinoma**. *Breast Cancer Res Treat* 2004, **88**(1):75-85.
432. Talvensaari-Mattila A, Pääkkö P, Höyhtyä M, Blanco-Sequeiros G, Turpeenniemi-Hujanen T: **Matrix metalloproteinase-2 immunoreactive protein: a marker of aggressiveness in breast carcinoma**. *Cancer* 1998, **83**(6):1153-1162.
433. Balduyck M, Zerimech F, Gouyer V, Lemaire R, Hemon B, Grard G, Thiebaut C, Lemaire V, Dacquembronne E, Duhem T *et al*: **Specific expression of matrix metalloproteinases 1, 3, 9 and 13 associated with invasiveness of breast cancer cells in vitro**. *Clin Exp Metastasis* 2000, **18**(2):171-178.
434. Francescone RA, Scully S, Faibish M, Taylor SL, Oh D, Moral L, Yan W, Bentley B, Shao R: **Role of YKL-40 in the angiogenesis, radioresistance, and progression of glioblastoma**. *J Biol Chem* 2011, **286**(17):15332-15343.

435. Johansen JS, Christensen IJ, Riisbro R, Greenall M, Han C, Price PA, Smith K, Brünner N, Harris AL: **High serum YKL-40 levels in patients with primary breast cancer is related to short recurrence free survival**. *Breast Cancer Res Treat* 2003, **80**(1):15-21.
436. Durand MK, Bødker JS, Christensen A, Dupont DM, Hansen M, Jensen JK, Kjelgaard S, Mathiasen L, Pedersen KE, Skeldal S *et al*: **Plasminogen activator inhibitor-I and tumour growth, invasion, and metastasis**. *Thromb Haemost* 2004, **91**(3):438-449.
437. Dellas C, Loskutoff DJ: **Historical analysis of PAI-1 from its discovery to its potential role in cell motility and disease**. *Thromb Haemost* 2005, **93**(4):631-640.
438. Jänicke F, Prechtl A, Thomssen C, Harbeck N, Meisner C, Untch M, Sweep CG, Selbmann HK, Graeff H, Schmitt M *et al*: **Randomized adjuvant chemotherapy trial in high-risk, lymph node-negative breast cancer patients identified by urokinase-type plasminogen activator and plasminogen activator inhibitor type 1**. *J Natl Cancer Inst* 2001, **93**(12):913-920.
439. Lek A, Evesson FJ, Sutton RB, North KN, Cooper ST: **Ferlins: regulators of vesicle fusion for auditory neurotransmission, receptor trafficking and membrane repair**. *Traffic* 2012, **13**(2):185-194.
440. Bernatchez PN, Sharma A, Kodaman P, Sessa WC: **Myoferlin is critical for endocytosis in endothelial cells**. *Am J Physiol Cell Physiol* 2009, **297**(3):C484-492.
441. Bernatchez PN, Acevedo L, Fernandez-Hernando C, Murata T, Chalouni C, Kim J, Erdjument-Bromage H, Shah V, Gratton JP, McNally EM *et al*: **Myoferlin regulates vascular endothelial growth factor receptor-2 stability and function**. *J Biol Chem* 2007, **282**(42):30745-30753.
442. Jones SL, Wang J, Turck CW, Brown EJ: **A role for the actin-bundling protein L-plastin in the regulation of leukocyte integrin function**. *Proc Natl Acad Sci U S A* 1998, **95**(16):9331-9336.
443. Wang J, Chen H, Brown EJ: **L-plastin peptide activation of alpha(v)beta(3)-mediated adhesion requires integrin conformational change and actin filament disassembly**. *J Biol Chem* 2001, **276**(17):14474-14481.
444. Shinomiya H: **Plastin family of actin-bundling proteins: its functions in leukocytes, neurons, intestines, and cancer**. *Int J Cell Biol* 2012, **2012**:213492.
445. Henmi Y, Tanabe K, Takei K: **Disruption of microtubule network rescues aberrant actin comets in dynamin2-depleted cells**. *PLoS One* 2011, **6**(12):e28603.
446. Joshi S, Perera S, Gilbert J, Smith CM, Mariana A, Gordon CP, Sakoff JA, McCluskey A, Robinson PJ, Braithwaite AW *et al*: **The dynamin inhibitors MiTMAB and OcTMAB induce cytokinesis failure and inhibit cell proliferation in human cancer cells**. *Mol Cancer Ther* 2010, **9**(7):1995-2006.
447. Chen JJ, Lin YC, Yao PL, Yuan A, Chen HY, Shun CT, Tsai MF, Chen CH, Yang PC: **Tumor-associated macrophages: the double-edged sword in cancer progression**. *J Clin Oncol* 2005, **23**(5):953-964.
448. Bretscher A, Chambers D, Nguyen R, Reczek D: **ERM-Merlin and EBP50 protein families in plasma membrane organization and function**. *Annu Rev Cell Dev Biol* 2000, **16**:113-143.
449. Sun CX, Robb VA, Gutmann DH: **Protein 4.1 tumor suppressors: getting a FERM grip on growth regulation**. *J Cell Sci* 2002, **115**(Pt 21):3991-4000.
450. Bretscher A, Edwards K, Fehon RG: **ERM proteins and merlin: integrators at the cell cortex**. *Nat Rev Mol Cell Biol* 2002, **3**(8):586-599.
451. Elliott BE, Qiao H, Louvard D, Arpin M: **Co-operative effect of c-Src and ezrin in deregulation of cell-cell contacts and scattering of mammary carcinoma cells**. *J Cell Biochem* 2004, **92**(1):16-28.
452. Kobayashi H, Sagara J, Kurita H, Morifuji M, Ohishi M, Kurashina K, Taniguchi S: **Clinical significance of cellular distribution of moesin in patients with oral squamous cell carcinoma**. *Clin Cancer Res* 2004, **10**(2):572-580.

453. Kanaan Z, Qadan M, Eichenberger MR, Galandiuk S: **The actin-cytoskeleton pathway and its potential role in inflammatory bowel disease-associated human colorectal cancer**. *Genet Test Mol Biomarkers* 2010, **14**(3):347-353.
454. Leong SP, Shen ZZ, Liu TJ, Agarwal G, Tajima T, Paik NS, Sandelin K, Derossis A, Cody H, Foulkes WD: **Is breast cancer the same disease in Asian and Western countries?** *World J Surg* 2010, **34**(10):2308-2324.
455. Saxena S, Szabo CI, Chopin S, Barjhoux L, Sinilnikova O, Lenoir G, Goldgar DE, Bhatanager D: **BRCA1 and BRCA2 in Indian breast cancer patients**. *Hum Mutat* 2002, **20**(6):473-474.
456. GW. S: **Cancer research in the developing world.** 41st Annual Meeting of ASCO 2005. Educational book, pp. 698–671; 2005.
457. Mohammad H Forouzanfar KJF, Allyne M Delossantos,, Rafael Lozano ADL, Christopher J L Murray, Mohsen, Naghavi: **Breast and cervical cancer in 187 countries between 1980 and 2010: a systematic analysis**. The Lancet; 2011.
458. Desai SB, Moonim MT, Gill AK, Punia RS, Naresh KN, Chinoy RF: **Hormone receptor status of breast cancer in India: a study of 798 tumours**. *Breast* 2000, **9**(5):267-270; discussion 270.
459. Navani S, Bhaduri AS: **High incidence of oestrogen receptor negative progesterone receptor positive phenotype in Indian breast cancer: fact or fiction?** *Indian J Pathol Microbiol* 2005, **48**(2):199-201.
460. Nair MK, Sankaranarayanan R, Nair KS, Amma NS, Varghese C, Padmakumari G, Cherian T: **Overall survival from breast cancer in Kerala, India, in relation to menstrual, reproductive, and clinical factors**. *Cancer* 1993, **71**(5):1791-1796.
461. Carter CL, Allen C, Henson DE: **Relation of tumor size, lymph node status, and survival in 24,740 breast cancer cases**. *Cancer* 1989, **63**(1):181-187.
462. G Kaur RI, L Suk Kam,, S Sabaratnam, N Ahmad.: **Assessment Of Correlation Between Clinicopathological Features And Lymph Node Metastases In Breast Cancer.** In., vol. 5. The Internet Journal of Pathology.; 2006.
463. Raina V, Bhutani M, Bedi R, Sharma A, Deo SV, Shukla NK, Mohanti BK, Rath GK: **Clinical features and prognostic factors of early breast cancer at a major cancer center in North India**. *Indian J Cancer* 2005, **42**(1):40-45.
464. Aaltomaa S, Lipponen P, Eskelinen M, Kosma VM, Marin S, Alhava E, Syrjänen K: **Hormone receptors as prognostic factors in female breast cancer**. *Ann Med* 1991, **23**(6):643-648.
465. Grann VR, Troxel AB, Zojwalla NJ, Jacobson JS, Hershman D, Neugut AI: **Hormone receptor status and survival in a population-based cohort of patients with breast carcinoma**. *Cancer* 2005, **103**(11):2241-2251.
466. Schultz JR, Petz LN, Nardulli AM: **Estrogen receptor alpha and Sp1 regulate progesterone receptor gene expression**. *Mol Cell Endocrinol* 2003, **201**(1-2):165-175.
467. Horwitz KB, Koseki Y, McGuire WL: **Estrogen control of progesterone receptor in human breast cancer: role of estradiol and antiestrogen**. *Endocrinology* 1978, **103**(5):1742-1751.
468. Ciocca DR, Fujimura FK, Tandon AK, Clark GM, Mark C, Lee-Chen GJ, Pounds GW, Vendely P, Owens MA, Pandian MR: **Correlation of HER-2/neu amplification with expression and with other prognostic factors in 1103 breast cancers**. *J Natl Cancer Inst* 1992, **84**(16):1279-1282.
469. Huang HJ, Neven P, Drijkoningen M, Paridaens R, Wildiers H, Van Limbergen E, Berteloot P, Amant F, Vergote I, Christiaens MR: **Hormone receptors do not predict the HER2/neu status in all age groups of women with an operable breast cancer**. *Ann Oncol* 2005, **16**(11):1755-1761.
470. Bardou VJ, Arpino G, Elledge RM, Osborne CK, Clark GM: **Progesterone receptor status significantly improves outcome prediction over estrogen receptor status alone for adjuvant endocrine therapy in two large breast cancer databases**. *J Clin Oncol* 2003, **21**(10):1973-1979.

471. Pawlowski V, Révillion F, Hornez L, Peyrat JP: **A real-time one-step reverse transcriptase-polymerase chain reaction method to quantify c-erbB-2 expression in human breast cancer**. *Cancer Detect Prev* 2000, **24**(3):212-223.
472. Gago FE, Fanelli MA, Ciocca DR: **Co-expression of steroid hormone receptors (estrogen receptor alpha and/or progesterone receptors) and Her2/neu (c-erbB-2) in breast cancer: clinical outcome following tamoxifen-based adjuvant therapy**. *J Steroid Biochem Mol Biol* 2006, **98**(1):36-40.
473. Kakarala M, Rozek L, Cote M, Liyanage S, Brenner DE: **Breast cancer histology and receptor status characterization in Asian Indian and Pakistani women in the U.S.--a SEER analysis**. *BMC Cancer* 2010, **10**:191.
474. Cobbs CS, Brenman JE, Aldape KD, Bredt DS, Israel MA: **Expression of nitric oxide synthase in human central nervous system tumors**. *Cancer Res* 1995, **55**(4):727-730.
475. Martin JH, Begum S, Alalami O, Harrison A, Scott KW: **Endothelial nitric oxide synthase: correlation with histologic grade, lymph node status and estrogen receptor expression in human breast cancer**. *Tumour Biol* 2000, **21**(2):90-97.
476. Vakkala M, Kahlos K, Lakari E, Pääkkö P, Kinnula V, Soini Y: **Inducible nitric oxide synthase expression, apoptosis, and angiogenesis in in situ and invasive breast carcinomas**. *Clin Cancer Res* 2000, **6**(6):2408-2416.
477. Loibl S, von Minckwitz G, Weber S, Sinn HP, Schini-Kerth VB, Lobysheva I, Nepveu F, Wolf G, Strebhardt K, Kaufmann M: **Expression of endothelial and inducible nitric oxide synthase in benign and malignant lesions of the breast and measurement of nitric oxide using electron paramagnetic resonance spectroscopy**. *Cancer* 2002, **95**(6):1191-1198.
478. Tschugguel W, Schneeberger C, Unfried G, Czerwenka K, Weninger W, Mildner M, Gruber DM, Sator MO, Waldhör T, Huber JC: **Expression of inducible nitric oxide synthase in human breast cancer depends on tumor grade**. *Breast Cancer Res Treat* 1999, **56**(2):145-151.
479. Nomelini RS, de Abreu Ribeiro LC, Tavares-Murta BM, Adad SJ, Murta EF: **Production of nitric oxide and expression of inducible nitric oxide synthase in ovarian cystic tumors**. *Mediators Inflamm* 2008, **2008**:186584.
480. Loibl S, Buck A, Strank C, von Minckwitz G, Roller M, Sinn HP, Schini-Kerth V, Solbach C, Strebhardt K, Kaufmann M: **The role of early expression of inducible nitric oxide synthase in human breast cancer**. *Eur J Cancer* 2005, **41**(2):265-271.
481. Bulut AS, Erden E, Sak SD, Doruk H, Kursun N, Dincol D: **Significance of inducible nitric oxide synthase expression in benign and malignant breast epithelium: an immunohistochemical study of 151 cases**. *Virchows Arch* 2005, **447**(1):24-30.
482. Calmels S, Hainaut P, Ohshima H: **Nitric oxide induces conformational and functional modifications of wild-type p53 tumor suppressor protein**. *Cancer Res* 1997, **57**(16):3365-3369.
483. Ambs S, Bennett WP, Merriam WG, Ogunfusika MO, Oser SM, Harrington AM, Shields PG, Felley-Bosco E, Hussain SP, Harris CC: **Relationship between p53 mutations and inducible nitric oxide synthase expression in human colorectal cancer**. *J Natl Cancer Inst* 1999, **91**(1):86-88.
484. Wang DY, Xiang YY, Tanaka M, Li XR, Li JL, Shen Q, Sugimura H, Kino I: **High prevalence of p53 protein overexpression in patients with esophageal cancer in Linxian, China and its relationship to progression and prognosis**. *Cancer* 1994, **74**(12):3089-3096.
485. Rajnakova A, Moochhala S, Goh PM, Ngoi S: **Expression of nitric oxide synthase, cyclooxygenase, and p53 in different stages of human gastric cancer**. *Cancer Lett* 2001, **172**(2):177-185.
486. Alsner J, Yilmaz M, Guldberg P, Hansen LL, Overgaard J: **Heterogeneity in the clinical phenotype of TP53 mutations in breast cancer patients**. *Clin Cancer Res* 2000, **6**(10):3923-3931.

487. Harris L, Fritsche H, Mennel R, Norton L, Ravdin P, Taube S, Somerfield MR, Hayes DF, Bast RC, Oncology ASoC: **American Society of Clinical Oncology 2007 update of recommendations for the use of tumor markers in breast cancer**. *J Clin Oncol* 2007, **25**(33):5287-5312.
488. Dookeran KA, Dignam JJ, Ferrer K, Sekosan M, McCaskill-Stevens W, Gehlert S: **p53 as a marker of prognosis in African-American women with breast cancer**. *Ann Surg Oncol* 2010, **17**(5):1398-1405.
489. Feki A, Irminger-Finger I: **Mutational spectrum of p53 mutations in primary breast and ovarian tumors**. *Crit Rev Oncol Hematol* 2004, **52**(2):103-116.
490. Di Leo A, Larsimont D, Gancberg D, Jarvinen T, Beauduin M, Vindevoghel A, Michel J, Focan CH, Ries F, Gobert PH *et al*: **HER-2 and topo-isomerase IIalpha as predictive markers in a population of node-positive breast cancer patients randomly treated with adjuvant CMF or epirubicin plus cyclophosphamide**. *Ann Oncol* 2001, **12**(8):1081-1089.
491. Jackson SP, Bartek J: **The DNA-damage response in human biology and disease**. *Nature* 2009, **461**(7267):1071-1078.
492. Rothkamm K, Löbrich M: **Evidence for a lack of DNA double-strand break repair in human cells exposed to very low x-ray doses**. *Proc Natl Acad Sci U S A* 2003, **100**(9):5057-5062.
493. Kinner A, Wu W, Staudt C, Iliakis G: **Gamma-H2AX in recognition and signaling of DNA double-strand breaks in the context of chromatin**. *Nucleic Acids Res* 2008, **36**(17):5678-5694.
494. Wasco MJ, Pu RT, Yu L, Su L, Ma L: **Expression of gamma-H2AX in melanocytic lesions**. *Hum Pathol* 2008, **39**(11):1614-1620.
495. Bartkova J, Tommiska J, Oplustilova L, Aaltonen K, Tamminen A, Heikkinen T, Mistrik M, Aittomäki K, Blomqvist C, Heikkilä P *et al*: **Aberrations of the MRE11-RAD50-NBS1 DNA damage sensor complex in human breast cancer: MRE11 as a candidate familial cancer-predisposing gene**. *Mol Oncol* 2008, **2**(4):296-316.
496. Tommiska J, Bartkova J, Heinonen M, Hautala L, Kilpivaara O, Eerola H, Aittomäki K, Hofstetter B, Lukas J, von Smitten K *et al*: **The DNA damage signalling kinase ATM is aberrantly reduced or lost in BRCA1/BRCA2-deficient and ER/PR/ERBB2-triple-negative breast cancer**. *Oncogene* 2008, **27**(17):2501-2506.
497. Melnikova VO, Dobroff AS, Zigler M, Villares GJ, Braeuer RR, Wang H, Huang L, Bar-Eli M: **CREB inhibits AP-2alpha expression to regulate the malignant phenotype of melanoma**. *PLoS One* 2010, **5**(8):e12452.
498. Deng X, Liu H, Huang J, Cheng L, Keller ET, Parsons SJ, Hu CD: **Ionizing radiation induces prostate cancer neuroendocrine differentiation through interplay of CREB and ATF2: implications for disease progression**. *Cancer Res* 2008, **68**(23):9663-9670.
499. Catalano S, Giordano C, Rizza P, Gu G, Barone I, Bonofiglio D, Giordano F, Malivindi R, Gaccione D, Lanzino M *et al*: **Evidence that leptin through STAT and CREB signaling enhances cyclin D1 expression and promotes human endometrial cancer proliferation**. *J Cell Physiol* 2009, **218**(3):490-500.
500. Kovach SJ, Price JA, Shaw CM, Theodorakis NG, McKillop IH: **Role of cyclic-AMP responsive element binding (CREB) proteins in cell proliferation in a rat model of hepatocellular carcinoma**. *J Cell Physiol* 2006, **206**(2):411-419.

6. ANNEXURE

6. Annexure

6.1 Antibodies and Chemicals

6.1.1 Fine chemicals

Name	Source	Catalogue number
1400W-inhibitor of iNOS	Sigma (St. Louis, MO, USA)	W4262
2-(5-Bromo-2-pyridylazo)-5-(diethylamino)phenol (BP blue stain)		180017
2-Mercaptoethanol		M6250
3-[(3-Cholamidopropyl)dimethylammonio]-1-propanesulfonate		C9426
Acetonitrile (ACN)		271004
Acrylamide		A3553
Ammonium persulfate		A3678
Ammonium Sulphate		A4418
Bovine Serum Albumin		A2153
Bradford reagent		B6916
Brilliant Blue G		B0770
Calcein AM	Life technologies, Invitrogen (Grand Island,	C3100MP

	NY, USA)	
CGK733	Sigma (St. Louis, MO,USA)	C9867
Crystal Violet		C3886
D.P.X Mountant	HiMedia (Mumbai, India)	RM655
DAF-FM-DA	Molecular probes, Invitrogen (Grand Island, NY, USA)	D-23842261
Dimethylsulfoxide (DMSO)	Sigma (St. Louis, MO, USA)	D2650
Dithiothreitol (DTT)	Sigma (St. Louis, MO, USA)	D0632
Ethylenediaminetetraacetic acid(EDTA)		E6758
Glycine		G8898
Gycerol		G5516
H2DCF-DA		D6883
Haematoxylin (Harris)	HiMedia (Mumbai, India)	S034-500ML
HRP chemiluminescent substrate	Millipore (Billerica, MA, USA)	WBKLS0500
Hydrogen Peroxide Solution 30% w/V	Thermo Fisher Scientific (Waltham, MA, USA)	18755
Igepal (NP-40)	Sigma (St. Louis, MO,	I7771

Iodoacetamide (IAA)	USA)	I1149
JC-1 dye	Molecular probes, Invitrogen (Grand Island, NY, USA)	T3168
LM agarose	Trevigen (Gaithersburg, MD,USA)	4250-050-02
Metal enhanced DAB Substrate Kit	Thermo Fisher Scientific (Waltham, MA, USA)	35065
Non-fat milk	HiMedia (Mumbai, India)	M530
PD 98059	Sigma (St. Louis, MO, USA)	P215
Peroxidase Suppressor	Thermo Fisher Scientific (Waltham, MA, USA)	35000PI
Phosphatase inhibitor cocktail tablets	Roche Applied Science (Germany)	4 906 837 001 262
PI	Sigma (St. Louis, MO, USA)	P4170
PKH26 Red Fluorescent Cell Linker Kit		PKH26GL
PMA		P8139
Poly-L-lysine hydrochloride		P9404
Ponceau S solution		P7170
Pre-stained Molecular weight marker	Bio-rad (Hercules, CA, USA)	161-0325

Protease inhibitor cocktail tablets	Roche Applied Science (Germany)	11 873 580 001
ProteoGel IPG Equilibration Buffer	Sigma (St. Louis, MO, USA)	I 7281
RNase A		R6513
SDS		L3771
Sodium azide		S2002
Sodium bicarbonate		S5761
SYBR green	Sigma (St. Louis, MO, USA)	S9430
TEMED		T9281
Thiourea		T8656
Tri Sodium Citrate	AR Cemico Fine Chemicals	
Trifluoroacetic acid (TFA)	Sigma (St. Louis, MO, USA)	T6508
Tris base		T1503
TrisHCl		T3253
Triton X 100		X100
Tween 20		P2287
Urea		U5378
α-Cyano-4-hydroxycinnamic acid (CHCA matrix)		03841

6.1.2 Antibodies

Name	Source	Catalogue number
Alexa Fluor 488 Donkey Anti-Mouse Antibody	Life technologies, Invitrogen (Grand Island, NY, USA)	A-21202
Alexa Fluor 488 Donkey Anti-Rabbit Antibody		A-21206263
Anti- ERK 2 (D-2) (Mouse monoclonal)	Santa Cruz Biotechnology (Santa Cruz, CA)	sc-1647
Anti-CREB antibody (clone 48H2)	Cell Signalling Technology (Danvers,MA)	9197
Anti-iNOS (Mouse monoclonal)	Santa Cruz Biotechnology (Santa Cruz, CA)	sc-7271
Anti-mouse FITC antibody	Sigma (St. Louis, MO, USA)	F2012
Anti-Mouse IgG HRP		A-9044
Anti-p53 (Mouse monoclonal)	Santa Cruz Biotechnology (Santa Cruz, CA)	sc-126264
Anti-PARP (Rabbit polyclonal)	Cell Signalling Technology (Danvers, MA)	9542L
Anti-phospho ATM (ser 1981, clone 10H11.E12;)	Upstate cell signaling solutions (Lake Placid, NY, USA)	05-740

Anti-phospho CREB (S133, clone 87G3)	Cell Signalling Technology (Danvers,MA)	9198
Anti-Phospho p53 (Ser15) (Rabbit polyclonal)		9284S
Anti-Rabbit IgG HRP	Santa Cruz Biotechnology (Santa Cruz, CA)	sc 2030
Anti-TGF-β, pan	Sigma (St. Louis, MO, USA)	T9429
Anti-vimentin antibody (clone V-9)	Santa Cruz Biotechnology (Santa Cruz, CA)	sc 6260
Anti-γH2AX (Ser 139) (Mouse monoclonal)	Upstate Millipore (Billerica, MA, USA)	05-636
Human IFN-γ ELISA Set	BD Biosciences (Franklin Lakes, NJ, USA)	555142
Human IL-1β ELISA Set		557953
Human IL-6 ELISA Set		555220
Human TGF-β1 ELISA Set		559119
Human TNF-α ELISA Set		555212
Phospho MAPK Family Antibody Sampler Kit	Cell Signalling Technology (Danvers,MA)	9910
Pro-Apoptosis Bcl-2 Family Antibody Sampler Kit		9942
Pro-Survival Bcl-2 Family Antibody Sampler Kit	Cell Signalling Technology (Danvers,MA)	9941
Vectastain Elite ABC kit	Vector Laboratories (CA, US)	PK-6200

(Universal)		

6.1.3 Tissue culture reagents

Name	Source	Catalogue number
DMEM	HiMedia (Mumbai, India)	AL151A
Heat inactivated fetal bovine serum		RM9955-100ML
Penicillin-Streptomycin		P4333
RPMI-1640		AL060A
Trypsin-EDTA solution		T3924

6.1.4 Molecular biology reagents

Name	Source	Catalogue number
ATM siRNA (h)	Santa Cruz Biotechnology (Santa Cruz, CA)	sc-29761
cDNA synthesis kit	Roche Applied Science (Germany)	11 483 188 001
Control siRNA-A	Santa Cruz Biotechnology (Santa Cruz, CA)	sc-37007

Deoxynucleotides Set	5 Prime GmbH (Hilden, Deutschland)	2201230266
Golgi Plug, Protein transport inhibitor	BD Biosciences (Franklin Lakes, NJ, USA)	555029
LightCycler® 480 SYBR Green I Master	Roche Applied Science (Germany)	04707516001
PerfectPure RNA isolation Kit	5 Prime GmbH (Hilden, Deutschland)	2302340
Primers	Sigma (St. Louis, MO, USA)	
Taq polymerase	Invitrogen (Grand Island, NY, USA)	10342-053
X-tremeGENE Transfection Reagent	Roche Applied Science (Germany)	04476093001

6.1.5 Miscellaneous

Name	Source	Catalogue number
Amicon® Ultra-4 Centrifugal Filter Units	Millipore (Billerica, MA, USA)	UFC800308
Cell culture inserts (8 μm)	BD Biosciences (Franklin Lakes, NJ, USA)	353097
PVDF membranes	Millipore (Billerica, MA,	1PVH00010

	USA)	
ReadyStrip IPG Strips, 11 cm, pH 3-10	Bio-rad (Hercules, CA, USA)	163-2015

6.2 Buffers and solutions

A. Phosphate Buffered Saline (PBS): 0.8 % NaCl, 2.7 mM KCl, 10 mM phosphate, pH 7.4

B. PBST: 0.05 % Tween 20 in PBS

C. Flowcytometry: Propidium Iodide (PI) Solution: 50 µg/ml PI, 50 µg/ml RNAase A in PBS

D. SDS-PAGE:

1. Whole cell lysis buffer: 50 mMTris.Cl (pH 6.8), 100 mM DTT, 2 % SDS, 0.1 % bromophenol blue, 10 % Glycerol, protease inhibitor cocktail and phosphatase inhibitor cocktail

2. 30% acrylamide mix: 29 % acrylamide, 1 % N,N'-Methylene bisacrylamide

3. Tris-Glycine Electrophoresis Buffer: 25 mM Tris base, 250 mM glycine (pH8.3) and 0.1 % SDS.

4. Transfer Buffer: 39 mM glycine, 48 mM Tris base and 10 % Methanol

5. 10 % SDS

6. SDS PAGE gels:

Components	Resolving Gels (10 ml)	
	10 %	**12 %**
Water	4	3.3
30 % Acrylamide Mix	3.3	4
1.5 M Tris (pH 8.8)	2.5	2.5
10 % SDS	0.1	0.1
10 % APS	0.1	0.1
TEMED	0.004	0.004
	5 % Stacking Gel (5 ml)	
Water	3.4	
30 % Acrylamide Mix	0.83	
1.5 M Tris (pH 6.8)	0.63	
10 % SDS	0.05	
10 % APS	0.05	
TEMED	0.005	

E: Silver Staining

Fixative solution: 50% methanol, 12% acetic Acid, 0.5 ml 37% formaldehyde/L

Sensitizer: 0.02% sodium thiosulfate

Silver Nitrate Solution: 2g/L $AgNO_3$, 0.75 ml of 37% formaldehyde/L

Developing Solution: 60g/L Na_2CO_3, 0.5 ml 37% formaldehyde/L, 4 mg/L $Na_2S_2O_3.5H_2O$

Stop Solution: 50% methanol and 12% acetic acid

F: ELISA

Coating carbonate buffer: 0.15 M sodium carbonate, 0.35 M sodium bicarbonate, pH 9.6

Phosphate Buffered Saline (PBS): 0.8 % NaCl, 2.7 mM KCl, 10 mM phosphate, pH 7.4

Blocking buffer: PBS, 1% BSA

Wash solution: PBS, 0.05% Tween-20

Dilution buffer: PBS, 0.05% Tween-20, 0.1% BSA

Stop Solution: 3 M HCl

G: Two dimensional SDS PAGE:

Rehydration Buffer: 8 M urea, 1 M thiourea, 2% CHAPS, 15 mM DTT, 2% IPG buffer, traces of bromphenol blue

Equilibration Buffer I: 6 M urea, 50 mM Tris, pH 6.8, 30% glycerol, 4% SDS, 20 mM DTT

Equilibration Buffer II: 6 M urea, 50 mM Tris, pH 6.8, 30% glycerol, 4% SDS, and 4.5% iodoacetamide

H:MALDI

Destaining buffer: 50 mM NH_4HCO_3/Acetonitrile (ACN) (1:1, v/v)

Reduction buffer: 10 mM DTT in 50 mM NH_4HCO_3

Alkylation buffer: 55 mM IAA in 50 mM NH_4HCO_3

Washing buffer: 50 mM NH_4HCO_3/ ACN (1:1, v/v)

Proteolytic cleavage buffer: Freshly prepared trypsin solution (20 ng in 25 mM NH_4HCO_3)

Peptide extraction buffer: (a) 0.1 % TFA, (b) 0.1% TFA: CAN and (c) ACN

Co-crystallized with CHCA : 5 mg/mL CHCA in 0.1% TFA with 50% ACN

I: Zymography:

2X sample loading buffer: 125 m*M* Tris-HCl, 20% glycerol, 4% SDS, and 0.005% bromophenol blue, pH 6.8

Renaturing Buffer: 2.5% Triton X-100 in H_2O, freshly prepared

Developing Buffer (10X): 500 mM Tris-HCl, 2 *M* NaCl, 50 mM $CaCl_2$, and 0.2% NP-40, pH 7.8

Staining solution: 0.5% Coomassie blue R-250, 5% methanol and 10% acetic acid in dH_2O.

Destaining solution: 10% methanol, 10% acetic acid in dH_2O.

J: Immunohistochemistry:

Peroxidase Suppressor: 3% H_2O_2 in methanol

Sodium Citrate Buffer: 10mM Sodium Citrate, 0.05% Tween 20, pH 6.0